Experimental Investigation of Residential Building Heating and Ventilation Systems Performance

Alula Assefa

A Thesis
In
The Graduate Program
Of
Building Science / Building Engineering

The School of Construction and the Environment

Presented in Partial Fulfillment of the Requirements
for the Degree of Master of Applied Science at
British Columbia Institute of Technology
Burnaby, British Columbia, Canada

May 2018

Burnaby, British Colombia, Canada

© Alula Assefa, 2018

BRITISH COLUMBIA INSTITUTE OF TECHNOLOGY

Building Science Graduate Program

BRITISH COLUMBIA
INSTITUTE OF TECHNOLOGY

Building Science Graduate Program
School of Construction
and the Environment
3700 Willingdon Avenue
Burnaby, British Columbia
Canada V5G 3H2

bcit.ca

This is to certify that the thesis prepared

By: Alula Assefa Yadete Student Number:

Entitled: **Experimental Investigation of Residential Building Heating and Ventilation Systems Performance**

And submitted in partial fulfillment of the requirement for the degree of:

Master of Applied Science in Building Engineering/Building Science

Complies with the regulations of the Institute and meets the accepted standards with respect to originality and quality.

Signed by the final Examining Committee:

Rodrigo Mora, PhD (Chair)

Wahid Maref, PhD (External Examiner)

May 14. 2018

Bo Li, MASc (Examiner)

Fitsum Tariku, PhD (Supervisor)

Approved by:

Graduate Program Director

ABSTRACT

The building sector is one of the most dynamically evolving field with an expectation to provide comfortable, clean and healthy indoor environment with less energy consumption. This acceptable indoor condition is created with a combination of heating/cooling systems and ventilation strategies. There are various systems available, which can deliver heating/cooling as well as ventilation to a dwelling space. These systems involve different heat transfer mechanisms and ventilation strategies: as a result, their performance would be different. Accordingly, the performance of these systems would affect indoor conditions. The process of providing an acceptable indoor environment with minimized energy use can be challenging. In addition to that, there is also a keen interest to reduce the current trend of the building energy consumption as low as possible without affecting the required, comfortable indoor environment. Therefore, the requirement of comprehensive field research that studies and compares most of currently available space heating systems, as well as ventilation strategies, is highly vital to provide information about their actual and relative performance in a real scenario.

This research project conducts a field experiment that studies, heating systems, ventilation strategies, and ventilation flow rates. The first part is done by running two different heating systems at a time out of four heating systems (electrical baseboard heater, portable radiator heater, heat pump, and Radiant floor heating systems) in identical full-scale test building with similar ventilation strategy and similar ventilation flow rate. Whereas, the second group of experiments compare two ventilation strategies (mixed ventilation and underfloor ventilation) inside two test buildings with similar heating systems and ventilation flow rate. The third group of comparison compares three ventilation flow rates (15 cfm, 7.5 cfm, and 5 cfm) in the test buildings with similar heating systems and ventilation strategies.

Various indicators and indoor environmental elements are used to conduct the comparisons. In the first case where heating systems are compared, the thermal energy provide by the systems are used for comparison. In addition, the thermal comfort, local thermal discomfort, temperature distribution and RH distribution are used to assess and compare the indoor environment produced by the systems. Whereas, the ventilation strategies are compared using indoor environmental element (temperature, relative humidity, CO2, and air velocity) distributions. Finally, the comparison of ventilation flow rates is performed using contaminant removal effectiveness, indoor air quality number, and indoor environmental element distributions.

The findings from the experiments indicate that all of the heating systems provide similar daily thermal energy between 10 kWh and 14 kWh based on the outdoor weather condition. In addition, all of the heating systems produce a thermally comfortable indoor environment for standing person. Whereas, the ventilation strategies comparison shows that mixed ventilation strategy performance is slightly better than an underfloor Ventilation strategy by creating marginally uniform CO2 and RH distribution. Moreover, the results of the ventilation flow rates comparison show that the temperature and air velocity distribution find similar while using all the three ventilation flow rates. But the higher ventilation flow rate removes relatively more RH and CO2 in comparison to the lower one. Accordingly, the higher ventilation flow rates depict higher contaminant removal rate and high indoor air quality number relative to lower ventilation flow rate.

Keyword: Thermal Energy, Portable Radiator Heater, Ventilation Effectiveness, Ventilation Flow Rate, Indoor Air Quality Number.

ACKNOWLEDGMENT

It is interesting to reflect on how things have rolled out at this point in this project. Primarily, I would like to thank God for giving me every piece of strength and hope to go through this learning curve with the patient as well as joy. Secondly, I would like to thank Dr. Fitsum Tariku who is my supervisor. I have learned so much about the process and basis of fundamental science research on this project working under your supervision. Thirdly, I'm thankful for the financial support from Natural Science and Engineering Council Canada (NSERC), Canada Research Chair (CRC) and School of Construction and the Environment at the British Columbia Institute of Technology (BCIT). Special thanks to Mr. Doug Horn, for his help when carrying out the experiments. Finally, I would like to thank family members, friends and colleagues for the support and encouragement they give me.

TABLE OF CONTENTS

Abstract i
Acknowledgment iii
Table of Contents iv
Table of Graphs vi
Acronyms xi
1 Introduction 1
2 Literature review 4
3 Problem statement 23
4 Research Framework 25
4.1 Objective 25
4.2 Scope 26
4.3 Methodology 26
5 Experimental Setup 28
5.1 Overview of the test buildings 28
5.1.1 General Description 28
5.1.2 Systems Descriptions 33
5.1.3 Occupant Simulators 38
5.2 Experimental Design 40
5.2.1 Sensors and Sensor Layouts 43
5.2.2 Measurement, Sensor specification, Calibration, and Data acquisition 49
6 Data analysis 54
6.1 Thermal Energy 55
6.1.1 Thermal Energy from Baseboard and Radiator Heating System 56
6.1.2 Thermal Energy Calculation from Heat Pump 56
6.1.3 Thermal Energy Calculation from Radiant Floor 59
6.2 Thermal Comfort 63
6.2.1 General Thermal Comfort 63
6.2.2 Local Thermal Comfort Analysis 69
6.3 Indoor Air Assessment 73
6.3.1 Indoor Air 73
6.3.2 Ventilation Effectiveness 73

6.4 The Weather Condition during the Experimental Period 75
7 Result and discussion 76
7.1 Heating Systems Comparison 76
7.1.1 Thermal Energy 76
7.1.2 Indoor Air Temperature and Relative Humidity Distributions 84
7.1.3 Thermal Comfort 91
7.2 Ventilation Strategies Comparison 106
7.2.1 Comparison of Mixed and Underfloor Ventilation Strategies 106
7.3 Ventilation Rate Comparison 116
7.3.1 Temperature Distribution: Ventilation Flow Rate Comparison 117
7.3.2 Air Velocity Distribution: Ventilation Flow Rate Comparison. 119
7.3.3 RH Distribution: Ventilation Flow Rate Comparison 121
7.3.4 CO2 Distribution: Ventilation Flow Rate Comparison. 125
7.3.5 Contaminant Removal Effectiveness (CRE): Ventilation Flow Rate Comparison 128
7.3.6 Indoor Air Quality Number: Ventilation Flow Rate Comparison 130
7.3.7 Global Contaminant Removal Effectiveness (GCRE) and Indoor Air Quality Number (IAQN) 132
7.3.8 Energy Penalty: Ventilation Flow Rate Comparison 134
8 Conclusion 136
9 Appendix I 140
10 APPENDIX II 144
11 Reference 179

TABLE OF GRAPHS

Figure 1: Thermal comfort zone (ASHRAE Fundamentals 2017) 7
Figure 2: Adaptive thermal comfort model (ASHRAE, RP-884)..... 8
Figure 3: Confluent Jet Ventilation..... 12
Figure 4: Wall confluent Jet ventilation..... 22
Figure 5: Research approach flow Chart. 28
Figure 6: Whole Building Performance Research Laboratory (WBPRL) 29
Figure 7: Section view of a foundation..... 30
Figure 8: Mechanical Room..... 32
Figure 9: Ventilation system components..... 33
Figure 10: Ventilation system schematic diagram..... 34
Figure 11: Ventilation strategies..... 34
Figure 12: Bath and accessories for RFHS. 36
Figure 13 Space heating systems. 38
Figure 14: Occupant simulator..... 39
Figure 15: CO2 and RH supply by the human simulator..... 40
Figure 16: Sensor layout, Horizontal and vertical. 44
Figure 17: Vertical sensor distribution (L3P3). 45
Figure 18: Anemometer. 46
Figure 19: RH transducer and CO2 Sensor..... 47
Figure 20: Revised Sensor layout. 48
Figure 21: ` Meter (Power Scout 24). 49
Figure 22: Thermocouple calibration: STB. 51
Figure 23: CO2 supply into the test rooms (NTB and STB). 52
Figure 24: Data Acquisition system..... 53
Figure 25: Room temperature profile of test rooms: PRH vs HP. 55
Figure 26: Thermal energy supply by EBH and HP (with COP). 57
Figure 27: Heat pump with inlet and outlet thermocouples..... 58
Figure 28: Section of test room for RFHS thermal energy analysis. 60
Figure 29: View factor for MRT calculation. 65
Figure 30: Mean radiant and globe temperature trend at the same position and location. 67
Figure 31: PMV comparison between Mat-lab and ISO 7730 (2005) using Table 7. 68
Figure 32: Local thermal discomfort as the result of radiant asymmetry (ASHRAE 55, 2013). . 70
Figure 33: Local thermal discomfort due to the vertical temperature difference (ASHRAE 55, 2013). 71
Figure 34: Local thermal discomfort caused by floor surface temperature (ASHRAE 55, 2013). 72
Figure 35: Outdoor weather condition over all the measurement period. 75
Figure 36 Thermal Energy profile of EBH and HP with indoor and outdoor conditions..... 77
Figure 37: Average outdoor weather condition and interior temperature difference during when thermal energy is compared. 78
Figure 38: Thermal energy profile of four heating systems for a single day..... 79

Figure 39: One-day total thermal energy supply at the same outdoor and indoor environmental conditions. 81
Figure 40: Components of thermal energy delivered by RFHS. 82
Figure 41: Thermal energy estimation using three film coefficients and actual thermal energy. 83
Figure 42: Sensor layout, Horizontal and vertical. 84
Figure 43: Indoor temperature distribution using four heating system within the period where thermal energy is compared. 85
Figure 44: Normalized interior temperature using four heating system within the period where thermal energy is compared. 86
Figure 45: Interior RH distribution using four heating system within the period where thermal energy is compared. 88
Figure 46: Surface temperature distribution using four heating systems within the period where thermal energy is compared. 90
Figure 47: Thermal comfort (PPD) for a seating & standing person: EBH vs HP. 93
Figure 48: Thermal comfort (PPD) for a seating & standing person: EBH vs PRH. 93
Figure 49: Thermal comfort (PPD) for a seating & standing person: PRH vs HP. 94
Figure 50: Thermal comfort (PPD) for a seating & standing person: RFHS vs EBH. 95
Figure 51: Thermal comfort (PPD) for a seating & standing person: RFHS vs HP. 96
Figure 52: Thermal comfort (PPD) for a seating & standing person: RFHS vs PRH. 96
Figure 53: Local thermal discomfort due to vertical temperature difference: PRH vs HP..... 99
Figure 54: Local thermal discomfort due to vertical temperature difference: RFHS vs EBH. 99
Figure 55: Local thermal discomfort due to surface temperature: PRH vs HP. 100
Figure 56: Local thermal discomfort due to surface temperature: RFHS vs EBH. 101
Figure 57: Local thermal discomfort due to cold window radiant asymmetry: PRH and HP. ... 102
Figure 58: Local thermal discomfort due to cold window radiant asymmetry: RFHS and EBH. 103
Figure 59: Local thermal discomfort due to ceiling to floor radiant asymmetry: PRH and HP. 104
Figure 60: Local thermal discomfort due to ceiling to floor radiant asymmetry: RFHS and EBH. 105
Figure 61: Temperature distribution in a room with similar heating bud different ventilation strategy (MV and UV). 107
Figure 62: Transient CO2 profile at L3P3 in a room with the similar heating system (EBH) and different ventilation strategy (MV and UV). 108
Figure 63: CO2 distribution in a room with similar heating system, but different ventilation strategy (MV and UV). 109
Figure 64: The relative humidity profile at L3P3 in a room with the similar heating system (RFHS) but different ventilation strategy (MV and UV). 110
Figure 65: Relative humidity distribution in a room with MV and UV but the similar heating system. 111
Figure 66: Air velocity distribution in a room with MV and UV but the similar heating system. 112
Figure 67: GVE in a test room with MV and UV both heated by EBH. 113

Figure 68: Contaminant removal effectiveness (CRE) in a room with MV and UV but the similar heating system. 114
Figure 69: Indoor air quality number (IAQN) in a room with MV and UV but the similar heating system. 115
Figure 70: Interior temperature distribution comparison of 15cfm, 7.5cfm, and 5cfm with MV. 118
Figure 71: Interior distribution comparison of 15cfm air velocity, 7.5cfm, and 5cfm with MV. 120
Figure 72: The relative humidity profile at L3P3 comparing 15cfm, 7.5cfm using RFHS with MV. 122
Figure 73: The relative humidity profile at L3P3 comparing 7.5cfm, 5cfm using EBH with MV. 122
Figure 74: Interior RH distribution comparison of 15cfm, 7.5cfm, and 5cfm with MV. 124
Figure 75: CO2 profile comparing 15cfm and 7.5cfm with RFHS and MV. 125
Figure 76: CO2 profile correlating 7.5cfm and 5cfm with EBH and MV. 126
Figure 77: Interior CO2 distribution comparison of 15cfm, 7.5cfm, and 5cfm with MV. 127
Figure 78: Interior CRE distribution comparison of 15cfm, 7.5cfm, and 5cfm with MV. 129
Figure 79: Interior IAQN distribution comparison of 15cfm, 7.5cfm, and 5cfm with MV..... 131
Figure 80: GCRE and IAQN: HP (15cfm vs 7.5cfm) MV. 133
Figure 81: GCRE and IAQN: HP (7.5cfm vs 5cfm) MV. 133
Figure 82: Energy profile of EBH with 15cfm and 7.5cfm. 134
Figure 83: Energy profile of EBH and MV with 7.5cfm and 5cfm. 135
Figure 84: View factor between the square floor and surrounding surfaces. 140
Figure 85 View factor between the rectangular floor and surrounding surfaces. 140
Figure 86: Thermocouple calibration: NTB. 143
Figure 87: Thermal Energy profile of PRH and HP with indoor and outdoor conditions. 144
Figure 88: Thermal Energy profile of PRH and EBH with indoor and outdoor conditions. 144
Figure 89: Thermal Energy profile of RFHS and HP with indoor and outdoor conditions..... 145
Figure 90: Thermal Energy profile of RFHS and EBH with indoor and outdoor conditions..... 145
Figure 91: Thermal Energy profile of EBH and HP with indoor and outdoor conditions..... 146
Figure 92 Components of thermal energy delivered by RFHS..... 147
Figure 93: Components of thermal energy delivered by RFHS. 147
Figure 94: Components of thermal energy delivered by RFHS. 148
Figure 95: Components of thermal energy delivered by RFHS. 148
Figure 96: Film coefficient comparisons during 7th Experiment. 149
Figure 97: Film coefficient comparisons during 8th Experiment. 149
Figure 98: Film coefficient comparisons during 9th Experiment. 150
Figure 99: Temperature distribution with four heating systems and UV. 151
Figure 100: Surface temperature distribution using four heating systems with UV..... 152
Figure 101: RH distribution with four heating systems and UV. 153
Figure 102: Local thermal discomfort due to a vertical temperature difference using EBH and HP. 154

Figure 103: Local thermal discomfort due to a vertical temperature difference using PRH and EBH. 154
Figure 104: Local thermal discomfort due to a vertical temperature difference using RFHS and HP. 155
Figure 105: Local thermal discomfort due to a vertical temperature difference using RFHS and PRH. 155
Figure 106: Local thermal discomfort due to surface temperature using EBH and HP. 156
Figure 107: Local thermal discomfort due to surface temperature using PRH and EBH. 156
Figure 108: Local thermal discomfort due to surface temperature using RFHS and HP. 157
Figure 109: Local thermal discomfort due to surface temperature using RFHS and PRH. 157
Figure 110: Local thermal discomfort due to cold window radiant asymmetry using EBH and HP. 158
Figure 111: Local thermal discomfort due to cold window radiant asymmetry using PRH and HP. 158
Figure 112: Local thermal discomfort due to cold window radiant asymmetry using RFHS and HP. 159
Figure 113: Local thermal discomfort due to cold window radiant asymmetry using RFHS and PRH. 159
Figure 114: Local thermal discomfort due to the ceiling to floor radiant asymmetry using EBH and HP. 160
Figure 115: Local thermal discomfort due to the ceiling to floor radiant asymmetry using PRH and EBH. 160
Figure 116: Local thermal discomfort due to the ceiling to floor radiant asymmetry using RFHS and HP. 161
Figure 117: Local thermal discomfort due to the ceiling to floor radiant asymmetry using RFHS and PRH. 161
Figure 118: Transient CO2 profile at L3P3 in a room with the similar heating system (HP) and different ventilation strategy (MV and UV). 162
Figure 119: Transient CO2 profile at L3P3 in a room with the similar heating system (RFHS) and different ventilation strategy (MV and UV). 162
Figure 120: The relative humidity profile at L3P3 in a room with the similar heating system (EBH) but different ventilation strategy (MV and UV). 163
Figure 121: The relative humidity profile at L3P3 in a room with the similar heating system (HP) but different ventilation strategy (MV and UV). 163
Figure 122: GVE in a test room with MV and UV both heated by HP. 164
Figure 123: GVE in a test room with MV and UV both heated by RFHS. 164
Figure 124: Interior temperature distribution comparison of 15 cfm, 7.5 cfm, and 5 cfm with UV. 165
Figure 125: Interior air velocity distribution comparison of 15 cfm, 7.5 cfm, and 5 cfm with UV. 166
Figure 126: Interior RH distribution comparison of 15 cfm, 7.5 cfm, and 5 cfm with UV. 167
Figure 127: The relative humidity profile at L3P3 comparing 15 cfm 7.5 cfm using EBH and UV. 168

Figure 128: The relative humidity profile at L3P3 comparing 15 cfm 7.5 cfm using EBH and UV. 168
Figure 129: The relative humidity profile at L3P3 comparing 15 cfm 7.5 cfm using HP and UV. 169
Figure 130: The relative humidity profile at L3P3 comparing 15 cfm 7.5 cfm using EBH and UV. 169
Figure 131: Interior CO2 distribution comparison of 15 cfm, 7.5 cfm, and 5 cfm with MV. 170
Figure 132: CO2 profile comparing 15 cfm and 7.5 cfm with RFHS and UV. 171
Figure 133: CO2 profile comparing 7.5 cfm and 5 cfm with EBH and UV. 171
Figure 134: Interior CRE distribution comparison of 15 cfm, 7.5 cfm, and 5 cfm with UV. 172
Figure 135: Interior IAQN distribution comparison of 15 cfm, 7.5 cfm, and 5 cfm with UV. .. 173
Figure 136: IAQN and GCRE room with RFHS (15 cfm vs 7.5 cfm) UV..... 174
Figure 137: IAQN and GCRE room with RFHS and UV. 174
Figure 138: IAQN and GCRE room with EBH (15 cfm vs 7.5 cfm) UV..... 175
Figure 139: IAQN and RVE room with EBH (15 cfm vs 7.5 cfm) MV..... 175
Figure 140: IAQN and RVE room with HP (15 cfm vs 7.5 cfm) UV. 176
Figure 141: IAQN and RVE room with EBH (7.5 cfm vs 5 cfm) UV. 176
Figure 142: IAQN and RVE room with EBH (7.5 cfm vs 5 cfm) MV..... 177
Figure 143: Energy profile of EBH and UV with 15 cfm and 7.5 cfm..... 178
Figure 144: Energy profile of EBH and UV with 7.5 cfm and 5 cfm..... 178

ACRONYMS

Short form	Long form
WBPRL	Whole Building Performance Research Laboratory
STB	South Test Building
NTB	North Test Building
RFHS	Radiant Floor Heating System
HP	Heat Pump
EBH	Electrical Baseboard Heater
PRH	Portable Radiator Heater
MV	Mixed ventilation
UV	Underfloor Ventilation
LPM	Liter Per Minute
ACH	Air Change Per Hour
MRT	Mean Radiant Temperature
Met	Metabolic Rate
ClO	Clothing
CRE	Contaminant Removal Effectiveness
GCRE	Globe Contaminant Removal Effectiveness
IAQN	Indoor Air Quality Number
TE	Temperature Effectiveness
SET	Standard Effective Temperature
Tm	Daily Mean Outdoor Air Temperature
Tcomf	Comfort Temperature
EDT	Effective Draft Temperature
HSR	Horizontal Solar Radiation
O/A	Outdoor Air
(O/I)/A	Outdoor and Indoor Air
(O/A) Temp	Outdoor Air Temp
(O/I)/A Temp	Outdoor and Indoor Air Temperature
ft	Feet
in	inch
m	Meter
PD	Percentage of Dissatisfied
PPD	Predicted Percentage of Dissatisfied
PMV	Predictive Mean Vote

1 INTRODUCTION

A typical living environment needs to be a healthy and comfortable space for dwellers, but it requires energy to provide these conditions. The conditioning involves a combined effort of heating/cooling systems and ventilation strategies. However, the performance of the systems varies from system to system. That means the energy performance of these systems would affect the dwelling space condition and overall building energy consumption. In addition, the cost of the energy is getting expensive over time leading a concern to consider energy efficient systems without compromising the thermal comfort and indoor air quality.

The thermal comfort is the state of human body perceiving the surrounding environment regarding temperature (ASHRAE 55, 2013). The state of thermal comfort shows substantial influence on the health and productivity of the dwellers. Consequently, the building industry firmly requires precise thermal comfort requirements, which are the focus of the mechanical design of air conditioning systems. In addition to thermal comfort, buildings also require maintaining acceptable indoor air quality, which deals with providing fresh air and removing polluted air. Moreover, the building code is demanding distributed ventilation design to reach every occupied space, so that acceptable indoor air quality is kept.

The concern of high contaminant particle concentration close to the floor brought the introduction of displacement ventilation and underfloor ventilation strategies. These ventilation strategies have shown higher momentum in comparison to mixed ventilation. Some research indicates that although the momentum is believed to remove the contaminant particulate indeed, there were concerns about the drawing of particles to the breathing zone. In addition, the particle at a lower level may pass through the breathing zone increasing the probability of inhaling the contaminant particles.

A different combination of mechanical systems can deliver the desired thermal comfort level and ventilation requirements. The mechanical systems include space heating/cooling systems and ventilation strategies. One of the most common mechanical systems is forced air system which combines space heating and ventilation altogether. The coupling of ventilation and space heating systems, on the one hand, discharges considerable amount of conditioned air to the exterior to keep acceptable indoor air quality level. On the other hand, this process consumes significant energy. Furthermore, there has been an attempt to separate and treat space heating and ventilation strategies, which potentially reduce the power spent on air conditioning. Thereby various studies have been conducted to investigate this approach and confirm that indeed energy saving is possible by differentiating ventilation and space heating systems. As a result, some independent space heating systems emerge and adopted by the building industry. One of the most known systems is radiant floor heating which covers wider floor area allowing uniform temperature distribution in the occupied space. The radiant floor heating system allows the heating medium recirculation rather than the breathing air which makes it advantageous than that of the forced air system.

Moreover, different independent space heating systems are introduced for heating purpose: heat distribution units (radiator heaters and electric baseboard heaters). These systems are adopted and used; through time, researchers unveil these systems have localized influence than over whole heating, especially for a wider dwelling. Despite this concern, those systems are found useful in avoiding cold from the cool part of the envelope such as windows that is why these systems most of the time install below the window.

As a result, various gaps and research opportunities are identified and addressed in this research. The first research opportunity for this thesis is energy. The building code is changing over time advancing into tighter building construction and energy requirements. This requires more research

into efficient energy systems for future implementation. Moreover, there are limited comparative investigations involving most of the available systems in the market. Those limited research studies either thermal comfort or energy performance separately. Thus, there is a demand for comprehensive whole performance investigation on heating systems, ventilation strategies, and ventilation flow rates.

Consequently, this research study focuses on three parts of air conditioning systems. The systems include four space heating systems (electrical baseboard heater, heat pump, portable radiator heater, and radiant floor heating system), two ventilation strategies (mixed ventilation and underfloor ventilation), and three ventilation flow rates (15 cfm, 7.5 cfm, and 5 cfm). Various performance indicators and indoor environmental element distributions are used to conduct this comparison based on experimental data. The data are gathered by running two systems in full-scale field experimental research facilities called Whole-Building Performance Research laboratory (WBPRL) at the BCIT Building Science Centre of Excellence.

2 LITERATURE REVIEW

The performance of a building can be characterized by different indicators which are collectively referred to the whole building performance. These indicators include energy use, thermal comfort, indoor air quality, and durability. The first three are closely related to indoor conditions, whereas, durability is linked to the structural and physical part of the building. A good understanding of these indicators enables designers and engineers to design and optimize high-performance building. Regardless of the outdoor climatic condition, buildings are expected to offer healthy and comfortable indoor environment while at the same time being energy efficient.

The building energy consumption includes space conditioning. The energy used for space conditioning is for heating/cooling of the living space. The common forms of energy sources are either electricity or fuel. These sources generate the required energy to run the mechanical system, which provides space heating for buildings.

The building envelope has been changed to improve the energy performance of buildings. The effort involves making the building enclosure more thermal resistant as well as airtight. The advancement in improving the envelope performance incorporates employing advanced insulation materials and reducing the thermal bridge in the building structure. Whereas, the air infiltration problem in the envelope can be minimized with an introduction of airtight envelope systems. Therefore, these two measures together boost the performance of buildings.

The building sector consumed a significant amount of energy to create comfortable, clean-living space. For example, Janbakhsh et al., 2014 showed buildings used 30% of the total energy produced globally. Moreover, the Heating ventilation air conditioning (HVAC) systems consumed a considerable amount of energy. These systems covered for 40% of the building's energy

consumption (Aleksander et al., 2015). Therefore, the performance of HVAC systems influenced energy consumption.

Thermal comfort is a state of mind in which human body perceives the surrounding environment. It is a scale of thermal neutrality, which is highly dependent on the thermal status of the body (Oleson et al., 1980). The goal of thermal comfort is not satisfying everyone thermally; instead, it is minimized thermal dissatisfaction as much as possible (Lin et al., 2008). As a result, the thermal comfort concept deals with defining thermally adequate living space for dwellers.

Therefore, a mathematical model formulated to calculate human thermal satisfaction. The analysis had evolved from representing human body as a single node like Fanger et al., 1972 to two eccentric cylinder model by Gagge et al., 1986. The two-node model represents the human body by a core (inner cylinder), which generates heat and carried by blood and transfer to the skin (outer cylinder), which eject heat to the surroundings. Whereas, a single node model considered the human body as a single node and correlate its interaction with the surrounding.

In addition, the thermal comfort calculation could be classified into two types based on the environment either indoor or outdoor. The two common ones are Fanger et al., 1972 for indoor space, and Gagge et al., 1986 which is based on outdoor context. Most researchers implement Fanger model, which have been widely accepted and vastly used both in the experimental investigation and numerical analysis. The Fanger model expressed thermal comfort with a predictive mean vote(PMV) and predictive percentage of dissatisfaction (PPD).

Where,

The predictive percentage of dissatisfaction (PPD), is expressed as follow:

$$\mathrm{PPD} = 100 - 95\exp\left[-(0.03353\mathrm{PMV}^4 + 0.2179\mathrm{PMV}^2)\right] \quad (1)$$

Where PMV is a mean predictive vote, which is dependent on the thermal load (L), and metabolic activity level (M). It is defined as follow:

$$PMV = [0.303exp\,(-0.036M) + 0.028]L \quad (2)$$

The thermal load on the human body (L) determined by calculating heat balance that includes radiative, conductive, convective and evaporative heat transfer.

ASHRAE developed a model (Figure 1) that depict the range of temperature and relative humidity at which thermal comfort could be achieved. Accordingly, the scope of operative temperature for winter and summer season specified in the graph regarding thermal comfort. It was shown that the effective temperature could range from 20°C to 25°C as well as the relative humidity reached 30% - 60% to feel thermal comfort. ASHRAE 55 (2013) also developed seven thermal sensation scales including hot, warm, slightly warm, neutral, slightly cool, cool, and cold to describe thermal perception for subjective evaluation.

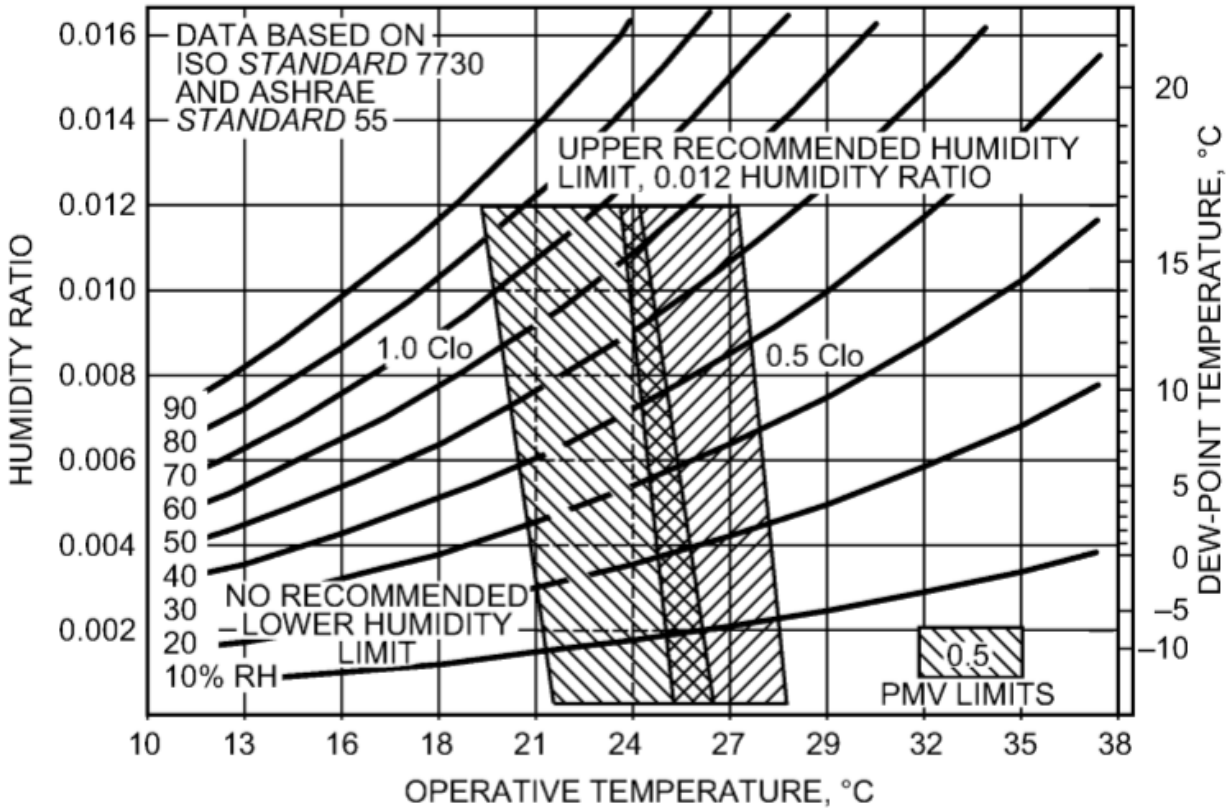

Figure 1: Thermal comfort zone (ASHRAE Fundamentals 2017)

The second model was by Gagge et al. (1986) to determine standard effective temperature (SET) as a thermal comfort indicator of outdoor dwelling environment. Although, the method used in the research involved several assumptions in numerical calculation, it is possible to come up with SET for a location given adequate weather data. Because the outdoor environment required a different variables unlike a conditioned space, the calculation had relatively higher assumed variables.

The physiology of the human body found adapting the surrounding conditions to some level like air temperature, which led to the development of the adaptive thermal comfort model by Richard et al., 2001. In addition, Leen et al., 2008, had indicated that individuals quickly adapt warm condition than cold weather conditions.

ASHRAE has created an adaptive thermal comfort model (Figure 2) accounting human adaptation to their thermal environment using survey data. The model produced a simplified way to describe thermal comfort in a naturally ventilated space with air temperature instead of calculating the complex standard effective temperature (SET). The adaptive model defined correlating the daily mean outdoor air temperature (T_m) in Equation 3 with expected comfort temperature (T_{comf}), or using the graph from ASHRAE 55, 2013 (Figure 2).

$$T_{comf} = 0.33\, T_m + 18.8 \tag{3}$$

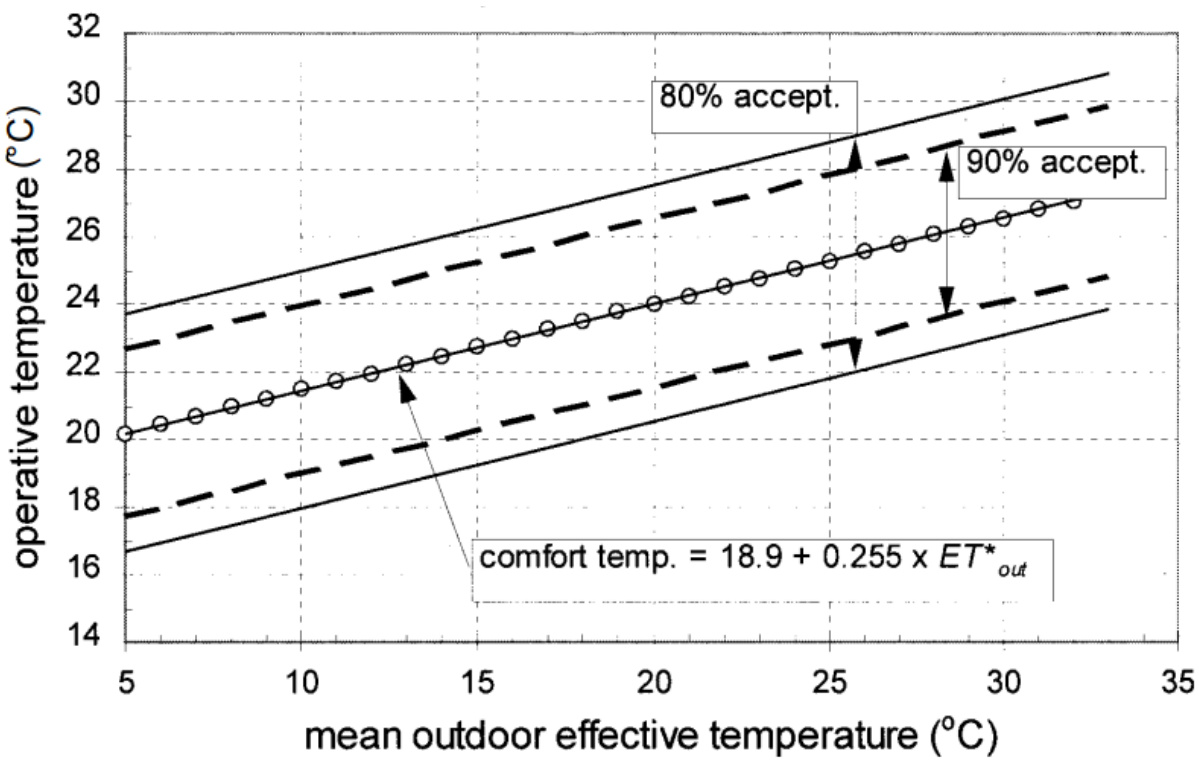

Figure 2: Adaptive thermal comfort model (ASHRAE, RP-884)

The human body not only adapt the surroundings but also affected by a different factor such as the draft. Effective draft temperature (EDT) is another thermal discomfort indicator related to air velocity around neck and ankle. It combines temperature difference between the average room temperature and local temperature with air velocity to describe the corresponding thermal status.

This approach was a conventional method to calculate EDT for cooling mode. After examining the cooling mode, a new model has been developed that can be used for heating mode (Shichao et al., 2015; equation 4).

$$\theta_1{}^* < EDT(\theta^*) = T_i - T_a - 9.1(v_i - 0.15) < \theta_2{}^* \quad (4)$$

Where

Furthermore, the effect of draft on different body parts such as ankle and neck level studied by different researchers. Twenty research works which investigated the impact of the draft on thermal comfort have been reviewed and discussed on Fountain et al., 2012. The review suggested that although it was essential to know the impact of air velocity on human thermal perception due to draft, the local thermal comfort might not reflect the whole body thermal comfort status.

Besides, different standards recommended requirements to maintain acceptable thermal comfort in mechanically air-conditioned space. For a typical residential house, the ISO 7730 standard suggested that the mean air velocity should be less than 0.25 m/s for summer and greater than 0.15 m/s in winter to achieve optimum thermal comfort. Moreover, regarding the vertical air temperature distribution, ISO 7730 also recommend that the vertical temperature difference (head - ankle) should be less than 3K. Whereas, ASHRAE suggested the vertical temperature gradient should be less than $2^{O}C$ to minimize local thermal discomfort as the result of vertical temperature difference.

The introduction of computational fluid dynamics (CFD) helped to understand air movement in a living space. Although it takes much time and memory to solve numerical analysis, the results were more illustrative as it was discussed in Zhai et al., 2005. Moreover, Hakan et al., 2007 used CFD to study human thermal preference in a controlled office environment. The agreement of

CFD simulation and experimental measurement discussed in various detailed research articles on living environments: Shuzo et al., 2000, Zhiqiang et al., 2005, Cataline et al., 2009, Wei-hwa et al., 2012.

In addition to ambient temperature, occupants' thermal comfort can be affected by airflow, radiation, and relative humidity. The airflow, radiation and moisture transfer has been analyzed to study the heat transfer between human body and their surroundings related to thermal comfort using experimental data and CFD tool (Shuzo et al., 2000). The approach was to determine the total heat loss from the human body, which was a combination of sensible and latent heat to attain thermal equilibrium. The result indicated that the human body had a different skin temperature for different body parts. The results also showed that CFD is a useful tool to study the whole-body heat transfer with its' surroundings.

Indoor space conditioning includes ventilation system. The ventilation system is tasked with keeping acceptable contaminant level in the occupied space by diluting as well as discharging the polluted air. There are two approaches to ventilation air supply. One of the methods is called dedicated outdoor ventilation system, which brought 100% outdoor air into the conditioned space. Whereas, the second one involves recirculating some portion of the indoor air and introducing makeup air from outdoors. ASHRAE recommended providing 7.5 cfm air per person into the occupied space to maintain acceptable indoor air quality level.

The indoor space has a variety of gaseous pollutants and particulate matters, which are harmful to a human being in high concentration. These materials include volatile organic compounds commonly known as VOCs, which cause a health concern above a certain level of concentration. Ventilation systems have been used to remove polluted air and replace it with a fresh one, so that acceptable indoor air quality is maintained consistently.

There are different types of ventilation strategies that could maintain acceptable indoor air quality level in a mechanically air-conditioned space. Based on supply and return location of the, ventilation systems are classified into five categories. These are mixed ventilation, underfloor ventilation, displacement ventilation, stratum ventilation and confluent ventilation.

Mixed ventilation strategy: the supply air is provided through the overhead unit. It is, then, distributed throughout the occupied space to create a stable condition by mixing with the existing air. Finally, the exhaust air leaves the space through the overhead unit.

Underfloor ventilation strategy: The Underfloor ventilation strategy provides the supply air through the floor and exhausts the polluted air through either the ceiling or floor (ASHRAE, 2009). The incoming air is supplied into the conditioned space with momentum to reach the breathing level in the occupied space. Then the contaminated air leaves the conditioned space through the exhaust mostly close to the ceiling. It is because if the exhaust is located close to the floor, the incoming air might directly go to the exhaust instead of rising above and diluting the air in a breathing zone.

Displacement ventilation strategy: It is a type of ventilation strategy, in which the air supplied through wall-mounted diffuser close floor (ASHRAE, 2009). Since the supply is at a lower level as it gets heated, it rises and mixes the air. The exhaust then discharged through wall mounted terminal unit opposite to the supply and close to ceiling as described by Zhang et al., 2005, Cho et al., 2002, Fong et al., 2011, and Olesen et al., 2011.

Zhang et al., 2005 studied the effect of air supply and return terminal locations for the performance of displacement ventilation in a typical office building during the cooling season using CFD simulation. Also, energy, thermal comfort, and indoor air quality were the indicator used to evaluate the performance of displacement ventilation strategy. The result indicated that the supply

unit was better to be located at the centre. However, the location of the return had shown the smallest effect on the performance.

Stratum ventilation strategy: this ventilation strategy provides the supply air directly into the breathing zone. As a result, the supply air is only the required amount of air for ventilation purpose, whereas the space heating is handled separately by heating systems. Moreover, since the supply air reaches the breathing zone directly the air needs to be treated or warm enough to minimize thermal discomfort (Lin et al., 2011).

Confluent ventilation strategy: the air is supplied to the occupied space through a supply unit mounted at the top part of the sidewall (Figure 3). This arrangement of ventilation strategy allows supplying air at a higher momentum to mix with the indoor air; then the exhaust air leaves the space on the opposite side of the supply (Cho et al., 2002; Youngjun et al., 2007). The air supplied into space is through circular holes of the supply unit, the air streamlines then start combining after the air leave the supply unit (Youngjun et al., 2008).

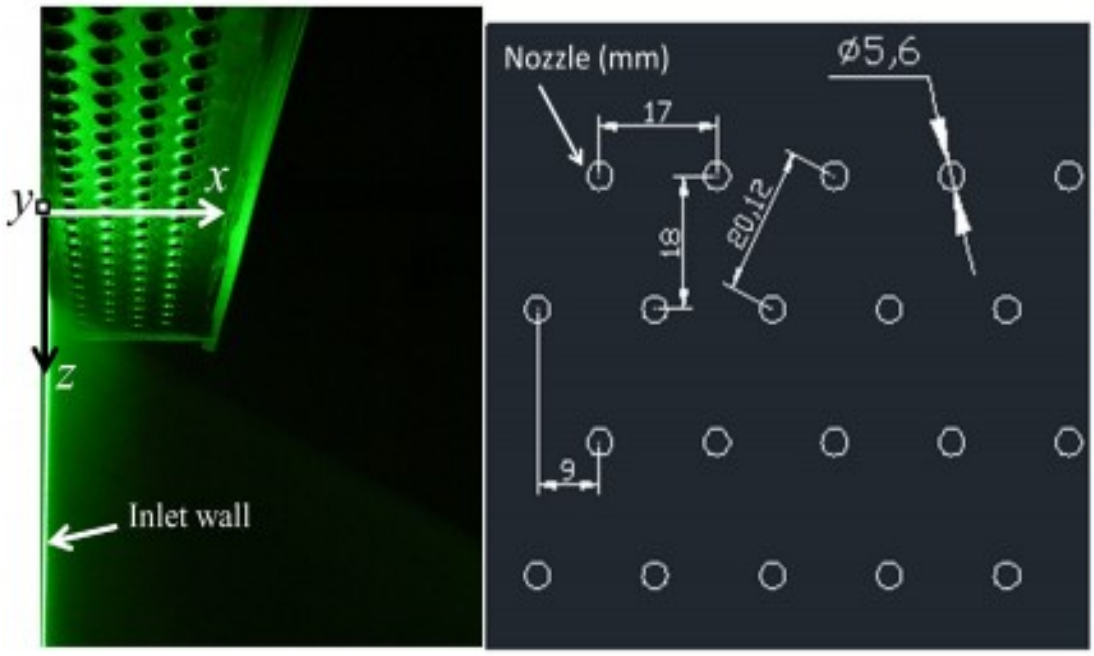

Figure 3: Confluent Jet Ventilation

The contaminant distribution was studied in a classroom with mixed ventilation and displacement ventilation strategies (Sture et al. 2003). As a result, the particle concentration in the classroom found between 50 and 200 μg/m^3, where the concentration rate 100 μg/m^3 represent the highest acceptable limit. Therefore, the result showed that for both ventilation strategies the particle concentration in the breathing zone was higher than the expected amount. Moreover, research indicated a cold surface could draw contaminants to the breathing zone, even with a displacement ventilation strategy (Francesco et al., 2010). This research applied equation 5 to calculate contaminant removal effectiveness (CRE).

$$CRE = \frac{C_{exit} - C_{supply}}{C_P - C_{supply}} \tag{5}$$

Where,

CRE = Contaminant removal effectiveness.

C_{exit} = Contaminant concentration in the exhaust air.

C_{Supply} = Contaminant concentration in the supply air.

C_p = Contaminant concentration at a specific point in the test room.

Young et al., 2008 investigated air distribution vertically and horizontally comparing two ventilation strategies: confluent ventilation strategy and displacement ventilation strategy. It was conducted in a full-scale experimental setup inside climate chamber. The result demonstrated that the confluent ventilation strategy performed better than displacement ventilation strategy providing a similar indoor condition as well as under similar outdoor conditions which were simulated using the climate chamber.

A demand control ventilation system introduced to the building industry with a promise of energy reduction by managing the ventilation flow rate based on occupancy density. The common one was CO2 based demand control ventilation which was examined by David et al., 2004. The result indicated that the risk of compromising indoor air quality was higher than the advantage of demand control ventilation since CO2 is not comprehensive indoor air quality indicator.

Conditioned space is categorized into two groups. The first one was treating ventilation and space heating/cooling together such as forced air heating system. Whereas, the second one was managing space heating/cooling and ventilation separately (Lin et al., 2011, Cho et al., 2002,). Both methods had been studied and compared using performance criteria as well as standards (Krajcik et al., 2012). As a result, separately treating heating/cooling and ventilation found to have a broader energy-saving advantage compared to addressing both together.

The Radiant floor space heating system either hydronic or electric powered was claimed to be an efficient approach to heat the occupied space. When it came to hydronic one, the actual design water temperature depended on economic and comfort considerations for the occupied space. The radiant floor heating system believed to be energy efficient and comfortable space heating system (Xiaozhou, 2016). That was why in the past decades, the system had been extensively adopted by countries such as Germany, Australia, and Denmark owe 30% to 50% of the newly built residential houses were equipped with the radiant floor heating system (Olsen et al., 200).

Nine different space heating systems were studied in a full-scale experimental test room built inside climate chamber (Oleson et al., 1980). A steady-state winter condition was simulated by the cold box on the front wall, and the experiment was based on two-hour data measurement. All systems that is (two electrical radiant floors, one convector, two radiators, one warm ceiling, two forced air heating) delivered acceptable thermal condition with 0.8 ACH infiltration-based

ventilation. The result indicated that the radiator had localized effect rather than heating the whole test space.

Energy-Plus building with two walls entirely window façade was used to investigate the energy performance of different space heating systems. The radiant floor heating and forced air systems were compared based on actual measurement and energy simulation (Jacob et al., 2011). The results indicated that the radiant floor heating demonstrated better energy performance than Forced air system heating depicting 23% energy savings compared to a forced air system.

Zhang et al., 2013 had tested low-temperature radiant floor heating system (LRFH) which used hydronic pipe laying on aluminum foil to improve radiation. Whereas, a conventional radiant floor heating system embedded hydronic pipelines inside concrete. The result revealed the LRFH could provide uniform temperature distribution and acceptable thermal comfort with less energy consumption compared to conventional radiant floor heating system.

Stefan et al. (2008) studied different heat pumps types that could be used for space heating and cooling in extreme weather condition. The test was for both heating and cooling season. The outcome indicated that it was possible to provide space heating even in extremely lower outdoor air temperature reaching -30°C using a heat pump. Moreover, the COP of heat pump reduced when the outdoor temperature falls to the extreme.

The thermal comfort and energy performance of the low-temperature heating system was studied in five newly built houses by Hesaraki et al., 2013. The houses comprised low-temperature hydronic floor heating system on the ground floor and ventilation radiator for upper two floors. Ventilation radiator was a unique design to harvest both radiation and convection. One-year actual energy consumption of these buildings indicated energy saving, as well as the thermal comfort analysis, showed PPD about 12% within the acceptable range (PPD = 15%).

The indoor environment components (air distribution and ventilation effectiveness) were investigated in a room equipped with the ventilation and heating/cooling systems (Olesen et al., 2011). The test was conducted in a climate chamber with radiant floor heating system combined with mixed and displacement ventilation strategies. The result showed that all combinations provide the intended thermal comfort for both heating and cooling mode. However, the outdoor weather condition was only simulated on the front wall by cold panels.

Similarly, the air distribution and ventilation effectiveness were studied in a room where the mixed ventilation is combined with the radiant floor heating system (Krajcik et al., 2012). The test room was inside laboratory hall, and one wall had cold panel simulating winter condition. Both mixed ventilation combined with radiant floor and forced air system had shown acceptable thermal comfort. But, the radiant floor heating coupled with the mixed ventilation had demonstrated uniform air distribution and better ventilation effectiveness. The research used temperature and contaminant removal effectiveness, Equation 3 and 4, respectively, to evaluate the performance of the system.

Temperature effectiveness,

$$\varepsilon_t = \frac{(T_e - T_s)}{(T_i - T_s)} \qquad (6)$$

Where,

ε_t is temperature effectiveness.

T_i is mean air temperature at engaged position.

T_s is mean air temperature of supply air.

T_e is mean air temperature of exhaust air.

Contaminant removal effectiveness

$$\mathrm{CRE} = \frac{(C_e - C_s)}{(C_i - C_s)} \tag{7}$$

Where

C_i is the mean contaminant at a given points in the test building.

$$Q = \frac{q_s}{1.2(T_r - T_s)} \tag{8}$$

Where

Q = required supply airflow rate to meet sensible load, L/s

q_s = net sensible heat gains in the space,

T_r= return or exhaust air temperature, °C

T_s = supply air temperature, °C

T_r = return air temperature, °C

The underfloor ventilation strategy was examined experimentally and with CFD simulation (Wan et al., 2005). The air distribution and temperature characteristics were evaluated to study the performance of the ventilation strategy. The result indicated that the thermal stratification was highly dependent on thermal length scale.

Tomasi et al., 2013 investigated the performance of mixed ventilation strategy by varying the position of supply and exhaust units. The test was conducted inside a climate chamber with private room arrangement having a low flow rate mixed ventilation and radiant floor. The thermal comfort, ventilation effectiveness, and contaminant removal were studied. The results were in line with the subjective investigation in a similar setup by Michal et al., 2013. As a result, in both cases, the

temperature distribution found uniform when radiant floor combined with mixed ventilation strategy.

On the other hand, experimental study and two-dimensional CFD simulation comparing underfloor and mixed ventilation strategies were carried out in the compartment office. The air distribution and thermal comfort were studied by varying the position of supply units for underfloor ventilation (Son et al., 2011). The results indicated that underfloor ventilation depicts better air distribution and energy saving than mixed ventilation systems at the breathing zone given a similar condition.

Fong et al. (2011) evaluated the energy performance of mixed ventilation, stratum ventilation, and displacement ventilation strategies of a room in the middle of the building. The result indicated that stratum ventilation system saved around 12% and 9% energy than mixed and displacement ventilation strategies respectively. Full-scale experimental and numerical analysis study of Francesco et al. (2010) suggested that a combination of radiant floor heating and displacement ventilation systems give ventilation effectiveness close to 1 (efficient).

Chanjuan et al., 2013 studied the energy performance of mixed ventilation with a local setpoint temperature different from the rest of the room. The analysis indicated it was possible to create an acceptable condition by providing tempered air targeting the chest and back level of individuals minimizing energy consumption in cooling mode.

Xiaozhou et al. (2013) showed a linear vertical temperature distribution for a room equipped with radiant floor heating and displacement ventilation. Unlike other research work, the numerical simulation result indicated that the vertical temperature distribution was within 80% (equation 10). However, most of the literature claims the temperature distribution was under 50%, for example, Olesen et al., 2011. In addition, Xiaozhou et al., 2013 used numerical analysis to demonstrate radiant floor heating system would create uniform thermal distribution.

The displacement ventilation was studied in a climate chamber using experiment and numerical analysis (Olesen et al., 2010). Also carried out a further study comparing mixed ventilation and displacement ventilation combined with space heating and cooling systems, in the same test room in which the window is simulated with the cold panel. The result demonstrated that displacement ventilation combined with floor heating showed a smaller vertical temperature difference and higher ventilation effectiveness. A similar effect was found by Michal et al., 2013 in which a subjective study was conducted in a similar scenario.

The confluent jet ventilation strategy was examined in contrast with mixed and displacement ventilation strategy by Cho et al., 2002. The full-scale experimental study revealed that mixed ventilation strategy was better regarding thermal comfort. However, the confluent ventilation showed better air distribution compared to the other two ventilation strategies. The introduction of Indoor air quality number (equation 9) that incorporating contaminant removal effectiveness and percentage of dissatisfaction based on ventilation flow rate gave a new perspective to evaluate ventilation strategies.

- Air quality number respectively could be determined as follows,

$$IAQN = \frac{\varepsilon_C}{PD} \tag{9}$$

Where,

N_c =

- The effectiveness of heat removal and contaminant respectively could be determined.

$$\varepsilon_t = \frac{T_o - T_i}{T_m - T_i} \tag{10}$$

$$\varepsilon_c = \frac{c_o - c_i}{c_m - c_i} \tag{11}$$

The research involving both numerical and experimental investigation was conducted to study confluent ventilation strategy (Janbakhsh et al., 2014). The result showed similar air movement and temperature distribution characteristics for both isothermal and non-isothermal conditions. In addition to air movement characteristics, the temperature distribution was also similar. The founder's of this article was in line with the previous study such as Cho et al., 2002.

Zhang et al., 2011 studied the airflow distribution of stratum ventilation system in a room built inside a full-scale climate chamber. The approach incorporated CFD simulation combined with the experimental measurement. The result indicated that the thermal comfort, air velocity, and contaminant concentration were within the acceptable state.

In addition, the airflow characteristics of stratum ventilation were studied in a classroom arrangement. The research outcome showed the supply temperature of Stratum ventilation should be 23°C since it was directed to the breathing zone (Cheng et al., 2015). The same scholars conducted an experimental study involving stratum ventilation by 2016. The focus was studying the interaction between a human body with room airflow and its impact on thermal comfort. The result indicated that although there were critics concerning about blocking of air at the back of the first row, the flow can overcome the blockade and reach the back row.

Moreover, the stratum ventilation was studied in a classroom compared with mixed and displacement ventilation strategies (Fong et al., 2011). The research aimed to determine the highest temperature limit without compromising thermal comfort. The study also involved 48 individuals in the subjective thermal comfort analysis of the cooling season. The result indicated that the stratum ventilation system was able to maintain thermal comfort by supplying 2.5^{o}C and 2°C above mixed ventilation and displacement ventilation, respectively.

The partial control system was studied in comparison with two points control system concerning energy saving possibility (Manohar et al., 2004). The results illustrated that the Partial control system showed precise set point temperature achievement than two position monitoring system, but the energy saving expected were not found from the energy simulation analysis. In addition, the real-time optimizing technique was investigated for energy saving in buildings by Attajariyakul et al., 2004. In which the control system was based on the average of actual performance and the designed set point condition. The research outcomes indicated that the control system with real-time optimizing had energy saving.

Moreover, some research work also experimented unique systems to see any energy-saving advantage. On the one hand, the passive solar space heating system was studied in full-scale experimental buildings by Ferna et al., 2006. The test considered five passive solar heating methods including sunspace and direct gain; the result showed that considerable temperature fluctuation which could cause radiant asymmetry discomfort. On the other hand, Dorer et al., 1998 conducted a full-scale experiment by embedding the supply duct through the ground. The result demonstrated that this system could improve energy saving in a particular environment.

There had also been researching that tested new innovative ideas. One of the attempts was to couple the ventilation duct with the ground and to provide ventilation into the house (Viktor et al., 1998). The significant aspect of the ventilation systems like energy consumption, air quality, ventilation efficiency, thermal comfort, and acoustical performance was investigated and found acceptable.

The other innovative test involved wall confluent ventilation strategy. In which the air was supplied directly to the corner with high momentum (Figure 4) so that the air bounce back and reach the occupied space. Different scenarios were tested by varying the supply flow rate and the

number of corners. The CFD simulation and measured result indicated that this confluent wall ventilation provides better performance than displacement ventilation. Moreover, the ventilation system also provided clean air than mixed ventilation (Karimipanah et al., 2007).

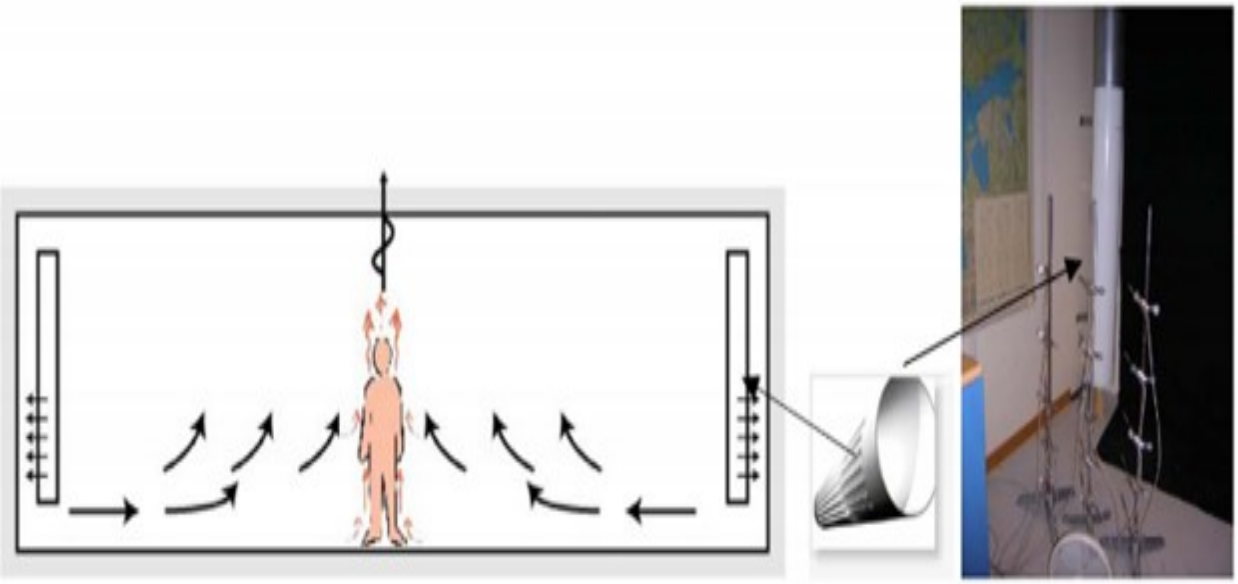

Figure 4: Wall confluent Jet ventilation.

3 PROBLEM STATEMENT

Buildings use different mechanical systems to create a comfortable living environment for occupants. The mode of heat transfer of the heating systems could be convective, radiative or combination of both. The thermal energy required to maintain the same indoor temperature using different heating systems with different mode of heat transfer could be different. In addition to thermal energy, the thermal comfort of the living space could be different. Thus, there was a need to investigate the impacts of different heating systems on the thermal energy use and thermal comfort of buildings operating in a field under the same outdoor boundary conditions (field exposure).

Extensive measurement of radiant floor heating and ventilation systems had been done, but not for other systems such as electrical baseboard heater, portable radiator heater and heat pump. Moreover, most of the research work presented in the literature were at steady state or quasi-steady states conditions in a climate chamber with isothermal surfaces and constant temperature difference across the surfaces. Although the information generated was quite useful, it needs to be extended to building operations in a field as the actual environment is much more dynamic, and complex involving solar, wind wash, longwave radiation, rain, and snow, and the different surfaces could experience different loads at a given time.

In the current building code, residential buildings not only are required to meet the code minimum ventilation rate, but also the fresh supply air needs to be distributed throughout the rooms. In a distributed ventilation air supply design, where the ventilation air requirement of each room in a building separately defined and delivered, the air that passes the diffuser could have a low trajectory velocity, which can limit its effectiveness in diluting the room air. In addition to ventilation rate, the ventilation system design, for example, the supply of the fresh air at the ceiling

level or under the floor may have an impact on the ventilation effectiveness of the distributed ventilation systems. In buildings, with the radiant floor heating system, portable radiator heater, electric baseboard heater, and split-head heat pump, fresh air is provided to the indoor space through a dedicated ventilation system. Usually, the two systems are designed separately. However, it is essential to understand the interrelationships between the different heating and ventilation systems and identify the best combinations that can reduce building energy use, increase occupants thermal comfort and ventilation effectiveness.

CFD can play a role in parametric sensitivity study and optimization of heating and ventilation systems. Unfortunately, a very limited data are available for benchmarking of CFD models with different combinations of systems and outdoor climatic conditions. There is a need to generate high-resolution data for validations and extend the application of CFD in building design to advance the existing building technology into more energy efficient technology.

4 RESEARCH FRAMEWORK

The main purpose of the mechanical systems is providing a comfortable living environment for occupants. As a result, the goal of this research is to compare the different mechanical systems (heating systems and ventilation strategies) employed in full-scale experimental test buildings. Therefore, by using energy performance, thermal comfort, and ventilation effectiveness as the indicator of the overall building performance, this study compares those mechanical systems and present the results.

4.1 Objective

The primary objective of this research is to study and compare the performance of space heating systems as well as ventilation strategies for residential buildings. The comparison involves evaluating the energy performance, thermal comfort, and ventilation effectiveness of four heating systems, two ventilation strategies, and two ventilation flow rates.

The specific objectives include,

- Evaluating thermal energy performance and thermal comfort of four heating systems with different heat transfer mode in a side-by-side field experiment.
- Determining the ventilation effectiveness of distributed ventilation system design.
- Evaluating the impacts of ventilation systems design, more specifically mixed and underfloor ventilation strategies as well as on the ventilation effectiveness of low-flow rate ventilation design.
- Examining the interrelationship of heating systems and ventilation strategies regarding energy consumption, thermal comfort, and ventilation effectiveness.

- Generating experimental data on building performances with different combinations of heating systems and ventilation strategies for future validation of CFD models.

4.2 Scope

The scope of this study includes four space heating system and two ventilation strategies in heating mode. The heating systems are a radiant floor heating system (RFHS), heat pump (HP), electrical baseboard heater (EBH), and portable radiator heater (PRH). In addition, the two ventilation strategies are mixed ventilation (MV) and underfloor ventilation (UV). Whereas, the ventilation flow rate cover in this study is 15 cfm, 7.5 cfm, and 5 cfm. However, no mechanical system efficiency is part of this project instead this study focused on thermal energy.

4.3 Methodology

Field experimental research methodology is followed in this study to investigate the performance of mechanical systems in test buildings, simulating a study room or small office building. Two different systems run side-by-side to provide a similar indoor environment in full-scale test buildings which are under similar climatic condition. Subsequently, the performance of the systems is compared using different performance indicators such as thermal energy, thermal comfort (general and local), and indoor environmental elements (temperature, relative humidity, air velocity, and CO2) distribution.

Consequently, by using this method three parts of indoor air conditioning systems such as heating systems, ventilation strategies, and ventilation flow rates are studied in this project. The space heating systems are RFHS, HP, EBH, and PRH, which represents the surface heat source, forced air heating system, line heat source, and a unit heat source respectively. These systems are already in place prior to the test. The ventilation strategies available in the test buildings are the two most common arrangements: ceiling mounted mixed ventilation and underfloor ventilation strategy.

Whereas, the ventilation flow rates are 15 cfm, 7.5 cfm, and 5cfm. Moreover, the measurement pattern and set up were identical, and all aspects of the buildings are carefully monitored to make sure similar test condition.

Thus, Figure 5 presents the task taken to carry out this study. The first task is converting the experimental design and preparing test buildings for the experiments. The work includes preparing system both heating as well as ventilation systems. The following task is sensor commissioning which deals with sensor preparation such as sensor calibration and sensor installation. Running experiments and data collection is the next task while monitoring the experiments is also another duty that covers all the measurement period. The following task deals with filtering and clearing the data collected by going through it, explicitly selecting a period to represent the experiment. Based on the data obtained the next task is analyzing for different indicators. The final task is discussing results which are explaining the observed behaviours and trends.

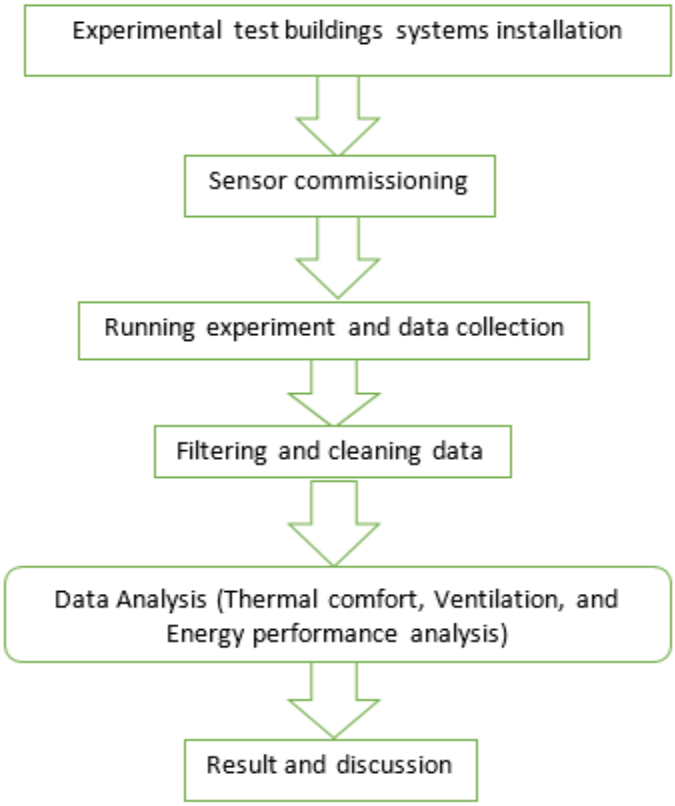

Figure 5: Research approach flow Chart.

5 EXPERIMENTAL SETUP

5.1 Overview of the test buildings

5.1.1 General Description

This study is conducted using two identical full-scale test buildings. They are located at BCIT, Burnaby campus, (Latitude: 49.24^{O}N, Longitude: 123.00^{O}W), British Colombia, Canada. The climatic zone of this location categorizes in a mild climate category with warmer summer and cold winter. In addition, both buildings have test room and mechanical room separated by an insulated wall. The test buildings have a similar floor area, orientation, and dimension. Moreover, every component of the buildings is constructed identically as discussed by Pedram et., al 2014, and Nghana et al., 2016.

A) STB B) NTB

Figure 6: Whole Building Performance Research Laboratory (WBPRL)

Figure 6 shows the test buildings which are used for this research. The overall dimension of these buildings is 16 ft x 12 ft floor area and 10 ft height. Whereas, they are constructed using 2 ft x 6 ft wood frame standard wall with R 20 fibreglass bat insulation between stud cavities. These buildings have a hollow structural section (HSS) steel superstructure with an insulated slab as shown in Figure 7, on top of the grade foundation as well as insulated engineered truss roof construction with R 40 insulation. Besides, both test buildings have air tight envelope with 0.43 cm2 /m2 and 0.49 cm2 /m2 air leakage area for NTB and STB respectively as discussed by Tariku et al., 2013. The buildings also have two double glazed air filled windows on the northern and southern walls of the buildings. Moreover, they have independent test rooms and mechanical rooms which are isolated by an insulated wall. In addition, the test buildings have two doors in the

mechanical rooms: one gives access to the test room from the mechanical room, the other provide exit.

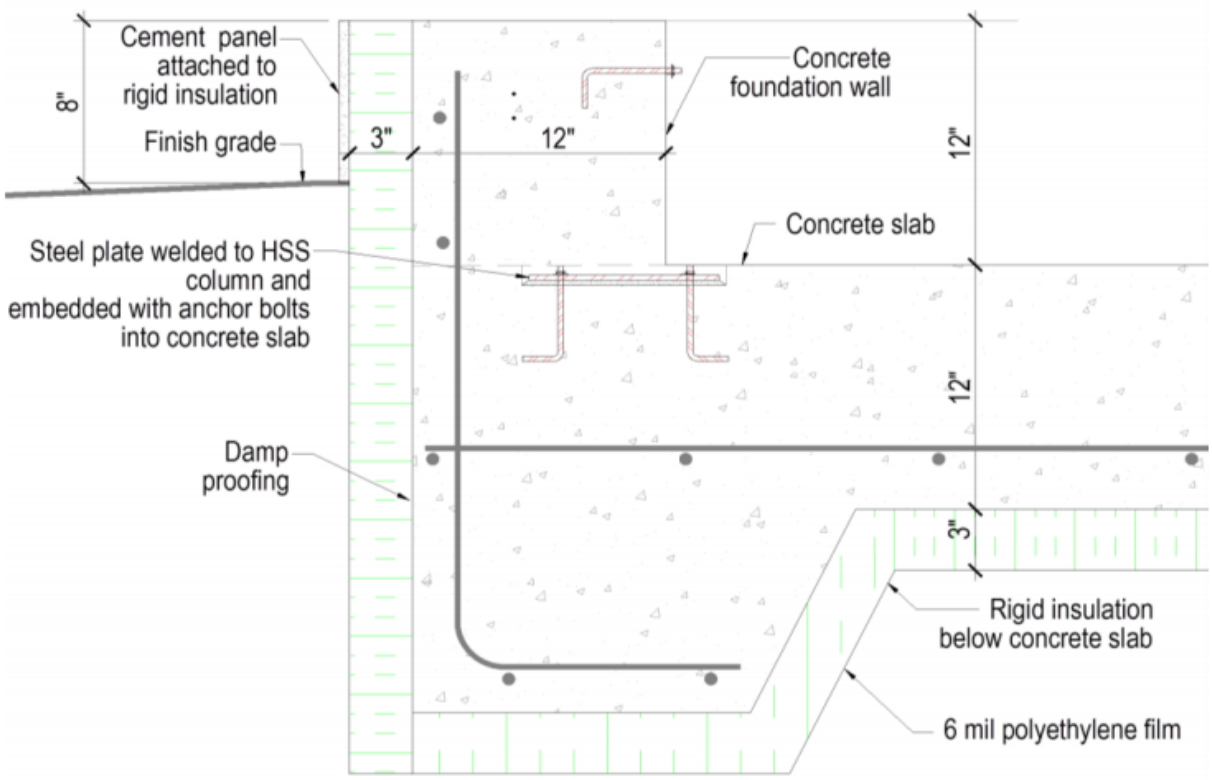

Figure 7: Section view of a foundation.

Since both buildings are identical, one of the buildings can be used as a control or both could be engaged in comparative research. Each building has independent mechanical systems to provide heating, cooling, ventilation, humidification, and dehumidification. Furthermore, these test buildings help to investigate various building systems, which includes selecting design parameters that could reduce the energy consumption while maintaining the indoor environment at the optimum level for occupant comfort, health, and sustainability of the building.

Both test buildings have mechanical systems (heating systems and ventilation strategies) before this study. The systems include mixed ventilation, radiant floor, heat pump, and portable radiator heater. Underfloor ventilation units and electric baseboard heater, then install once the experiment

starts running. Those systems are needed because the test combines ventilation and space heating system operating together to provide fresh air for breathing and thermal comfort for the occupants of these test buildings.

The mechanical room accommodates different systems as shown in Figure 8, which condition the supply air; then deliver the conditioned air from the mechanical room to the test space. Therefore, for this purpose, the mechanical room houses most of the systems (bath, Chiller, blower, and data acquisition systems). The air conditioning unit, which treats the incoming air is also part of the mechanical room; it is insulated to reduce the influence of mechanical room conditions such as temperature on the supply air. The mechanical room also has an independent air condition unit to maintain similar condition like the test room to minimize its impact. Overall, having independent adjacent mechanical room creates an opportunity to control and make changes without affecting the experiments.

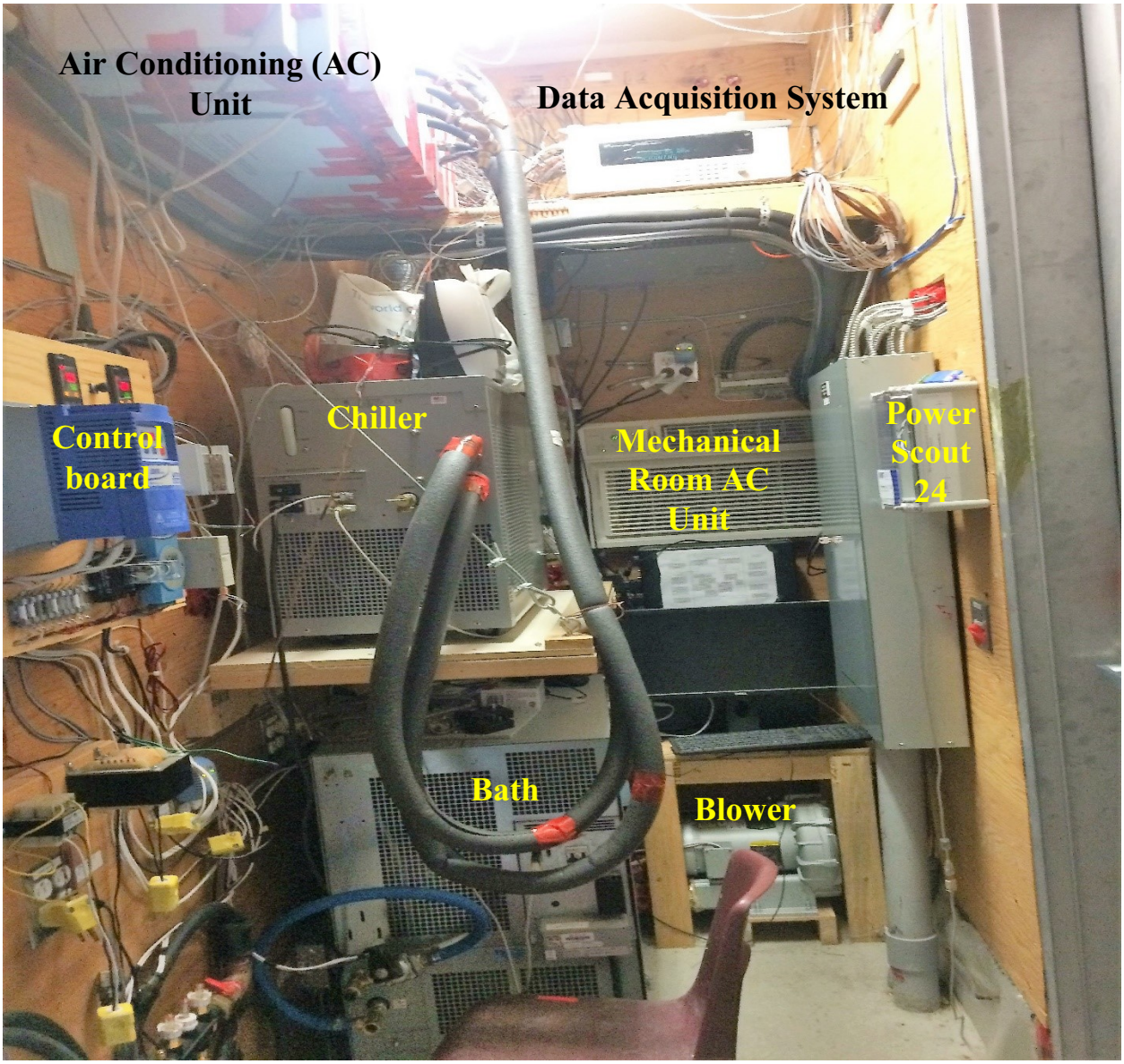

Figure 8: Mechanical Room

In addition, both of these test buildings are equipped with green roof except for the portion of the mechanical room. These green roof samples are running experimental measurement. The southern test roof holds four test samples without the plant. Two of the experimental samples are different; one fully covers and the other open and empty. The remaining two samples are filled with soil. Whereas on the north building all four samples have green plants and like the south one the surrounding of the samples is filled with soil.

5.1.2 Systems Descriptions

The overall system set up have separate heating and ventilation systems running simultaneously to create comfortable living space. For instance, the ventilation system involves variable speed blower, air-conditioning (AC) unit, flow rate control, a supply terminal (MV or UV), exhaust, flow control and control actuator as shown in Figure 8. The control actuator helps to set the proportion air, which is supplied to the test room. Therefore, it's possible to use either 100% outdoor air or a mix of external air and return air.

Flow control | AC unit & Chiller | Control | Control actuator

Figure 9: Ventilation system components.

In this study, 100% outdoor air is used for ventilation. As a result, the blower draws fresh air from outdoors based on the set point flow rate (15 cfm, 7.5 cfm, or 5 cfm) as shown in Figure 10. The air conditioning unit then heats the incoming air to 18°C. It is done by using a chiller in heating mode. Moreover, two temperature probes measure the air temperature before the air touch the heating coil and after it leaves the coil in the air conditioning unit. The temperature probes are used to set the chiller water temperature that goes to the air conditioning unit to heat the incoming air. Subsequently, the flow rate control measures how much air is supplied into the test room either from ceiling mounted mixed ventilation terminal (MV) or underfloor ventilation strategy terminals as shown in Figure 11.

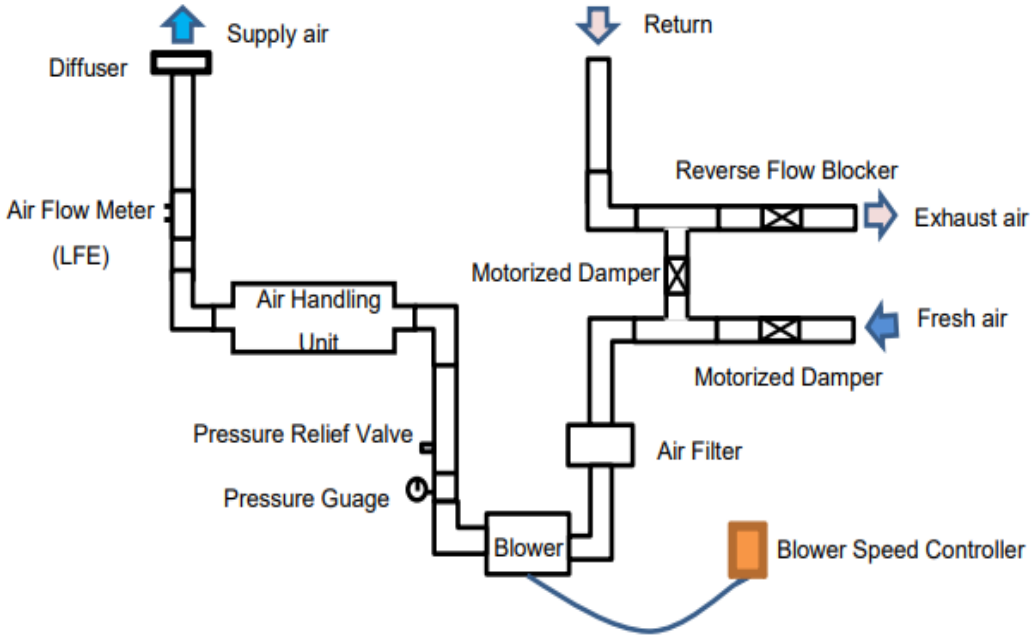

Figure 10: Ventilation system schematic diagram.

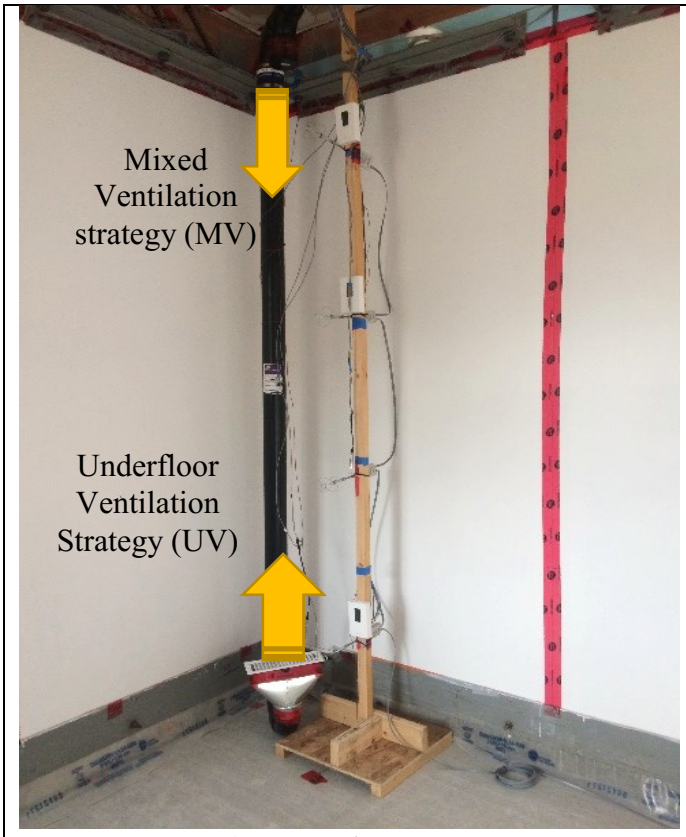

A) UV and MV Strategy

B) Exhaust

Figure 11: Ventilation strategies.

The heating system is the second component of the test buildings, mainly responsible for providing heat to the test space. Four common types of heating systems are selected for this test. Besides, all the heating systems in the test building use a similar source of power, which is electric power. The systems are RFHS, HP, EBH, and PRH: Furthermore, their corresponding capacity was 3.9 kW, 2.3 kW, 1.5 kW, and 1 kW respectively. The following section discusses each one.

The radiant floor heating system uses the bath to heat the recirculating water. The bath and the accessories that are used for radiant floor heating system are shown in Figure 12. The numbers 1, 2 and 3 in Figure 12 represent three solenoid valves on the corresponding supply tube (5), return tube (6) and recirculation loop (4) respectively. The bath heats the water, then circulate through the loops in the floor and come back to the bath reservoir. The three-solenoid valves help to avoid overheating the test room by recirculating the hot water in the mechanical room once the room setpoint temperature attains. The recirculation is possible by closing the supply as well as return solenoid valve and opening the solenoid valve in the recirculating loop. Whereas, once the room temperature gets below the set point, the opposite process happens, and the water starts to recirculate in the floor again.

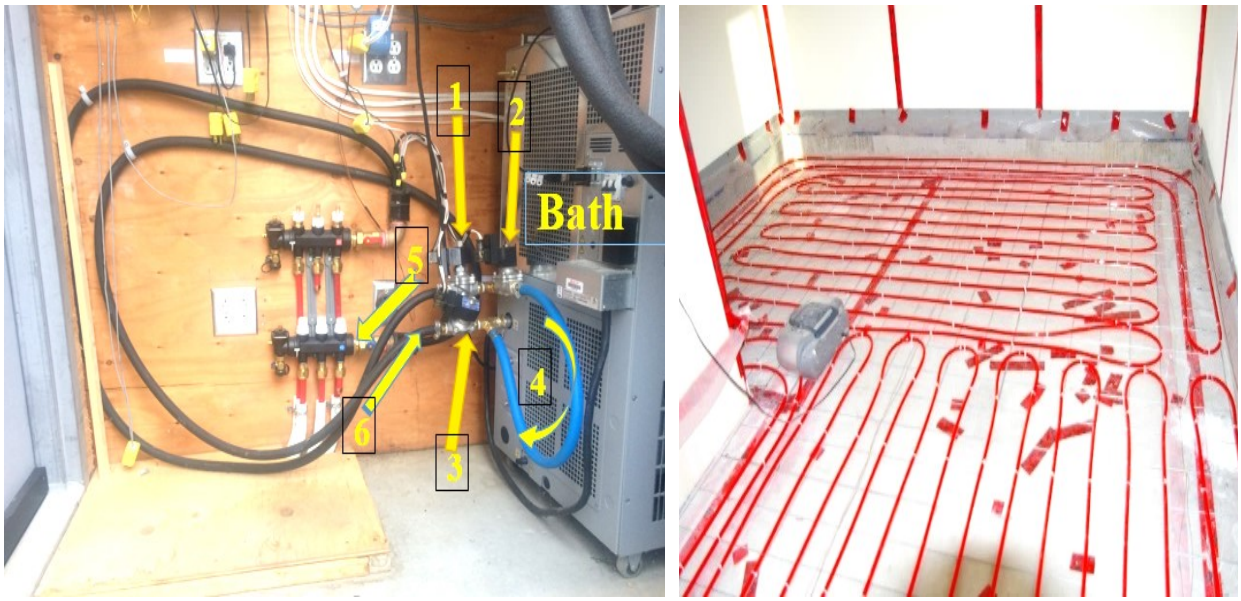

Figure 12: Bath and accessories for RFHS.

Whereas, both electrical baseboard heater and Portable radiator heater are placed immediately below the south window as shown in Figure 13. The EBH (A) has an external control (B), which is placed close to the centre to operate according to the test room temperature profile because L3P3 represent the test room. Whereas the PRH (C) has the control inside itself that control the unit temperature as well as room temperature. Since the unit has the internal control that monitors its temperature, as a result, the unit will not overheat itself (T > 24°C) and cause a fire. The fact that the thermostat is inside the unit causes the control to be affected by its heat. The thermostat is taken out for an additional testing experiment which demonstrates the same behaviour, therefore, this approach abandons. Moreover, the heat pump (HP) indoor unit installed on the wall adjacent to the mechanical room. The HP has an indoor unit (D) consist of the condenser tubes, fan, and louvre, which temper as well as recirculate air in the test room. The temperature entering and leaving the unit is recorded with two thermocouples. The remote-control (E) for the HP gave access to set the control.

A) EBH heating unit B) Control

C) PRH heating unit

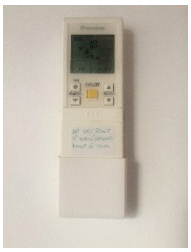

D) HP indoor unit E) Control

Figure 13 Space heating systems.

5.1.3 Occupant Simulators

The test buildings are equipped with occupant simulator that simulates a single person from 10 PM to 6 AM assuming a night time where most individuals stay in the dwelling room. Two of the common elements that every individual produce (CO2 and RH) are simulated in this project. Consequently, extra CO2 and moisture are supplied into the test rooms for 8 hours to simulate occupant. For this reason, these two systems (Humidifier and CO2 system) are prepared, tested, and installed in the test buildings as shown Figure 14. Moreover, these systems are installed at the corner of the test room to minimize the impact of the setup on the indoor environment.

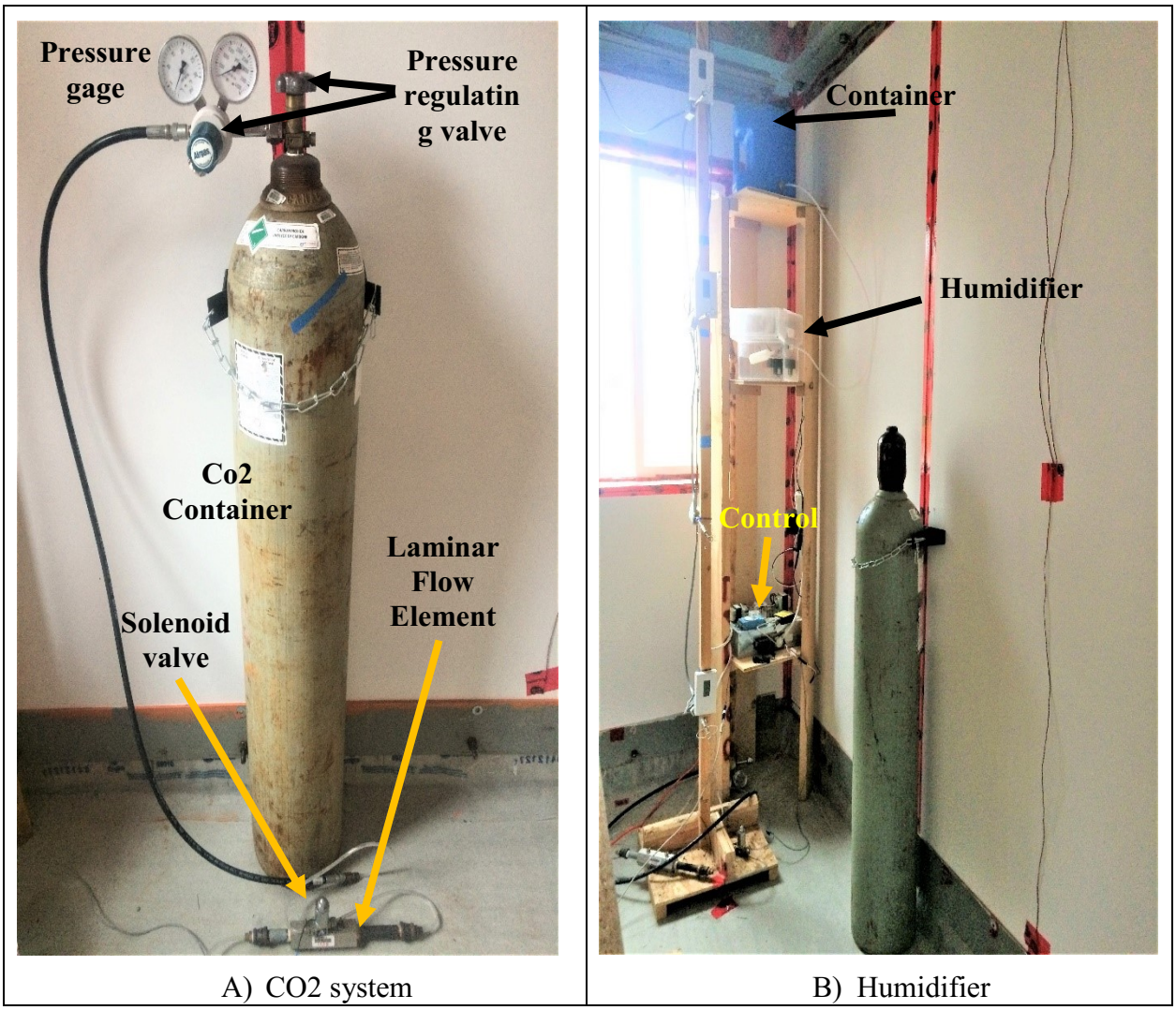

A) CO2 system B) Humidifier

Figure 14: Occupant simulator.

These systems have different components and accessories to carry out the desired task. The CO2 system has a container and accessories which are prepared to deliver consistent CO2 supply (0.25 litre per minute) to the test room as shown in Figure 15. The pressure regulating valve and solenoid valve control the CO2 supply; besides, the pressure gauges indicate the remaining CO2 in the container. Moreover, the laminar flow element measures the actual CO2 supply using the pressure difference across the component. On the other hand, moisture produced by a single individual is simulated using a humidifier which operates from 10:00 PM to 6:00 AM like the CO2 system. Furthermore, assuming that average person exhales 100 grams per hour overnight the same amount

is supplied in the test room as depicted in Figure 15. It is possible to do that by using a water container, a control and humidifier working together.

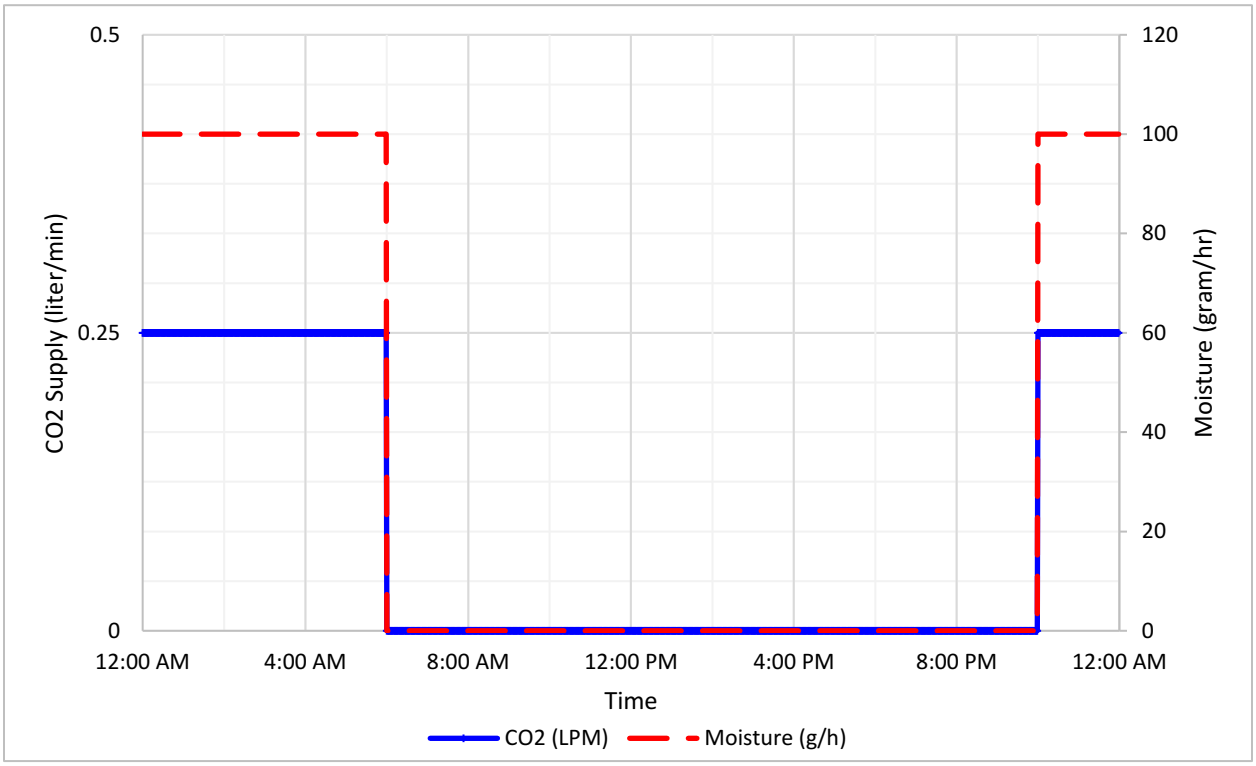

Figure 15: CO2 and RH supply by the human simulator.

5.2 Experimental Design

The experimental design is to run two different systems simultaneously and compare the outcome. For example, the first six pairs of experiments, two heating systems with similar ventilation strategy run to provide similar indoor temperature. Since the two test buildings are identical and the measurement is conducted in the same climatic condition, the thermal energy supply and the indoor environment produced by the heating systems can be compared. Overall, six pairs of experiments are needed to compare four heating systems as shown in Table 1.

Table 1: List of Experiments

Groups	Experiments	Systems				Ventilation flow rate (cfm)	
		Heating		Ventilation			
		NTB	STB	NTB	STB	NTB	STB

<table>
<tr><td rowspan="6">Heating System Comparison</td><td>1th</td><td>EBH</td><td>HP</td><td colspan="2" rowspan="6">UV</td><td colspan="2" rowspan="9">15cfm</td></tr>
<tr><td>2th</td><td>PRH</td><td>EBH</td></tr>
<tr><td>3th</td><td>PRH</td><td>HP</td></tr>
<tr><td>4th</td><td>RFHS</td><td>HP</td></tr>
<tr><td>5th</td><td>RFHS</td><td>EBH</td></tr>
<tr><td>6th</td><td>RFHS</td><td>PRH</td></tr>
<tr><td rowspan="3">Ventilation strategy comparison</td><td>7th</td><td colspan="2">EBH</td><td rowspan="3">MV</td><td rowspan="3">UV</td></tr>
<tr><td>8th</td><td colspan="2">HP</td></tr>
<tr><td>9th</td><td colspan="2">RFHS</td></tr>
<tr><td rowspan="9">Ventilation flow rate comparison</td><td>10th</td><td colspan="2">RFHS</td><td colspan="2">MV</td><td rowspan="6">15</td><td rowspan="6">7.5</td></tr>
<tr><td>11th</td><td colspan="2">RFHS</td><td colspan="2">UV</td></tr>
<tr><td>12th</td><td colspan="2">EBH</td><td colspan="2">UV</td></tr>
<tr><td>13th</td><td colspan="2">EBH</td><td colspan="2">MV</td></tr>
<tr><td>14th</td><td colspan="2">HP</td><td colspan="2">MV</td></tr>
<tr><td>15st</td><td colspan="2">HP</td><td colspan="2">UV</td></tr>
<tr><td>16nd</td><td colspan="2">HP</td><td colspan="2">UV</td><td rowspan="4">7.5</td><td rowspan="4">5</td></tr>
<tr><td>17rd</td><td colspan="2">HP</td><td colspan="2">MV</td></tr>
<tr><td>18th</td><td colspan="2">EBH</td><td colspan="2">UV</td></tr>
<tr><td>19th</td><td colspan="2">EBH</td><td colspan="2">MV</td></tr>
</table>

A similar method is adapted to compare two ventilation strategies: mixed ventilation (MV) and underfloor ventilation (UV). The 7th, 8th, and 9th pair of experiments compare the performance of these ventilation strategies as shown in Table 1. The experimental design is to use north test building (NTB) with MV and south test building (STB) with UV in all three cases while running the same heating system in both test buildings for each experiment. The corresponding heating systems are EBH, HP, and RFHS respectively. Since the heating system in both test buildings is similar and the only difference is the ventilation strategy, the performance of the ventilation strategies is possible for comparison.

The last experimental design in this study compares low ventilation flow rates. The low ventilation flow rates contrast in this study are 15 cfm, 7.5 cfm, and 5 cfm. The last ten pair of experiments focuses on carrying out these comparisons. The design is to run both test buildings with the same heating system as well as ventilation strategy while providing different ventilation flow rate for each one. For instance, during 12th Experiment, the NTB is at 15 cfm and STB is at 7.5 cfm: In this experiment, both test buildings are running EBH with UV. For the following experiment (13th)

it is only switching the ventilation strategy from UV to MV. Therefore, by doing so, it is possible to compare the impact of ventilation flow rates on the indoor environment.

The experimental design also involves conducting measurement throughout the test room, both vertically and horizontally. The measurement variables are temperature, RH, air velocity, and CO2 concentration. The temperature measurement points range from the floor vertically at different level up to the ceiling as well as on wall surfaces and windows. The air velocity and Co2 distributions within the indoor space are determined using 16 point measurements in each building as discussed in the following section. Overall, a comprehensive experimental measurement design is used to conduct these experiments.

5.2.1 Sensors and Sensor Layouts

Sensors are distributed throughout the test room based on the criticalness of the location. For instance, sensors are installed close to windows which represent the weakest section of the envelope thermally. They are also located close to both supply and return terminals which are part of the boundary conditions. Moreover, as a representative to the test room, sensors are located at the geometrical centre. Besides, sensors are placed all over the surface enclosing the conditioned space including floor and ceiling. Additional sensors are also placed on the exterior to collect data from the outdoor environment. Overall, more than 170 sensors are used to gather data in both test buildings as shown in Table 2.

Table 2 Type of sensor and estimated number of sensors

		Number of sensors			Wiring length (ft)		
Sensor types	Measurement	STB	NTB	Total	STB	NTB	Total
Thermocouple	Temperature	38	38	76	705.25	705.25	1410.5
RHT	Relative humidity	18	18	36	258	258	516
Air Velocity	Air velocity	16	16	32	163	163	326
CO_2 sensor	CO_2 sensor	12	12	24	80	80	160
Glob Thermometer	Mean radiant temperature	1	1	2	15	15	30
Total		85	85	170	1269.25	1269.25	2538.5

The test rooms are equipped with sensors measuring air temperature, air velocity, globe temperature, relative humidity, and CO2 concentration throughout the test rooms. Therefore, the corresponding sensors such as thermocouples, anemometers, globe thermometer, RH chips and CO2 sensors are used to collect data (Table 2). These sensors are collected five-minute average data and stored it in database system, which then can be accessed from a remote location.

The sensor location initially designed is revised halfway through the test based on observation of the first six experiments. In the first sensor layout, five locations are selected to position vertical stands: two in front of windows, two in the proximity of supply and return terminals, and one at the centre as shown in Figure 16 A. Moreover, five vertical positions are chosen to install the

sensors. Starting on the floor surface, 1 ft above the floor, 5 ft above the floor, 1 ft below the ceiling, and on the ceiling as shown in Figure 16 B. Besides, similar positions are selected to place wall surface temperature at the middle section of the wall at three vertical positions (one foot above the floor, mid-height, one foot below the ceiling). At the corners, thermocouples are positioned at mid-height and on both windows surface midpoint.

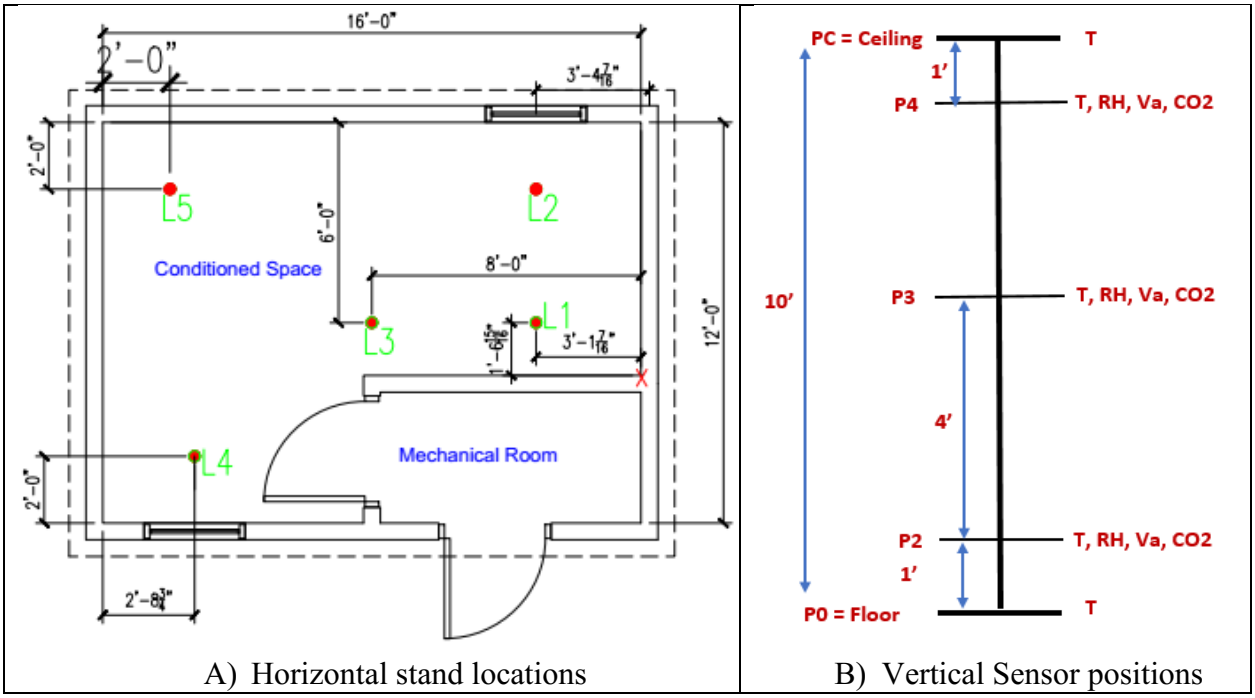

A) Horizontal stand locations B) Vertical Sensor positions

Figure 16: Sensor layout, Horizontal and vertical.

The temperature measurement is conducted at various levels ranging from floor to ceiling. The temperature data collection is undertaken using thermocouples, anemometers as well as globe thermometer. At four locations (L1, L2, L4, L5) and five vertical positions (P0, P2, P3, P4, PC), the air temperature is measured with thermocouples as shown in Figure 17. However, at the centre, thermocouples are only used to carry out temperature measurement on the floor and ceiling. Except for those surfaces (floor and ceiling), at the centre, the air temperature is recorded by the same sensor that measured air velocity. Also, globe thermometer measures the temperature at L3P3 which is the central location for the test building.

Figure 17: Vertical sensor distribution (L3P3).

The air velocity is measured using anemometer at different vertical levels as well as locations in the test room (Figure 18). During the first 12 pair of experiments, each room has only four sets of anemometers at the centre. On location two and four (L2 and L4), air velocity sensors are positioned above the floor at one foot and below the ceiling. Since the wiring has the limitation of 2 feet between two anemometers, that is why four sets of anemometers put at the centre (L3). Accordingly, at the central vertical stand (L3) have four anemometers which are mounted at one, three, five, and seven feet above the floor.

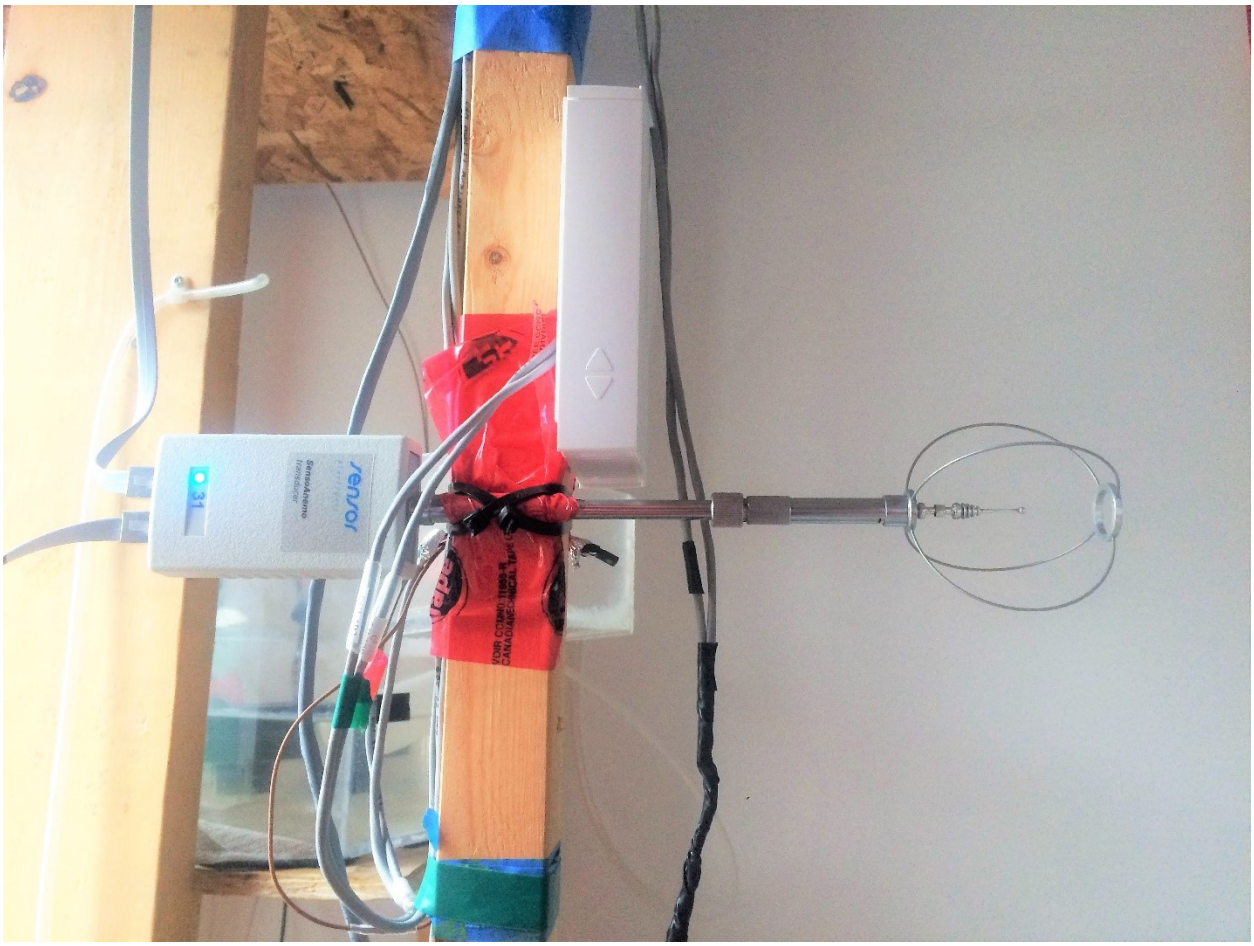

Figure 18: Anemometer.

The relative humidity is measured using relative humidity transducer for the first six pairs of experiments. They are installed at all locations (L1, L2, L3, L4, and L5) and three positions (P2, P3, and P4) as shown in Figure 19. Also, at the beginning of the experiments, there are six CO2 sensors in each test building. Moreover, they are installed at three locations (L1, L3, and L4) and two vertical positions (P3, P4).

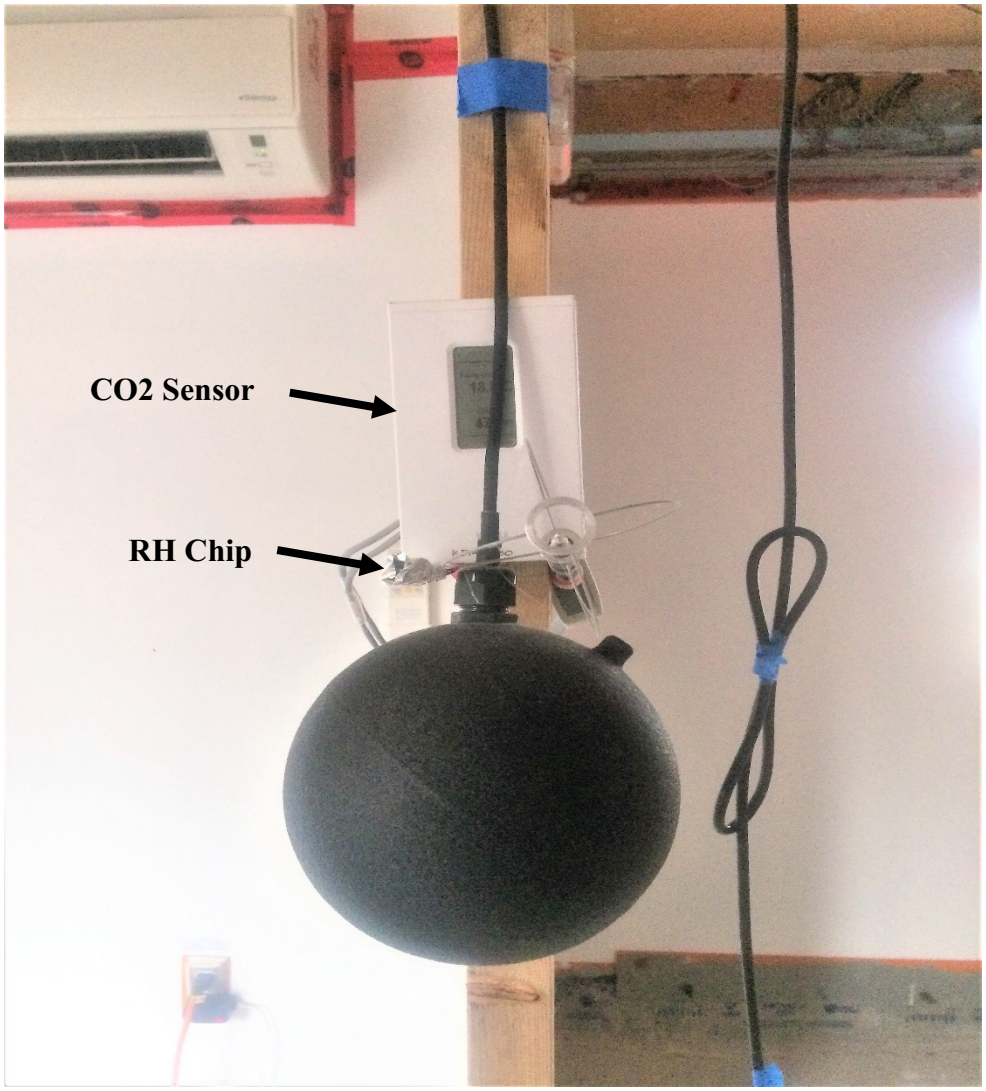

Figure 19: RH transducer and CO2 Sensor.

After finishing the first six pairs of experiments and going through all the data, the sensor layout is revised to meet the objectives of the following experiments which is investigating ventilation strategies and ventilation flow rates. As a result, the vertical stand reduces from five to four, by eliminating L1 and bringing L2 more to the centre. Moreover, the central stand (L3) moves to mid-distance between the south wall and mechanical room, which is a central point specifically for the test room. Whereas, the vertical sensor layout adds a new position at P1 (1'6'' above the floor) and CO2 sensor at P1, P3, and P4 in all locations

except L3. The central stand at L3 as shown in Figure 20 (B) have one more CO2 and RH sensor at P2. Furthermore, every stand is equipped with a set of four anemometers, relative humidity, and CO2 sensors. For the rest of the experiments, the new sensors are used which, coupled both CO2 and RH measurement. These sensors measure both CO2 and RH together, which reduce the power cable requirements for the sensors. Moreover, the elimination of L1 provides more RH sensors so that all the four-vertical stands have additional one RH sensors. Since the preceding experiments (from 7th and 19th) focus on ventilation strategies, additional CO2 sensors are installed in the outdoor to determine the incoming CO2 concentration. Furthermore, RH sensors are added at the supply and exhaust terminal to measure the RH value of the incoming and exhaust air. Besides, the outdoor climatic conditions are obtained from the locally available weather station at the test site.

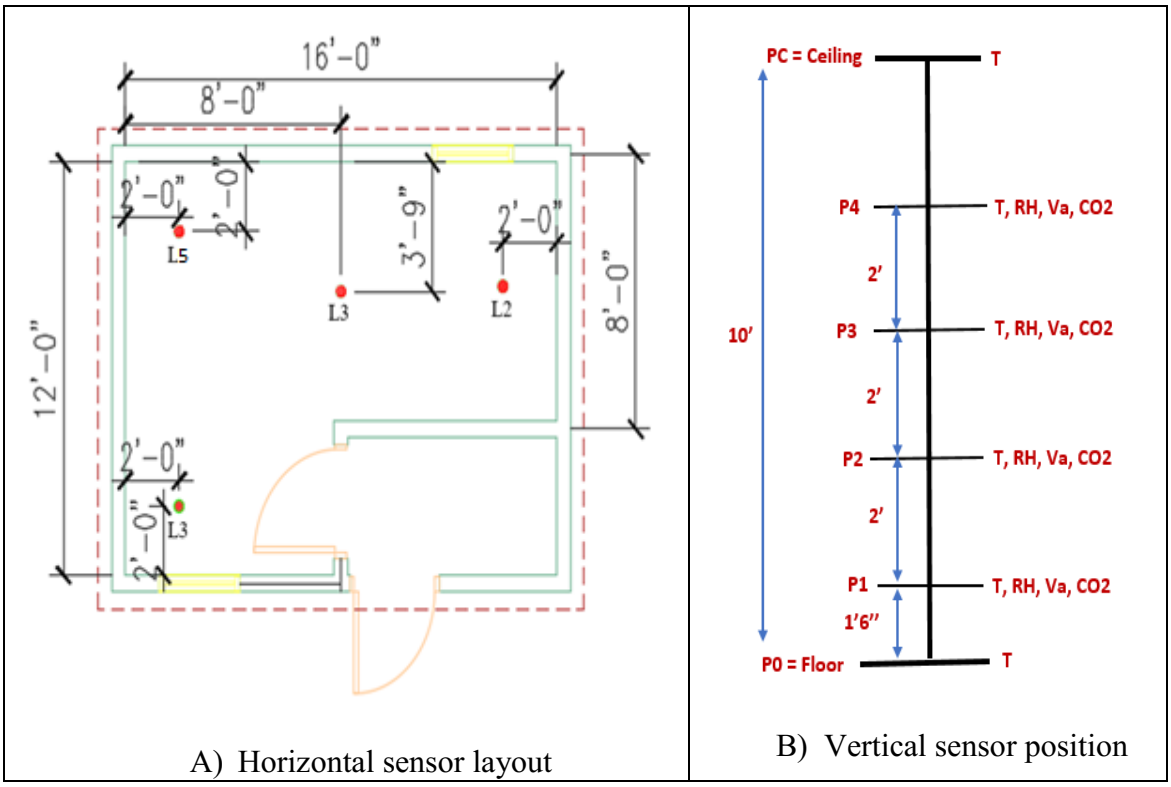

Figure 20: Revised Sensor layout.

5.2.2 Sensor specification, Calibration, Data acquisition, and Measurement

5.2.2.1 Energy Measurement

Heating system's energy performance is the primary focus of this study. As a result, the energy consumption of the systems is recorded using Power Scout 24 (Figure 21), based on the amount of electric power draw by each system. The power scout reading is verified using an independent power meter. Furthermore, verification is performed by running similar systems and check the Power Scout 24 readings in both test buildings. Besides, since the energy monitoring system (Power Scout 24) is already integrated into the test room's circuits, it makes it easier to change systems without affecting energy data collection.

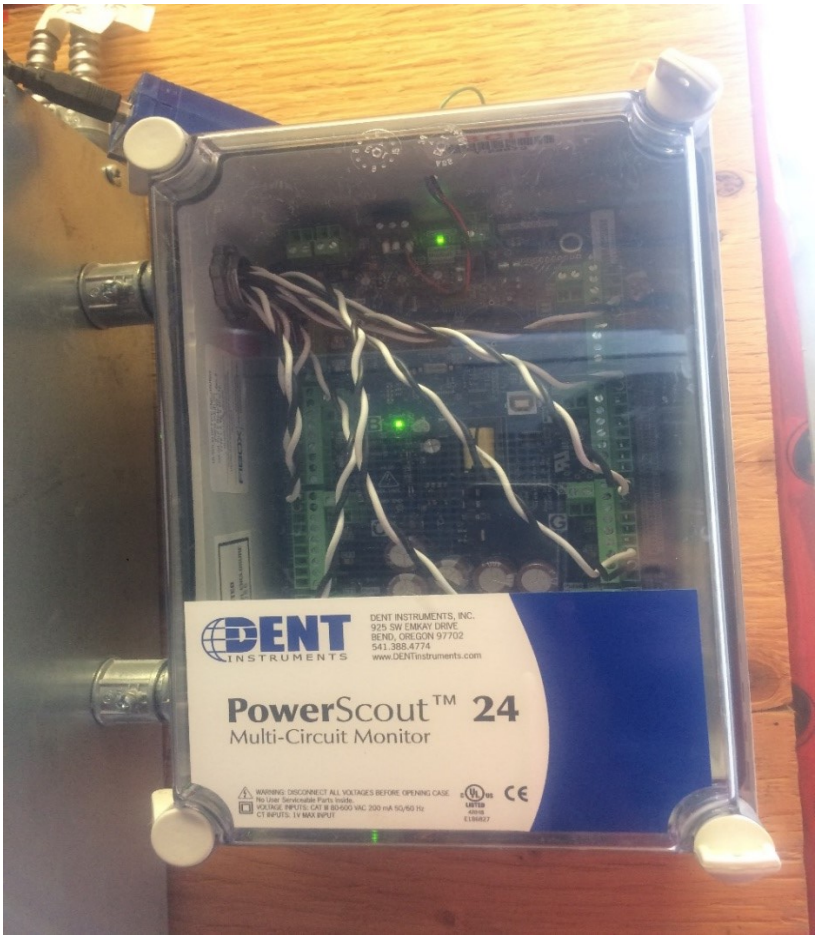

Figure 21: ` Meter (Power Scout 24).

5.2.2.2 Sensor Specification

Four different types of sensors are used in this study as summarized in Table 3. The temperature measurement in the test rooms is conducted using a thermocouple with the deviation of -0.5°F at 212°F. Whereas, the anemometers that measure air temperature has a measurement range of -10°C to 50°C and accuracy of 0.2°C. Besides, the CO2 sensor that is used in the experiments are two types, first one (VAISAL GMW90) have a measurement range 0 to 5000 PPM and the second one (C7262CO2) has a measurement range 0 to 2000 PPM. Both of these CO2 sensors have around 30 PPM accuracy. Moreover, the RH chip install in the test rooms has an accuracy of 3.5% at 25°C. In addition, the air velocity sensors have 0.02 m/s and 0.03 m/s accuracy as shown in Table 3.

Table 3: Sensors and specifications.

Measurement parameter	Sensor type	Model	Measurement range	Accuracy	Deviation
Temperature	Thermocouple	TT-T-24-3LF(ROH3)			-0.5^{0}F at 212^{0}F
	Anemometer		-10 to 50^{0}C	0.2^{0}C	
CO2	CO2 sensor	VAISAL GMW90	0 to 5000PPM	±(30 PPM +2%)	
	CO2 sensor	C7262CO2	0 to 2000PPM	±(30 PPM +3%)	
Relative humidity	RH chip	HIH-4021-003	0 to 100 %RH	3.5% RH at 25^{0}C	
Air velocity	Anemometer	AirDistSys5000	0.05-5m/s	±0.02 m/s	±2.5% above 2m/s
	Air velocity transducer	8475-03	0 – 2.5m/s	0.03 m/s	

5.2.2.3 Sensor Calibration

All sensors in this project are either calibrated in the lab, or the manufacturers provide the calibration information. For instance, the anemometers, CO2, RH chip, and CO2 sensors are calibrated, and their calibration documents are provided by the manufacturers. Whereas, thermocouples are calibrated in the lab by using a thermometer. The calibration is done by immersing the thermostat and the thermocouple into the water inside the cup and measure the temperature reading from both meters. The temperature reading after the reading stabilize is selected for comparison between those sensors as shown in Figure 22. Then the thermocouple is calibrated using the thermometer reading. Similar thermocouple calibration for NTB is presented in Appendix I section 6.

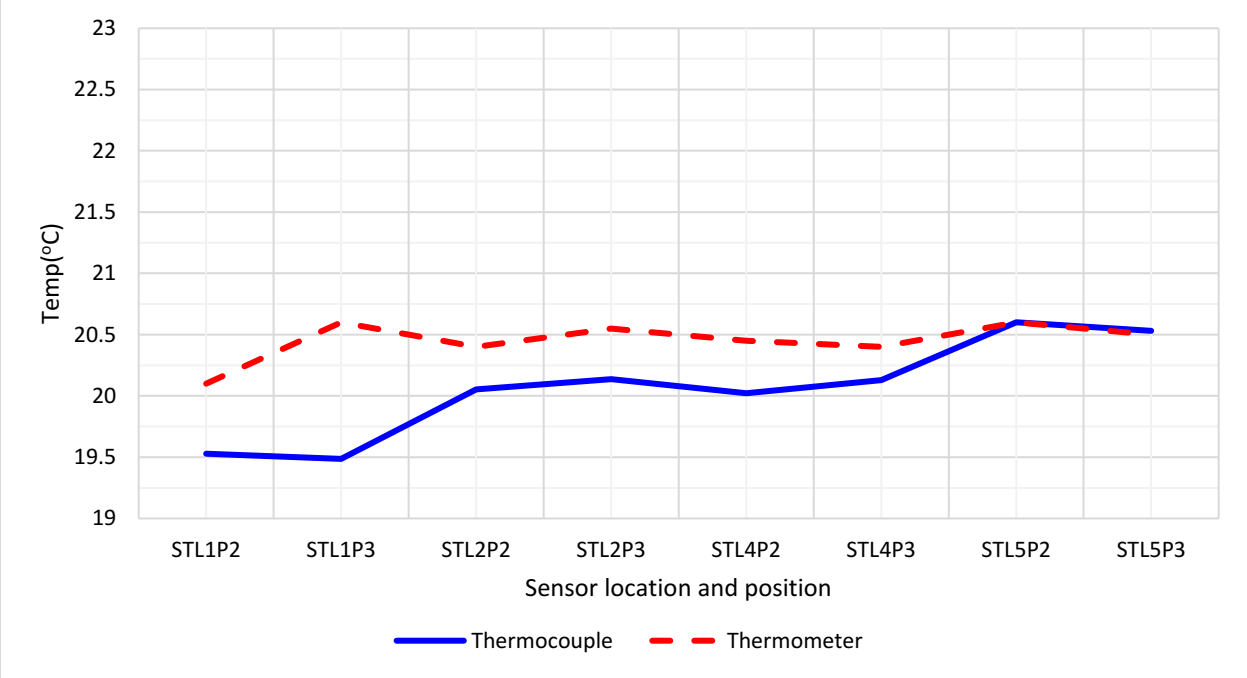

Figure 22: Thermocouple calibration: STB.

The calibration of moisture generators is different because this unit is a system (have different component and accessories): not a single sensor. The moisture generator is calibrated using a balance scale. A balance scale is placed under the water container and runs the humidifier for 20

minutes several times repeatedly. Simultaneously measuring the mass of water container because the moisture supply to the test room is from the container. After that, the humidifier is recalibrated to meet the specified target (100 grams per hours) by using a ratio of time. It is done by calculating the number of minutes in a single hour required to run the humidifier to supply the desire moisture amount based on the hourly balance scale reading. As a result, 75% of the minutes in one hour provides 100 g/h which is the goal of the humidifier.

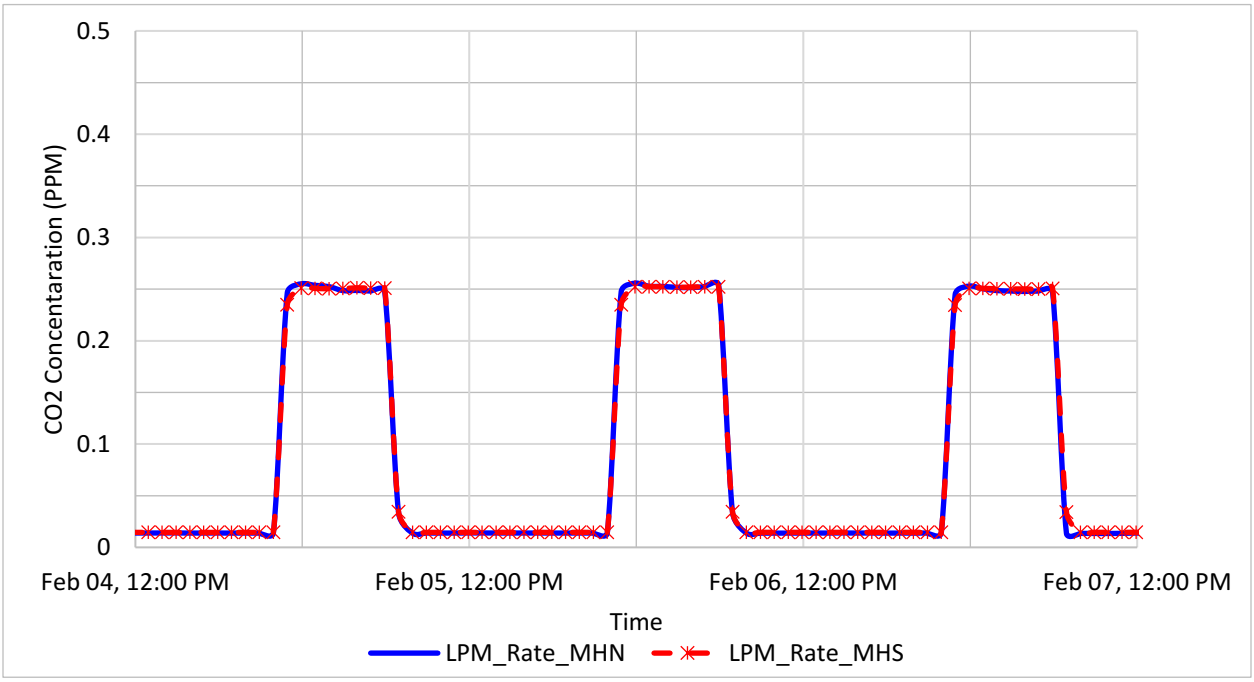

Figure 23: CO2 supply into the test rooms (NTB and STB).

The CO2 system is calibrated using a similar approach like moisture generator, but a bit different. It is calibrated using the pressure reading from the CO2 container. The CO2 supply in 10 seconds is measured using laminar flow element which then used to calibrate the CO2 supply to meet the desired supply amount (0.25 litre per minute). A solenoid valve is used to open and close the CO2 supply for the specific period. Therefore, a repetitive measurement is carried out, and the CO2 supply is recorded. As the result, of opening the CO2 supply for just 3 seconds out of 60 seconds, it is possible to deliver 0.25 lpm into the test room as shown in Figure 23.

5.2.2.4 Data Collection System

The collected data immediately send to a data logging instrument called 34980A Keysight (Figure 24). The data then sent to a computer server to store it for further analysis and discussion. The sequence of measurement is a five-minute interval for the entire sensors except for air velocity sensors where the data is one-minute average to get more detail change in the reading. The data from anemometers do not go to the data logger instead go to the computer where the data is stored. This data collection system is so flexible and allowed to treat each data collection system independently without affecting one another.

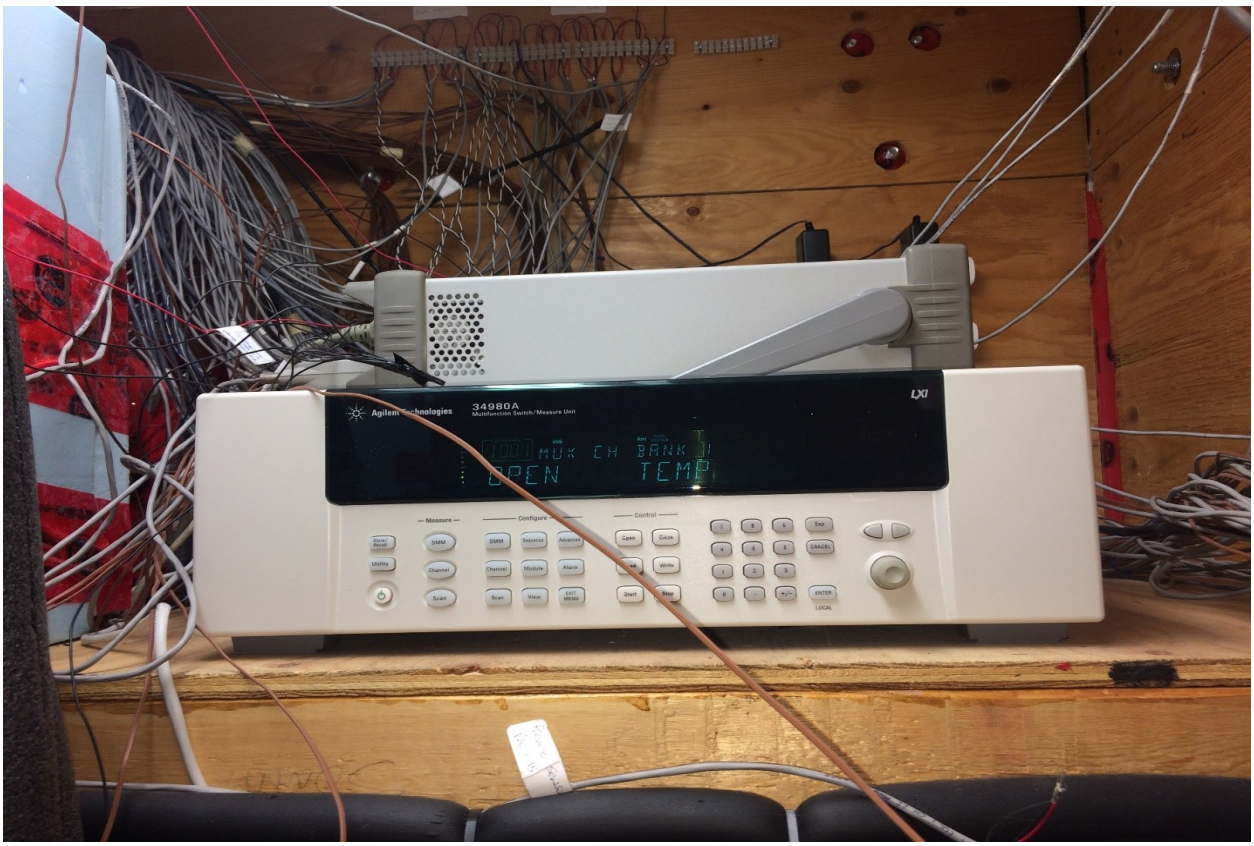

Figure 24: Data Acquisition system.

6 DATA ANALYSIS

The experimental data undergoes through the data analysis process. The data analysis process involves methodically applying scientific and statistical techniques to illustrate and interpret the collected experimental data. Two groups of data analysis are conducted to evaluate the indoor environment produced by the heating and ventilation systems. The first data analysis includes calculation of the thermal energy, thermal comfort, local thermal discomfort assessment, temperature distribution, and relative humidity distributions for six pairs of experiments in the test buildings as the result of the different combinations of the heating and ventilation systems. The second data analysis examines data collected from the last eight pairs of experiments which focus on ventilation performance effectiveness assessment. In this study, average hourly data is used for all experiments except for heat pump COP analyses in which one-minute data are used.

6.1 Thermal Energy

The thermal energy analysis focuses on determining the amount of heat energy supply to the indoor space to maintain the building at a specific set point temperature (21°C). As a result, the thermal energy analysis assesses the heat supply by four space-heating systems to produce the specified indoor temperature. The assessment covers the data collected from 6-pair of experiments comparing those four heating systems in parallel using the two side by side test buildings. Each pair of experiment runs for four days. For comparison purpose, a 24-hour data when the indoor temperature difference between the two buildings is less than 0.5°C is used. For instance, Figure 25 represents the room temperatures where PRH and HP are compared, the thermal energy analysis, therefore, selects the data after the first two days where the temperature difference between the rooms stay below 0.5°C. As shown in Figure 25 the room temperature difference stays below 0.5°C mostly, except at the beginning of the experiment.

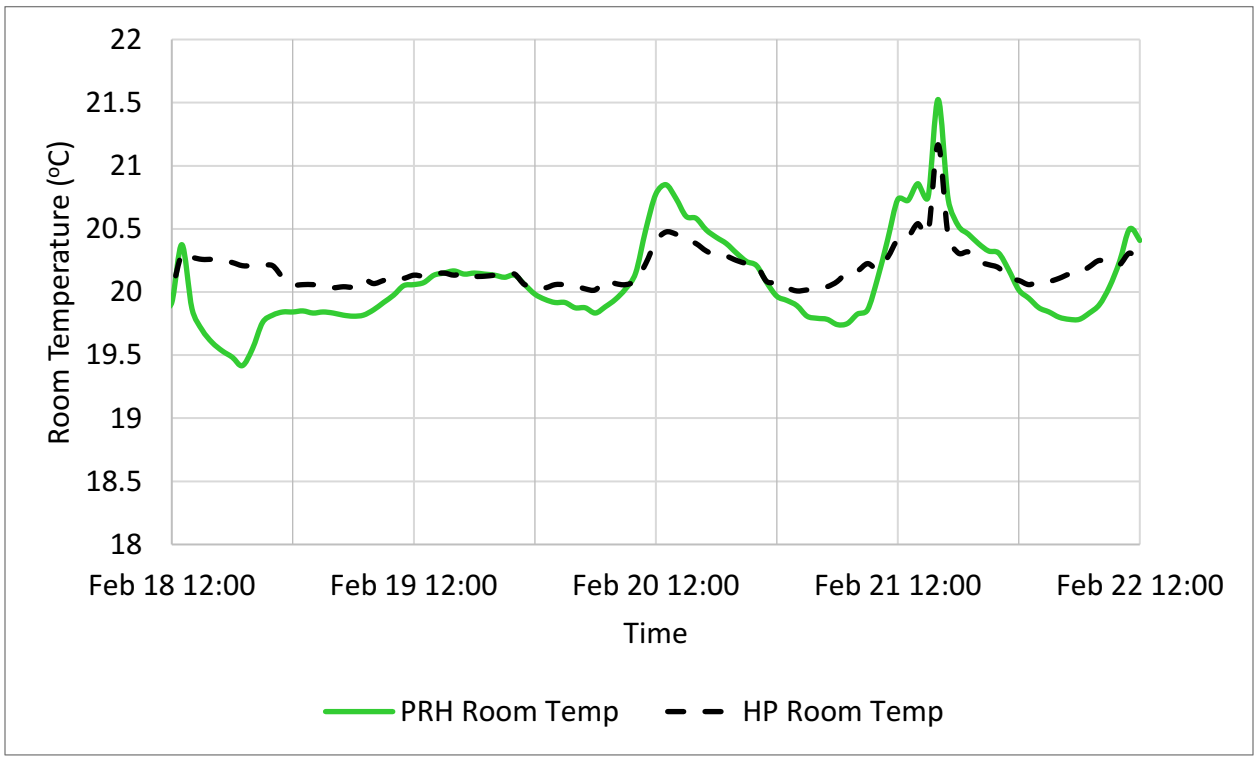

Figure 25: Room temperature profile of test rooms with: PRH vs HP.

6.1.1 Thermal Energy from Baseboard and Radiator Heating System

The thermal energy analysis of EBH and PRH is straightforward. The analysis assumes both heater's efficiency is 100%, meaning all the electrical energy consumed, turn into thermal energy (heat). Thus, energy measurement from the Power Scout is regarded thermal energy provided to the building to maintain the indoor air temperature.

6.1.2 Thermal Energy Calculation from Heat Pump

The thermal energy supply by the heat pump is not straightforward because it requires further calculation and analysis. Consequently, the heat pump thermal energy is calculated by multiplying the measured electrical energy from power scout with the heat pump coefficient of performance (COP). Although, as part of the equipment specification, the maximum and the minimum COPs of the heat pump are given, these values are based on laboratory tests at specific indoor and outdoor temperature conditions and may not be applied in real building operation with random combinations of indoor and outdoor conditions. Thus, in this thesis, the actual COP of the system for the test conditions is determined by conducting a separate experimental test. In the experiment, the heat pump in the south test building and the baseboard heater in north test building is run, and the measured energy consumption of the two buildings is used to determine the COP of the Heat pump. Since, both the indoor and outdoor conditions are the same, similar thermal energy is required to maintain both test rooms at the same temperature set point as shown in Figure 27. The COP of the heat pump is found by dividing the energy consumption of baseboard heater by the energy consumption of heat pump.

The COP value is verified by calculating the thermal energy supplied by the heat pump indoor unit and the from the energy consumption measurement of the heat pump. It is done by measuring the inlet and outlet air temperatures of the indoor heat pump unit using thermocouples as shown in

Figure 27, and the manufacturer specified air flow rate to calculate the thermal energy using Equation (12). Similarly, the COP of the heat pump is determined by dividing the calculated thermal energy and the measured heat pump energy consumption, 2.1. Estimation of the thermal energy of the building using the twin building or from the indoor unit inlet and outlet air temperature measurements lead to comparable COP value determinations as shown in Figure 26.

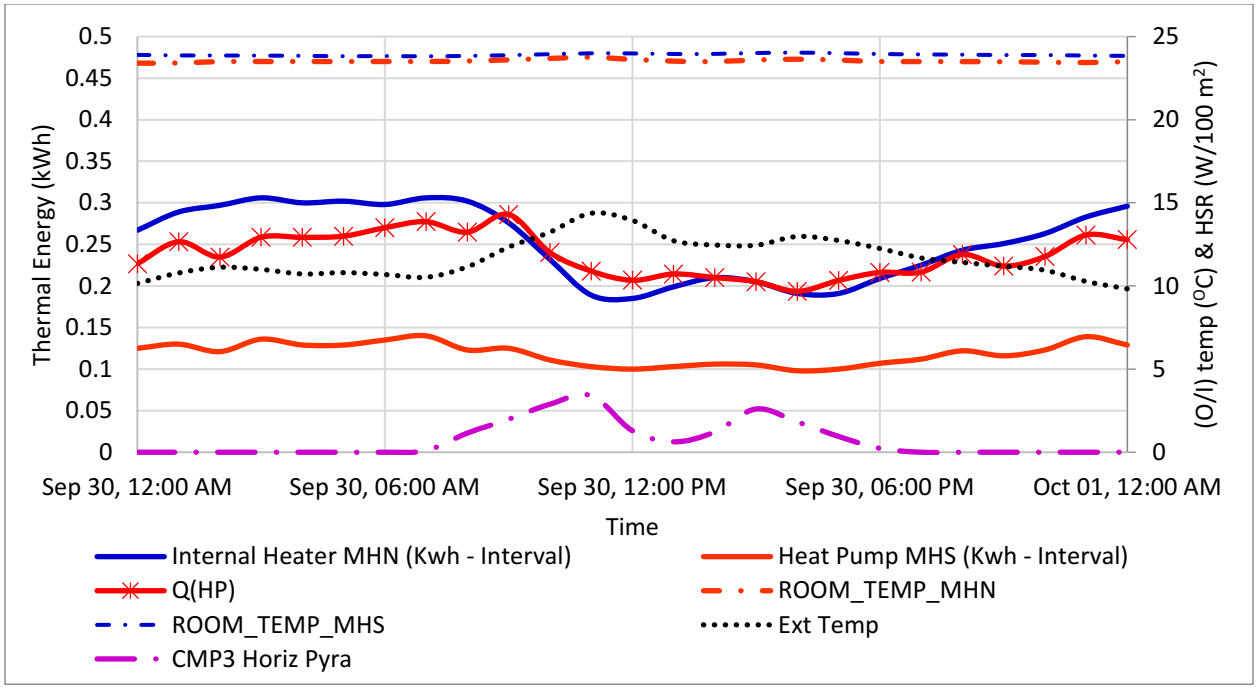

Figure 26: Thermal energy supply by EBH and HP (with COP).

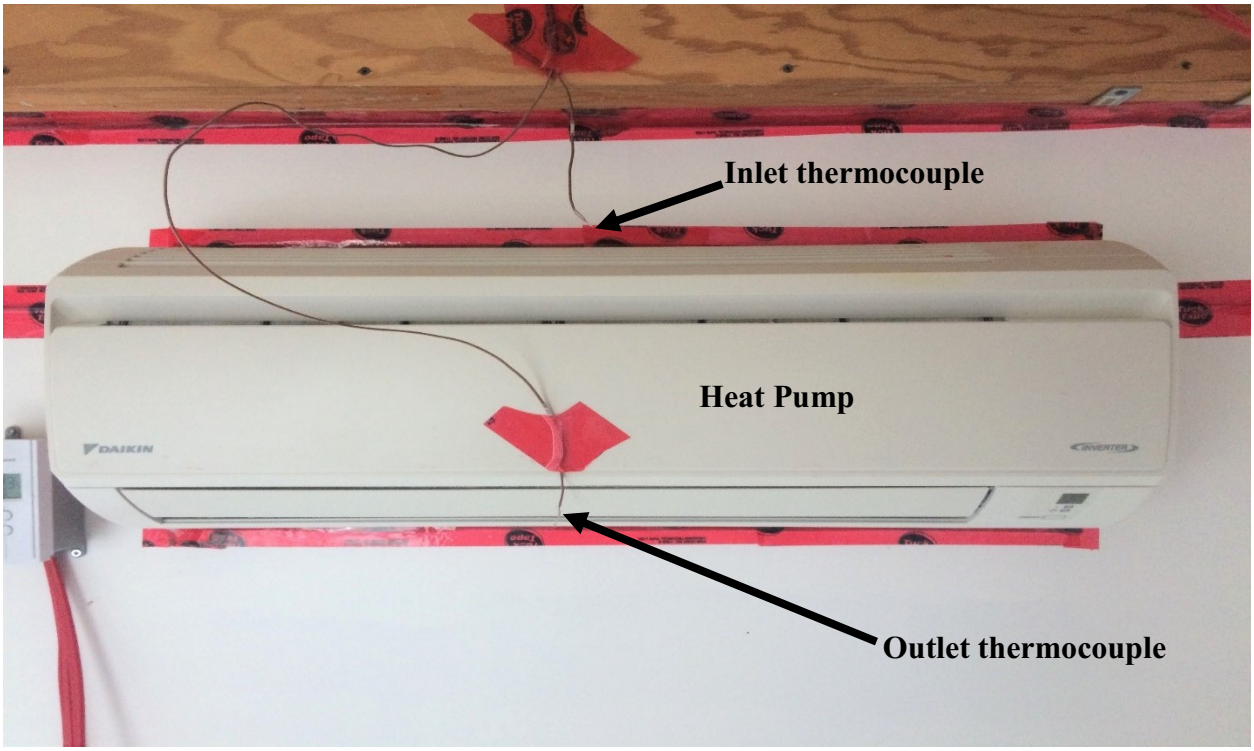

Figure 27: Heat pump with inlet and outlet thermocouples.

$$Q = \dot{m} C_p \Delta T \tag{12}$$

Where,
Q = Thermal energy (Watts)
$\dot{m}$ = mass flow rate (kg/s)
C_p = Specific heat capacity ($Kj/K_g\ K$)
ΔT = Temperature difference between in let and out let air (K).

6.1.3 Thermal Energy Calculation from Radiant Floor

The radiant floor heating system thermal energy calculation requires combining convective heat transfer and radiation heat transfer between the floor and the entire surrounding surfaces as illustrated in Equation 13. The radiant heat exchange between the floor and interacting surfaces is calculated using ASHRAE Systems 2016 (Chapter 5) Equation 14 and the convection heat transfer between the floor and indoor air is determined using Equation 15.

$$Q_{Total} = q_r + q_c \tag{13}$$

$$q_r = A_f \varepsilon \sigma \, [T_f^4 - T_r^4] \tag{14}$$

$$q_c = 0.39 \, \frac{(T_f - T_a)|T_f - T_a|^{0.31}}{D_e^{0.08}} \tag{15}$$

Where,

q_r = Radiation heat exchange, Kw.

q_c = Convective heat exchange, Kw.

A_f = floor area, m^2.

ε = emissivity.

σ = Stefan-Boltzmann constant ($5.67 * 10^{-8} \, W/m^2K^4$).

T_f = floor temperature, ^{O}C.

T_r = Mean radiant temperature of the surfaces, ^{O}C.

T_a = Air temperature at 1.5m above the floor, ^{O}C.

D_e = perimeter of the floor, m.

The radiative energy is dependent on the orientation (view factor) of the surfaces. The shape of the test room in this study is not simple like a rectangle instead it is L shaped. Also, the asymmetric

position of the two windows concerning the walls, they are mounted on making the radiation heat transfer calculation is complex. These two geometrical problems create a challenge to adopt ASHRAE calculation method for determination of view factors readily. In this work, the view factors between the non-rectangular floor and the enclosures are computed by dividing the test space with imaginary wall into two rooms of the square and rectangular floor areas as shown in Figure 28. Applying, the basic fundamental constraints in view factor determination such as the sum of view factors from a surface, is unity and using the superposition and reciprocity rules.

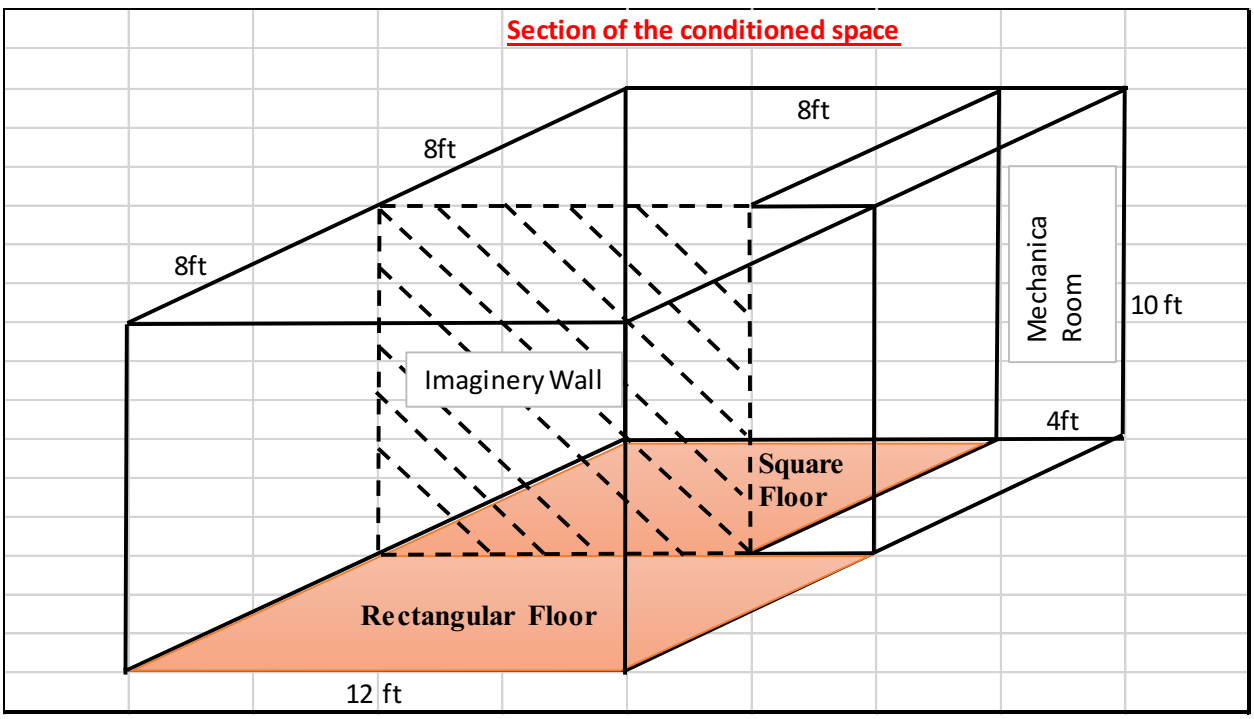

Figure 28: Section of test room for RFHS thermal energy analysis.

Table 4 presents the calculated view factors of radiation from the floor. The calculation procedure is documented in Appendix I, Section 1. As can be seen from the table, the summation of the view factors between the floor and the surrounding surfaces is one.

Table 4: View factor summery between the floor and surrounding wall.

Part of the test room	Symbol	Surface	Area (ft^2)	Radiation exchanging surfaces	View factor
Square Floor	S.wall	South Wall	80	F_S.floor -S.wall	0.192261527
	I.wall	Imaginery wall	80	F_S.floor -I.wall	0.213408418
	W.wall	west wall	80	F_S.floor -W.wall	0.213408418
	N_m.wall	North_mech.room adjacent wall	80	F_S.floor -N_m.wall	0.213408418
	S.ceiling	Square Ceiling	64	F_S.floor - S.ceilling	0.14636633
	S.Win	South Window		F_S.Floor-S.Win	0.02114689
	S.Floor	Square Floor	64	Sum	1
Rectangular floor	S.Wall	South wall	80	F R.floor – S.wall	View factor
	N.Wall	North wall	80	F_R.floor - S.wall	0.161336191
	E.wall	East wall	120	F_R.floor - N.wall	0.145018569
	W_m.wall	West_mech.room adjacent wall	120	F_R.floor - E.wall	0.243061987
	I.wall	Imaginary wall	80	F_R.floor - W_m.wall	0.076531104
	R.Ceiling	West_mech.wall	40	F_R.floor - I_m.wall	0.166530883
	N.Win	North Window	80	F_R.floor - Ceilling	0.191203644
	R.Floor	Rectangular floor	96	F_S.Floor-N.Win	0.016317622
				Total	1

These view factors are used to calculate equivalent mean radiant temperature or the equivalent temperature of the surrounding surfaces using Equation 17. The radiation that is intercepted by the imaginary wall needs to be distributed to the adjacent room based on the view factor of the imaginary wall and the surrounding surfaces. Since radiation emitted from the floor in the rectangular section will not pass through the imaginary wall and come back to the floor again in the square section and vice versa, the view factors of the imaginary wall are calculated accordingly. Table 5 presents the calculated view factors. Equation 17 is used to calculate equivalent mean radiant temperature of the surrounding surfaces, where the view factor of a surface is determined by superposing the view factor values of the surface given in Table 4, 5 and the measured surface temperature.

$$T_r = \left(\sum_{j=1}^{n} F_{f-j}\, T_j^{\,4}\right)^{\frac{1}{4}} \tag{17}$$

Where,
T_r = Mean radiant temperature surrounding surfaces (K)
F_{f-j} = View factor between floor and a surface J
T_j = Temperature of surfaces (j)
N = Number of surfaces

Table 5: View factor of the Imaginary wall without a floor.

Rectangular Floor	Radiation exchanging surfaces	View Factor	Symbol	Surfaces.	Area (Ft^2)
	F_I.wall-S.Ceiling	0.205875121	S.Ceiling	Square ceiling	64
	F_I.wall-S.wall	0.232342195	S.wall	South wall	80
	F_I.wall-N.wall	0.258943868	N_m.wall	North wall	80
	F_I.wall-E.wall	0.276237143	E.wall	Eest wall	80
	F_I.wall-S.Win	0.026601673	S.Win	South window	80
	Sum	1	I.wall	Imaginary wall	
Square Floor	Radiation exchanging surfaces	View Factor	Symbol	Surfaces.	Area (ft^2)
	F_I.wall-R.Ceiling	0.249745457	S.Wall	Rectangular ceiling	80
	F_I.wall-S.wall	0.268364375	N.Wall	South wall	80
	F_I.wall-N.wall	0.08845032	E.wall	North wall	120
	F_I.wall-E.wall	0.373277836	W.wall	Eest wall	120
	F_I.wall-R.Win	0.020162011	W_m.Wall	North window	40
	Sum	1	I.Wall	Imaginary wall	80

6.2 Thermal Comfort

6.2.1 General Thermal Comfort

The thermal energy supply of the heating system is responsible for creating a thermally comfortable environment. Thus, this study simulates small study rooms heated by four different heating systems and inspect the thermal environment created by the systems. Accordingly, the two groups of thermal comfort analysis: general thermal comfort and local thermal comfort assessment are conducted in this study. Overall, the analysis examines the environment produced by heating systems regarding comfortableness of space for a dweller thermally.

The general thermal comfort is calculated at the centre of the test area (L3) and two vertical positions for a seated person 0.6 m (24 in) and standing person 1.1 m (43 in) assuming waist level in both cases as specified in ASHRAE 55, 2013. Moreover, the general thermal comfort analysis requires four environmental inputs: air temperature, air velocity, Relative humidity, and mean radiant temperature as well as two personal inputs: clothing and metabolic rate to carry out the calculation. Mean radiant temperature (MRT) is determined using walls, floor, ceiling, and windows surface temperatures and the corresponding view factors between the point of interests (seating and standing positions) and the surrounding surfaces as illustrated in Equation 18. The temperatures of the surrounding surfaces are obtained from the experiments, whereas the view factors are calculated based on the geometrical relationship between the position where thermal comfort is calculated and the surrounding surfaces.

$$\bar{t}_r{}^4 = t_1{}^4 F_{P-1} + t_2{}^4 F_{P-2} + \cdots + t_n{}^4 F_{P-n} \qquad (18)$$

Where,

$\bar{t}_r$ = mean radiant temperature, K.

F_{P-n} = view factor between a surface and surface N.

t_n = surface temperature of surface N, K.

ASHRAE Fundamentals (2017) provide Equations for determining the view factors for both seating person and standing person. However, the formulas assume a person face rectangular surfaces of uniform temperature, which cannot be readily applied due to the presence of windows in the middle of the rectangular surfaces that creates different surface temperatures. In addition, the actual geometry of the test room in this study has different geometry to that of the provided by ASHRAE, which produce a challenge to calculate the view factor precisely.

As a result, the view factor of a differential area to a rectangular surface area like a wall, floor and ceiling are determined using Hamilton and Morgan (1965) (Figure 29 (a) and Equation 19). The view factors between differential area and small rectangular surface like window are determined using Nusselt Analogy Form Factor (Tobler et al. 1998) (Figure 29 (b) and Equation 20). Section By applying this two Equations the view factor is calculated at the location where seating and standing person is simulated. Table 7 lists the view factors for both seating and standing position relative to each surface. A can be seen in the table, the view factor summations for both seating and standing position are one. Since both test buildings had a similar orientation, the view factor remains the same for both test rooms. Finally, the measured surface temperatures and the corresponding view factors from Table 7 are used to calculate the mean radiant temperature, which is one of the inputs for general thermal comfort calculation.

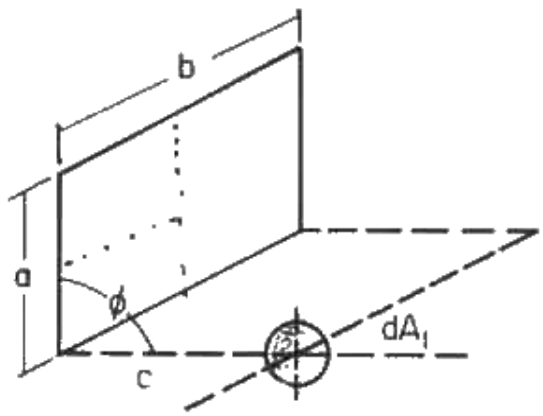

Definitions: A=a/c; B=b/c

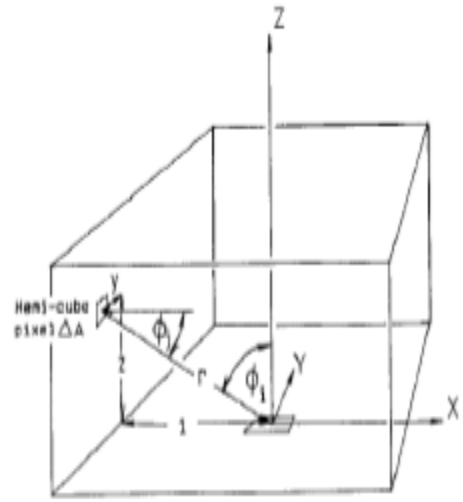

View factor between differential area and rectangular surface

A) Hamilton and Morgan 1965 (Eq. 19)

View factor between differential area and small rectangular surface like a window

B) Nusselt Analogy Form Factor (Eq. 20)

Figure 29: View factor for MRT calculation.

$$F_{dA1-2} = \frac{1}{4\pi}\left(tan^{-1}\left(\frac{AB}{(1+B^2+A^2)^{\frac{1}{2}}}\right)\right); \quad \left(\emptyset = \frac{\pi}{2}\right) \tag{19}$$

$$F_{dA1-\Delta A} = \left(\frac{Z}{\pi(Y^2+Z^2+I)^2}\right) * \Delta A \tag{20}$$

Table 6: View factor from different surfaces for two positions.

Surface	Symbol	Seating	standing
West wall	FPW	0.064887	0.068763
Est wall	FPE	0.092977	0.098428
South wall	FPS	0.145642	0.15653
North wall	FPN	0.070023	0.075467
North mech. R wall	FPNm	0.157728	0.170419
South Window	FPSw	0.005597	0.005596
North Window	FPNw	0.005597	0.005596
Floor	FPF	0.339235	0.280438
Ceiling	FPC	0.118316	0.138762
sum	sum	1.000	1.000

For verification purpose, results of the presented mean radiant temperature (MRT) calculation method is compared with the results that are driven from a globe temperature sensor that is installed at the centre of the test room (L3P3). At the same location, anemometers and thermocouple are installed to measure the local air velocity and air temperature, which are essential for the determination of MRT. The MRT calculation using the globe thermometer reading is conducted by Equation 21. Figure 30 shows a typical result of MRT calculated based on surface temperature measurements and view factors, and globe thermometer. The results of the two MRT determination methods are nearly identical. Consequently, in this thesis, the first method will be used as it allows to calculate MRT at any point of interest in the test room.

$$\bar{t}_r = \left[\left(t_g - 273\right)^4 + \frac{1.10 * 10^8 {V_a}^{0.6}}{\varepsilon D^{0.4}}(t_g - t_a)\right]^{1/4} \tag{21}$$

Where,

t_g = globe temperature, ºC.

V_a = air velocity, m/s.

t_a = air temperature, ºC.

D = globe diameter, m.

ε = emissivity (0.95 for black globe).

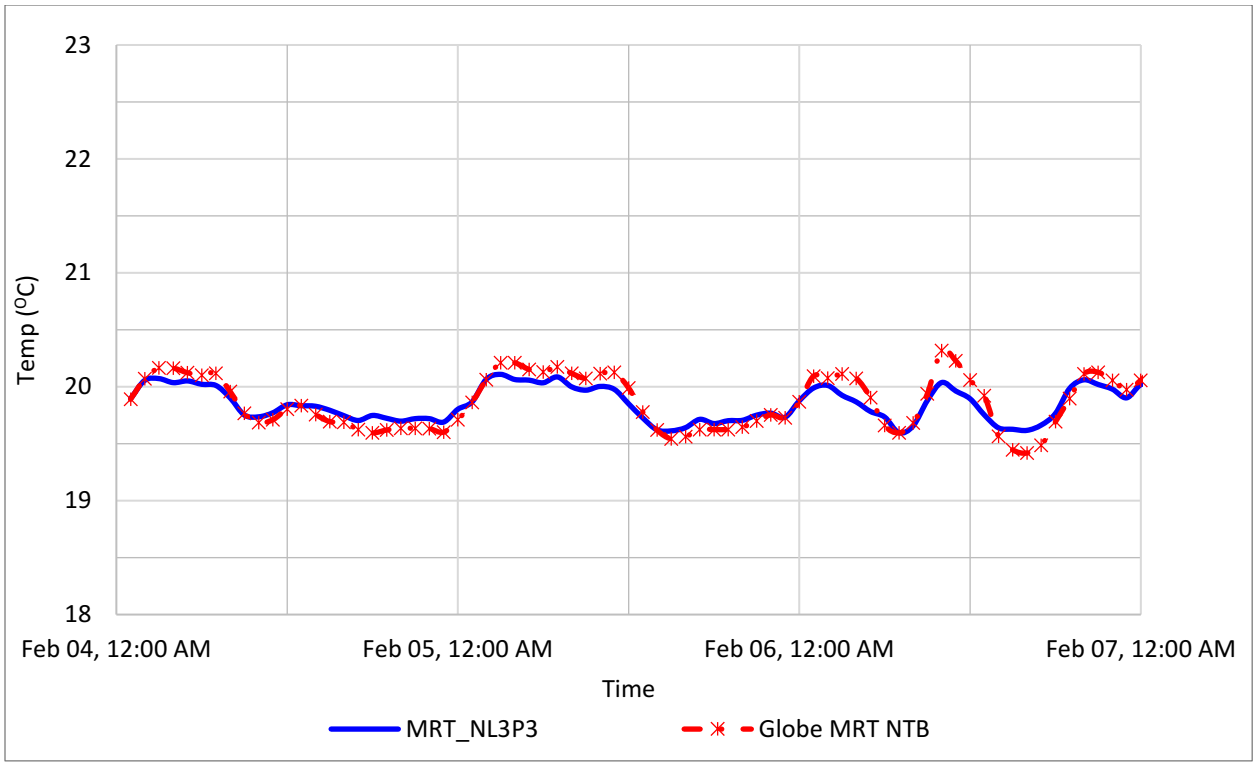

Figure 30: Mean radiant and globe temperature trend at the same position and location.

The other inputs for general thermal comfort calculation are air temperature, relative humidity, external-work (assume 0), air velocity, metabolic-rate and clothing. The air temperature, air velocity, and RH used in the analysis are measured values. The assumed metabolic rates are 1 and 1.2 met for a seating person and standing person respectively, based on ASHRAE 55 (2013), Table 5.2.1.2. Also, the supposed clothing values are typical winter clothing (1 CLO).

Finally, for general thermal comfort computation, a Matlab code based on the ASHRAE computer program script (Appendix I, Section 2) is adapted to calculate PMV and PPD. Furthermore, for validation purpose, the Matlab code results are compared to the results from ISO 7730 (2005) standard (Table 7). The closeness between the two lines in Figure 31 depicts that the Matlab code adapted from ASHRAE 55 (2013) produce a similar result as ISO 7730 (2005) standard.

Table 7: Thermal comfort verifying with ISO 7730 (2005) standard values

Cases	Air Temp	MRT	Va	RH	Meta	Clo	ISO 7730	Mat-lab
1	22	22	0.1	60	1.2	0.5	-0.75	-0.76
2	27	27	0.1	60	1.2	0.5	0.77	0.76
3	27	27	0.3	60	1.2	0.5	0.44	0.43
4	23.5	25.5	0.1	60	1.2	0.5	-0.01	-0.02
5	23.5	25.5	0.3	60	1.2	0.5	-0.55	-0.56
6	19	19	0.1	40	1.2	1	-0.6	-0.6
7	23.5	23.5	0.1	40	1.2	1	0.5	0.36
8	23.5	23.5	0.3	40	1.2	1	0.12	0.12
9	23	21	0.1	40	1.2	1	0.05	0.05
10	23	21	0.3	40	1.2	1	-0.16	-0.17
11	22	22	0.1	60	1.6	0.5	0.05	0.05
12	27	27	0.1	60	1.6	0.5	1.17	1.17
13	27	27	0.3	60	1.6	0.5	0.95	0.95

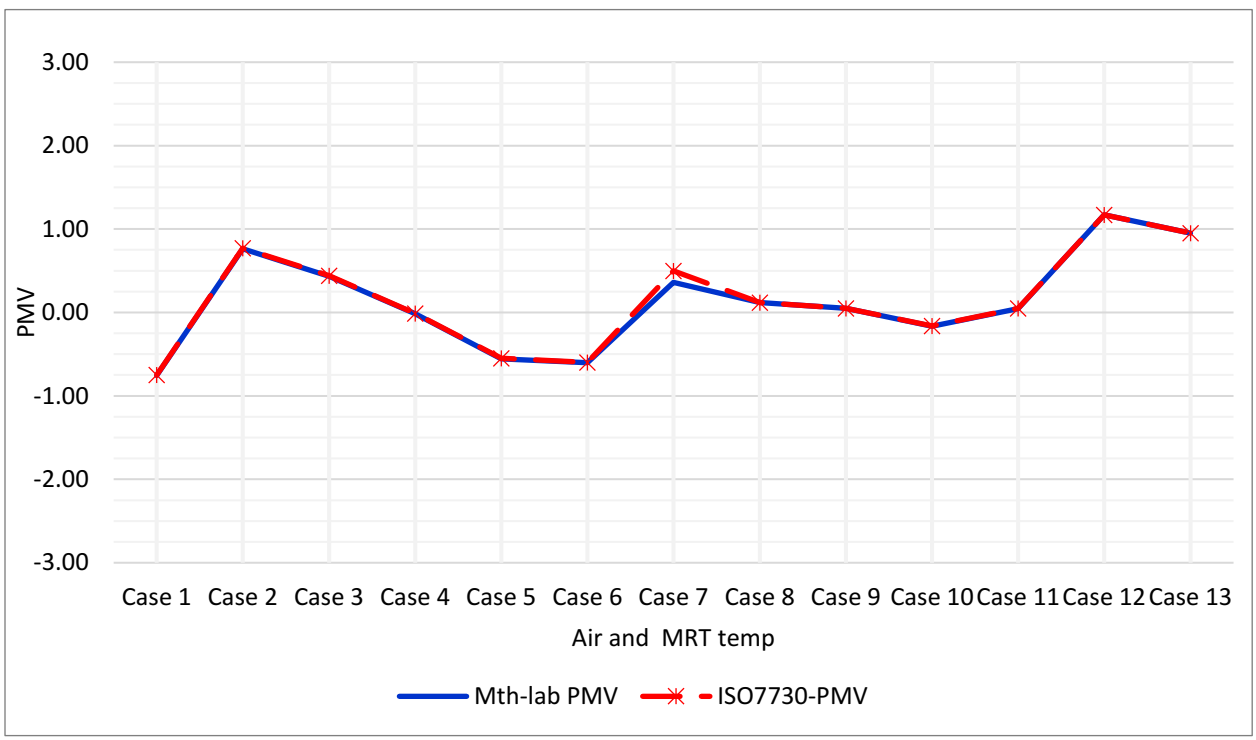

Figure 31: PMV comparison between Mat-lab and ISO 7730 (2005) using Table 7.

6.2.2 Local Thermal Comfort Analysis

Three local thermal comfort analyses are conducted using the data collected from the first six pairs of experiments, which compares the performance of four heating systems. These are local thermal discomfort as the result of radiant asymmetry, vertical temperature difference, and floor surface temperature. The approach suggested by ISO 7730 (2005) and ASHRAE 55 (2013) standards are implemented to assess potential local discomforts created in the test rooms heated by four different heating systems.

The radiant temperature asymmetry analysis has two components, radiant temperature asymmetry as the result of the floor to ceiling temperature difference and radiant symmetry due to the cold window using Equation 22 to 25 and Figure 32. The average of floor surface temperature and average ceiling surface temperature are used to determine floor to ceiling radiant asymmetry. Whereas, the radiant temperature asymmetry as the result of the cold window is analyzed for a position in front of both south and north windows.

Warm ceiling

$$PD = \frac{100}{1+\exp(2.84-0.174*\Delta T)} - 5.5; \quad \Delta T<23^{O}C \tag{22}$$

Cool wall

$$PD = \frac{100}{1+\exp(9.93-0.5*\Delta T)}; \quad \Delta T<15^{O}C \tag{23}$$

Cool ceiling

$$PD = \frac{100}{1+\exp(6.61-0.345*\Delta T)}; \quad \Delta T<15^{O}C \tag{24}$$

Warm wall

$$PD = \frac{100}{1+\exp(3.72-0.052*\Delta T)} - 3.5; \quad \Delta T<35^{O}C \tag{25}$$

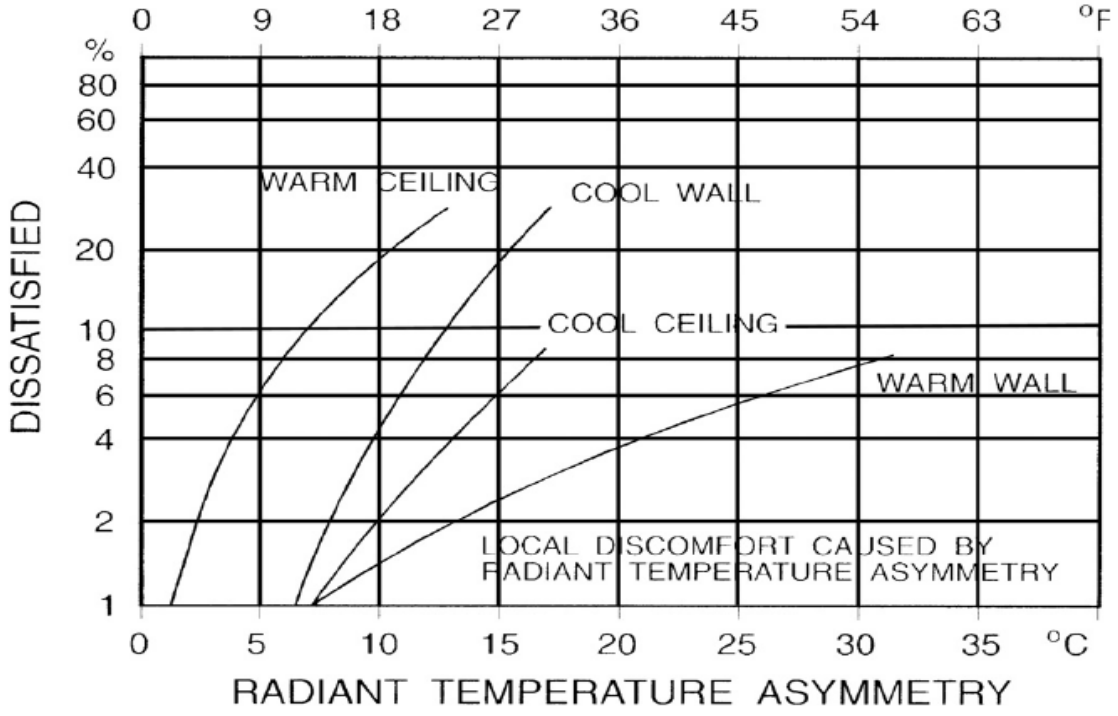

Figure 32: Local thermal discomfort as the result of radiant asymmetry (ASHRAE 55, 2013).

The temperature difference between the ankle and neck level is used to determine local thermal discomfort because of vertical temperature difference for both seatings as well as standing position at the centre of the test room (L3) using Equation 26 or Figure 33. Local thermal discomfort due to vertical temperature difference for both seating and standing person is calculated using temperature measurements at the ankle (0.1 m) and neck positions (1.1 m for seating and 1.7 m for standing person). Air temperature at 0.1 m from the floor level is determined by interpolating the temperature measurement results of the floor and the air at 0.3 m foot above the floor. In addition, similar interpolation is applied between L3P2 and L3P3 as well as between L3P3 and L3P4 to determine the air temperature at 1.1 m and 1.7 m which are the corresponding neck levels for the seating and standing person, respectively.

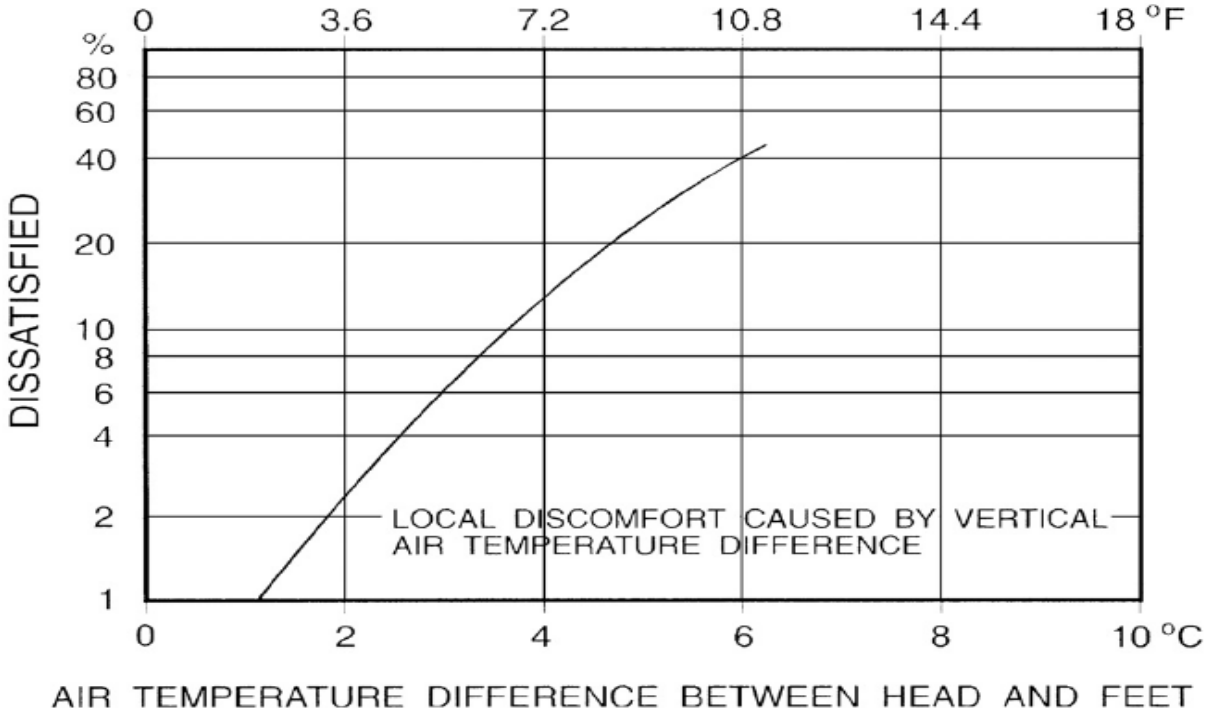

Figure 33: Local thermal discomfort due to the vertical temperature difference (ASHRAE 55, 2013).

$$PD = \frac{100}{1+\exp(6.61-0.856*\Delta T)}; \quad \Delta T<8^{o}C \tag{26}$$

The average of five-floor surface temperature reading is used in Equation 27 and Figure 34 (ISO 7730, 2005) to analyze the percentage of dissatisfied as the result of floor surface temperature. This analysis is applied to the data collected from the first six pairs of experiments where four heating systems are compared.

$$PD = 100 - 94 * \exp(-1.387 + 0.118 - 0.0025 * T_f^2) \tag{27}$$

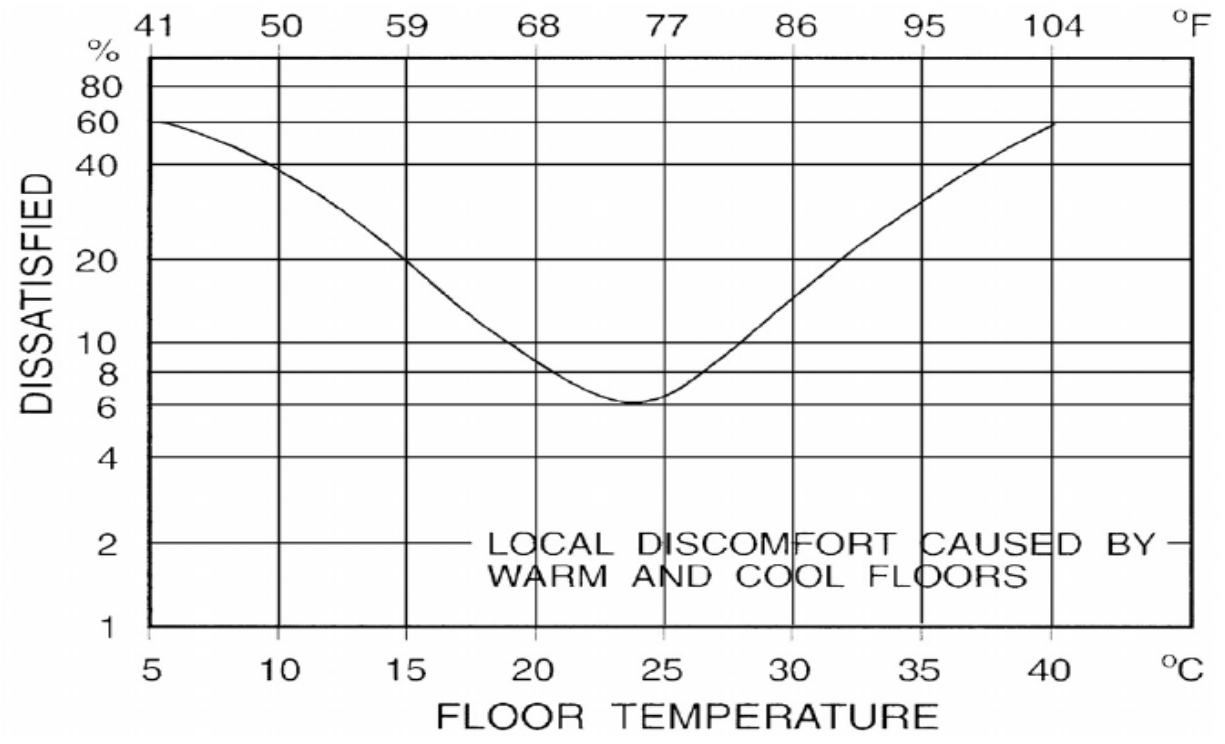

Figure 34: Local thermal discomfort caused by floor surface temperature (ASHRAE 55, 2013).

6.3 Indoor Air Assessment

6.3.1 Indoor Air

The indoor air temperature and relative humidity distributions are analyzed for the six pairs of experiments where the thermal energy comparisons are carried out. Whereas, for the last 13 pair of experiments where ventilation strategies and ventilation flow rates are compared, additional two indoor environmental parameters are added. They are CO2 distribution and air velocity distribution. The distribution of these parameters in the test room at a given time snapshot is mapped using the gradient of colours. The time that is selected for analysis is 6 AM, which is intended to avoid the interference of solar radiation in the analysis.

6.3.2 Ventilation Effectiveness

The data collected from the last eight pairs of experiments are used to analyze the performance of ventilation strategies as well as ventilation rates. The 7th to the 9th pair of experiments are intended to investigate the relative performance of mixed ventilation and underfloor ventilation strategies. The remaining analysis of 10 pairs of experiments is used to analyze the effect of ventilation flow rates in the indoor environment.

The ventilation performance analyzes is conducted by determining the ability of ventilation strategies or ventilation flow rates in removing pollutants from a given space. When examined for a specific point in the test area, it is called contaminant removal effectiveness (CRE), but when it is used to calculate for entire test room, it became global contaminant removal effectiveness (GCRE) (Sandberg et al., 1981). CRE at specific locations are calculated using Equation 28 (Krajčík et al. 2012) and measured CO2 and relative humidity at the location of interest. GCRE (Equation 29) determination, average contaminant concentration from all points are used.

$$CRE = \frac{C_o - C_i}{C_m - C_i} \tag{28}$$

$$GCRE = \frac{C_o - C_i}{\bar{C}_m - C_i} * 100\% \tag{29}$$

Equation 30 is adapted from Fanger et al. (1972) in which the percentage of dissatisfied (PD) expressed regarding ventilation flow rate ($\dot{v}$). The last analysis looks at the indoor air quality number (IAQN) where CRE and PD are related as given in Equation 31. Color plots of contaminant distributions at a time snapshot of 6 AM are used to interpret and analyze the impacts of ventilation strategies and ventilation flow rates in the indoor contaminant distribution.

$$PD = 395 * \exp(-1.83 * \dot{v}^{0.25}) \tag{30}$$

$$IAQN = \frac{CRE}{PD} \tag{31}$$

6.4 The Weather Condition during the Experimental Period

Figure 35 presents the outdoor weather condition during the experimental measurement period (Jan 1 to Jun 30). The average RH value is 75% with 18% standard deviation. Whereas, the outdoor air temperature and horizontal solar radiation gradually increase as the experimental period progresses from winter to summer season. The outdoor air temperature when the heating system comparisons are carried out varies between 0ºC to 15ºC, and 15ºC to 20ºC during the rest of the experimental period.

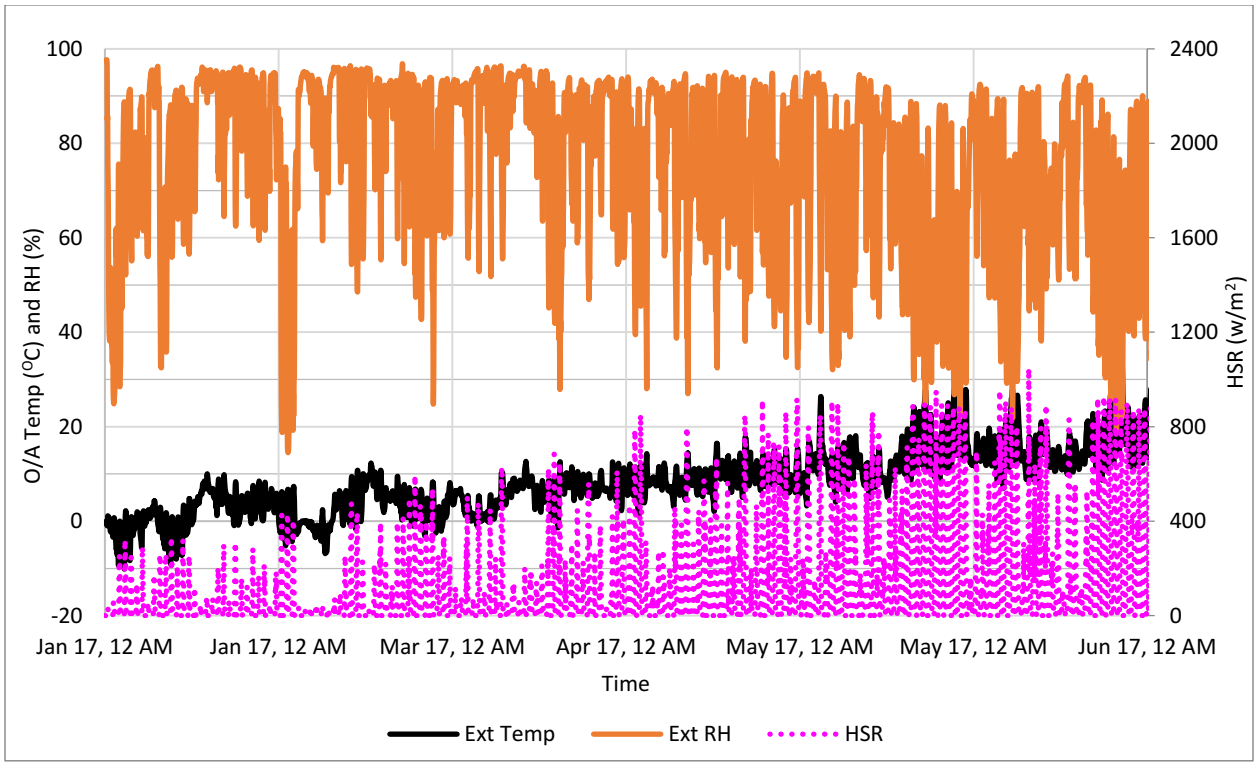

Figure 35: Outdoor weather condition over all the measurement period.

7 RESULT AND DISCUSSION

7.1 Heating Systems Comparison

7.1.1 Thermal Energy

Thermal energy is vital to keep dwelling space warm enough for occupants during the winter season. Therefore, the thermal energy supply by four heating systems (EBH, HP, PRH, and RFHS) over the four-day period is evaluated using the result from six pairs of experiments. As presented in the Data Analysis (Section 6), both EBH and PRH are assumed to be 100% efficient that is all the electrical energy used by these devices convert to the thermal energy which is equal to the power scout reading. The thermal energy of the HP is calculated using a COP of 2.1 as determined in the previous section.

Figure 36 presents hourly average thermal energy provide by EBH and HP, which depicts similar trend over a four-day period. The indoor temperatures of the two test buildings, outdoor temperature, and horizontal solar radiation are superimposed; whereas, the hourly average thermal energy of EBH and HP are represented separately using solid blue and black lines respectively. As illustrated in Figure 36, the thermal energy supply to the test rooms varies with outdoor weather conditions to maintain similar set point temperature. For example, during the night time, due to lack of solar radiation, and low outdoor temperature, the thermal energy supply of the systems increases to maintain the setpoint temperature. Whereas, in the daytime, solar heat gain increases and outdoor temperature increases thereby reducing the thermal energy required to reach the setpoint temperature. Similar thermal energy profile plots of the five remaining experiments are reported in Appendix II section 1.

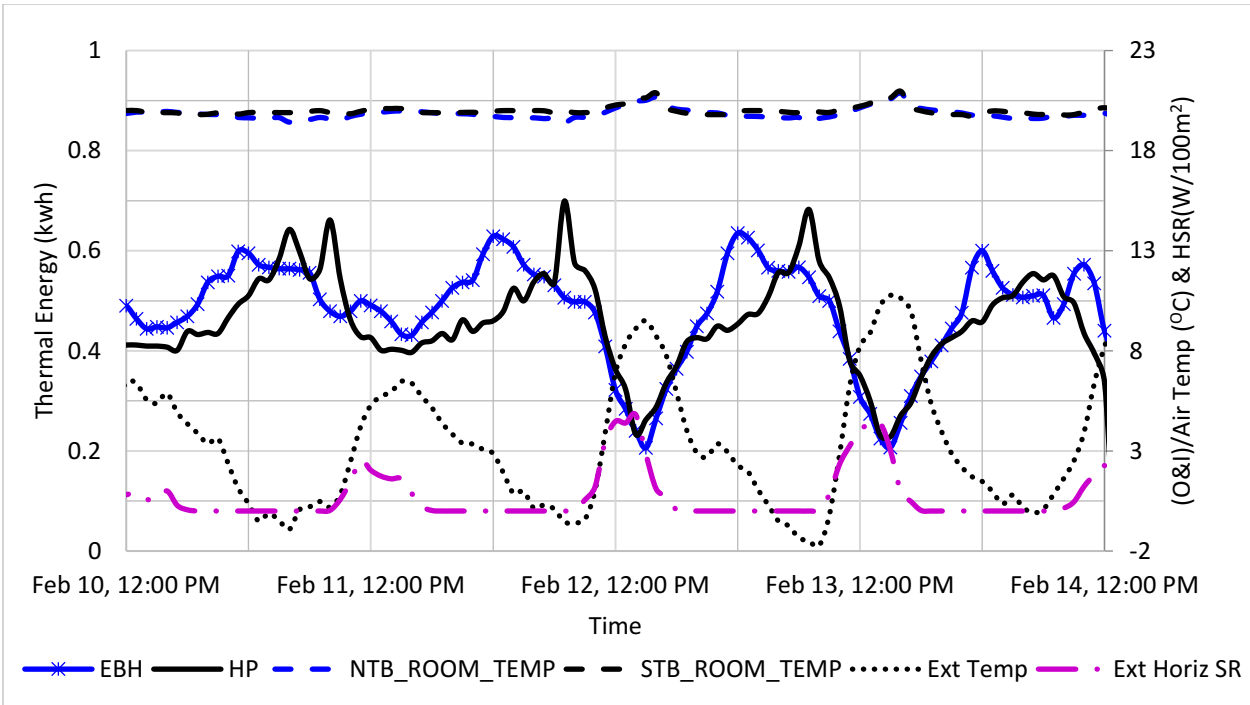

Figure 36 Thermal Energy profile of EBH and HP with indoor and outdoor conditions.

A pairwise comparison of the thermal energy supply by four heating systems over the course of 24-hours of the four-day period in which the maximum room temperature difference is less than 0.5ºC. Figure 37 shows both the indoor and outdoor conditions as well as maximum room temperature differences which is the baseline for the comparison. Figure 37 shows the maximum temperature difference for all experiments in which the temperature difference remains between 0.3ºC and 0.45ºC. Whereas, the outdoor temperature stays less than 8ºC in all comparisons.

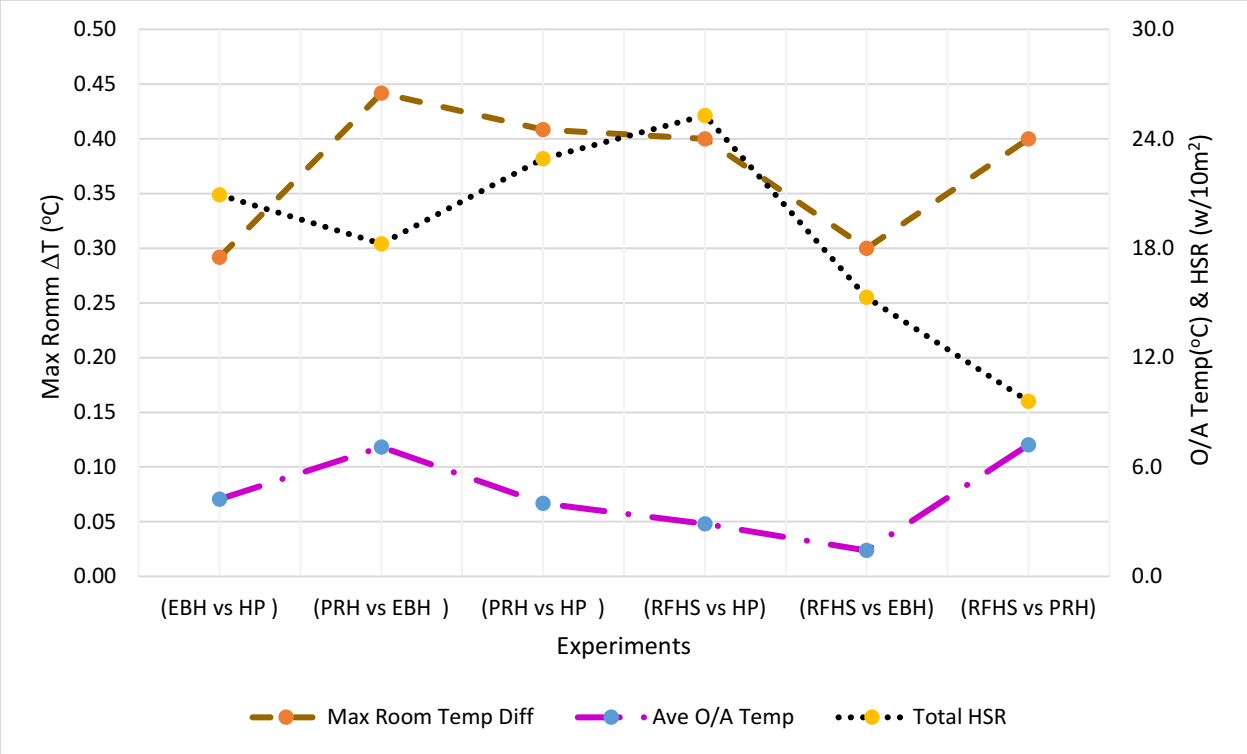

Figure 37: Average outdoor weather condition and interior temperature difference during when thermal energy is compared.

HP and EBH demonstrate a smooth trend (as shown Figure 38 A and B) whereas PRH shows fluctuating thermal energy profile as shown in Figure 38 B and C. Overall, 0.3 kWh to 0.6 kWh of thermal energy is supplied by all heating systems depending on the outdoor temperature and solar radiation. Additionally, Figure 38 A, C and E show that the thermal energy supply of all the heating systems responds to outdoor conditions change. Decreasing during the daytime where the outdoor temperature and solar radiation are high and increasing overnight where the outdoor temperature is low. For example, the effect of outdoor conditions is apparent in Figure 38 A where both EBH and HP provides slightly over 0.2 kWh during the daytime when the outdoor temperature is close to 10.5ºC. While, when the outdoor temperature is close to -2ºC around 6:00 AM, both heating systems deliver around 0.5kWh.

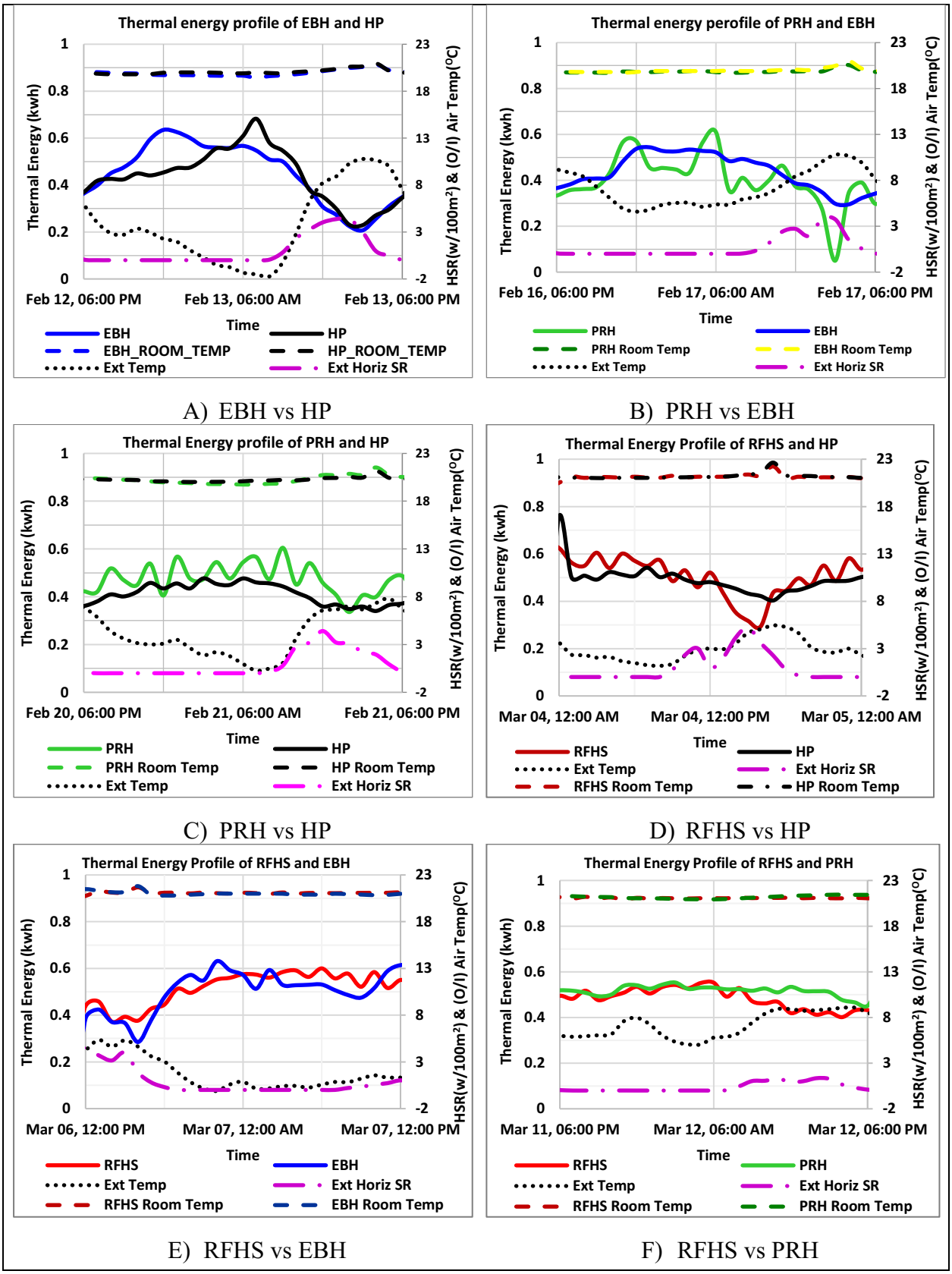

Figure 38: Thermal energy profile of four heating systems for a single day.

Table 8 presents a summary of the total daily thermal energy consumptions of the four heating systems in the six pairs of experiments: that is RFHS vs HP, RFHS vs EBH, EBH vs PRH, EBH vs HP, PRH vs HP, and PRH vs RFHS. The RFHS supplies 3.4% and 1.8% more thermal energy than HP and EBH, respectively. The EBH, in contrast, supplies 7.8% more than PRH and 4.0% more than HP. Whereas, PRH provides 13.1 % more thermal energy than HP and 6.3% more than RFHS. The reason why PRH outputs more thermal energy in comparison to HP and RFHS can be attributed to the fact that the thermostat resides inside the unit, which is positioned close to the window. Overall, all heating systems are able to maintain a similar set point by providing similar (small difference) thermal energy. As shown in Table 8 and Figure 39, depending on the outdoor weather conditions, 10 kWh to 14 kWh total daily thermal energy is required to heat the rooms during the experimental period.

Table 8: Summary of total thermal energy and outdoor/indoor conditions over 24 hours.

Experiments	Ave O/A Temp (^{O}C)	Max Room Temp Diff (^{O}C)	Total HSR (W/m2)	Energy(kwh)				Diff	%
				HP	**EBH**	**PRH**	**RFHS**		
(HP vs EBH)	4.2	0.29	20.92	10.1	10.6			0.4	4.0
(EBH vs PRH)	7.1	0.44	18.23		10.5	9.7		0.8	7.8
(HP vs PRH)	4.0	0.41	22.9	9.9		11.4		1.5	13.1
(HP vs RFHS)	2.9	0.40	25.28	11.5			11.9	0.4	3.4
(EBH vs RFHS)	1.4	0.30	15.30		13.4		13.6	0.2	1.8
(PRH vs RFHS)	7.2	0.40	9.61			12.4	11.6	0.8	6.3

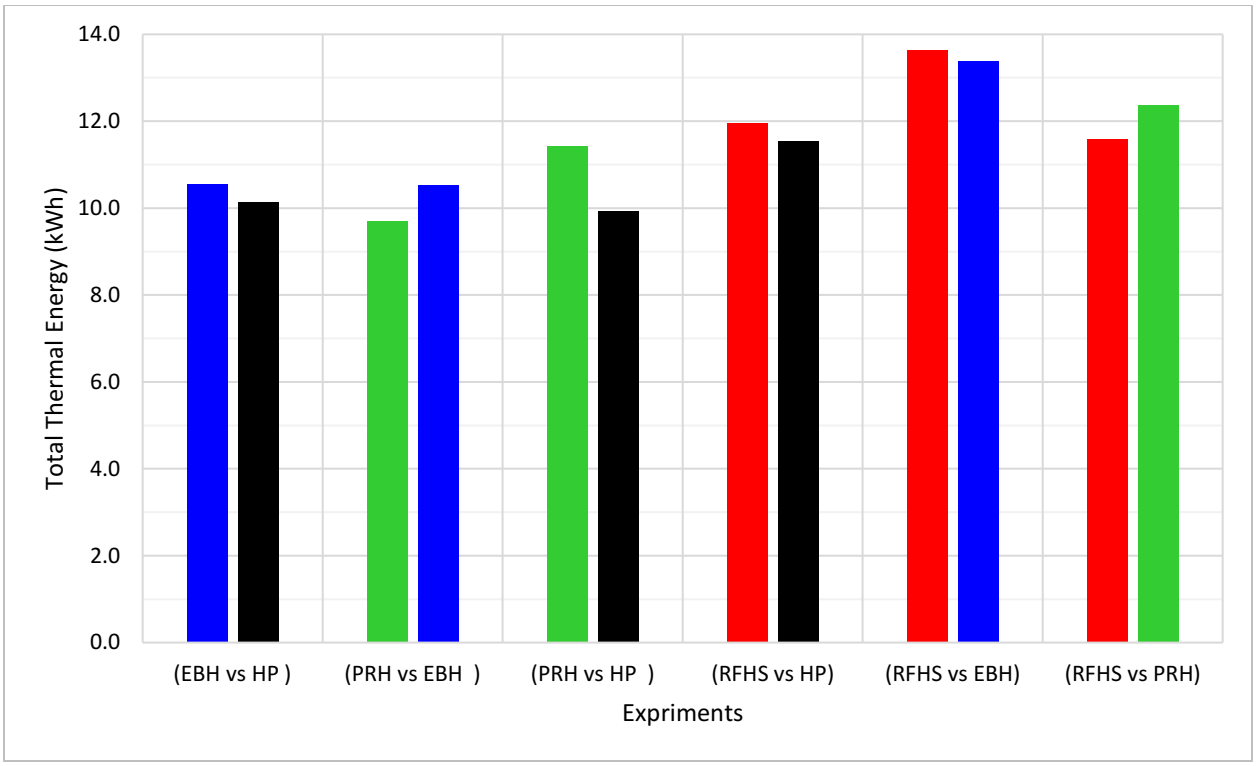

Figure 39: One-day total thermal energy supply at the same outdoor and indoor environmental conditions.

The radiant floor heating system provides thermal energy by two methods of heat transfer: convective and radiative heat transfer mechanisms. Of the total thermal energy in the test room and supply by radiant floor heating system, the contribution from convective energy (qc) is found to be less than 30% while the remaining amount, an excess of 70% supply by radiative energy (qr) as shown in Figure 40. This result is in agreement with Xiaozhou et al. (2013) finding, which suggests that the thermal energy supply of the radiant floor heating system is not evenly distributed (50% convective, 50% radiative). But instead, the radiative heat transfer has the upper hand in delivering the required thermal energy to the test space.

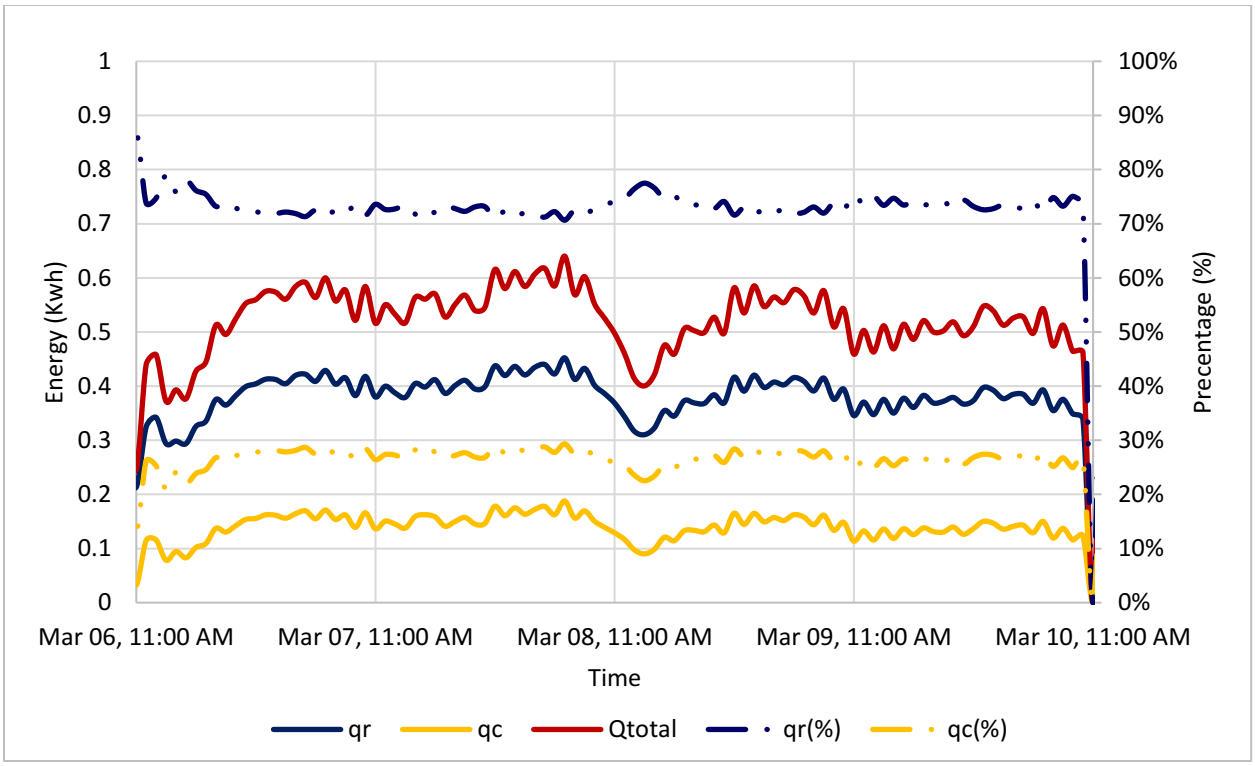

Figure 40: Components of thermal energy delivered by RFHS.

The thermal energy supply by the RFHS is determined using a fundamental heat transfer equation of both convective and radiation heat exchange using the corresponding view factors of the surrounding surfaces relative to the floor. Use of heat transfer coefficient (convective plus radiation heat transfer coefficient) like ASHRAE Fundamentals (2017) h = 9.26 W/m^2 K (for horizontal surface heat transfer upward) underestimate the actual thermal energy supply as shown in Figure 41. A better agreement, within ± 10%, depending on the temperature difference between the floor and the mid-height of the test room, is obtained when using h = 11 W/m^2 K from EN15377 (2005). When the floor temperature reaches around 22°C, the temperature difference gets smaller, as a result; it underestimates the thermal energy up to 10%. Whereas, when the floor temperature increases the estimation gets much closer to the actual thermal energy supply to the test room.

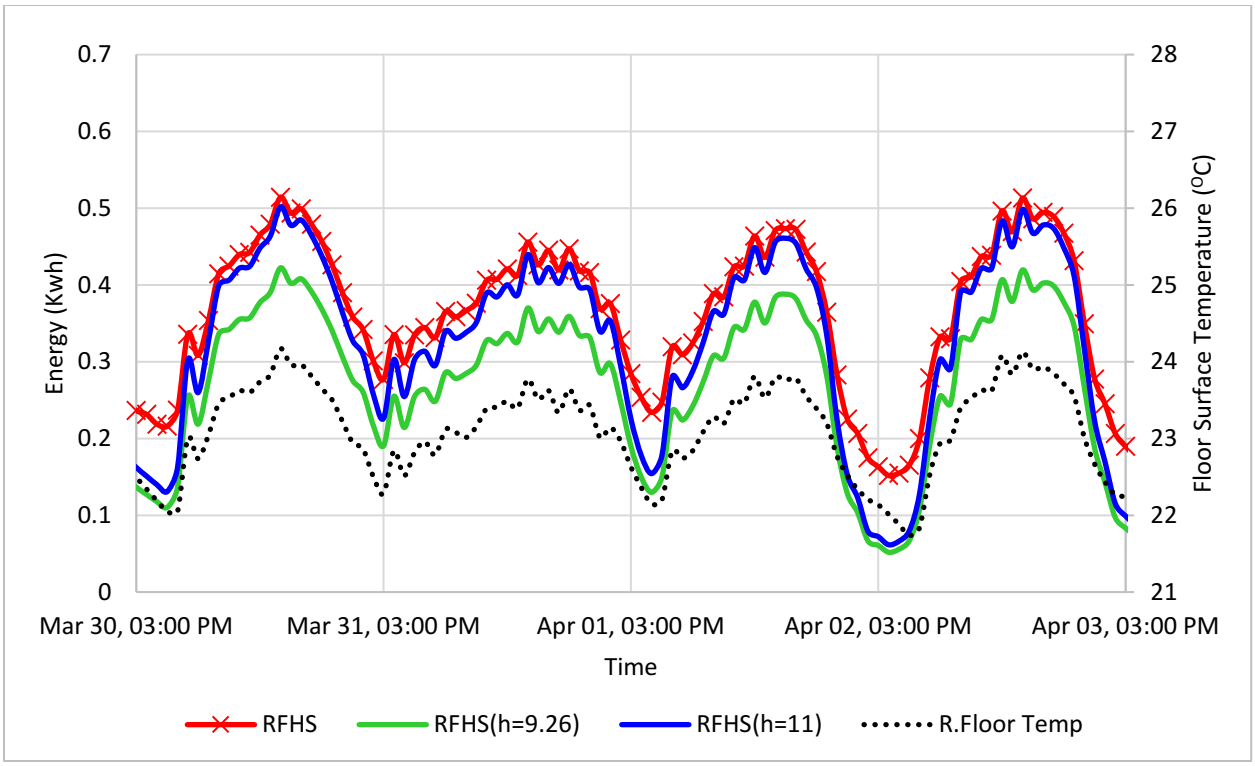

Figure 41: Thermal energy estimation using three film coefficients and actual thermal energy.

7.1.2 Indoor Air Temperature and Relative Humidity Distributions

This section discusses the indoor air temperature, relative humidity and the surface temperature distributions in the test buildings while using different heating systems. Figure 42 shows the horizontal and vertical sensor layouts which are used to collect data. The temperature measurements at five horizontal locations (L1, L2, L3, L4, L5) and five vertical positions (P0, P1, P2, P3, P4, PC) are discussed. In addition, relative humidity measurements from those five horizontal locations and three vertical positions (P2, P3, and P4) are presented. Similarly, the surface temperature distribution of the corresponding vertical positions on the surrounding wall surfaces is discussed. With the intention of avoiding solar radiation interference, the temperature and RH distributions in the test buildings at 6 AM are presented. Four heating systems in of the 6 pairs of experimental tests conducted for heating systems comparison, four representative test cases are presented here, and the indoor and surface temperature profiles of the rest of the test cases are documented in Appendix II section 4, 5, and 6.

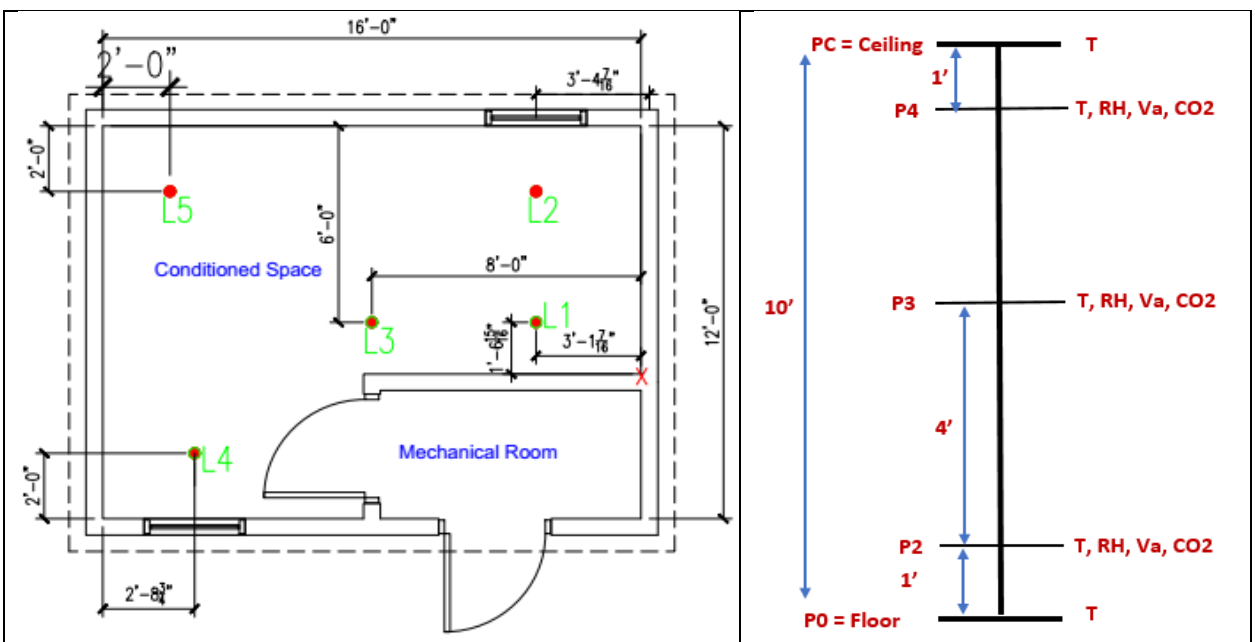

A) Horizontal stand locations

B) Vertical Sensor positions

Figure 42: Sensor layout, Horizontal and vertical.

7.1.2.1 Indoor Air Temperature Distribution: Heating System Comparison

The temperature distribution from 1ft above the floor up to 1 ft below the ceiling are presented using a colour gradient as shown in Figure 43. Two colour gradient plots are presented in this section: the first one is a plot that shows the temperature gradient from floor to the ceiling in the test room, and the second one is a plot that shows a gradient of temperature difference from a reference point, centre of the test room (L3P3). The centre point (L3P3) is monitored to keep within 21±1°C for all cases.

The highest temperature is measured when using HP, EBH and PRH is close to the ceiling: 21°C. Whereas, the coldest temperature measured is 1 ft above the floor (across P2) for all heating systems except RFHS. In addition, the temperature difference between P4 and P2 remain around 3°C for those three heating systems, but in the case of RFHS, the vertical temperature difference is less than 0.4°C. As illustrated in Figure 43 the temperature distribution when using RFHS is more uniform (21±0.5°C) relative to a room with HP, EBH, or PRH.

RFHS					
P4	20.9	20.8	21.2	20.7	20.3
P3	21.1	20.7	21.3	20.7	20.6
P2	21.0	20.7	21.3	20.7	20.7
4th	L5	L4	L3	L2	L1

HP					
P4	20.8	20.8	21.3	21.0	20.1
P3	20.4	19.7	20.8	19.9	19.3
P2	19.3	18.8	19.8	19.4	18.0
3th	L5	L4	L3	L2	L1

EBH					
P4	21.4	20.9	21.4	21.3	21.0
P3	20.7	19.9	21.0	20.2	19.6
P2	18.9	18.5	19.5	18.6	18.0
2th	L5	L4	L3	L2	L1

PRH					
P4	21.0	20.9	21.2	21.4	20.9
P3	20.5	20.0	20.8	20.0	19.6
P2	19.2	18.8	19.9	19.3	18.5
5th	L5	L4	L3	L2	L1

Color Legend		
Ave of Min	Ave	Ave of Max
15	20	25

Figure 43: Indoor temperature distribution using four heating system within the period where thermal energy is compared.

Figure 44 illustrates the temperature difference between the centre point and the other measurement point in the test rooms. Above the floor, the HP creates a temperature distribution ranging less than 2°C close to the floor and over 1.4°C at L2PC, which is in front of the unit. In the case of both EBH and PRH, the temperature distribution below P3 (5ft or half way between ceiling and floor) is -3°C to 0°C relative to the centre. However, above P3 the temperature profile shows warm trend even over 1°C (relative to the centre) for instance at L2P4, which is straight above the heating units. Also, RFHS creates more uniform temperature distribution relative to the centre. For example, above the floor, the temperature difference relative to the centre remains between -1°C and 0°C throughout the measurement points.

RFHS					
P4	-0.4	-0.5	-0.1	-0.6	-1
P3	-0.2	-0.6	0	-0.6	-0.7
P2	-0.3	-0.6	0	-0.6	-0.6
4th	L5	L4	L3	L2	L1

HP					
P4	0	0	0.5	0.2	-0.7
P3	-0.4	-1.1	0	-0.9	-1.5
P2	-1.5	-2	-1	-1.4	-2.8
3th	L5	L4	L3	L2	L1

PRH					
P4	0.2	0.2	0.4	0.7	0.1
P3	-0.2	-0.8	0	-0.8	-1.2
P2	-1.6	-2	-0.9	-1.4	-2.3
2th	L5	L4	L3	L2	L1

EBH					
P4	0.4	0	0.4	0.4	0
P3	-0.3	-1	0	-0.7	-1.3
P2	-2	-2.4	-1.5	-2.3	-3
2th	L5	L4	L3	L2	L1

Color Legend		
Min	Ave	Max
-1	0	1

Figure 44: Normalized interior temperature using four heating system within the period where thermal energy is compared.

7.1.2.2 Indoor Humidity Distribution: Heating System Comparison

The objective of this section is to discuss Relative humidity (RH) distribution in the test room using the same experimental data which is used to compare four heating systems. The RH distribution for all heating systems is between 40% and 50% with an average of 45% throughout the room as illustrated in Figure 45. The RH distribution in the test room demonstrates acceptable RH value for a dwelling space. The RH Distribution in the case of RFHS shows 45 ± 1% in all locations except L2 (above 46%) which is in front of the south window. While for the other heating systems the RH distributions in the test room inversely relate to the temperature distributions presented in Figure 43. High RH measurements are across P2, which are close to the cold floor surface. Low RH values are obtained across P4 the warmest region of the test room since it is close to the ceiling.

In the case of HP, the RH distribution is below the average RH (45%) except close to the floor. Whereas, across the centre (P3) it is between 45% and 48%. Close to the floor (across P2) it is slightly more compare to the midsection which is 45±1%. The reverse is true in the upper section (P4). Overall, the RH distribution in all cases is within the range of acceptable value according to ASHRAE Fundamentals (2017), which recommend 30% to 60% for a living space. The RH distribution in the test room with RFHS is uniform compared to the other heating systems. Whereas, the RH distribution of the test rooms using EBH and HP are similar having the lowest concentration at L5P4, L4P4, and L3P4 which are close to the ceiling. While using PRH the highest RH measurement is across P2 (around 50%), and the lowest data is measured across P4 (about 43 %).

RFHS

P4	45.3	45.3	44.8	46.7	45.5
P3	45.0	45.4	45.0	46.2	44.5
P2	44.3	45.4	45.3	46.4	44.3
7th	L5	L4	L3	L2	L1

EBH

P4	39.0	40.3	39.7	42.9	42.1
P3	45.0	44.8	43.3	46.8	47.3
P2	45.4	45.1	46.1	48.3	46.5
8th	L5	L4	L3	L2	L1

HP

P4	41.9	41.2	41.9	43.5	43.5
P3	44.6	44.8	42.7	45.8	46.9
P2	46.8	45.5	47.0	47.3	45.9
6th	L5	L4	L3	L2	L1

PRH

P4	43.2	42.8	42.5	45.5	46.2
P3	47.4	47.5	46.5	48.4	47.5
P2	48.0	47.5	48.2	51.1	48.2
5th	L5	L4	L3	L2	L1

Color Legend

Ave of Min	Ave	Ave of Max
35	45	55

Figure 45: Interior RH distribution using four heating system within the period where thermal energy is compared.

7.1.2.3 Surface Temperature Distribution: Heating System Comparison

This section discusses the surface temperature distribution in the test rooms as the result of using different heating systems. Surface temperature has an effect on envelope durability due to condensation and mould growth, and also occupant's thermal comfort as it is involved in radiation heat transfer exchange with occupants.

As shown in Figure 46, when using RFHS, the surface temperature on the south and west walls are close to 21 ± 0.5°C (in line with room temperature) whereas the east wall is 20 ± 0.5°C which is 1°C below the room set point temperature. While using HP, EBH, and PRH, the surrounding walls (East, South, and West) are around 20 ± 1°C in most measurement points. Besides, the coldest surface is a north window, which is far from the heat source. Whereas, the East wall in case of PRH is a little bit cold (-1°C) at P3 and P4 relative to EBH, which is far from the heating units in both cases. The wall temperature also follows the room temperature profile getting warmer going up from the floor for both EBH and PRH with a small difference. Overall, the surrounding wall surface temperature is relatively cold compared to the room temperature setpoint while using all heating systems except RFHS.

The surface temperature with EBH and PRH shows that the South and West wall is slightly warmer in comparison to East wall. It is because the East wall is relatively far from the heat source. The warmest surface temperature measured is the floor when using RFHS as shown in Figure 46. Whereas, when using EBH, PRH and HP, the floor is relatively cold to the other surfaces. L2P3 and L2P4 measurement points are relatively warm (21°C) compared to room temperature (20°C) when using EBH and PRH. Overall, the RFHS creates a relatively more uniform surface temperature compared to EBH, HP and PRH.

EBH

PC	20.8		22.8		20.0		21.3
P4	20.2		21.1		21.6		
P3	20.0	19.5	20.2	20.0	20.5	19.6	
P2	18.1		19.4		19.2		
P0	16.1		17.7		18.1		16.8
Win			19.0				17.7
UV5	E/L5	ES-C3	S/L2	SW-C2	W/L1	NE-C1	N/L4

RFHS

PC	20.9		21.3		21.2		21.2
P4	20.1		20.9		21.0		
P3	19.6	18.2	21.2	19.5	21.0	18.7	
P2	20.5		21.6		21.4		
P0	25.3		21.8		25.4		25.3
Win			18.4				17.8
	E/L5	ES-C3	S/L2	SW-C1	W/L1	NE-C3	N/L4

PRH

PC	20.5		22.6		21.4		20.8
P4	19.0		20.9		21.5		
P3	18.3	19.9	20.2	19.5	20.4	18.0	
P2	17.7		19.2		19.5		
P0	16.9		19.0		18.3		16.9
Win			18.5				16.6
UV6	E/L5	ES-C3	S/L2	SW-C2	W/L1	NE-C1	N/L4

HP

PC	20.6		22.2		19.3		21.1
P4	19.8		21.0		21.0		
P3	19.7	19.1	20.7	20.2	20.0	19.1	
P2	18.0		19.7		18.9		
P0	16.8		18.1		17.8		17.1
Win			19.3				16.5
	E/L5	ES-C3	S/L2	SW-C2	W/L1	NE-C1	N/L4

Color Legend

Ave of Min	Ave	Ave of Max
14	20	24

Figure 46: Surface temperature distribution using four heating systems within the period where thermal energy is compared.

7.1.3 Thermal Comfort

In this section, the general and local thermal comforts results for cases with four heating systems are presented. For the analysis, the test buildings are assumed to simulate small study rooms with occupant's metabolic activity of Met = 1 for seating and reading, and Met = 1.2 for relax standing position, and a typical winter clothing value of 1 CLO.

7.1.3.1 General Thermal Comfort

The graphs in Figure 47 to 52 present the transient thermal comfort at the centre of the test rooms. Two cases are presented here, general thermal comfort for seating and standing position with four heating systems using the experimental data that are used for thermal energy comparison. In this analysis, the measured indoor air temperature, surface temperatures, relative humidity and air velocity are used to calculate thermal comfort. A time period between 6:00 AM to 10:00 PM are selected to discuss these results by excluding the sleeping period where the closing value and the metabolic rate is different.

As it is discussed in the Section 7.1.2.1, the floor surface temperature in the test room is found low with HP, PRH, and EBH which leads to relatively small mean radiant temperature, which consequently creates slightly cold thermal indoor environment. The room setpoint temperature is 21°C Although the thermostat maintains the air temperature at set point, the surrounding wall temperatures are relatively cold compared to the indoor air temperature as discussed in section 7.1.2.3. It is known that thermal comfort does not merely depend on the air temperature but also on mean radiant as well, which includes the temperature of the surrounding surfaces.

Figure 47 shows the thermal comfort (PPD) with EBH and HP where the room temperature is similar for a single day from 6:00 AM to 10:00 PM. The PPD profile shows a higher value for seating person for both heating systems between 25% and 32.5%. It is because the seating position

(0.6 m above the floor) is relatively close to the floor in contrast to standing person (1.1 m above the floor). The floor is relatively cold compared to the other surfaces which affect the PPD of seating in addition to lesser metabolic rate (1 met) compared to standing person (1.2 met). Whereas, for the seating person PPD remain between 7.5% to 10%.

solar radiation does not reach to the central points where thermal comfort is calculated, but incoming solar radiation hit the floor which heats the room. It is evident that the impact of solar radiation is seen in multiple cases (Figure 47 and 48). For an instant, in the case of 1st Experiment (EBH vs HP) during the daytime, the solar radiation and exterior temperature increases, as a result, the room temperature gets a little bit high, causing PPD to fall. However, early in the morning, there is no solar radiation, and the outdoor temperature is low, which lead to higher PPD. In this particular experiment, the higher PPD is after 6:00 AM, and it is around 32.5% for EBH as well as between 25% and 27.5% for HP. Whereas, the PPD fell to 22.5% for EBH and close to 20% for HP during the daytime in which the solar radiation and exterior temperature are high. These values show higher response by EBH compares to HP.

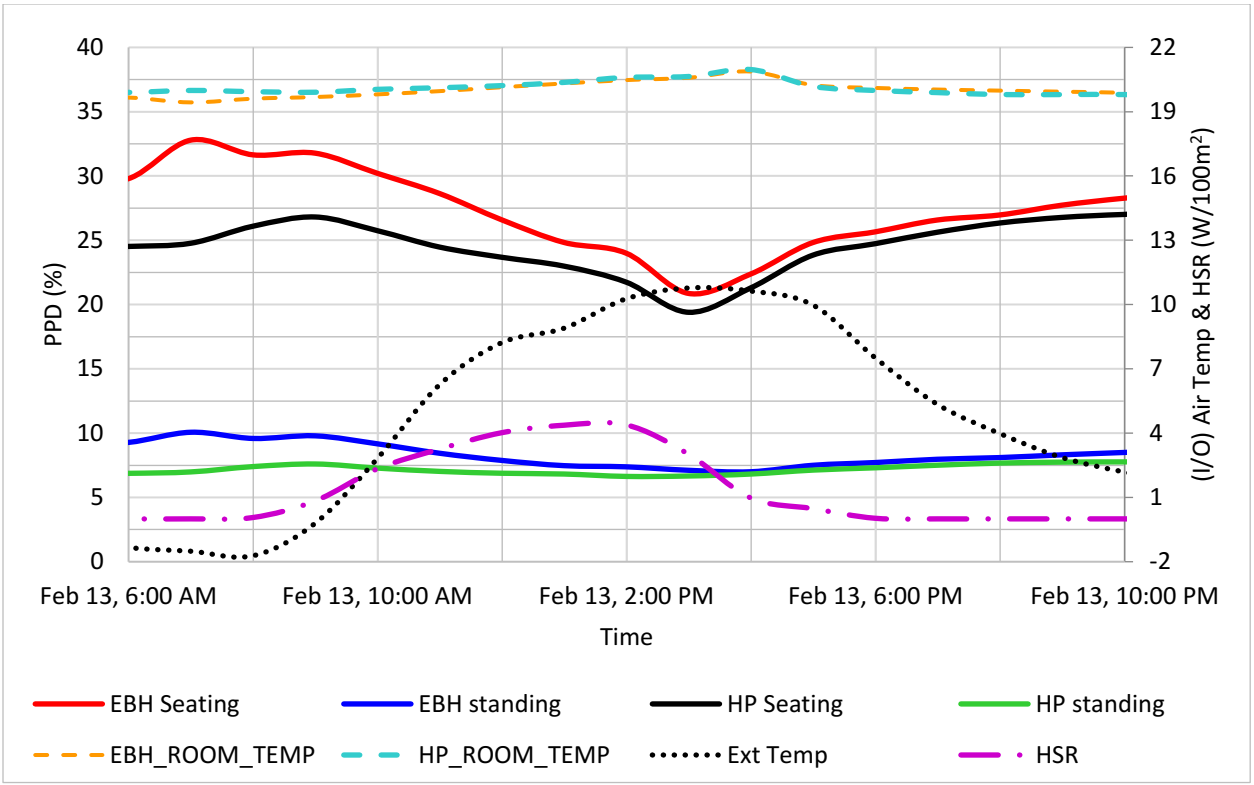

Figure 47: Thermal comfort (PPD) for a seating & standing person: EBH vs HP.

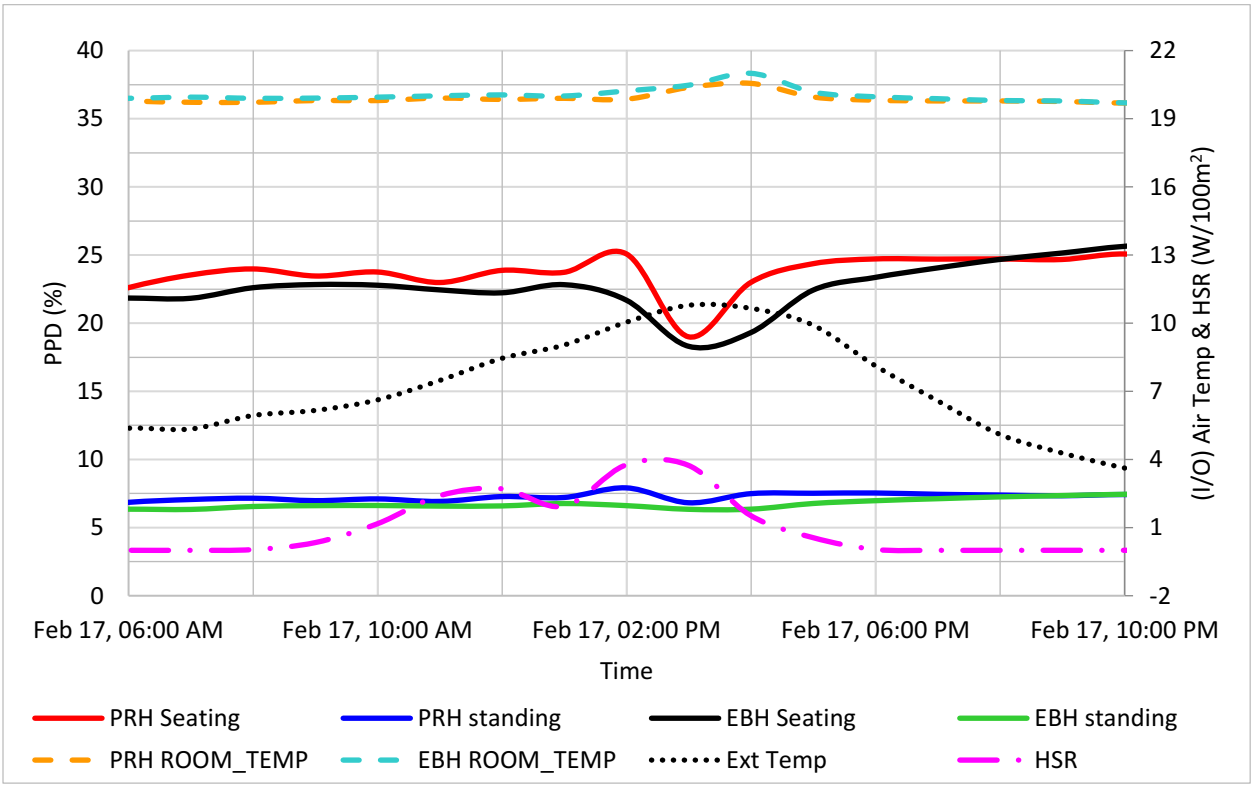

Figure 48: Thermal comfort (PPD) for a seating & standing person: EBH vs PRH.

The thermal comfort profile in Figure 49 present PPD in a room with HP and PRH. The HP repeats similar behaviour like the previous experiments, which is a relatively smooth trend in both thermal comfort and room temperature profile. Whereas, the room with PRH reflects similar outline like EBH, which is more reaction to the outdoor condition. When the solar radiation and exterior air temperature is high, PPD is low. Overall, both heaters, the PPD for seating person stay 25% ± 5% over the measurement period for this experiment depending on outdoor weather condition. However, throughout this experiment, the PPD is mostly within 7.5% to 10% for standing person using both heaters.

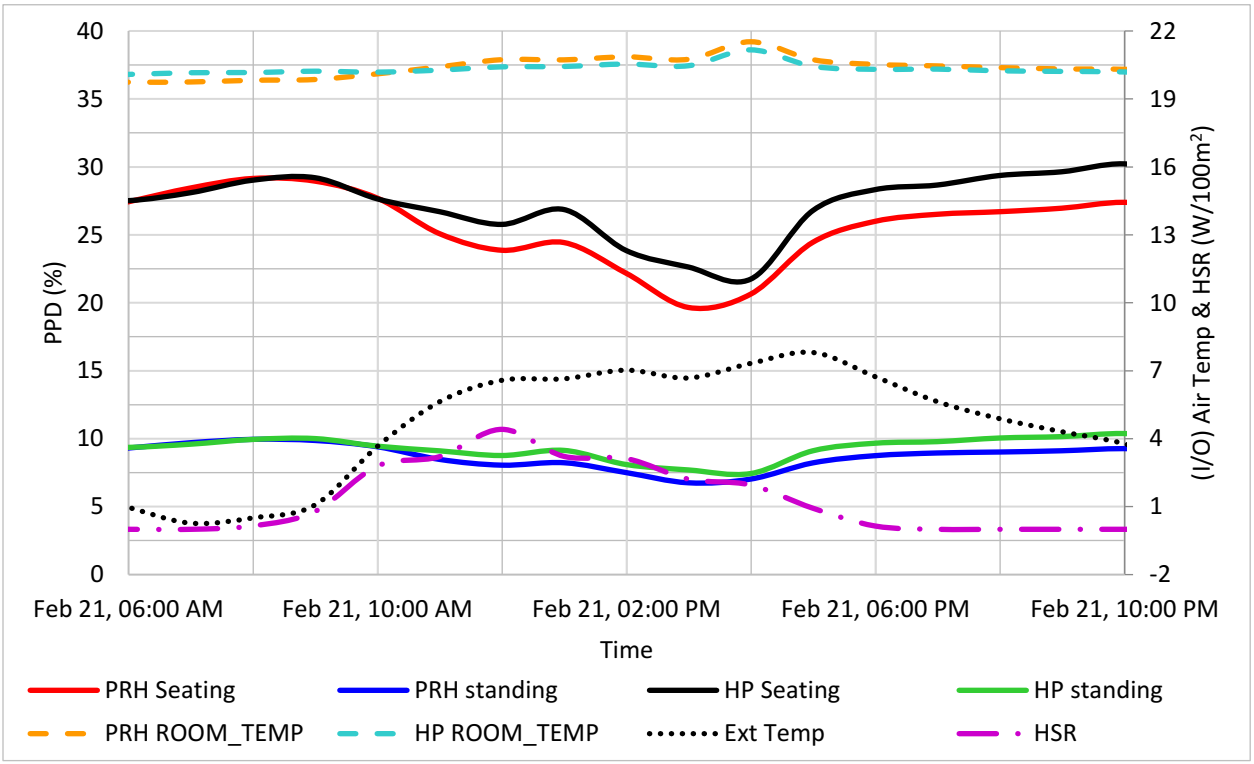

Figure 49: Thermal comfort (PPD) for a seating & standing person: PRH vs HP.

The thermal comfort when using RFHS shows PPD about 5% for standing person, which is the maximum to achieve. Moreover, in the case of seating person, RFHS again provide an acceptable thermal environment PPD = 10% ± 2.5% (Figure 50, 51, and 52) in all three experiments. It is

evident that high floor temperature radiates the heat energy and create a warm surface temperature leading to higher MRT unlike the rest of heating systems. In general, RFHS provides an acceptable thermal environment for both sitting and standing positions.

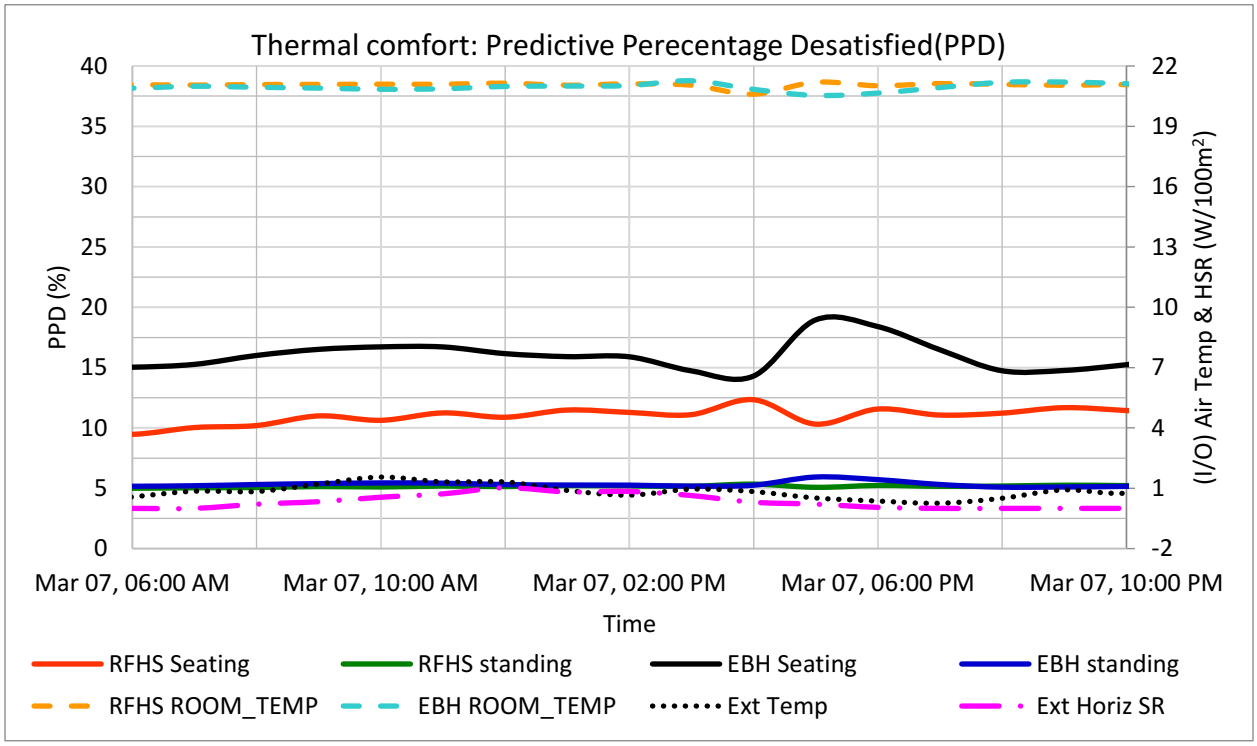

Figure 50: Thermal comfort (PPD) for a seating & standing person: RFHS vs EBH.

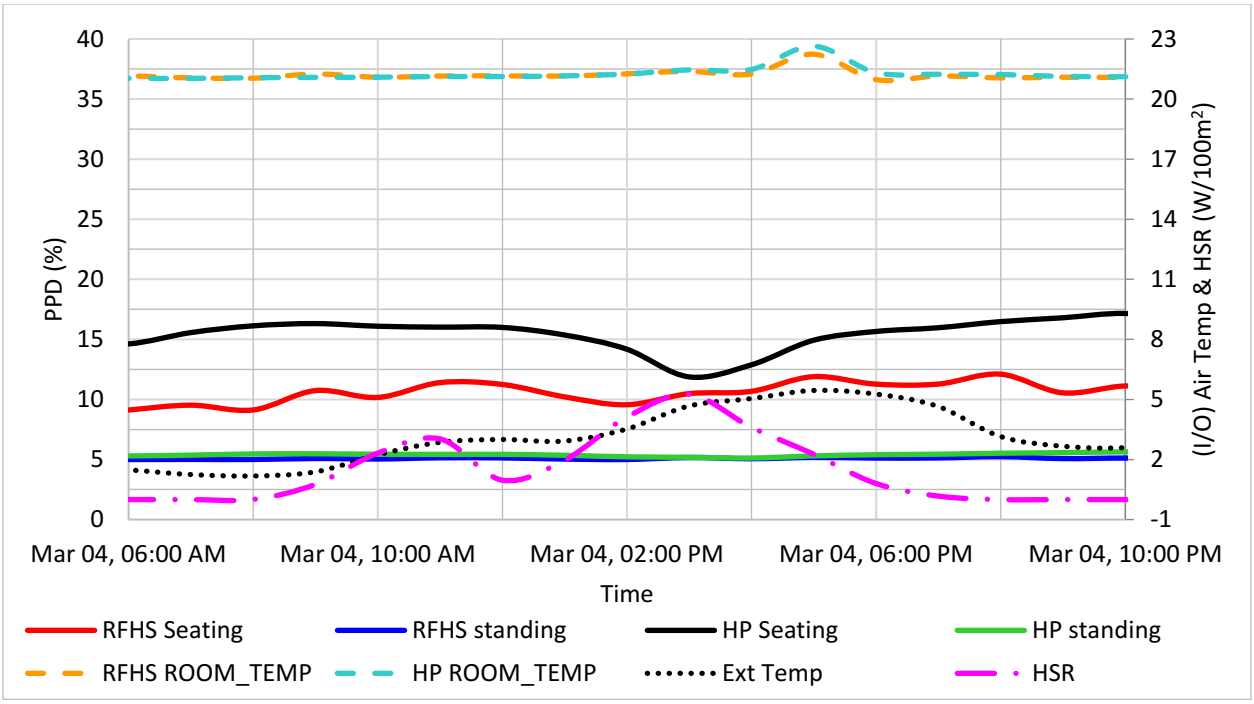

Figure 51: Thermal comfort (PPD) for a seating & standing person: RFHS vs HP.

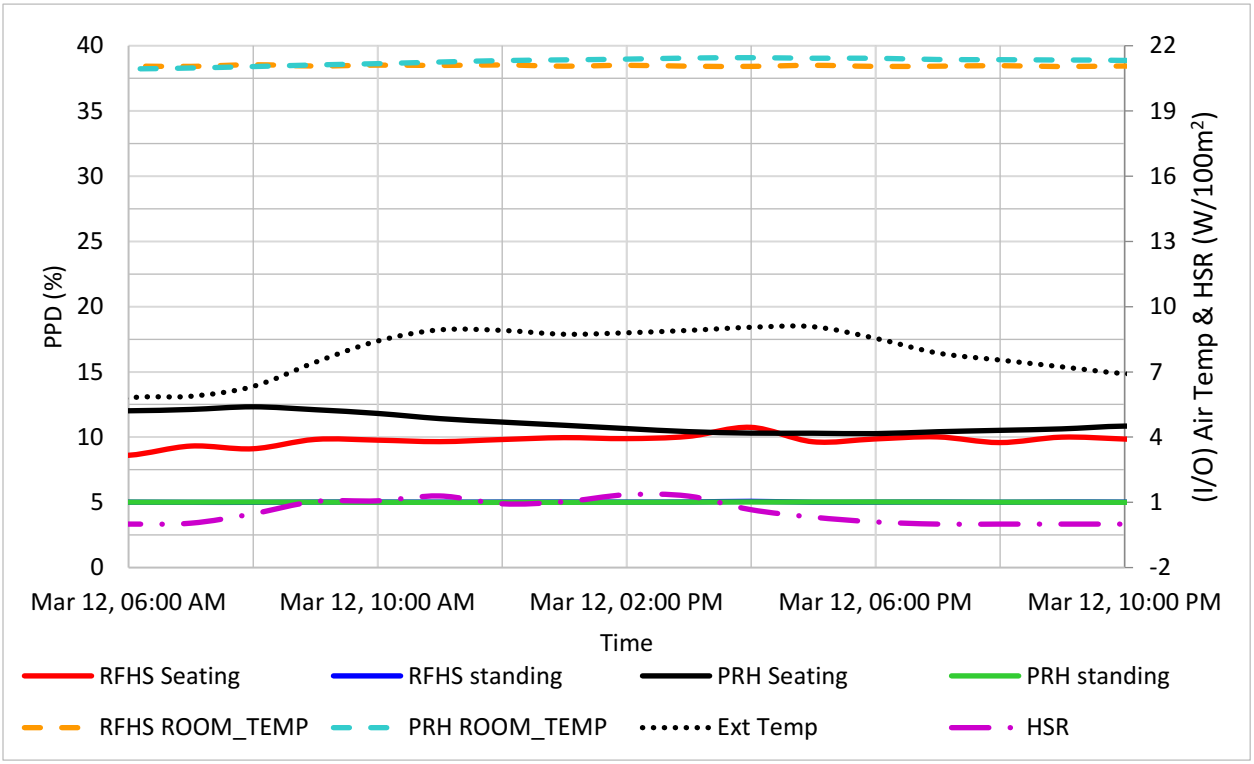

Figure 52: Thermal comfort (PPD) for a seating & standing person: RFHS vs PRH.

Table 9 shows the thermal comfort (PPD) of four heating systems and outdoor air temperature at 6:00 AM. As shown in the table, the thermal dissatisfaction (PPD) decreases as the outdoor temperature increase. For instance, in the case of RFHS, when the outdoor temperature is 5.3°C, the corresponding PPD is 9.5%, and the PPD is 8.6% when the outdoor temperature is 5.8. In case of PRH, PPD is 27.4%, 22.6%, and 12.0% for the corresponding outdoor temperatures 1°C, 5.4°C, and 5.8°C respectively.

Table 9: Thermal comfort (PPD) using four heating systems and outdoor air temperature at 6:00 AM.

Experiments	O/A Temp(°C)	Thermal comfort (PPD)			
		HP	EBH	PRH	RFHS
(EBH vs HP)	-1.3	24.5	29.8		
(PRH vs HP)	1.0	27.5		27.4	
(RFHS vs EBH)	3.0		15.0		9.5
(RFHS vs HP)	5.3	15.0			9.5
(PRH vs EBH)	5.4		21.8	22.6	
(RFHS vs PRH)	5.8			12.0	8.6

Overall, all heating systems provide acceptable thermal comfort (PPD < 20%) for standing person, but the occupant might feel slightly cool for a seating case depending on outdoor weather conditions. It is because a typical winter clothing value is assumed (1 CLO), the dweller might need to adjust clothing to avoid the slightly cold thermal sensation for a seating scenario. Otherwise, the occupant would feel thermally comfortable in a standing position with all heating systems.

7.1.3.2 Local Thermal Comfort

Three local thermal indicators apply to assess the local thermal comfort associated with the four heating systems. The indicators include local thermal discomfort as the result of radiant asymmetry, vertical temperature difference, and floor surface temperature. The radiant asymmetry has two parts: radiant asymmetry from floor to ceiling and radiant asymmetry due to a cold window. The summary of local thermal comfort using each heating system is discusses below. The single experimental result for each heating systems depict in the following section, and additional similar graphs are reported in the Appendix II section 7 to 10.

7.1.3.2.1 Local Thermal Discomfort as the Result of Vertical Temperature Difference

The local thermal discomfort due to vertical temperature difference is calculated at L3, which represent the centre of the test room. As stated on ASHRAE 55 (2013), thermal discomfort because of the vertical temperature difference should be less than 5%. As shown in Figure 53, the percentage of dissatisfied due to vertical temperature difference is between 0.75% and 2.25% for both seating and standing person when using both HP and PRH. While using EBH, the percentage dissatisfy stay between 1.25% and 2.75% for both seating and standing person as depicted in Figure 54. Whereas, while using RFHS, the PD is close to 0% for both seating and standing person. Also, the difference between the seating and standing is minimal. The difference between the seating and standing in the case of HP and PRH is close to 0.25% and over 0.25% for PRH. In general, the percentage of dissatisfied is less than 3% for all heating systems. As a result, all heating system creates acceptable local thermal discomfort as the result of vertical temperature difference for both seating and standing person.

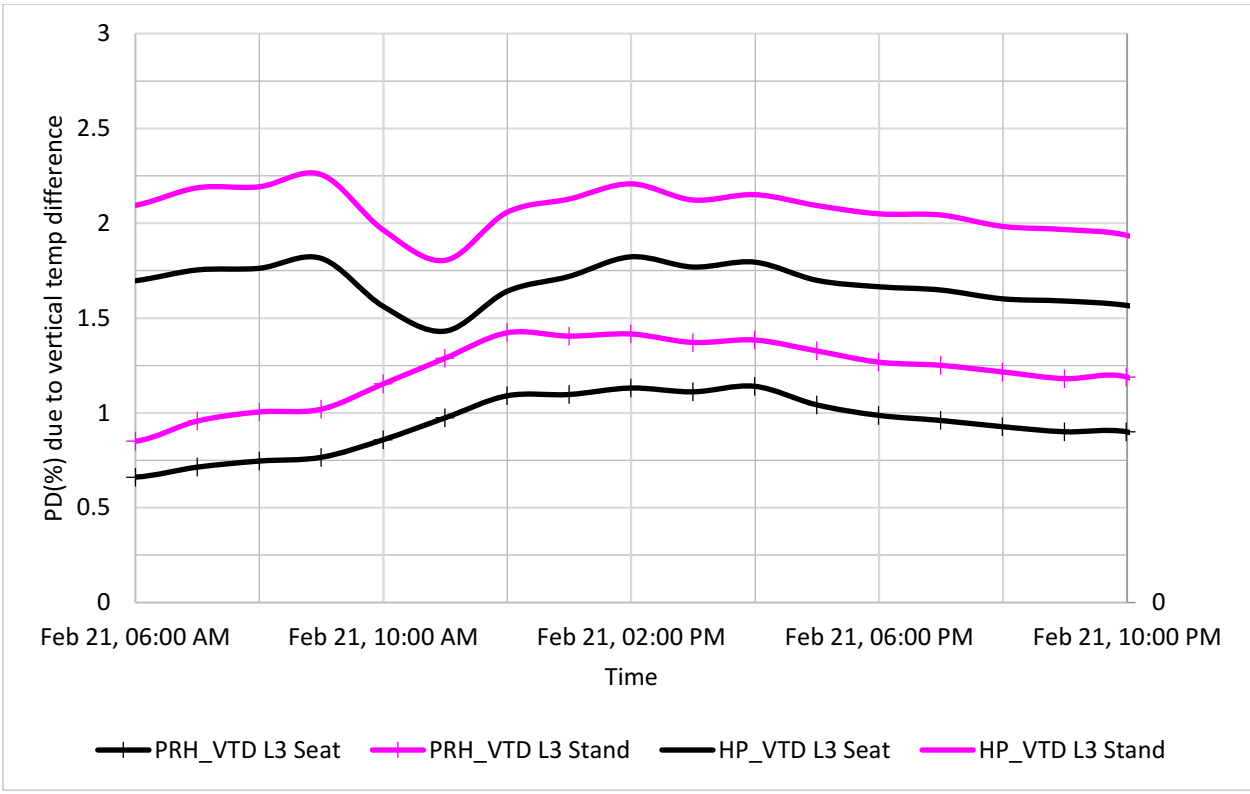

Figure 53: Local thermal discomfort due to vertical temperature difference: PRH vs HP.

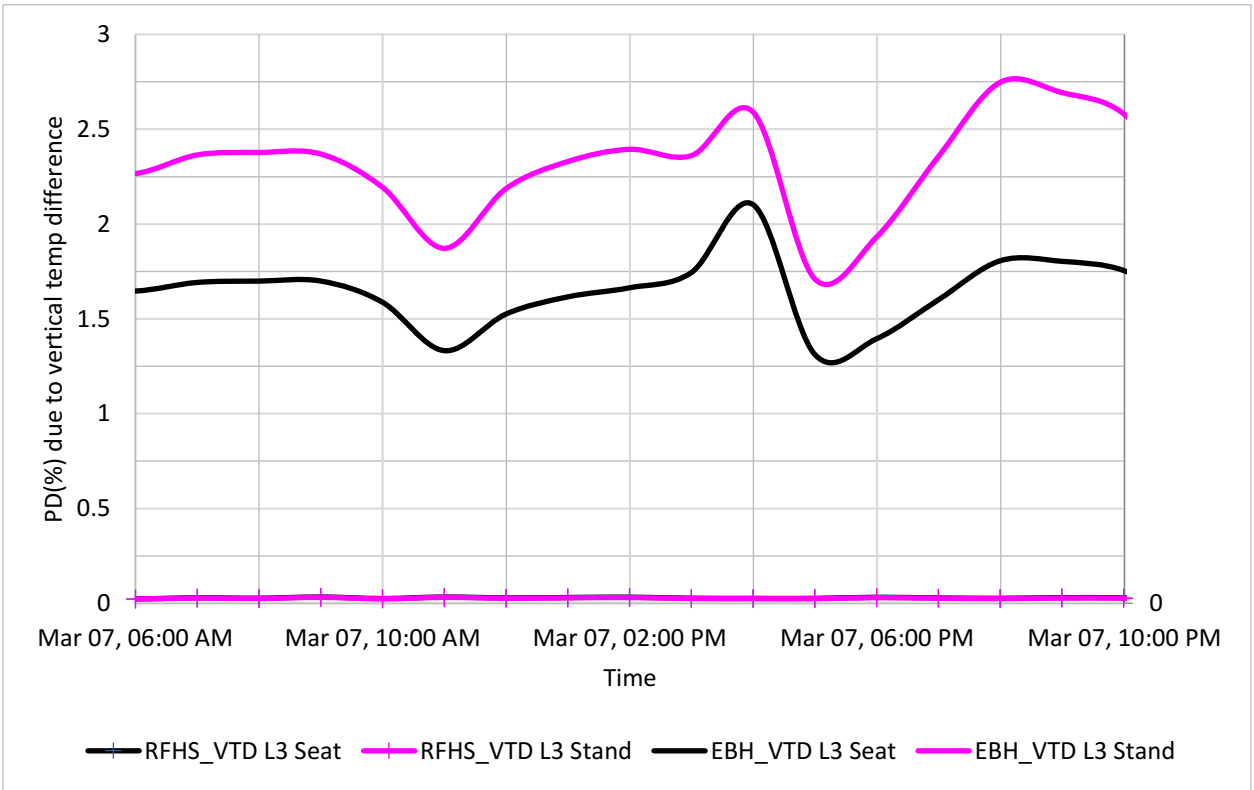

Figure 54: Local thermal discomfort due to vertical temperature difference: RFHS vs EBH.

7.1.3.2.2 Local Thermal Comfort as the Result of Floor Surface Temperature

According to ASHRAE 55 (2013), the percentage of acceptable dissatisfaction of local thermal discomfort due to floor surface temperature is 10%. The average floor temperature reading from five thermocouples is used to calculate PD due to floor temperature. The percentage of dissatisfied while using RFHS is within 6 ± 1%. While running HP, PRH, and EBH, the PD is between 12% and 15% as illustrated in Figure 55 and Figure 56. Overall, out of the four heating systems, only RFHS provides thermally acceptable floor surface temperature. Whereas for the remaining three heating systems it is beyond the acceptable range.

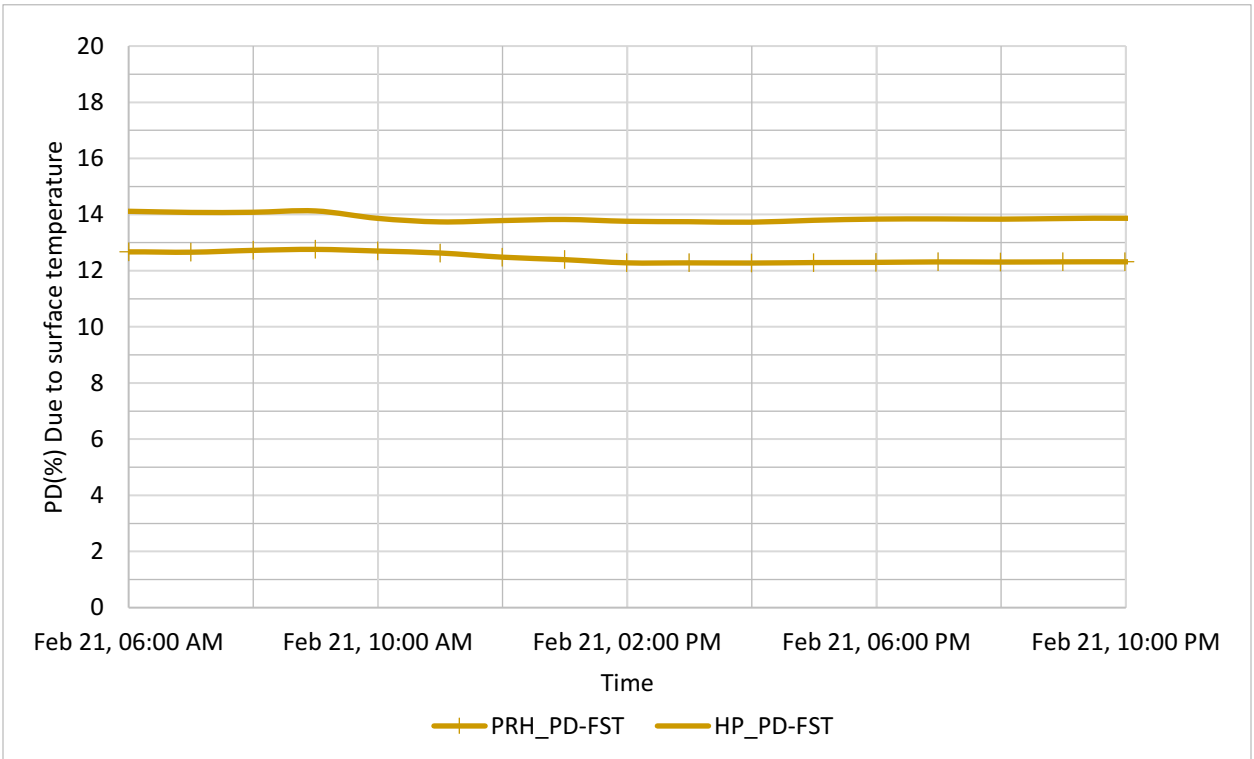

Figure 55: Local thermal discomfort due to surface temperature: PRH vs HP.

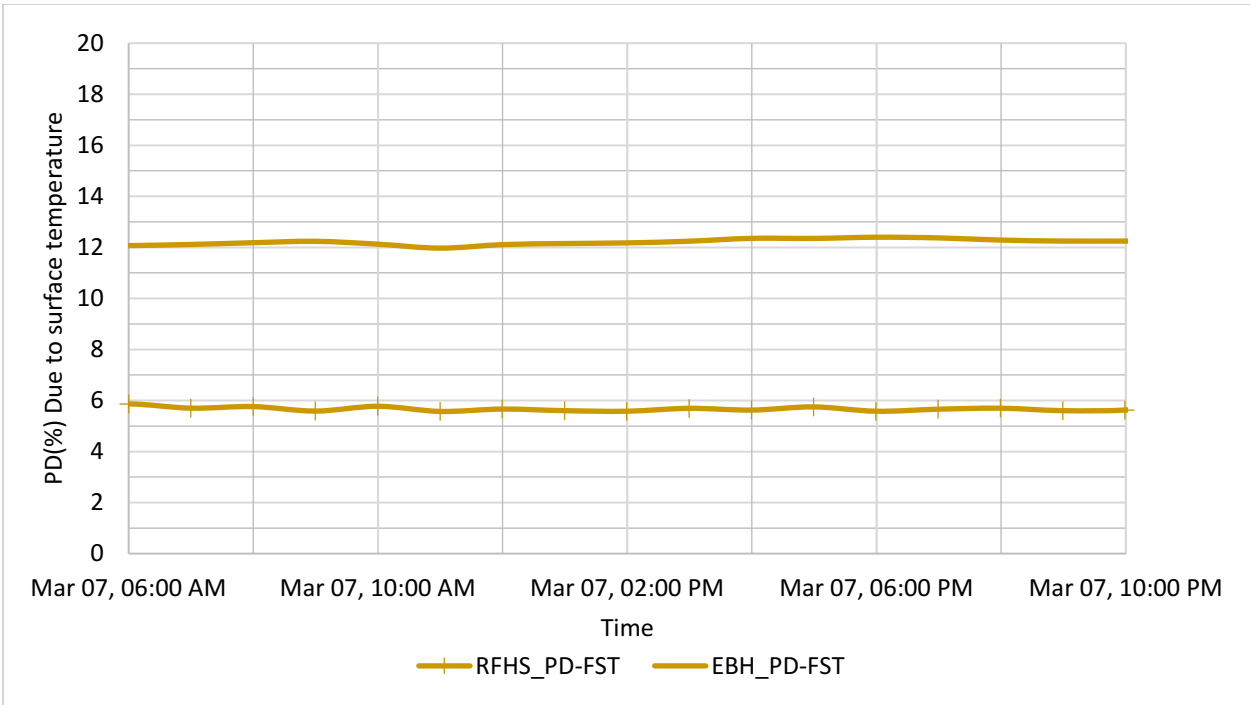

Figure 56: Local thermal discomfort due to surface temperature: RFHS vs EBH.

7.1.3.2.3 Local Thermal Discomfort as the Result of Radiant Asymmetry

7.1.3.2.3.1 Local Thermal Discomfort as the Result of Cold Window Radiant Asymmetry

Thermally, the windows are the weakest part of the envelope. As a result, it is the coldest surface as illustrate in section 7.1.2.3, which can cause thermal discomfort nearby. ASHRAE 55 (2013) specifies the maximum acceptable local thermal discomfort due to radiant asymmetry to 5%. While using HP, EBH, PRH, and RFHS, the average PD are mostly below 1.5% for both windows as illustrated in Figure 57 and 58. During the daytime when the sun hits the window, the temperature rises, and the radiant asymmetry then turns from cold window to warm for a brief moment. As a result, the PD goes up but still stay within the acceptable limit. This behaviour exhibits more in the south-facing window rather than north facing, which do not have the same temperature fluctuation and solar exposure as the south-facing window. Overall, the radiant asymmetry due to the cold window for all heating systems is within the acceptable range.

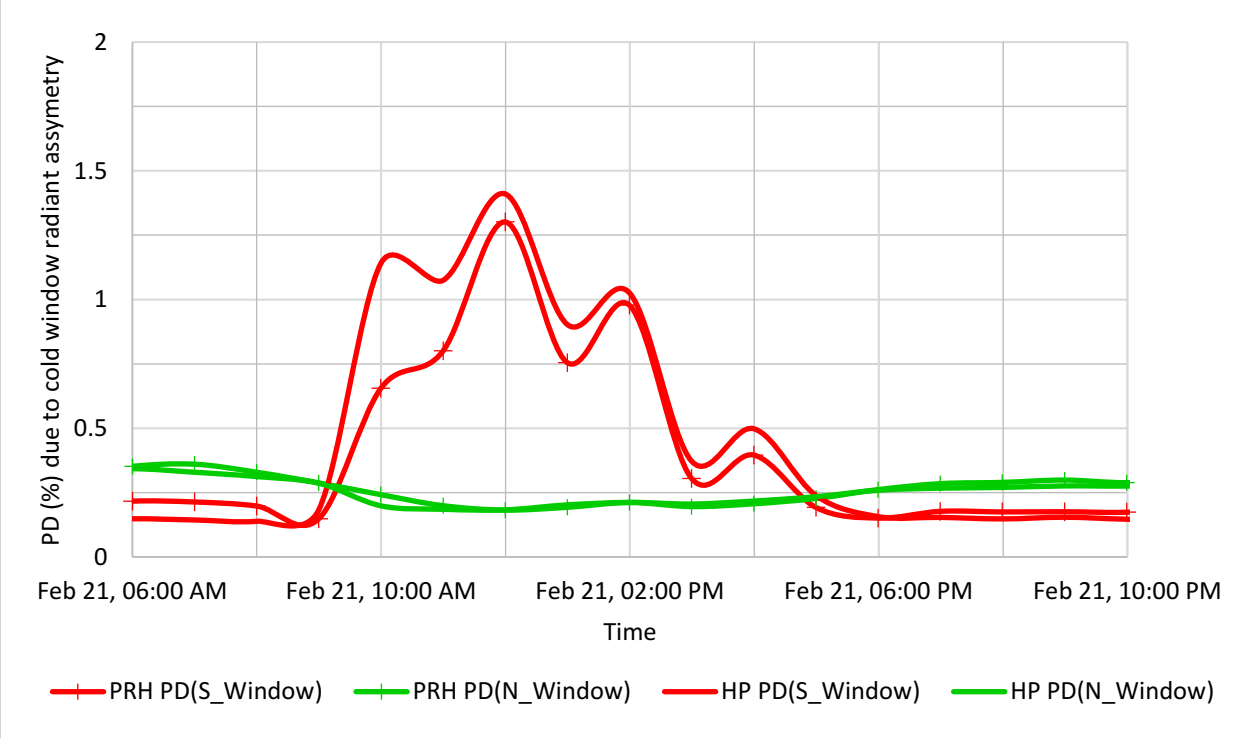

Figure 57: Local thermal discomfort due to cold window radiant asymmetry: PRH and HP.

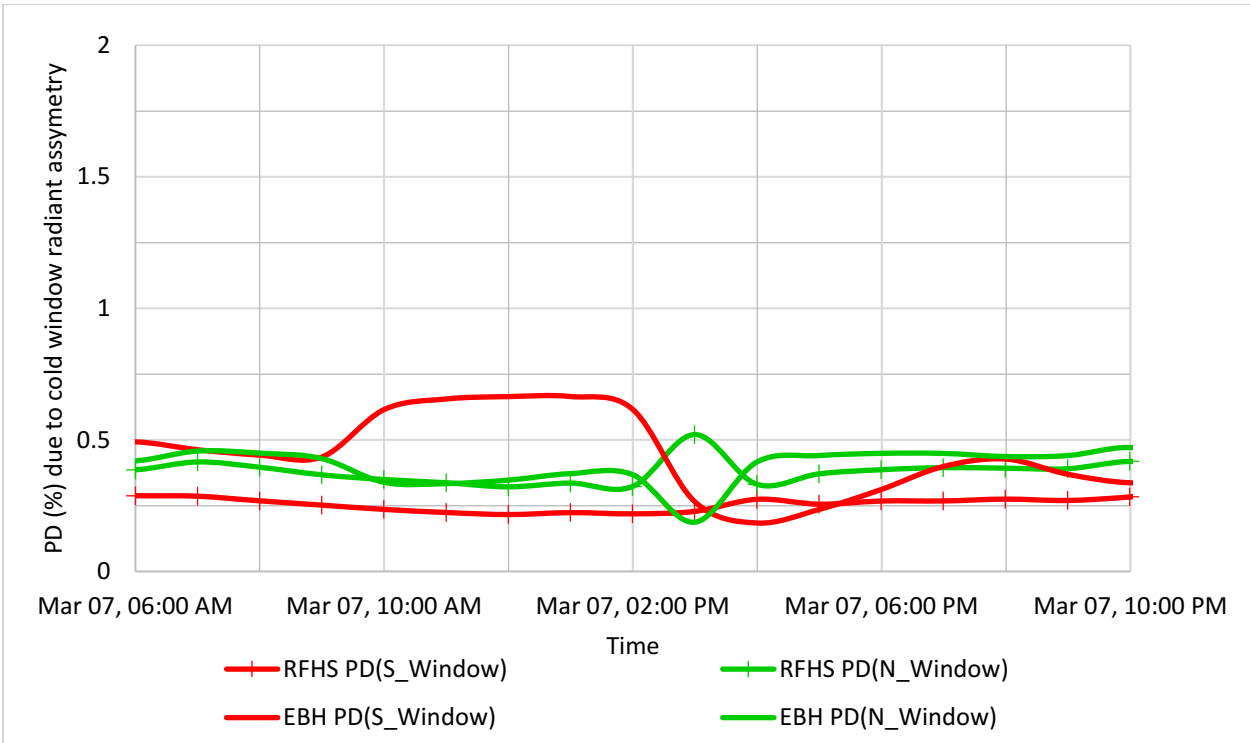

Figure 58: Local thermal discomfort due to cold window radiant asymmetry: RFHS and EBH.

7.1.3.2.3.2 Local Thermal Discomfort Due to the Floor to Ceiling Radiant Asymmetry

The radiant asymmetry can also be due to cool ceiling or warm floor. The RFHS creates a warm floor compared to the ceiling; the corresponding asymmetry then is cool ceiling radiant asymmetry. The other three systems (EBH, PH and HP) create a warm ceiling in contrast to the floor; the asymmetry becomes warm ceiling radiant asymmetry. According to ASHRAE 55 (2013), the allowable thermal discomfort due to radiant asymmetry is less than 5 %. The results in Figure 60 indicate that RFHS provides close to 0% PD due to the floor to radiant ceiling asymmetry, and the other heating systems (EBH, HP, and PRH) also create an acceptable floor to ceiling radiant asymmetry. The percentage of dissatisfied while using these heating systems are around 5 ± 1% as depicted in Figure 59 and Figure 60. Overall, all heating systems create acceptable local thermal discomfort due to the floor to ceiling radiant asymmetry.

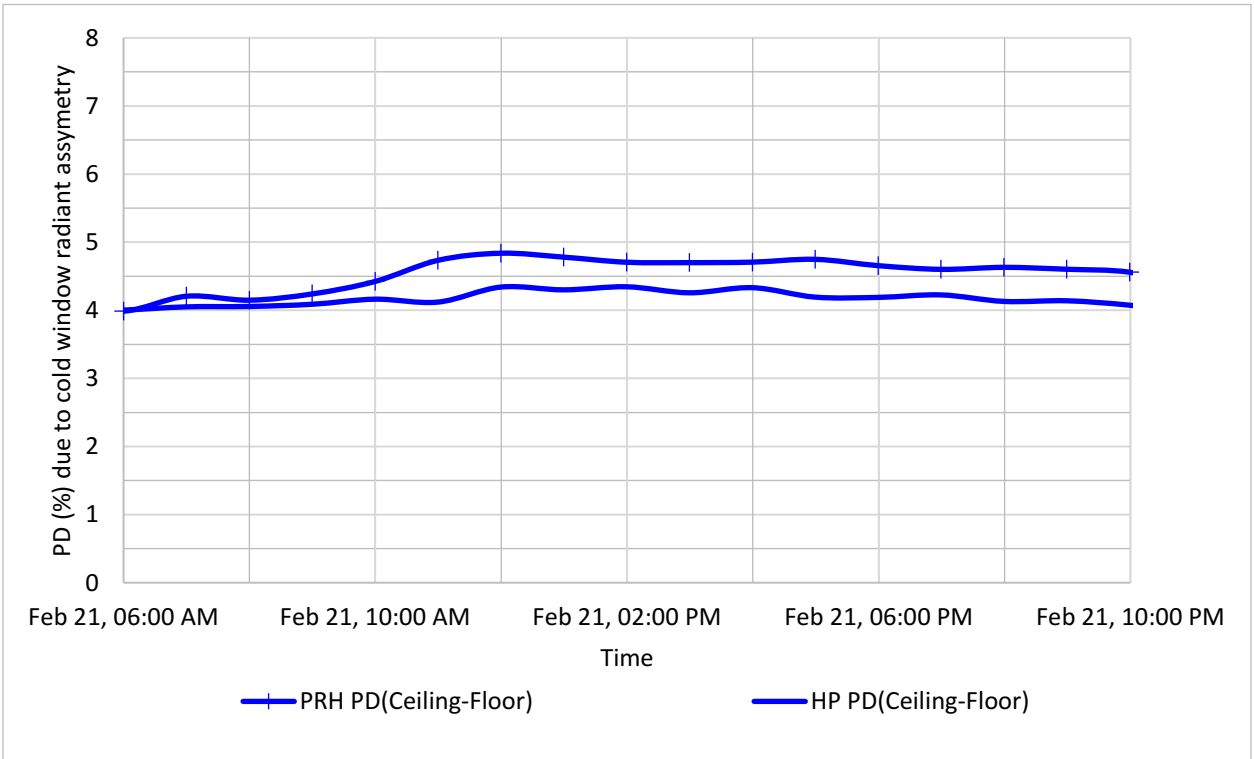

Figure 59: Local thermal discomfort due to ceiling to floor radiant asymmetry: PRH and HP.

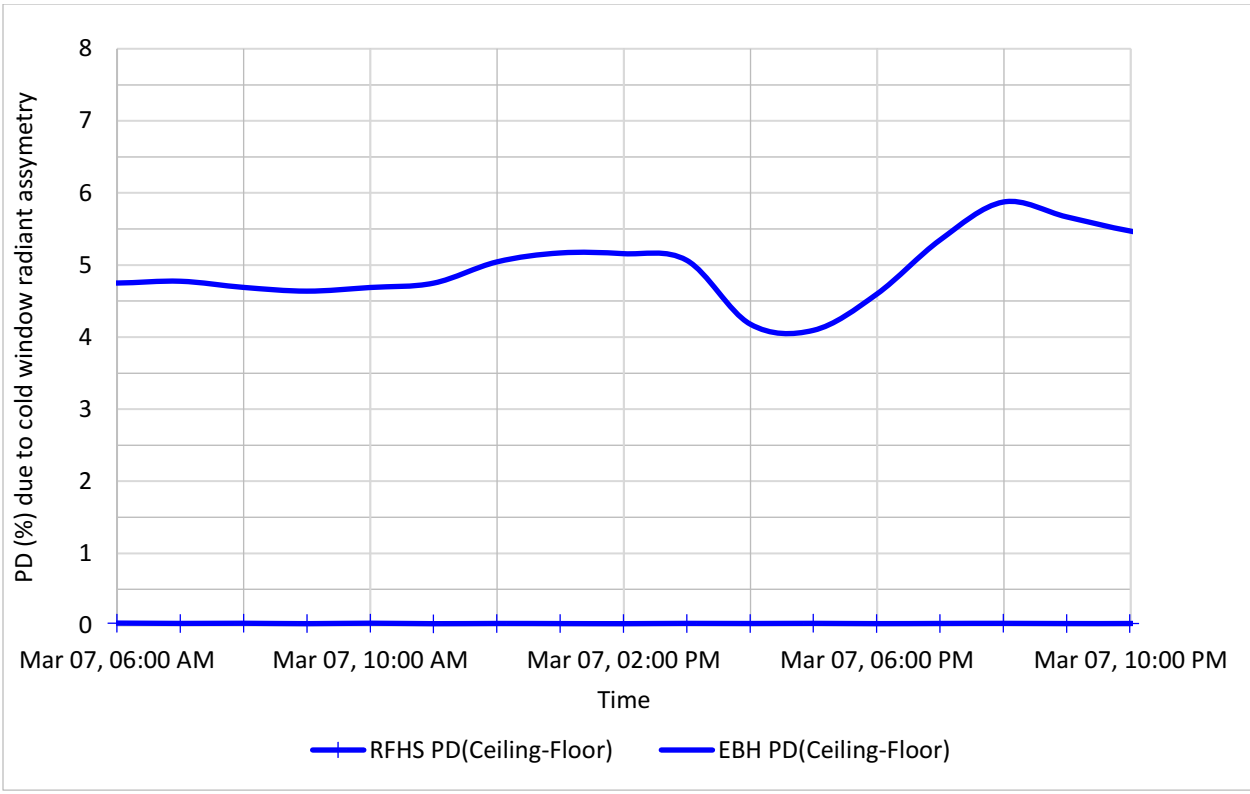

Figure 60: Local thermal discomfort due to ceiling to floor radiant asymmetry: RFHS and EBH.

7.2 Ventilation Strategies Comparison

7.2.1 Comparison of Mixed and Underfloor Ventilation Strategies

Mixed and underfloor ventilation strategies coupled with EBH, HP, and RFHS are compared in 7th, 8th and 9th experiments, respectively. Temperature, RH, CO2 and air velocity distributions in the test room, as well as ventilation effectiveness, are used to evaluate the relative performance of the two ventilation strategies in combinations with three different heating systems. In addition, the impact of the heating systems on the ventilation strategies is also discussed in this section.

7.2.1.1 Indoor Air Temperature Distribution: Comparison of MV and UV

The influence of ventilation strategies in the interior temperature distribution is discussed based on the data collected from parallel experiments running with the same heating system but different ventilation strategies, namely, MV and UV. Figure 61 depicts the interior temperature distribution of the test rooms at 6 AM. In the case of the experiment where EBH is used in both test rooms, the lowest temperature reading is around 19.5^{o}C at L5P3 with MV and around 20.5^{o}C at L5P1 with UV. The location where the lowest temperature is recorded, L5P3 for MV and L5P1 for UV, is closely situated to the supply terminals where the incoming air has a temperature of approximately 18°C. Whereas, when using HP, the coldest region in the room is across P1 (1 ft above floor) around 22 ± 0.3^{o}C for both MV and UV. The warmest region is above P3 (5ft above the floor), where the temperature reaches 23°C for both UV and MV. Whereas, when using RFHS, the room temperature distribution remains within 22 ± 0.5^{o}C and the coldest region is at L4P3 (21.3^{o}C) which is close to the north window for both UV and MV. Overall, when using RFHS and HP, similar interior temperature distribution (temperature difference of less than 0.5^{o}C) is observed in most measurement points for both MV and UV. However, when using EBH with UV, the result indicates relatively uniform temperature distribution compare to MV. In General, Figure 61 shows

that ventilation strategies have some effect on the indoor temperature distribution in a room with EBH but has an insignificant impact on temperature distribution when HP and RFHS heating systems are used due to air mixing and dominance of radiative heat transfer, respectively.

Heating systems	Ventilation Strategy														
	Mixed Ventilation (MV)					Underfloor Ventilation (UV)					Temperature Difference				
Eclectic baseboard Heather (EBH)	P4	20.8	21.6	22.1	21.6	P4	22.6	22.7	22.9	22.4	P4	1.8	1.1	0.8	0.8
	P3	19.5	22.6	21.2	20.2	P3	22.5	22.2	22.2	22.0	P3	2.9	0.4	1.0	1.8
	P2	21.0	22.2	22.3	20.7	P2	21.9	21.6	21.3	21.7	P2	0.9	0.6	1.0	1.0
	P1	22.0	22.8	22.5	22.7	P1	20.5	22.0	22.0	20.8	P1	1.5	0.8	0.5	1.9
		L5	L4	L3	L2		L5	L4	L3	L2		L5	L4	L3	L2
Heat Pump (HP)	P4	22.6	22.0	23.0	22.9	P4	22.7	21.5	22.8	23.1	P4	0.1	0.5	0.2	0.2
	P3	22.7	22.6	22.6	22.6	P3	22.5	22.3	22.4	22.4	P3	0.2	0.3	0.2	0.2
	P2	22.5	22.4	22.4	22.5	P2	22.0	22.0	22.1	22.1	P2	0.5	0.5	0.3	0.5
	P1	22.2	22.2	22.1	22.3	P1	21.7	21.7	21.8	21.7	P1	0.6	0.5	0.3	0.7
		L5	L4	L3	L2		L5	L4	L3	L2		L5	L4	L3	L2
Radiant Floor Heating system (RFHS)	P4	22.1	21.4	22.4	22.4	P4	22.2	21.2	22.2	22.2	P4	0.0	0.2	0.2	0.2
	P3	22.4	22.1	22.4	22.3	P3	22.3	22.0	22.3	22.1	P3	0.1	0.1	0.1	0.2
	P2	22.4	22.1	22.3	22.5	P2	22.1	21.8	22.2	22.2	P2	0.3	0.3	0.2	0.2
	P1	22.3	22.3	22.4	22.6	P1	22.2	22.1	22.3	22.3	P1	0.1	0.2	0.1	0.3
		L5	L4	L3	L2		L5	L4	L3	L2		L5	L4	L3	L2

Color Legend				
Ave of Min	Ave	Ave of Max	Min	Ave of Max
20	22	24	0	2

Figure 61: Temperature distribution in a room with similar heating bud different ventilation strategy (MV and UV).

7.2.1.2 CO2 Distribution: Comparison of MV and UV

Figure 62 shows the CO2 readings at L3P3, which represents the test room. The solid lines represent the CO2 concentration in the rooms, whereas, a dashed line represents the CO2 supply (simulating CO2 generation by a single person) and the dotted line represents the ambient CO2 concentration in the incoming air. The CO2 concentration in the test room starts increasing once the CO2 began injecting into the test rooms at 10:00 PM and peaks at 800 – 900 PPM after 8 hours of constant CO2 supply at a rate of 0.25 lpm. During the daytime, the CO2 concentration decreases and remains low at a concentration that is equivalent to the ambient concentration (between 400 PPM and 500 PPM). A little change of the CO2 reading during mid-day in the room with UV is due to solar radiation impinging on the sensor. As can be seen in Figure 62, the CO2 concentration profiles at the centre of the test rooms, which use different ventilation strategies are nearly identical.

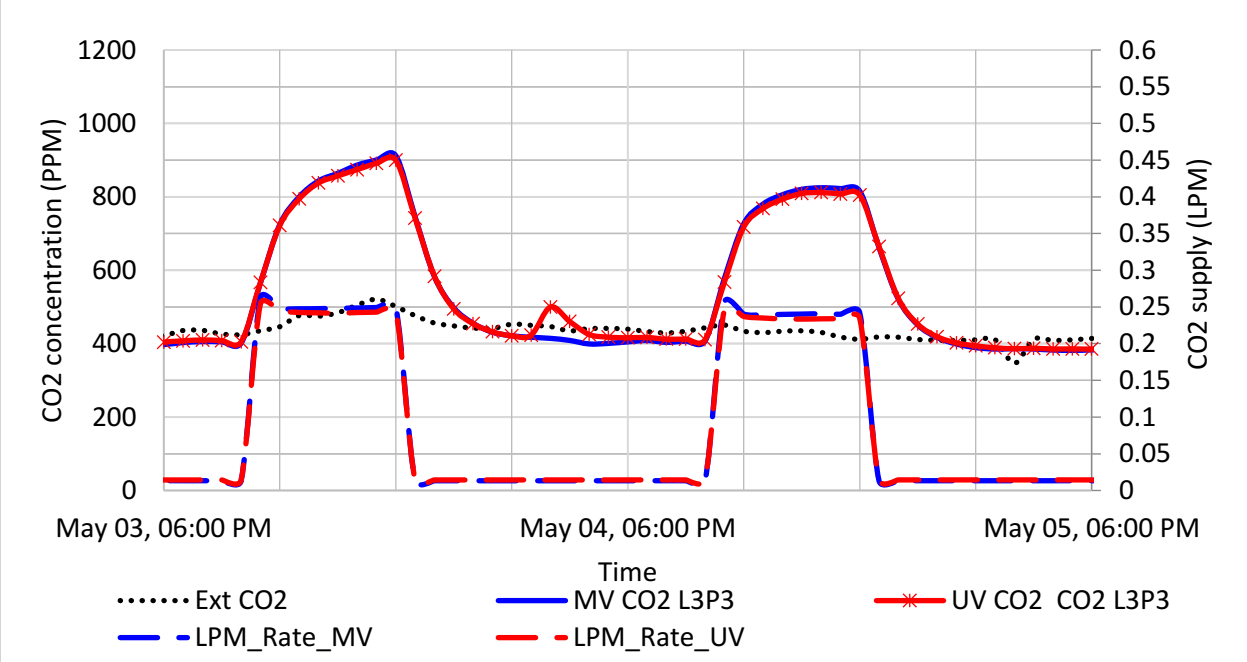

Figure 62: Transient CO2 profile at L3P3 in a room with the similar heating system (EBH) and different ventilation strategy (MV and UV).

The CO2 distributions normalized using outdoor CO2 in the test rooms with mixed and underfloor ventilation strategies are provided with colour plots in Figure 63. The CO2 concentration at 6 AM, which is the maximum concentration in the test rooms, is used to assess the CO2 distribution in the test rooms relative to the ventilation strategy in place. In both MV and UV, the maximum CO2 concentration (around 400 PPM at L3P4) is measured in the case where EBH is running in both rooms. In the case of experiments where HP and RFHS are used in both rooms, the maximum concentration is found at L3P3 and L3P4, which is in front of the CO2 supply unit. Irrespective of the heating system types and ventilation strategies used, the lowest concentration in the test rooms is observed close to the exhaust at L2 and L3. Relatively, the CO2 concentration demonstrates the UV strategy remove and create less CO2 concentration close to the floor and exhaust. This behaviour is more apparent when using EBH and HP than RFHS.

Heating systems	Ventilation Strategy																			
	Mixed Ventilation (MV)					Underfloor Ventilation (UV)					Difference									
Eclectic baseboard Heather (EBH)	P4	396	509	399	405	P4	481	504	403	418	P4	85		6	3	13				
	P3	358	470	404	395	P3	385	453	393	415	P3	27		17	11	20				
	P2	326	433	413	384	P2	461	374	350	313	P2	135		59	63	71				
		L5	L4	L3	L2		L5	L4	L3	L2		L5		L4	L3	L2				
Heat Pump (HP)	P4	388	537	423	437	P4	459	487	389	408	P4	70	50	33	29					
	P3	420	515	416	432	P3	364	455	373	391	P3	57	61	44	41					
	P2	404	444	439	427	P2	463	394	385	358	P2	59	50	53	69					
		L5	L4	L3	L2		L5	L4	L3	L2		L5	L4	L3	L2					
Radiant Floor Heating system (RFHS)	P4	326	474	374	382	P4	449	503	392	412	P4	123	30	18	30					
	P3	374	456	365	380	P3	350	519	377	394	P3	25	63	12	14					
	P2	350	399	383	377	P2	383	422	388	372	P2	33	23	5	5					
		L5	L4	L3	L2		L5	L4	L3	L2		L5	L4	L3	L2					
	Color Legend																			
	Ave of Min					Ave			Ave of Max			Min				Ave of Max				
	750					850			950			0				100				

Figure 63: CO2 distribution in a room with similar heating system, but different ventilation strategy (MV and UV).

7.2.1.3 Relative Humidity Distribution: Comparison of MV and UV

This section discusses the impact of ventilation strategies on the relative humidity profile in the test rooms. As illustrated in Figure 64, the RH profile in the test room gradually decreases to the ambient RH level (42%) during the daytime where there is no moisture supply. Once the indoor moisture generation starts supplying the RH level in the test room increases until it peaks (around 50%) at 6 AM after 8 hours of continuous moisture supply at a rate of 100 g/h. As shown in Figure 64, the RH profiles of the test rooms with MV and UV are similar. Overall, throughout the measurement period, the RH reading stays within the acceptable limit (30% to 60 %) as recommended by ASHRAE 55, 2013.

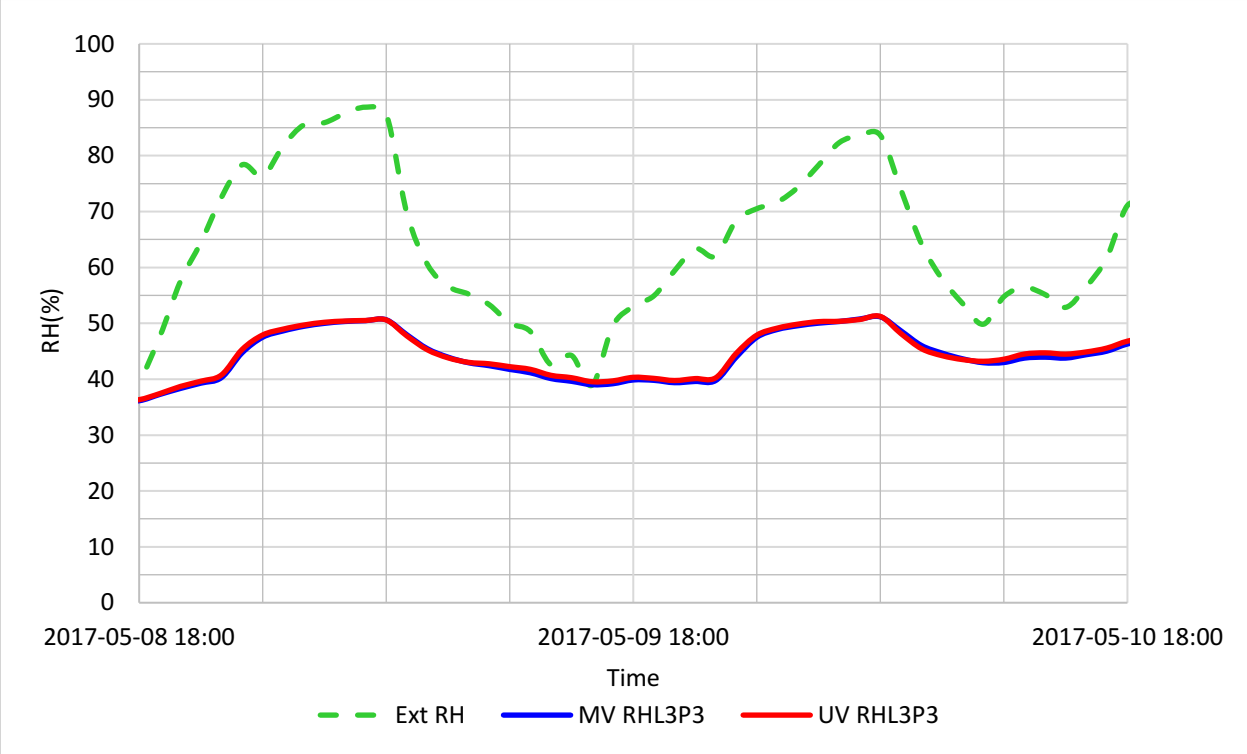

Figure 64: The relative humidity profile at L3P3 in a room with the similar heating system (RFHS) but different ventilation strategy (MV and UV).

In Figure 65, relative humidity distributions (at 6 AM) in the test rooms with different ventilation strategies and similar heating system is presented. In the experiment where EBH and RFHS are used, both MV and UV yield slightly high RH value (above 50%) in contrast to the experiment with HP cases (about 45%). The highest difference is 2% to 7.5% at L5P2, L5P3, and L5P4, which is during the experiment with EBH. The RH distribution while using EBH and RFHS, both MV and UV strategies provide uniform distribution. Whereas, The RH distribution is slightly less uniform when using HP. Besides, the most common difference occurs at L4P3 and L4P4, which are close to the moisture source. However, in most measurement points, the RH difference between the room with MV and UV remain less than 2%. Hence, the MV remove relatively more moisture compared to UV. Overall, The RH distribution indicates with all heating systems, the MV show relatively less RH value in contrast to UV.

Heating systems	Ventilation Strategy															
	Mixed Ventilation (MV)					Underfloor Ventilation (UV)					RH Difference (MV -UV)					
Eclectic baseboard Heather (EBH)	P4	49.6	57.6	49.6	48.6	P4	50.1	60.6	50.4	49.8	P4	0.5	3.1	0.8	1.2	
	P3	49.5	53.8	51.4	51.1	P3	56.7	56.1	51.4	53.5	P3	7.2	2.3	0.0	2.3	
	P2	48.9	52	51.4	51.9	P2	51.2	52	52.5	52.8	P2	2.3	0.0	1.0	0.9	
	P1	50.5	54.3	53	51.8	P1	55.2	54.5	52.9	52.4	P1	4.8	0.2	0.1	0.6	
		L5	L4	L3	L2		L5	L4	L3	L2		L5	L4	L3	L2	
Heat Pump (HP)	P4	45	51.4	45	44.8	P4	46	55.1	46	45.5	P4	1.0	3.7	1.0	0.6	
	P3	46.3	47.3	46	45.9	P3	50.1	50.8	45.9	47.7	P3	3.8	3.6	0.1	1.8	
	P2	46.5	47.9	46.7	46.7	P2	45.6	47.9	47	47.6	P2	0.9	0.0	0.4	0.9	
	P1	47	48.1	47	46.8	P1	49.2	49.8	48.6	48.6	P1	2.3	1.8	1.6	1.8	
		L5	L4	L3	L2		L5	L4	L3	L2		L5	L4	L3	L2	
Radiant Floor Heating system (RFHS)	P4	50.5	57.8	51.3	51.3	P4	52.2	61.4	52.4	52.4	P4	1.6	3.6	1.1	1.1	
	P3	51.6	53	51.2	51.3	P3	54.4	55.6	51.2	52.9	P3	2.9	2.7	0.1	1.6	
	P2	51.7	52	50.7	51.7	P2	48.8	52	49.9	51.6	P2	2.9	0.0	0.8	0.1	
	P1	50.5	51.7	50	50.6	P1	51.9	53	52	51.4	P1	1.4	1.3	2.0	0.8	
		L5	L4	L3	L2		L5	L4	L3	L2		L5	L4	L3	L2	

Color Legend				
Ave of Min	Ave	Ave of Max	Min	Ave of Max
30	45	60	0	5

Figure 65: Relative humidity distribution in a room with MV and UV but the similar heating system.

7.2.1.4 Air Velocity Distribution: Comparison of MV and UV

The air velocity profiles in the test rooms with the similar heating system, but different ventilation strategy (MV and UV) are presented here. As shown in Figure 66, the air velocity throughout the test rooms is less than 0.2 m/s except at L4P4, where the humidifier fun is near. When using EBH, the air velocity remains less than 0.05m/s throughout the test room with both ventilation strategies. In case of RFHS, the velocity distribution is similar either using UV or MV (between 0 to 0.1 m/s). HP with MV shows relatively high air velocity (between 0.07 and 0.1 m/s) in contrast to UV in most measurement points. Overall, both MV and UV demonstrate low air velocity and uniform distribution throughout the test room. The air velocity magnitude is relatively high for both ventilation strategies in the HP and RFHS cases. The HP has a blower and louvre, which induce air movement in the test room. The air velocity in RFHS is mainly due to buoyancy flow created by warm floor.

Heating systems	Ventilation Strategy															
	Mixed Ventilation (MV)					Underfloor Ventilation (UV)					Air Velocity Difference					
Eclectic baseboard Heather (EBH)	P4	0.03	0.12	0.05	0.02	P4	0.00	0.13	0.01	0.03	P4	0.02	0.00	0.04	0.01	
	P3	0.02	0.03	0.00	0.00	P3	0.00	0.05	0.01	0.00	P3	0.02	0.01	0.01	0.00	
	P2	0.04	0.02	0.01	0.00	P2	0.00	0.02	0.01	0.00	P2	0.04	0.01	0.00	0.00	
	P1	0.04	0.02	0.01	0.00	P1	0.00	0.02	0.00	0.00	P1	0.04	0.00	0.01	0.00	
		L5	L4	L3	L2		L5	L4	L3	L2		L5	L4	L3	L2	
Heat Pump (HP)	P4	0.11	0.18	0.08	0.13	P4	0.07	0.17	0.04	0.14	P4	0.04	0.01	0.04	0.01	
	P3	0.09	0.06	0.06	0.12	P3	0.04	0.06	0.05	0.10	P3	0.05	0.00	0.01	0.01	
	P2	0.08	0.05	0.08	0.10	P2	0.03	0.03	0.05	0.08	P2	0.05	0.02	0.03	0.02	
	P1	0.07	0.05	0.09	0.11	P1	0.02	0.04	0.06	0.05	P1	0.05	0.01	0.03	0.06	
		L5	L4	L3	L2		L5	L4	L3	L2		L5	L4	L3	L2	
Radiant Floor Heating system (RFHS)	P4	0.10	0.19	0.07	0.07	P4	0.04	0.14	0.07	0.08	P4	0.05	0.04	0.00	0.01	
	P3	0.04	0.06	0.05	0.08	P3	0.03	0.05	0.03	0.08	P3	0.01	0.01	0.01	0.00	
	P2	0.03	0.05	0.09	0.08	P2	0.03	0.04	0.04	0.07	P2	0.01	0.01	0.05	0.01	
	P1	0.04	0.04	0.09	0.07	P1	0.03	0.03	0.05	0.05	P1	0.00	0.00	0.04	0.02	
		L5	L4	L3	L2		L5	L4	L3	L2		L5	L4	L3	L2	

Color Legend				
Ave of Min	Ave	Ave of Max	Min	Ave of Max
0	0.05	0.15	0	0.05

Figure 66: Air velocity distribution in a room with MV and UV but the similar heating system.

7.2.1.5 Global Contaminant Removal Effectiveness (GCRE): Comparison of MV and UV

The global contaminant removal effectiveness expresses the contaminant removal capability of the ventilation system in a room. Since CO2 is assumed as a contaminant; GCRE is calculated by using the average CO2 concentration in the test room, the CO2 level in the incoming air and exhaust air as illustrated in section 6.4.2. MV and UV strategies in the three heating systems (HP, EBH, and RFHS) are compared using GCRE. Figure 67 shows a plot of two-day hourly GCRE data: a red line for mixed ventilation and blue for underfloor ventilation.

In all three heating systems, MV provides high GCRE than UV. The GCRE is only significant during the nighttime in which internal CO2 generation is active and added into the test room. Whereas during the daytime the CO2 concentration remains as low as the incoming air CO2 that leads low GCRE (0%). As illustrated in Figure 65, MV produces around 100 ± 10% GCRE, and UV creates 80 ± 10%. Consequently, MV shows approximately 20% more GCRE than UV. Overall, MV depicts better global contaminant removal effectiveness in contrast to UV. Similar behaviour is found when using HP and RFHS and reported in Appendix II section 12.

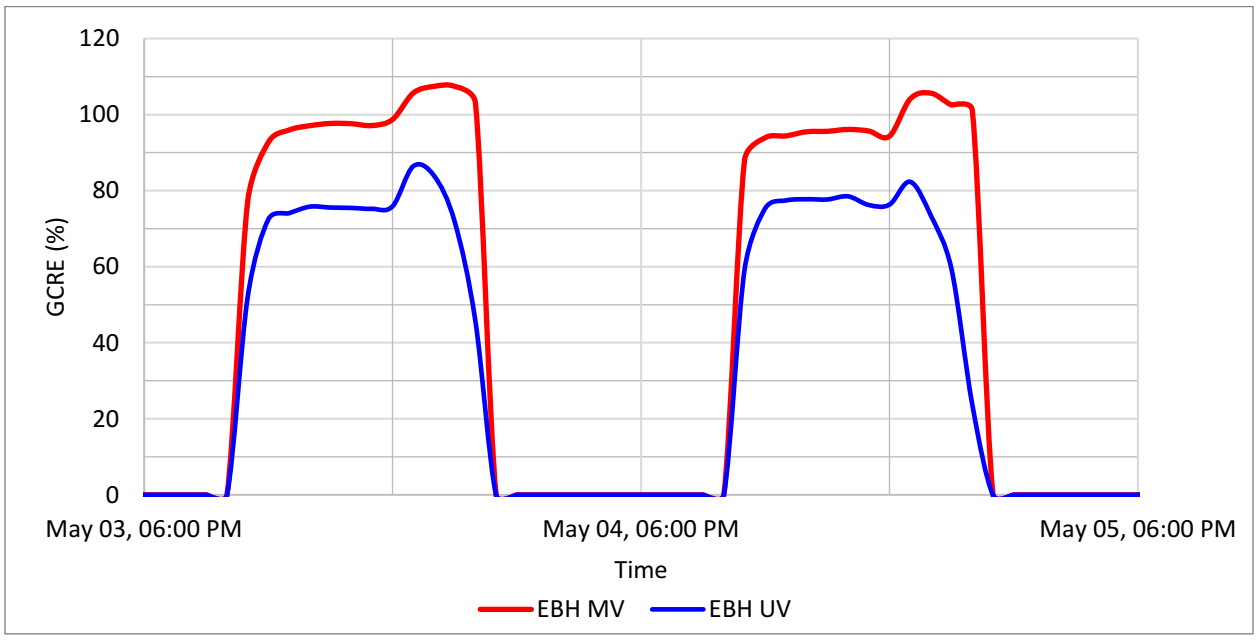

Figure 67: GVE in a test room with MV and UV both heated by EBH.

7.2.1.6 Contaminant (CO2) Removal Effectiveness:

Similar behaviour is found when it comes to contaminant removal effectiveness (CRE). As can be seen in Figure 68, in all cases MV provides higher CRE number in most of the measurement spots relative to UV. The only identical CRE measurement is found at L2P2 (100%) in every case; this is because this point is close to the exhaust, which represents the room air average CO2 concentration. Low CRE value is measured while using EBH with UV during the 7th experiment (70 ± 10%). High CRE is recorded at L5 in all three experiments in a room with MV, and it is 100% to 120%. Since high CRE means the good pollutant removal rate, MV removes more CO2 than UV.

Heating systems		Ventilation Strategy											
		Mixed Ventilation (MV)				Underfloor Ventilation (UV)				CRE Difference			
Eclectic baseboard Heather (EBH)	P4	97.0	75.5	96.3	94.8	65.1	62.2	77.8	74.9	31.9	13.3	18.4	19.9
	P3	107.4	81.8	95.2	97.4	81.4	69.1	79.7	75.6	26.0	12.6	15.5	21.8
	P2	118.0	88.8	93.0	100.0	68.0	83.7	89.5	100.0	50.0	5.1	3.5	0.0
		L5	L4	L3	L2	L5	L4	L3	L2	L5	L4	L3	L2
Heat Pump (HP)	P4	110.0	79.6	101.1	97.7	78.0	73.5	91.9	87.7	31.9	6.1	9.2	10.0
	P3	101.6	82.9	102.6	98.9	98.4	78.6	96.0	91.5	3.2	4.2	6.6	7.4
	P2	105.8	96.2	97.4	100.0	77.3	90.8	92.8	100.0	28.5	5.4	4.6	0.0
		L5	L4	L3	L2	L5	L4	L3	L2	L5	L4	L3	L2
Radiant Floor Heating system (RFHS)	P4	115.6	79.7	100.9	98.7	82.8	73.9	94.9	90.2	32.8	5.7	6.0	8.5
	P3	100.8	82.8	103.4	99.3	106.4	71.7	98.6	94.5	5.6	11.1	4.8	4.9
	P2	107.8	94.5	98.5	100.0	97.2	88.2	96.0	100.0	10.6	6.3	2.6	0.0
		L5	L4	L3	L2	L5	L4	L3	L2	L5	L4	L3	L2

Color Legend				
Ave of Min	Ave	Ave of Max	Ave	Ave of Max
60	90	120	0	100

Figure 68: Contaminant removal effectiveness (CRE) in a room with MV and UV but the similar heating system.

7.2.1.7 Indoor Air Quality Number Comparing MV and UV:

The indoor air quality number couples contaminant removal effectiveness with the percentage of dissatisfaction due to ventilation flow rate. However, since the ventilation flow rate is equal (15 cfm) for both ventilation strategies, PD is constant and the same for both. Therefore, the only changing variable, in this case, is contaminant removal effectiveness. In addition, high indoor air quality number imply better contaminant removal subsequently good indoor air quality. Comparing MV with UV, MV reflect high IAQN than UV. The highest IAQN find at L5, which is close to the supply especially with MV. In the case of UV, high IAQN is across P2 (1 ft 6 in above the floor). It is because underfloor ventilation supplies fresh air close to the floor and create high contaminant removal effectiveness near the floor. In all three experiments, MV produce around 5 IAQN whereas UV creates around 4 IAQN in most measurement points except (L4P3 and L4P4). Overall, MV show 20% more IAQN than UV as depicted in Figure 69.

Heating systems	Ventilation Strategy														
	Mixed Ventilation (MV)					Underfloor Ventilation (UV)					IAQN Difference				
Eclectic baseboard Heather (EBH)	P4	4.9	3.8	4.8	4.8	P4	3.3	3.1	3.9	3.8	P4	1.6	0.7	0.9	1.0
	P3	5.4	4.1	4.8	4.9	P3	4.1	3.5	4.0	3.8	P3	1.3	0.6	0.8	1.1
	P2	5.9	4.4	4.7	5.0	P2	3.4	4.2	4.5	5.0	P2	2.5	0.3	0.2	0.0
		L5	L4	L3	L2		L5	L4	L3	L2		L5	L4	L3	L2
Heat Pump (HP)	P4	5.5	4.0	5.1	4.9	P4	3.9	3.7	4.6	4.4	P4	1.6	0.3	0.5	0.5
	P3	5.1	4.2	5.1	5.0	P3	4.9	3.9	4.8	4.6	P3	0.2	0.2	0.3	0.4
	P2	5.3	4.8	4.9	5.0	P2	3.9	4.5	4.6	5.0	P2	1.4	0.3	0.2	0.0
		L5	L4	L3	L2		L5	L4	L3	L2		L5	L4	L3	L2
Radiant Floor Heating system (RFHS)	P4	5.8	4.0	5.1	4.9	P4	4.1	3.7	4.8	4.5	P4	1.6	0.3	0.3	0.4
	P3	5.0	4.1	5.2	5.0	P3	5.3	3.6	4.9	4.7	P3	0.3	0.6	0.2	0.2
	P2	5.4	4.7	4.9	5.0	P2	4.9	4.4	4.8	5.0	P2	0.5	0.3	0.1	0.0
		L5	L4	L3	L2		L5	L4	L3	L2		L5	L4	L3	L2

Color Legend				
Ave of Min	Ave	Ave of Max	Min	Ave of Max
3	5	7	0	2

Figure 69: Indoor air quality number (IAQN) in a room with MV and UV but the similar heating system.

7.3 Ventilation Rate Comparison

The comparison of low ventilation flow rate is discussed in this section, mainly 15 cfm vs 7.5 cfm and 7.5 cfm vs 5cfm. The indoor conditions such as temperature, RH, CO2, and air velocity distribution are used to conduct the ventilation flow rate performance comparison. In addition, ventilation performance assessment (CRE, GCRE, and IAQN) is used to examine the effect of ventilation flow rate on indoor air quality. Moreover, the impact of ventilation flow rate difference in the energy consumption briefly present at last. In all the comparisons both the heating systems and ventilation strategies maintain similar in both buildings, the only difference is the supply ventilation flow rate, which is the subject of the study in these experiments. The pair of experiments is (15 cfm vs 7.5 cfm) MV RFHS, (15 cfm vs 7.5cfm and 7.5 cfm vs 5 cfm) MV EBH, (15 cfm vs 7.5 cfm and 7.5 cfm vs 5 cfm) MV HP and the all the above with UV. Colour plots for a single time instant at 6 AM with MV present here, similar colour plot with a UV report in Appendix II section 13.

7.3.1 Temperature Distribution: Ventilation Flow Rate Comparison.

In this section, the experimental result from two rooms with similar heating systems and ventilation strategy, but with different ventilation flow rate is discussed. Since both heating systems and ventilation strategies are the same, it is possible to see the impact of ventilation flow rate on indoor temperature distributions. The temperature distribution present in Figure 70 shows a similar temperature trend with a small difference. Except for the East wall, all the temperature difference stays below 0.5^{o}C throughout the test rooms. It is mainly because the ventilation air is treated separately and independently: Moreover, the heating and ventilation strategy is the same in both buildings that lead the creation of a similar thermal environment despite the ventilation flow rate difference. The thermocouple reading at L4P3 and L4P4 show slightly less because the sensors are close to humidifiers and north window which is the coldest region in the test room. Therefore, the reduction of the ventilation flow rate from 15 cfm to 7.5 cfm, then to 5 cm do affect the temperature distribution in the test room. Similar behaviour is observed when the MV switch by UV (Appendix II section 6.1).

Heating systems	Ventilation flow rate													Difference Abs (15cfm – 7.5cfm)			
	15cfm					7.5cfm											
Radiant Floor Heating system (RFHS)	P4	22.9	22.0	23.1	23.1	P4	22.9	21.8	23.1	23.1	P4	0.1	0.2	0.0	0.0
	P3	23.1	22.8	23.1	23.1	P3	23.0	22.7	23.2	23.0	P3	0.1	0.1	0.1	0.1
	P2	23.1	22.8	23.1	23.2	P2	22.8	22.9	23.1	23.0	P2	0.3	0.0	0.0	0.2
	P1	22.9	23.0	23.1	23.3	P1	23.0	22.8	23.1	23.1	P1	0.0	0.2	0.0	0.2
		L5	L4	L3	L2		L5	L4	L3	L2		L5	L4	L3	L2
Eclectic baseboard Heather (EBH)	P4	24.3	23.1	24.4	24.7	P4	24.3	22.8	24.2	24.5	P4	0.1	0.3	0.2	0.2
	P3	24.0	23.8	24.0	24.0	P3	23.8	23.7	23.8	23.9	P3	0.2	0.1	0.2	0.1
	P2	23.9	23.8	23.9	24.0	P2	23.7	23.5	23.6	23.8	P2	0.3	0.3	0.3	0.2
	P1	23.8	23.7	23.7	23.9	P1	23.6	23.5	23.6	23.6	P1	0.2	0.2	0.0	0.3
		L5	L4	L3	L2		L5	L4	L3	L2		L5	L4	L3	L2
Heat pump (HP)	P4	24.1	23.3	24.4	24.4	P4	24.4	23.3	24.6	24.7	P4	0.3	0.0	0.2	0.3
	P3	24.1	23.9	24.1	24.1	P3	24.2	24.1	24.3	24.2	P3	0.1	0.2	0.2	0.1
	P2	23.9	23.9	23.9	24.1	P2	24.0	23.9	23.8	24.1	P2	0.1	0.1	0.0	0.0
	P1	23.6	23.8	23.6	24.0	P1	23.7	23.8	23.7	24.0	P1	0.1	0.0	0.1	0.0
		L5	L4	L3	L2		L5	L4	L3	L2		L5	L4	L3	L2
	7.5cfm					5cfm					Abs (7.5cfm – 5cfm)				
Heat pump (HP)	P4	24.3	23.6	24.6	24.6	P4	24.4	23.2	24.6	24.7	P4	0.1	0.4	0.0	0.1
	P3	24.3	24.4	24.3	24.3	P3	24.2	24.1	24.3	24.3	P3	0.1	0.2	0.0	0.1
	P2	24.1	24.1	24.1	24.3	P2	24.0	23.8	23.9	24.2	P2	0.1	0.3	0.2	0.1
	P1	23.7	23.9	23.9	24.1	P1	23.7	23.8	23.8	24.0	P1	0.0	0.1	0.1	0.1
		L5	L4	L3	L2		L5	L4	L3	L2		L5	L4	L3	L2
Eclectic baseboard Heather (EBH)	P4	24.7	23.1	24.6	24.8	P4	24.4	23.1	24.3	24.6	P4	0.2	0.0	0.3	0.3
	P3	24.0	23.9	24.0	24.1	P3	23.8	23.7	23.8	24.0	P3	0.2	0.2	0.3	0.1
	P2	24.0	23.8	23.9	24.1	P2	23.7	23.5	23.6	23.9	P2	0.2	0.3	0.3	0.2
	P1	23.5	23.6	23.7	23.8	P1	23.5	23.4	23.6	23.5	P1	0.1	0.1	0.1	0.3
		L5	L4	L3	L2		L5	L4	L3	L2		L5	L4	L3	L2

Color Legend				
Ave of Min	Ave	Ave of Max	Min	Ave of Max
22	23.5	25	0	1

Figure 70: Interior temperature distribution comparison of 15cfm, 7.5cfm, and 5cfm with MV.

7.3.2 Air Velocity Distribution: Ventilation Flow Rate Comparison.

The air velocity distribution present in Figure 71 shows instant air velocity measurement in the test rooms at 6 AM and the difference between the two rooms, which is running similar heating system with mixed ventilation strategy. The velocity difference between the rooms is explained relative to the ventilation flow rate. The air velocity in the experiments where EBH is the heating system is very low, close to 0m/s in most measurement points with all three-ventilation flow rates. Whereas, in those experiments where RFHS and HP are the heating systems, the air velocity in the rooms stays above 0.5 m/s in most of the measurement points with all three ventilation flow rates. The air velocity reading at L4P4 is relatively very high; it is because the sensors are picking up the air movement generated by the humidifier fan which is nearby. The difference between the rooms is less than 0.03m/s in most of the measurement points regardless of the ventilation flow rate difference in the rooms. This behaviour is true for both 15cfm vs 7.5 cfm as well as 7.5 cfm vs 5 cfm. Therefore, low ventilation flow rate shows not to affect the air movement in the room. The same result is found using UV and the report in the Appendix II section 6.2.

Heating systems	Ventilation flow rate																Difference Abs (15cfm – 7.5cfm)			
	15cfm					7.5cfm														
Radiant Floor Heating system (RFHS)	P4	0.09	0.20	0.08	0.08	P4	0.06	0.18	0.06	0.08	P4	0.03	0.02	0.01	0.00
	P3	0.04	0.07	0.05	0.08	P3	0.05	0.06	0.03	0.08	P3	0.01	0.01	0.02	0.01
	P2	0.03	0.06	0.09	0.08	P2	0.07	0.02	0.03	0.08	P2	0.04	0.03	0.06	0.00
	P1	0.04	0.04	0.09	0.07	P1	0.05	0.05	0.08	0.07	P1	0.01	0.00	0.01	0.00
		L5	L4	L3	L2		L5	L4	L3	L2		L5	L4	L3	L2
Eclectic baseboard Heather (EBH)	P4	0.06	0.14	0.05	0.03	P4	0.00	0.15	0.02	0.03	P4	0.06	0.01	0.03	0.00
	P3	0.02	0.03	0.01	0.01	P3	0.02	0.02	0.01	0.01	P3	0.00	0.01	0.00	0.00
	P2	0.02	0.01	0.01	0.00	P2	0.04	0.01	0.01	0.00	P2	0.01	0.00	0.00	0.00
	P1	0.03	0.01	0.01	0.01	P1	0.01	0.01	0.02	0.01	P1	0.02	0.01	0.00	0.00
		L5	L4	L3	L2		L5	L4	L3	L2		L5	L4	L3	L2
Heat pump (HP)	P4	0.13	0.18	0.07	0.13	P4	0.08	0.18	0.04	0.12	P4	0.05	0.00	0.03	0.02
	P3	0.09	0.06	0.06	0.11	P3	0.07	0.05	0.04	0.11	P3	0.02	0.00	0.01	0.00
	P2	0.07	0.06	0.08	0.11	P2	0.06	0.04	0.07	0.11	P2	0.01	0.02	0.01	0.00
	P1	0.06	0.06	0.11	0.08	P1	0.06	0.04	0.08	0.08	P1	0.00	0.01	0.03	0.00
		L5	L4	L3	L2		L5	L4	L3	L2		L5	L4	L3	L2
	7.5cfm					5cfm					Abs (7.5cfm – 5cfm)				
Heat pump (HP)	P4	0.09	0.20	0.07	0.12	P4	0.08	0.18	0.04	0.12	P4	0.01	0.02	0.03	0.00
	P3	0.08	0.06	0.06	0.11	P3	0.07	0.05	0.04	0.11	P3	0.01	0.01	0.02	0.01
	P2	0.06	0.04	0.08	0.10	P2	0.06	0.04	0.07	0.11	P2	0.01	0.00	0.01	0.01
	P1	0.04	0.04	0.10	0.09	P1	0.04	0.04	0.08	0.08	P1	0.00	0.00	0.02	0.01
		L5	L4	L3	L2		L5	L4	L3	L2		L5	L4	L3	L2
Eclectic baseboard Heather (EBH)	P4	0.01	0.19	0.05	0.03	P4	0.01	0.11	0.02	0.04	P4	0.00	0.08	0.03	0.01
	P3	0.04	0.04	0.03	0.00	P3	0.04	0.03	0.02	0.00	P3	0.00	0.00	0.01	0.00
	P2	0.03	0.03	0.02	0.00	P2	0.00	0.01	0.01	0.00	P2	0.03	0.02	0.00	0.00
	P1	0.00	0.03	0.00	0.00	P1	0.00	0.01	0.00	0.00	P1	0.00	0.02	0.00	0.00
		L5	L4	L3	L2		L5	L4	L3	L2		L5	L4	L3	L2

Color Legend				
Ave of Min	Ave	Ave of Max	Min	Ave of Max
0	0.05	0.15	0	0.05

Figure 71: Interior distribution comparison of 15cfm air velocity, 7.5cfm, and 5cfm with MV.

7.3.3 RH Distribution: Ventilation Flow Rate Comparison

Figure 72 and 73 presents the RH profile at the centre of the test rooms (L3P3) which represent the room air condition. The RH concentration in the test rooms with different ventilation flow rate is compared in this section using these two graphs. The RH concentration in a room with the higher ventilation flow rate is represented by red lines and the RH in a room with a lower flow rate in the comparison represent with a blue line. A broken green line represents the outdoor RH. Whereas, in the background, the ventilation flow rate is plotted by a dashed line with the colour match corresponding RH in the test rooms. The RH concentration in the test rooms stays low during the daytime. Once the external moisture starts supplying at 10 PM the RH start rising till reaching the maximum after 8 hours consistence 100 g/h supply. At the pick, the maximum RH in the test rooms reached around 50% with all three ventilation flow rates. The room with 15 cfm shows higher RH (2.5%) in contrast to a room with 7.5 cfm as shown in Figure 72. Whereas, the RH comparison in a room with 7.5 cfm and 5 cfm is small as illustrated in Figure 73. Overall, the room with lower ventilation rate demonstrates slightly higher RH relative to higher ventilation flow rate. The impact of ventilation flow rate in RH profile decreases as the ventilation flow rates decrease.

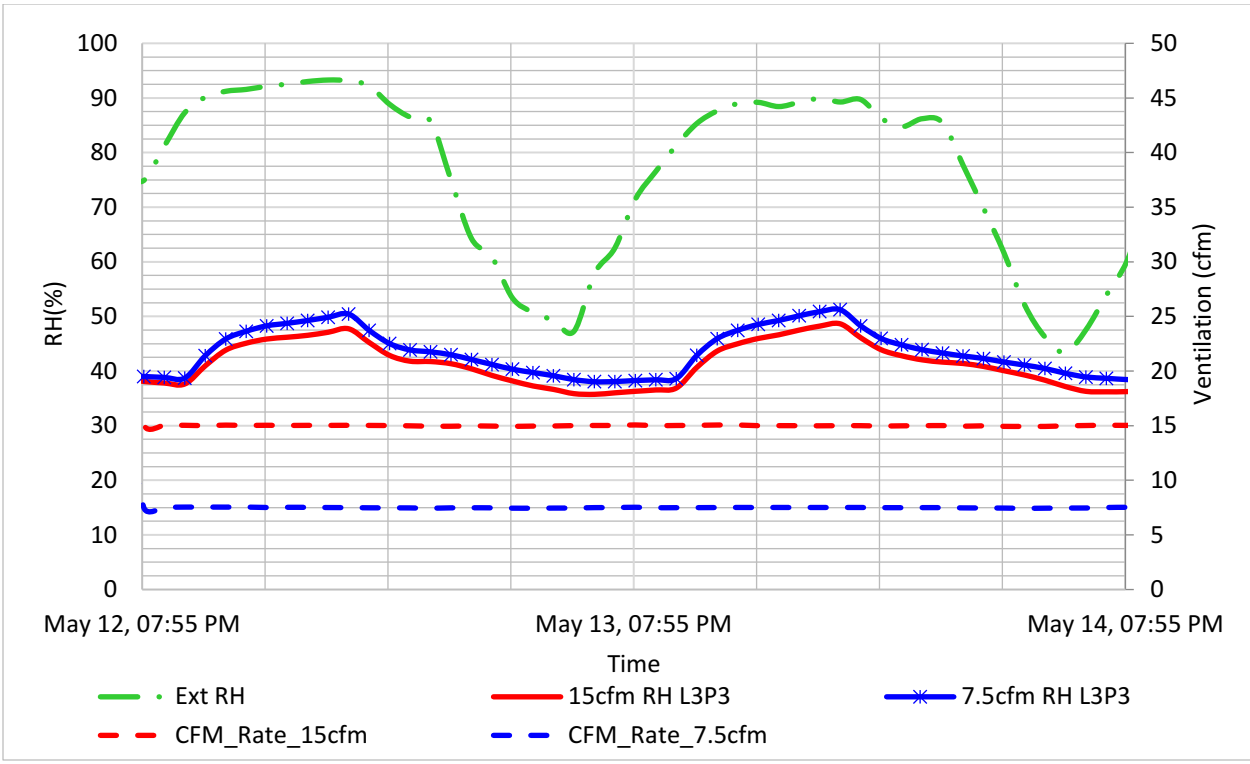

Figure 72: The relative humidity profile at L3P3 comparing 15cfm, 7.5cfm using RFHS with MV.

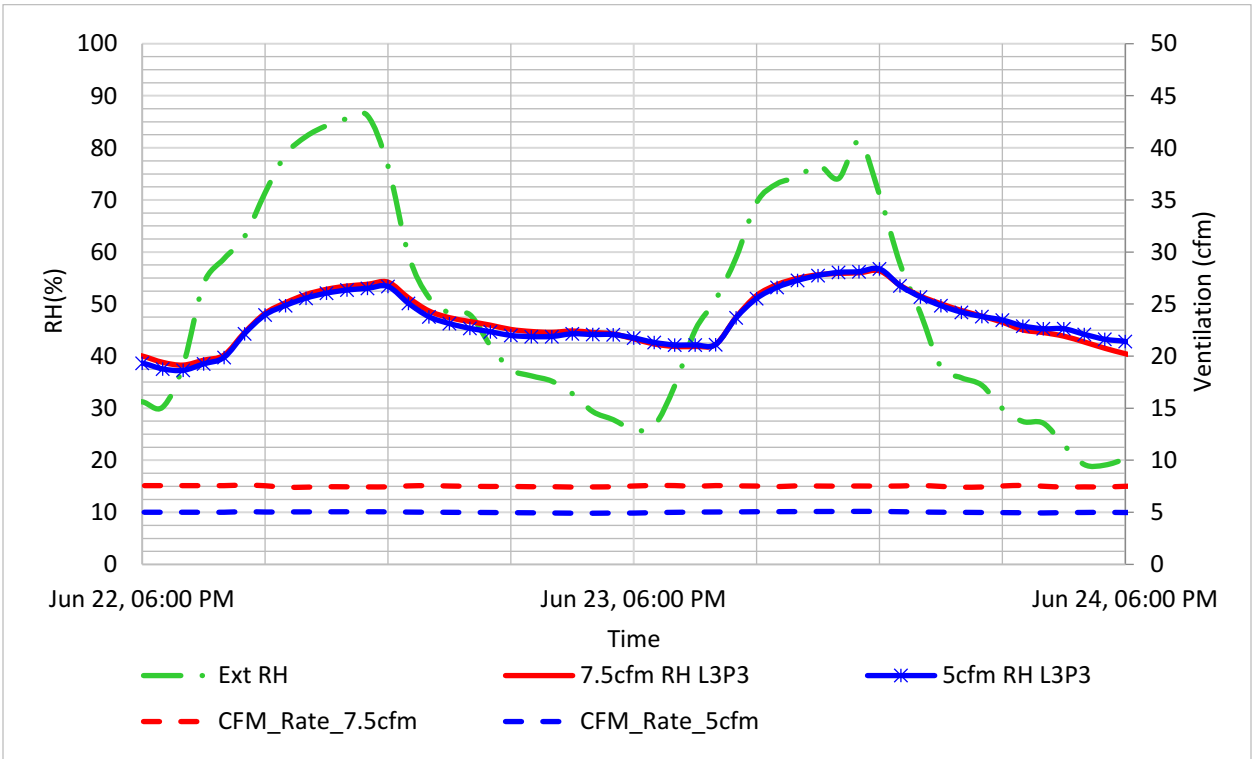

Figure 73: The relative humidity profile at L3P3 comparing 7.5cfm, 5cfm using EBH with MV.

The effect of ventilation flow rate on temperature and air velocity distribution, provide the same heating system and ventilation strategy, found to have a small impact as presenters in section 7.3.2. Unlike that, the flow rate has more to do with moisture and contaminant removal from the space. This section discusses RH distribution as the result of the ventilation flow rate difference. Like the previous sections, only the result with MV presents here, the remaining (with UV) report in appendix section 6.2. The RH concentration in throughout the test rooms with different ventilation flow rate is shown in Figure 74. The RH reading from all sensors is between 40 and 55% in most measurement points with all ventilation flow rates. The highest reading finds at L4P4 and L4P3 in all cases because the sensors are in front of the humidifiers. The RH distribution also shows the room with 7.5 has 2% to 5% more RH in comparison to the other room with 15 cfm. It is because the higher the flow rate (15 cfm), the higher moisture is removed from the space, which leads low RH in the space, comparable to low ventilation flow rate (7.5 cfm). However, the RH difference in the test rooms becomes small when comparing 7.5 cfm and 5 cfm, for instance, look at 19th experiment on Figure 74 where EBH is used to heat both of the test rooms. Overall, the higher the flow rate, the higher moisture is removed from the space, however, this effect decrease when the ventilation flow rate became small.

Heating systems	Ventilation flow rate															Difference Abs (15cfm – 7.5cfm)			
	15cfm					7.5cfm													
Radiant Floor Heating system (RFHS)	P4	47.4	54.4	47.7	47.7	P4	51.7	60.9	51.5	51.4	P4	4.3	6.5	3.9	3.7	P4	4.3	6.5	3.9	3.7
	P3	48.0	49.6	47.7	47.7	P3	53.8	55.4	50.5	52.0	P3	5.8	5.7	2.8	4.3	P3	5.8	5.7	2.8	4.3
	P2	48.6	51.1	47.2	48.4	P2	48.4	51.1	49.2	51.3	P2	0.2	0.0	2.0	3.0	P2	0.2	0.0	2.0	3.0
	P1	46.9	48.2	46.4	46.8	P1	51.0	52.2	51.2	50.2	P1	4.1	4.0	4.8	3.3	P1	4.1	4.0	4.8	3.3
		L5	L4	L3	L2		L5	L4	L3	L2		L5	L4	L3	L2		L5	L4	L3	L2
Eclectic baseboard Heather (EBH)	P4	53.4	58.5	52.4	51.0	P4	54.7	64.1	55.6	54.6	P4	1.3	5.5	3.1	3.6	P4	1.3	5.5	3.1	3.6
	P3	53.3	56.0	53.9	52.8	P3	58.0	60.0	55.5	57.2	P3	4.8	4.0	1.6	4.4	P3	4.8	4.0	1.6	4.4
	P2	52.8	55.8	53.3	53.5	P2	52.1	55.8	55.7	56.2	P2	0.7	0.0	2.3	2.7	P2	0.7	0.0	2.3	2.7
	P1	53.0	55.9	53.5	53.3	P1	56.6	58.3	57.6	56.8	P1	3.6	2.4	4.1	3.5	P1	3.6	2.4	4.1	3.5
		L5	L4	L3	L2		L5	L4	L3	L2		L5	L4	L3	L2		L5	L4	L3	L2
Heat pump (HP)	P4	49.1	55.2	48.4	47.9	P4	50.1	58.2	50.6	50.5	P4	1.0	3.0	2.2	2.6	P4	1.0	3.0	2.2	2.6
	P3	49.7	51.0	49.2	49.0	P3	54.2	53.8	49.4	51.9	P3	4.5	2.8	0.2	2.9	P3	4.5	2.8	0.2	2.9
	P2	49.9	51.0	49.8	49.5	P2	48.8	51.0	51.1	51.1	P2	1.0	0.0	1.4	1.6	P2	1.0	0.0	1.4	1.6
	P1	50.7	51.3	50.0	49.7	P1	52.4	53.3	52.5	51.2	P1	1.6	2.0	2.6	1.5	P1	1.6	2.0	2.6	1.5
		L5	L4	L3	L2		L5	L4	L3	L2		L5	L4	L3	L2		L5	L4	L3	L2
	7.5cfm					5cfm					Abs (7.5cfm – 5cfm)								
Heat pump (HP)	P4	51.1	56.6	50.7	50.4	P4	47.4	55.5	51.2	51.2	P4	3.8	1.1	0.5	0.8	P4	3.8	1.1	0.5	0.8
	P3	51.8	52.7	51.5	51.4	P3	55.0	51.1	46.8	52.6	P3	3.2	1.6	4.6	1.2	P3	3.2	1.6	4.6	1.2
	P2	51.9	51.8	52.3	51.7	P2	49.7	51.8	51.9	51.9	P2	2.2	0.0	0.4	0.2	P2	2.2	0.0	0.4	0.2
	P1	53.7	53.6	52.7	52.3	P1	49.4	50.1	49.8	48.4	P1	4.3	3.5	2.9	3.9	P1	4.3	3.5	2.9	3.9
		L5	L4	L3	L2		L5	L4	L3	L2		L5	L4	L3	L2		L5	L4	L3	L2
Eclectic baseboard Heather (EBH)	P4	52.6	60.2	52.5	51.6	P4	52.5	59.5	53.0	52.4	P4	0.1	0.7	0.4	0.8	P4	0.1	0.7	0.4	0.8
	P3	52.8	56.3	54.2	53.7	P3	56.4	57.3	53.4	54.9	P3	3.6	1.0	0.8	1.2	P3	3.6	1.0	0.8	1.2
	P2	52.3	53.5	54.9	54.0	P2	51.3	53.5	53.2	53.7	P2	1.0	0.0	1.7	0.3	P2	1.0	0.0	1.7	0.3
	P1	56.1	56.8	55.2	53.9	P1	55.3	56.7	55.7	54.4	P1	0.7	0.1	0.5	0.5	P1	0.7	0.1	0.5	0.5
		L5	L4	L3	L2		L5	L4	L3	L2		L5	L4	L3	L2		L5	L4	L3	L2

Color Legend				
Ave of Min	Ave	Ave of Max	Min	Ave of Max
30	55	80	0	5

Figure 74: Interior RH distribution comparison of 15cfm, 7.5cfm, and 5cfm with MV.

7.3.4 CO2 Distribution: Ventilation Flow Rate Comparison.

The CO2 profile in the test rooms demonstrates the CO2 concentration change over two-day period, comparing two ventilation flow rates at a time such as 15 cfm vs 7.5 cfm and 7.5 cfm vs 5cfm as shown in Figure 75 and 76. In the figures, the CO2 concentration in a room with higher ventilation flow rate represented by a red line and the lower with the blue line; in addition, the outdoor CO2 concentration is plotted with a black dot-line. Whereas, in the background, the extra CO2 supply (0.25 lpm) is represented by a broken line in the corresponding colour to the room CO2 profile. In comparing 15 cfm to 7.5 cfm, the room with 7.5 cfm shows 100 PPM more CO2 at the peak in contrast to 15 cfm as illustrated in Figure 75. Whereas comparing 7.5 cfm with 5 cfm, both rooms show a close CO2 profile as presents in Figure 76. Similar graphs are presented in Appendix II, section 6.2. Overall, the CO2 pattern in the room with higher ventilation flow rate is small in comparison to lower flow rate. However, the relative CO2 difference gets smaller when the flow rate decreases.

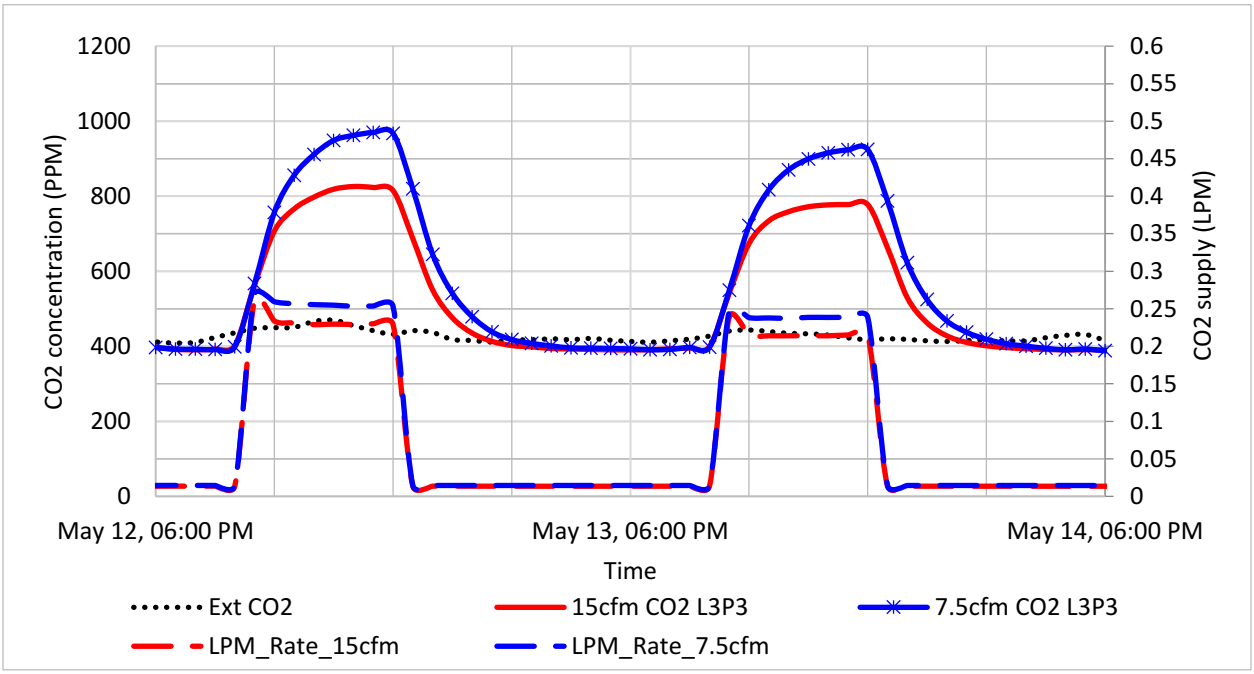

Figure 75: CO2 profile comparing 15cfm and 7.5cfm with RFHS and MV.

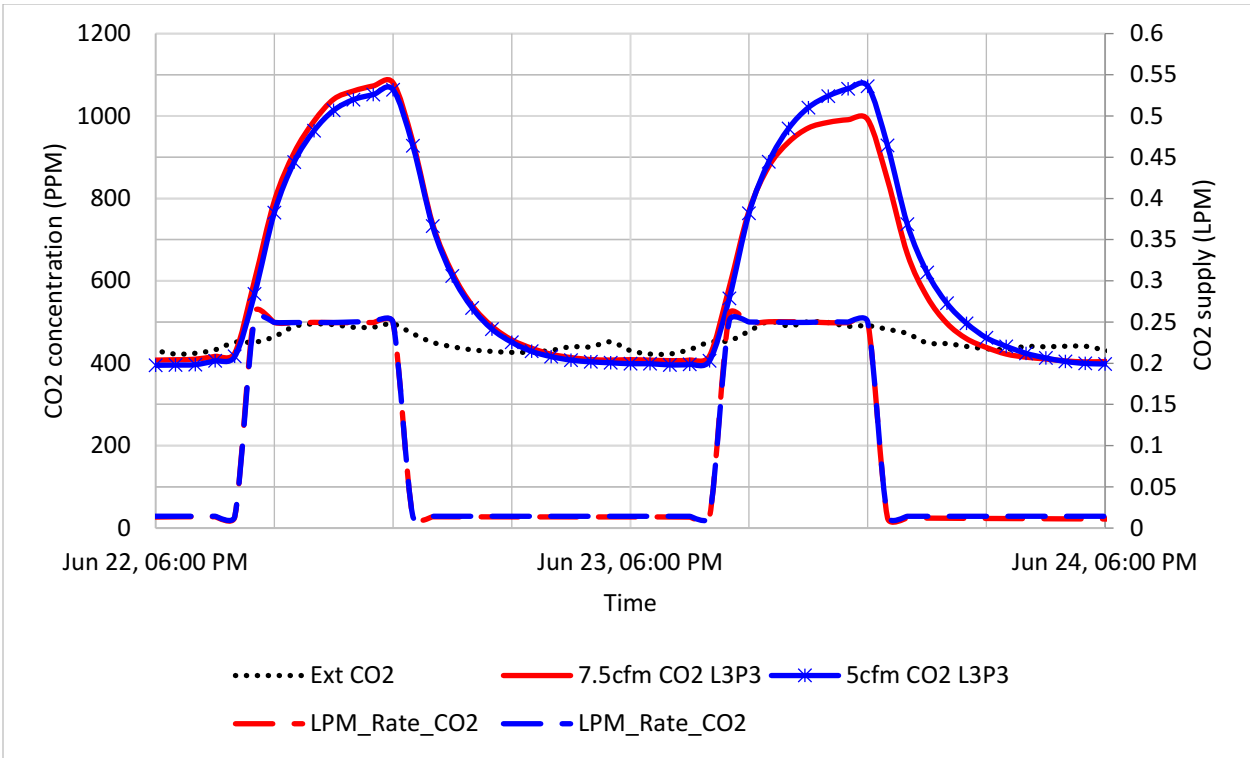

Figure 76: CO2 profile correlating 7.5cfm and 5cfm with EBH and MV.

Furthermore, close-up look at the CO2 concentration at a single time instance (6 AM) from each measurement point normalized by the incoming air CO2 concentration is illustrated in Figure 77. The CO2 concentration colour plot shows similar behaviour to that of RH distribution. The result depicts that during comparison of 15 cfm and 7.5 cfm, the CO2 concentration in a room with 7.5 cfm is high (close 1000 PPM). In the second case, 7.5 cfm vs 5 cfm, the CO2 level in 5 cfm is again higher than 7.5 cfm, but the difference is less than the first comparison. The higher value at L4 is due to the CO2 supply position is close to those sensors, that is why the sensors pick up high CO2 concentration. Overall, the comparison of 15 cfm and 7.5 cfm, the 15 cfm removes more CO2 than 7.5 cfm (over 100 PPM), as depicted on the colour plot. Whereas contrasting 7.5 cfm and 5 cfm, the 7.5 cfm removes more CO2 than 5 cfm. However, the difference is small in most of the measurement spots less than 20 PPM. As a result, the high ventilation flow rate removes more contaminant than lower flow rate.

Heating systems	Ventilation flow rate														Difference				
	15cfm					7.5cfm					Abs (15cfm – 7.5cfm)				
Radiant Floor Heating system (RFHS)	P4	319	473	347	358	P4	572	595	506	525	P4	253	123	159	167
	P3	352	407	344	356	P3	464	577	484	499	P3	112	170	141	143
	P2	335	377	363	354	P2	500	521	498	482	P2	165	144	135	129
		L5	L4	L3	L2		L5	L4	L3	L2		L5	L4	L3	L2
Eclectic baseboard Heather (EBH)	P4	421	496	418	424	P4	521	626	533	554	P4	100	130	115	129
	P3	389	489	428	421	P3	443	619	520	538	P3	54	130	92	116
	P2	359	443	421	418	P2	507	547	537	514	P2	149	104	116	96
		L5	L4	L3	L2		L5	L4	L3	L2		L5	L4	L3	L2
Heat pump (HP)	P4	433	534	432	441	P4	545	654	544	562	P4	112	120	113	121
	P3	437	488	428	437	P3	505	664	524	541	P3	68	176	96	103
	P2	427	441	439	434	P2	538	557	538	513	P2	111	116	100	79
		L5	L4	L3	L2		L5	L4	L3	L2		L5	L4	L3	L2
	7.5cfm					5cfm					Abs (7.5cfm – 5cfm)				
Heat pump (HP)	P4	580	692	593	610	P4	608	722	601	629	P4	29	30	8	18
	P3	597	692	593	607	P3	571	692	585	607	P3	27	1	7	0
	P2	597	610	619	604	P2	615	625	601	584	P2	18	15	18	20
		L5	L4	L3	L2		L5	L4	L3	L2		L5	L4	L3	L2
Eclectic baseboard Heather (EBH)	P4	587	705	586	605	P4	609	606	589	621	P4	21	99	4	16
	P3	519	656	585	606	P3	514	656	569	591	P3	5	362	17	15
	P2	586	610	635	608	P2	632	680	659	597	P2	46	70	24	11
		L5	L4	L3	L2		L5	L4	L3	L2		L5	L4	L3	L2

Color Legend				
Ave of Min	Ave	Ave of Max	Min	Ave of Max
700	950	1200	0	200

Figure 77: Interior CO2 distribution comparison of 15cfm, 7.5cfm, and 5cfm with MV.

7.3.5 Contaminant Removal Effectiveness (CRE): Ventilation Flow Rate Comparison

The contaminant removal effectiveness expresses how the contaminant particle is removed from a given space based on the relative contaminant concentration difference between a measurement point and the contaminant concentration between supply and exhaust air. Therefore, in this section, the CRE is discussed with having a higher ventilation flow rate in comparison to the lower one. Figure 78 presents colour plots of CRE at a single time instance for (15 cfm vs 7.5 cfm) as well as (7.5 cfm vs 5 cfm) all with MV; similar trend also is found when using UV and report in Appendix II section 6.3. The CRE in the rooms indicates that CRE is found mostly similar. In all cases, either using RFHS or HP or EBH, the room with 15 cfm show relatively less CRE in comparison to 7.5 cfm. Furthermore, the difference is less than 7.5% in most measurement points. Similar trend finds when comparing 7.5 cfm and 5 cfm, in which a room with 7.5 cfm show high CRE relative to a room with 5 cfm. In this case, the difference is less than 6% in most of the measurement points. Overall, high CRE discovers close to the air supply (L5), and 100% is determined by the proximity of the exhaust (L2P2). In general, 15 cfm provides better CRE than 7.5 cfm, and it is also true comparing 7.5 cfm to 5cfm because of the higher the ventilation flow rates, the more contaminant removal, which leads higher CRE in comparison to lower ventilation flow rate.

Heating systems	Ventilation flow rate											Difference				
	15cfm					7.5cfm						Abs (15cfm – 7.5cfm)				
Radiant Floor Heating system (RFHS)	P4	110.9	74.8	101.8	98.8	P4	84.3	81.0	95.3	91.8		P4	26.6	6.2	6.5	7.0
	P3	100.5	86.8	102.8	99.4	P3	104.0	83.5	99.5	96.7		P3	3.5	3.3	3.3	2.7
	P2	105.6	93.8	97.5	100.0	P2	96.4	92.5	96.9	100.0		P2	9.2	1.2	0.6	0.0
		L5	L4	L3	L2		L5	L4	L3	L2			L5	L4	L3	L2
Eclectic baseboard Heather (EBH)	P4	99.3	84.3	100.2	98.5	P4	98.6	82.0	96.5	92.9		P4	0.7	2.3	3.7	5.7
	P3	107.5	85.6	97.7	99.3	P3	116.0	83.0	98.8	95.6		P3	8.5	2.6	1.1	3.7
	P2	116.6	94.4	99.4	100.0	P2	101.3	94.0	95.8	100.0		P2	15.3	0.4	3.6	0.0
		L5	L4	L3	L2		L5	L4	L3	L2			L5	L4	L3	L2
Heat pump (HP)	P4	100.1	81.2	100.5	98.4	P4	94.0	78.4	94.2	91.3		P4	6.1	2.8	6.2	7.2
	P3	99.3	89.0	101.4	99.2	P3	101.5	77.2	97.9	94.9		P3	2.2	11.7	3.5	4.4
	P2	101.6	98.2	98.9	100.0	P2	95.3	92.0	95.3	100.0		P2	6.3	6.2	3.6	0.0
		L5	L4	L3	L2		L5	L4	L3	L2			L5	L4	L3	L2
	7.5cfm					5cfm						Abs (7.5cfm – 5cfm)				
Heat pump (HP)	P4	104.1	87.2	101.8	98.9	P4	95.9	80.8	97.0	92.8		P4	8.2	6.4	4.7	6.0
	P3	101.1	87.2	101.8	99.4	P3	102.3	84.3	99.7	96.2		P3	1.2	2.8	2.1	3.3
	P2	101.1	99.0	97.5	100.0	P2	94.8	93.4	97.1	100.0		P2	6.2	5.6	0.4	0.0
		L5	L4	L3	L2		L5	L4	L3	L2			L5	L4	L3	L2
Eclectic baseboard Heather (EBH)	P4	103	86	104	101	P4	98	99	101	96		P4	5.4	12.3	2.4	4.4
	P3	117	93	104	100	P3	116	59	105	101		P3	1.0	34.0	1.2	0.7
	P2	104	100	96	100	P2	94	88	91	100		P2	9.3	11.8	5.1	0.0
		L5	L4	L3	L2		L5	L4	L3	L2			L5	L4	L3	L2
	Color Legend															
	Ave of Min					Ave			Ave of Max			Min			Ave of Max	
	700					950			1200			0			200	

Figure 78: Interior CRE distribution comparison of 15cfm, 7.5cfm, and 5cfm with MV.

7.3.6 Indoor Air Quality Number: Ventilation Flow Rate Comparison

Indoor air quality number (IAQN) is the ratio of contaminant removal effectiveness and PD based on ventilation flow rate. Since, in this section, lower ventilation flow rates are compared using IAQN, it is possible to assess the effect of ventilation flow rate difference on IAQN. Consequently, IAQN in the room with 15 cfm, 7.5 cfm, and 5 cfm are illustrated in Figure 79. In the first comparison (15 cfm vs 7.5 cfm), the IAQN is around 5 in a room with 15 cfm and around 3 for the 7.5 cfm. In the second comparison, it is around 3 in the room with 7.5 cfm and about 2.4 cfm in a room with 5 cfm. The indoor air quality number (IAQN) present in the Figure 79 indicates that the higher ventilation flow rate produces higher IAQN in comparison to lower ventilation flow rate. It is because the higher ventilation flow rate creates higher contaminant removal rate as illustrated in section 7.3.6 which lead higher IAQN. The higher the number represents better indoor air quality, whereas the low number depicts the opposite. Overall, the higher the ventilation flow rate the highest IAQN in contrast to the lower flow rate. The different, however, decrease when the flow rate gets smaller as demonstrated in the comparison of 7.5 cfm and 5 cfm. The same behaviour is found in the rest of experiments in which the ventilation strategy switches from MV to UV as illustrated in Appendix II section 6.4.

Heating systems	Ventilation flow rate															Difference				
	15cfm					7.5cfm										Abs (15cfm – 7.5cfm)				
Radiant Floor Heating system (RFHS)	P4	5.6	3.7	5.1	5.0	P4	2.6	2.5	3.0	2.9						P4	2.9	1.2	2.1	2.1
	P3	5.0	4.3	5.2	5.0	P3	3.2	2.6	3.1	3.0						P3	1.8	1.7	2.1	2.0
	P2	5.3	4.7	4.9	5.0	P2	3.0	2.9	3.0	3.1						P2	2.3	1.8	1.9	1.9
		L5	L4	L3	L2		L5	L4	L3	L2							L5	L4	L3	L2
Eclectic baseboard Heather (EBH)	P4	5.0	4.2	5.0	4.9	P4	3.1	2.6	3.0	2.9						P4	1.9	1.7	2.0	2.0
	P3	5.4	4.3	4.9	5.0	P3	3.6	2.6	3.1	3.0						P3	1.8	1.7	1.8	2.0
	P2	5.8	4.7	5.0	5.0	P2	3.2	2.9	3.0	3.1						P2	2.7	1.8	2.0	1.9
		L5	L4	L3	L2		L5	L4	L3	L2							L5	L4	L3	L2
Heat pump (HP)	P4	5.0	4.1	5.0	4.9	P4	2.9	2.4	2.9	2.8						P4	2.1	1.6	2.1	2.1
	P3	5.0	4.5	5.1	5.0	P3	3.2	2.4	3.0	3.0						P3	1.8	2.0	2.0	2.0
	P2	5.1	4.9	5.0	5.0	P2	3.0	2.9	3.0	3.1						P2	2.1	2.1	2.0	1.9
		L5	L4	L3	L2		L5	L4	L3	L2							L5	L4	L3	L2
	7.5cfm					5cfm										Abs (7.5cfm – 5cfm)				
Heat pump (HP)	P4	3.2	2.7	3.2	3.1	P4	2.3	2.0	2.4	2.3						P4	0.9	0.7	0.8	0.8
	P3	3.1	2.7	3.2	3.1	P3	2.5	2.1	2.4	2.4						P3	0.6	0.7	0.7	0.7
	P2	3.1	3.1	3.0	3.1	P2	2.3	2.3	2.4	2.4						P2	0.8	0.8	0.7	0.7
	HP	L5	L4	L3	L2		L5	L4	L3	L2							L5	L4	L3	L2
Eclectic baseboard Heather (EBH)	P4	3.2	2.7	3.2	3.1	P4	2.4	2.4	2.5	2.4						P4	0.8	0.3	0.8	0.8
	P3	3.6	2.9	3.2	3.1	P3	2.8	1.4	2.6	2.5						P3	0.8	1.5	0.7	0.7
	P2	3.2	3.1	3.0	3.1	P2	2.3	2.1	2.2	2.4						P2	0.9	1.0	0.8	0.7
		L5	L4	L3	L2		L5	L4	L3	L2							L5	L4	L3	L2

Color Legend				
Ave of Min	Ave	Ave of Max	Min	Ave of Max
0	3	6	0	4

Figure 79: Interior IAQN distribution comparison of 15cfm, 7.5cfm, and 5cfm with MV.

7.3.7 Global Contaminant Removal Effectiveness (GCRE) and Indoor Air Quality Number (IAQN)

The GCRE and the IAQN in the test room present in Figure78 and 79 show two-day plots for the experiments comparing the influence of ventilation flow rate on indoor air quality. The plots use the room average CO2 concentration to calculate GCRE and then use it to determine IAQN in the test rooms. Therefore, the result represents the entire room contaminant distribution produce while providing different ventilation flow rate. In both cases (GCRE and IAQN), significant reading is measured only once the extra CO2 start supplying at 10 PM in both rooms. Furthermore, both rooms exhibit similar trend despite the difference in magnitude. The room with 15 cfm shows higher GCRE in contrast to a room with 7.5 cfm as shown in Figure 80. Whereas in the case of the second comparison 7.5 cfm provide slightly more GCRE to 5 cfm as shown in Figure 81. Moreover, the IAQN in the room with 15 cfm is close to 40% more than a room with 7.5 cfm, which is similar to the behaviour observed in the colour plot discussed in the previous section (section 7.3.5). In addition, in the case of 7.5 cfm vs 5 cfm, the room with 7.5 cfm create 25% more IAQN in comparison to a room with 5 cfm, which is again in line with the colour plot in section 7.3.5. The GCRE in the test rooms is high in all cases, and it is between 80% - 100%. The same trend is found when repeating these experiments with UV and the result present in Appendix II section 6.8.

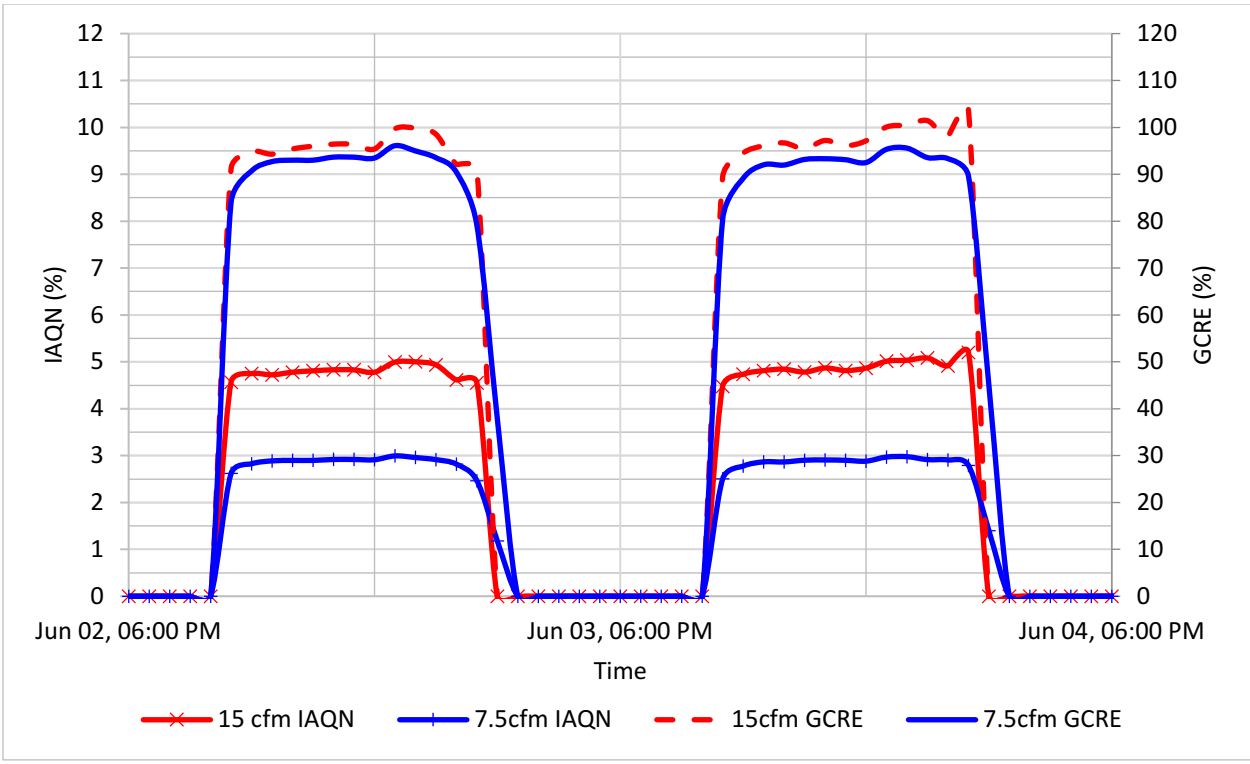

Figure 80: GCRE and IAQN: HP (15cfm vs 7.5cfm) MV.

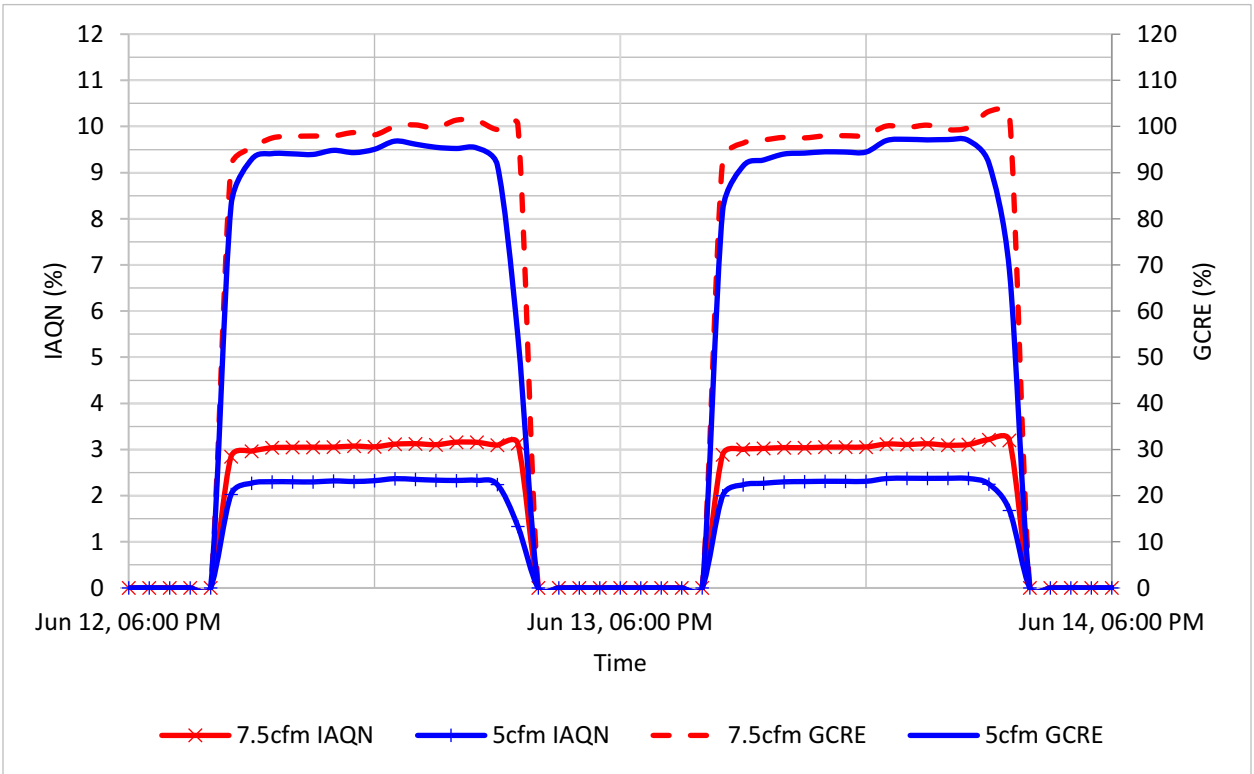

Figure 81: GCRE and IAQN: HP (7.5cfm vs 5cfm) MV.

7.3.8 Energy Penalty: Ventilation Flow Rate Comparison

The ventilation air supply into the test room gets heat while mixing inside and discharged. These exhaust air costs energy. Therefore, this section compares the energy penalty due to ventilation flow rate difference between 15 cfm, 7.5 cfm and 5 cfm in a test room with the same heating system and ventilation strategies. The room with 15cfm shows higher energy consumption relative to a room with 7.5 cfm as illustrated in Figure 82. The peak energy consumption with 15 cfm is 0.25 kWh and 0.2 kWh in a room with 7.5 cfm. Similarly, a room with 7.5 cfm consumes more energy relative to a room with 5 cfm as depicted in Figure 83. The energy usage difference in the first comparison (15 cfm vs 7.5 cfm) is higher than the second comparison (7.5 cfm vs 5 cfm). Overall, the higher ventilation flow rate consumes more energy relative to less flow rate. However, the corresponding energy penalty due to ventilation gets lower when the ventilation flow rates get lower. Similar plots present in Appendix II, section 6.9.

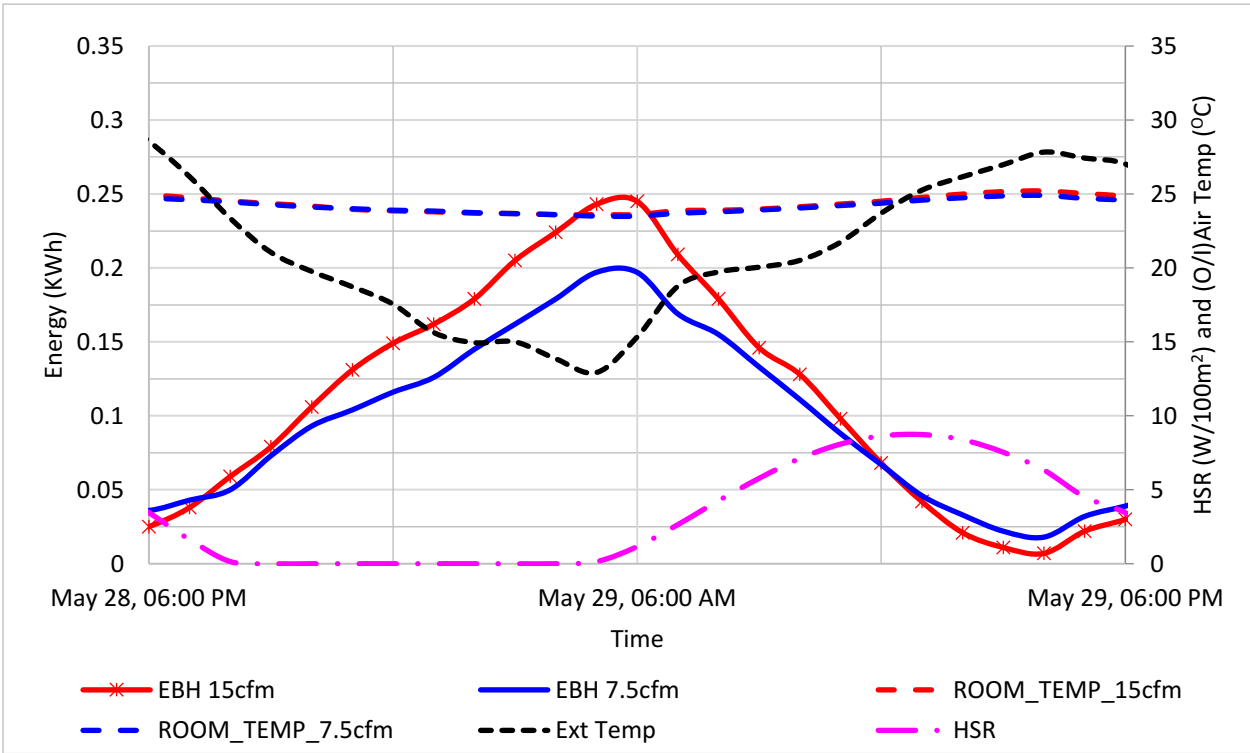

Figure 82: Energy profile of EBH with 15cfm and 7.5cfm.

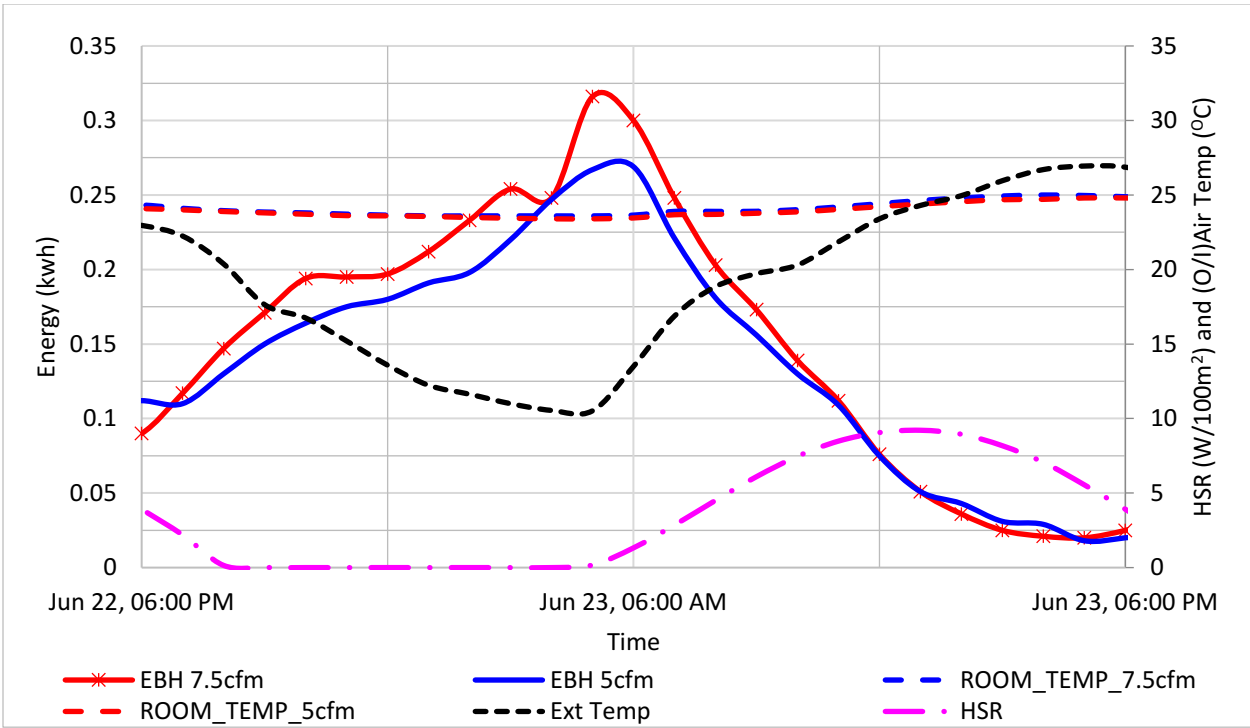

Figure 83: Energy profile of EBH and MV with 7.5cfm and 5cfm.

8 CONCLUSION

To sum up, this study conducts 19 pairs of field experiments comparing four heating systems, two ventilation strategies, and three ventilation flow rates. The first comparison involves analyzing the relative thermal energy performance and general/local thermal comfort of the heating systems as well as investigate various aspects of the indoor environment condition by the systems such as temperature distribution and RH distribution to understand how the system performs. The second comparison studies the two ventilation strategies and compare the relative performance and in pact on the indoor environment. The last section in this study deal with the comparative analysis of three-ventilation flow rates. Therefore, after going through all the data analysis and results in the following conclusion find outstanding.

1) In this study, four heating systems are compared based on the thermal energy they provide to the test rooms. All heating systems supply similar thermal energy into the test room between 10 kWh and 14 kWh depending on outdoor weather condition. The RFHS provide 3.4% and 1.79% more thermal energy than HP and EBH respectively. The EBH, in contrast, supply 7.79% more than PRH and 3.96% more than HP. Whereas, PRH produces 13.10 % more thermal energy than HP and 6.3% more than RFHS. The difference is due to the difference in heat transfer mode, type of control system and the relative location of the control system to the heating systems.
2) The thermal energy supply by radiant floor surface has two components: Convective and Radiative. The convective thermal energy contributes around 30%, and the 70% is provided by radiative thermal energy to provide the total thermal energy. Moreover, these two thermal energy components combined can be estimated using film coefficient (convective plus radiative thermal conductivity). The film coefficient h = 11 W/m^2 K (from

EN15377) estimates the thermal energy within ± 10 %. Whereas, the film coefficient h = 9.26 W/m^2 K (ASHRAE) might under or overestimate based on the temperature difference between the floor and 1.5 m above the floor.

3) The indoor environment produces by different heating systems is investigated using temperature and RH distribution. The temperature distribution shows that EBH, HP, and PRH provide cold floor temperature. Whereas, RFHS produce warm floor temperature (over 24°C). Above the floor, the RFHS also create more uniform temperature distribution in contrast to the rest of heating systems. The temperature distribution with those three remaining heating systems depicts a less uniform temperature profile. In addition, the coldest wall is East wall, and the coldest spot in the measurement is a north window since it is far from the heat source for all heating systems. The RH distribution for all heating systems mostly is between 40% and 50% with an average of 45% throughout the measurement with an addition 100 gram per hour moisture supply after 8 consecutive hours.
4) The indoor environment produces by the heating systems is assessed for thermal comfort for a single person either standing or seating person. All heating systems provide acceptable thermal comfort (PPD < 20%) for standing position, but the occupant might feel slightly cold for seating position (PPD < 40%) except using RFHS which provides acceptable thermal comfort for seating person as well.
5) The local thermal comfort is investigated while running four heating systems using local thermal discomfort due to radiant asymmetry, vertical temperature difference, and floor temperature. All heating systems create acceptable local thermal discomfort (PD < 5%) due to vertical temperature difference for both sitting and standing person. Out of the four

heating systems, only RFHS deliver thermally acceptable floor surface temperature (PD = 6±1%). Whereas for the remaining three heating systems it is beyond the acceptable range, which is higher than 10%. The radiant asymmetry due to the cold window (south and north) or floor to ceiling for all heating systems is within the acceptable range (PD < 5%).

6) The second major part of this study investigates the performance of two ventilation strategies (MV and UV). The temperature and air velocity distribution are found less affected by the ventilation strategy in use (MV or UV). Whereas, the RH and CO2 distribution indicate that MV show slightly less value and slightly uniform distribution in contrast to UV. In addition, comparing MV and UV, MV depict around 20% more GCRE than UV. The same result reflects while using IAQN for comparison where MV show 20% more IAQN compare to UV. Overall, MV show relatively better performance in contrast to UV.

7) The third major part of this study compares three ventilation flow rates (15 cfm, 7.5 cfm, and 5 cfm). Various aspects of the indoor environment are studied relative to the ventilation flow rates. The reduction of the ventilation flow rate from 15 cfm to 7.5 cfm even to 5 cfm is found to have no significant effect on the temperature distribution and air movement. Whereas, the RH distribution shows that the higher ventilation flow rate demonstrates slightly lesser RH compare to lower ventilation flow rate. Moreover, the high ventilation flow rate comparatively removes more contaminant than low ventilation flow rate. As a result, the CO2 concentration in a room with 15 cfm is relatively less than in a room with 7.5 cfm, and it is the same when comparing 7.5 cfm to 5 cfm. But the difference gets lesser when the flow rate becomes small.

8) In General, the CRE in the test rooms is high in all cases (15 cfm, 7.5 cfm, and 5 cfm) and it is 80% to 100%. Moreover, 15 cfm provides relatively high CRE than 7.5 cfm, and it is also true comparing 7.5 cfm to 5 cfm because of the higher the ventilation flow rates, the more contaminant removal, which led higher CRE in comparison to lower ventilation flow rate. In addition, the room with 15 cfm crate 40% higher IAQN than 7.5 cfm. Whereas, the room with 7.5 cfm crates 25% more IAQN in contrast to a room with 5 cfm. It is because the higher the ventilation flow rate creates the highest IAQN relative to the lower flow rate. Overall, the higher the ventilation flow rate better indoor air quality relative to the lesser flow rate.

Further study

Since this study focus to maintain similar set point in the test room, a recirculating bypass mechanism is used to avoid overheating as explained in section 5.1.2. In this system, in addition to energy loss during the recirculation period, some energy will be lost into the ground. Thus, for instance, the thermal energy supply by RFHS as shown in Table 9 is 25 ± 2% of the total electric energy consumption by the RFHS; the rest dissipates to the ground and in the mechanical room. Therefore, further study is recommended to investigate RFHS energy consumption relative to the thermal energy supply.

9 Appendix I

Section 1: View factor calculation for the radiant floor.
Summary of Square Floor (S.Floor) between floor and Radiation exchanging surfaces in *square floor.*

Radiation exchanging surfaces	View factor
F_S.floor -S.wall	0.192261527
F_S.floor -I.wall	0.213408418
F_S.floor -W.wall	0.213408418
F_S.floor -N_m.wall	0.213408418
F_S.floor - S.ceilling	0.14636633
F_S.Floor-S.Win	0.02114689
Sum	1

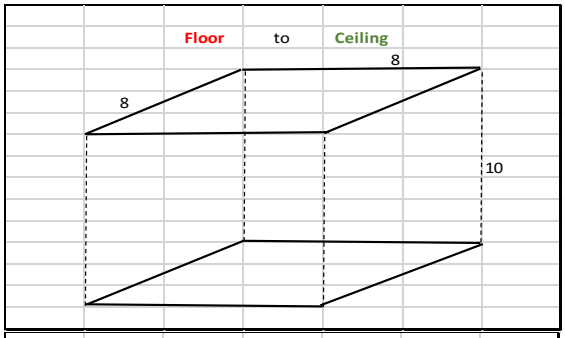

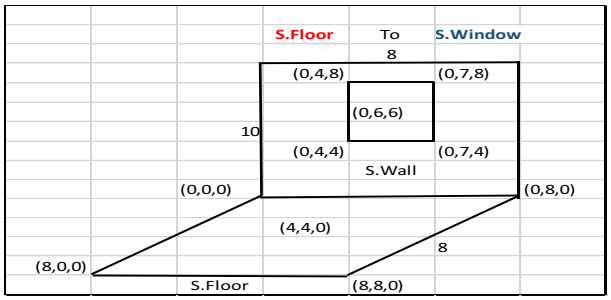

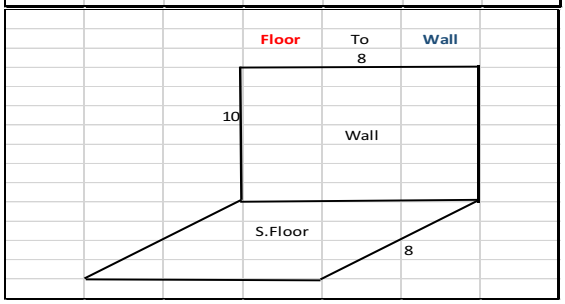

Figure 84: View factor between the square floor and surrounding surfaces.

View factor of Rectangular Floor (R.Floor) with radiation exchanging surfaces - a common arrangement for *Rectangular section(R.)*

Radiation exchanging surfaces	View factor
F_R.floor - S.wall	0.1613362
F_R.floor - N.wall	0.1450186
F_R.floor - E.wall	0.243062
F_R.floor - W_m.wall	0.0765311
F_R.floor - I_m.wall	0.1665309
F_R.floor - Ceilling	0.1912036
F_S.Floor-R.Win	0.0163176
Total	**1**

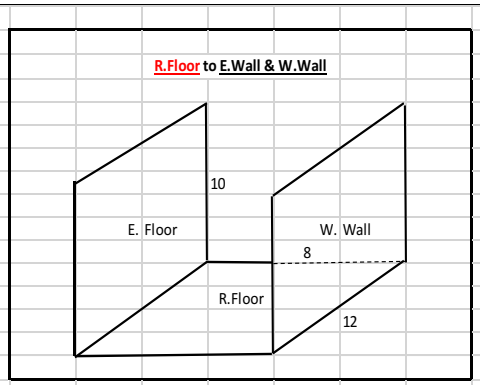

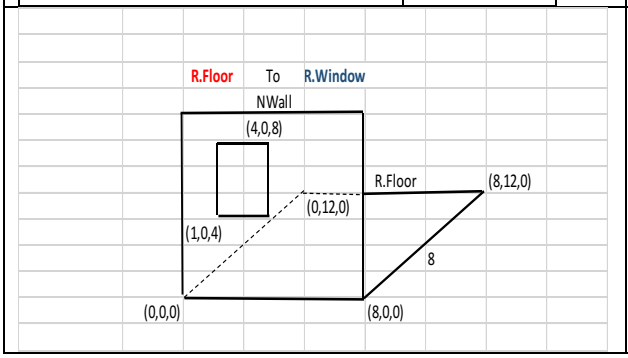

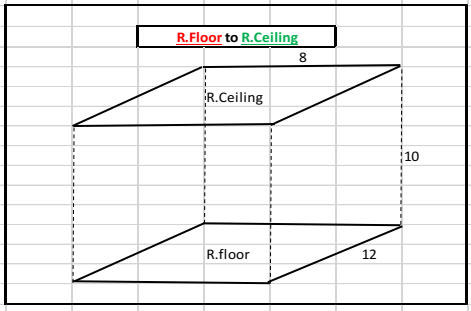

Figure 85 View factor between the rectangular floor and surrounding surfaces.

Section 2

```
%Thermal comfort calculation PMV and PPD
clc
close all
a=1:1:119;
b=1:1:4;
TA(a,b)=xlsread('Tcomf input.xlsx', 'Tair', 'B2:E120');
RH(a,b)=xlsread('Tcomf input.xlsx', 'RH', 'B2:E120');
VEL(a,b)=xlsread('Tcomf input.xlsx', 'Va', 'B2:E120');
TR(a,b)=xlsread('Tcomf input.xlsx', 'MRT', 'B2:E120');
CLO(a,b)=xlsread('Tcomf input.xlsx', 'Iclo', 'B2:E120');
MET(a,b)=xlsread('Tcomf input.xlsx', 'MET', 'B2:E120');
WME(a,b)=zeros(119,4);
for a=1:1:119
   for b=1:1:4
   FNPS(a,b)=exp(16.6536-4030.183/(TA(a,b)+235));
   PA(a,b)=RH(a,b)*10*FNPS(a,b);
   ICL(a,b)=0.155*CLO(a,b);
   M(a,b)=MET(a,b)*58.15;
   W(a,b)=WME(a,b)*58.15;
   MW(a,b)=M(a,b)-W(a,b);
   if(ICL(a,b)<0.078)
   FCL(a,b)=1+1.3*ICL(a,b);
   else
   FCL(a,b)=1.05+0.645*ICL(a,b);
   end
   HCF(a,b)=12.1*sqrt(VEL(a,b));
   TAA(a,b)=TA(a,b)+273;
   TRA(a,b)=TR(a,b)+273;
   TCLA(a,b)=TAA(a,b)+(35.5-TA(a,b))/(3.5*(6.45*ICL(a,b)+0.1));
   P1(a,b)=ICL(a,b)*FCL(a,b);
   P2(a,b)=P1(a,b)*3.96;
   P3(a,b)=P1(a,b)*100;
   P4(a,b)=P1(a,b)*TAA(a,b);
   P5(a,b)=308.7-0.028*MW(a,b)+P2(a,b)*(TRA(a,b)/100)^4;
   XN(a,b)=TCLA(a,b)/100;
   XF(a,b)=XN(a,b);
   EPS=0.00015;
   XF(a,b)=(XF(a,b)+XN(a,b))/2;
   HCN(a,b)=2.38*abs(100*XF(a,b)-TAA(a,b))^0.25;
   if(HCF(a,b)>HCN(a,b))
   HC(a,b)=HCF(a,b);
   else
   HC(a,b)=HCN(a,b);
   end
   XN(a,b)=(P5(a,b)+P4(a,b)*HC(a,b)-P2(a,b)*(XF(a,b))^4)/(100+P3(a,b)*HC(a,b));
   N=1;
   while abs(XN(a,b)-XF(a,b))>EPS
   XF(a,b)=(XF(a,b)+XN(a,b))/2;
   HCN(a,b)=2.38*abs(100*XF(a,b)-TAA(a,b))^0.25;
   if(HCF(a,b)>HCN(a,b))
   HC(a,b)=HCF(a,b);
   else
   HC(a,b)=HCN(a,b);
   end
   XN(a,b)=(P5(a,b)+P4(a,b)*HC(a,b)-P2(a,b)*(XF(a,b))^4)/(100+P3(a,b)*HC(a,b));
```

```
    N=N+1;
    end
    TCL(a,b)=100*XN(a,b)-273;
    HL1(a,b)=3.05*0.001*(5733-6.99*MW(a,b)-PA(a,b));
    if(MW(a,b)>58.15)
    HL2(a,b)=0.42*(MW(a,b)-58.15);
    else
    HL2(a,b)=0;
    end
    HL3(a,b)=1.7*0.00001*M(a,b)*(5867-PA(a,b));
    HL4(a,b)=0.0014*M(a,b)*(34-TA(a,b));
    HL5(a,b)=3.96*FCL(a,b)*((XN(a,b))^4-(TRA(a,b)/100)^4);
    HL6(a,b)=FCL(a,b)*HC(a,b)*(TCL(a,b)-TA(a,b));
    TS(a,b)=0.303*exp(-0.036*M(a,b))+0.028;
    PMV(a,b)=TS(a,b)*(MW(a,b)-HL1(a,b)-HL2(a,b)-HL3(a,b)-HL4(a,b)-HL5(a,b)-HL6(a,b));
    PPD(a,b)=100-95*exp(-(0.03353*(PMV(a,b))^4+0.2179*(PMV(a,b))^2));
    end
end
% xlswrite('Tcomf.xlsx',PMV,'PMV');
% xlswrite('Tcomf.xlsx',PPD,'PPD');
```

Section 3

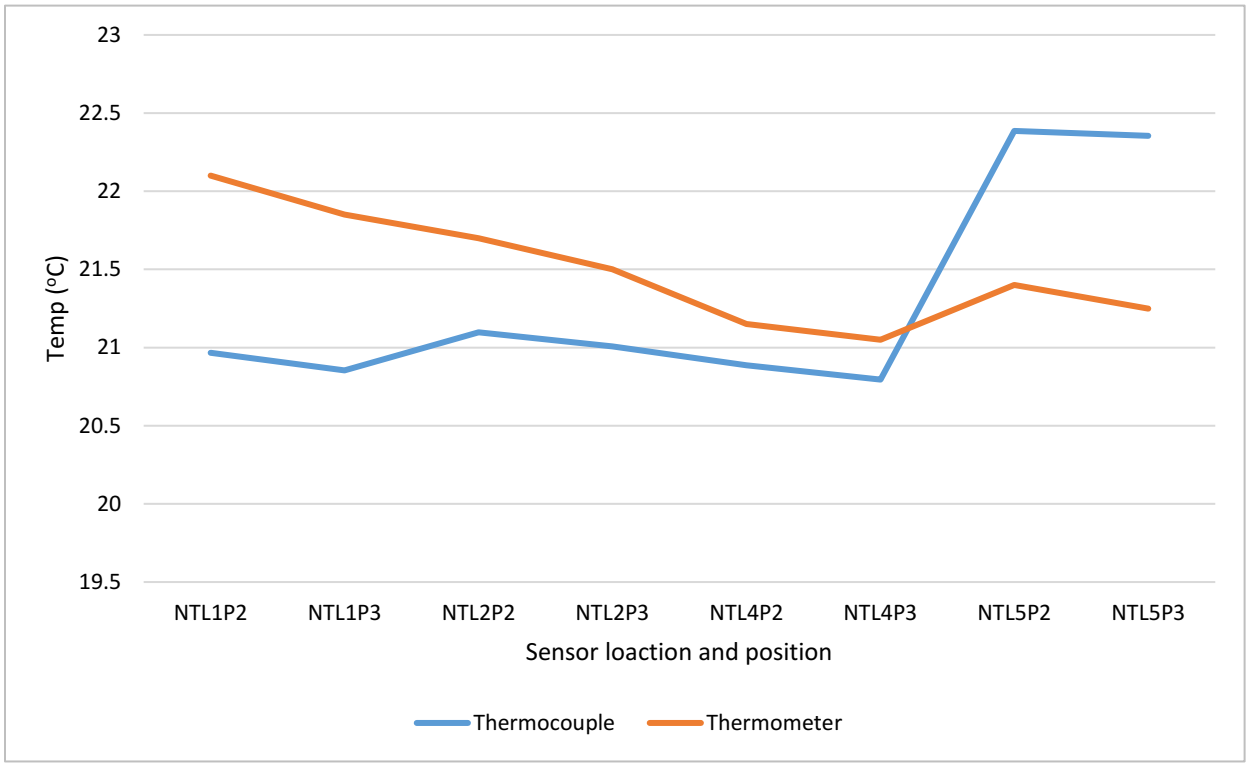

Figure 86: Thermocouple calibration: NTB.

10 Appendix II

Section 1

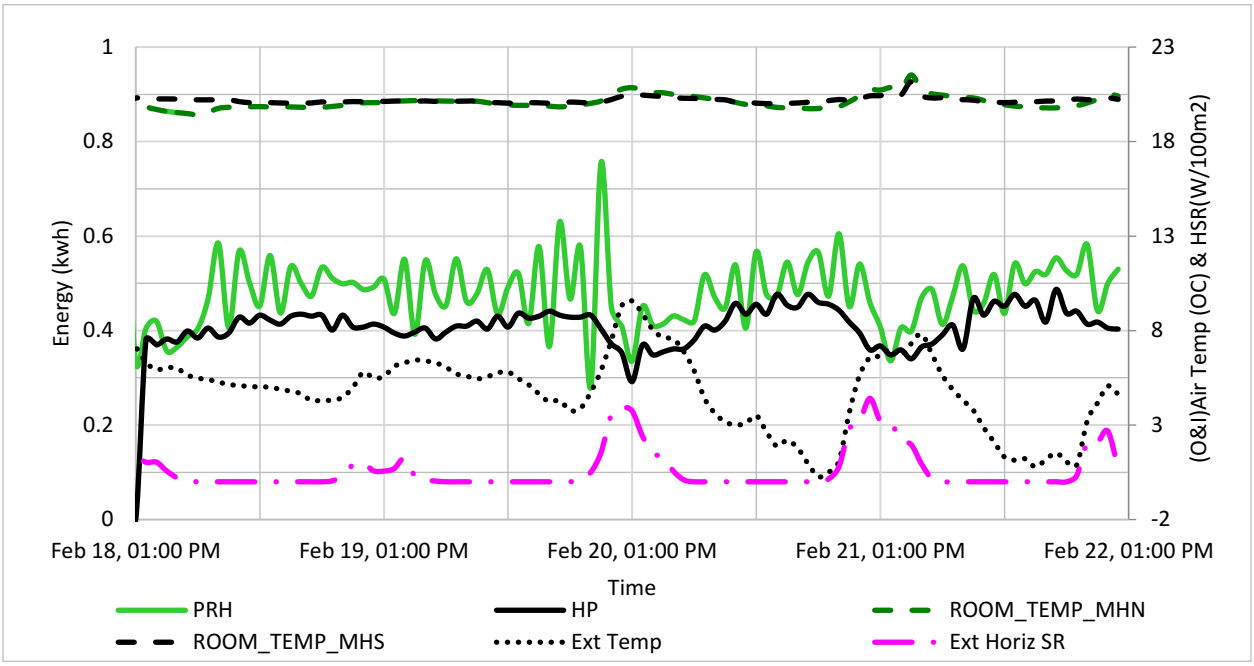

Figure 87: Thermal Energy profile of PRH and HP with indoor and outdoor conditions.

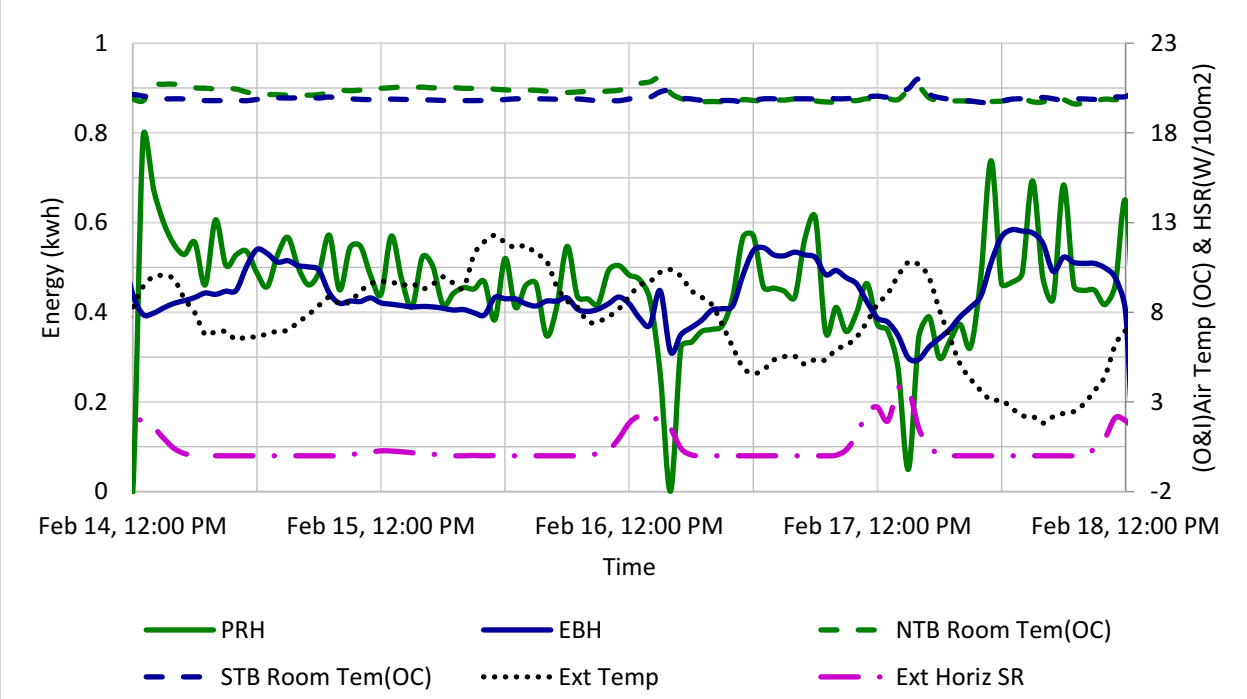

Figure 88: Thermal Energy profile of PRH and EBH with indoor and outdoor conditions.

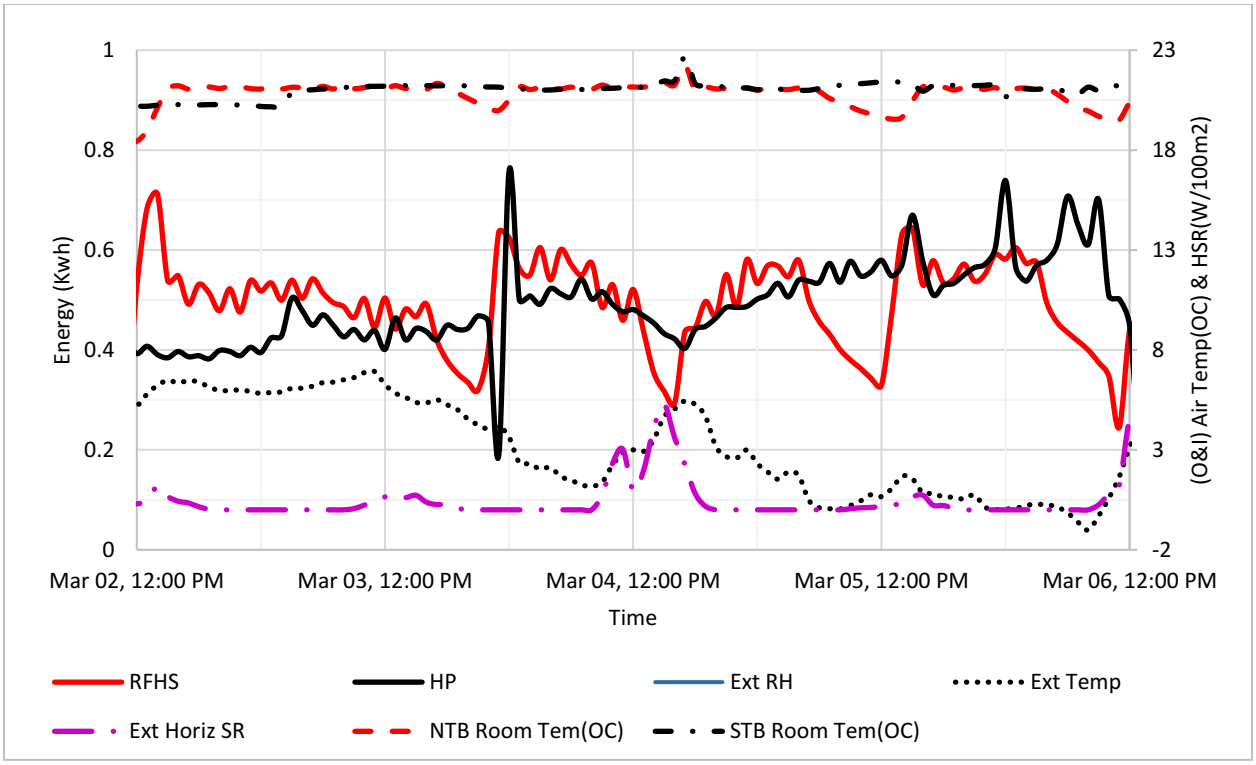

Figure 89: Thermal Energy profile of RFHS and HP with indoor and outdoor conditions.

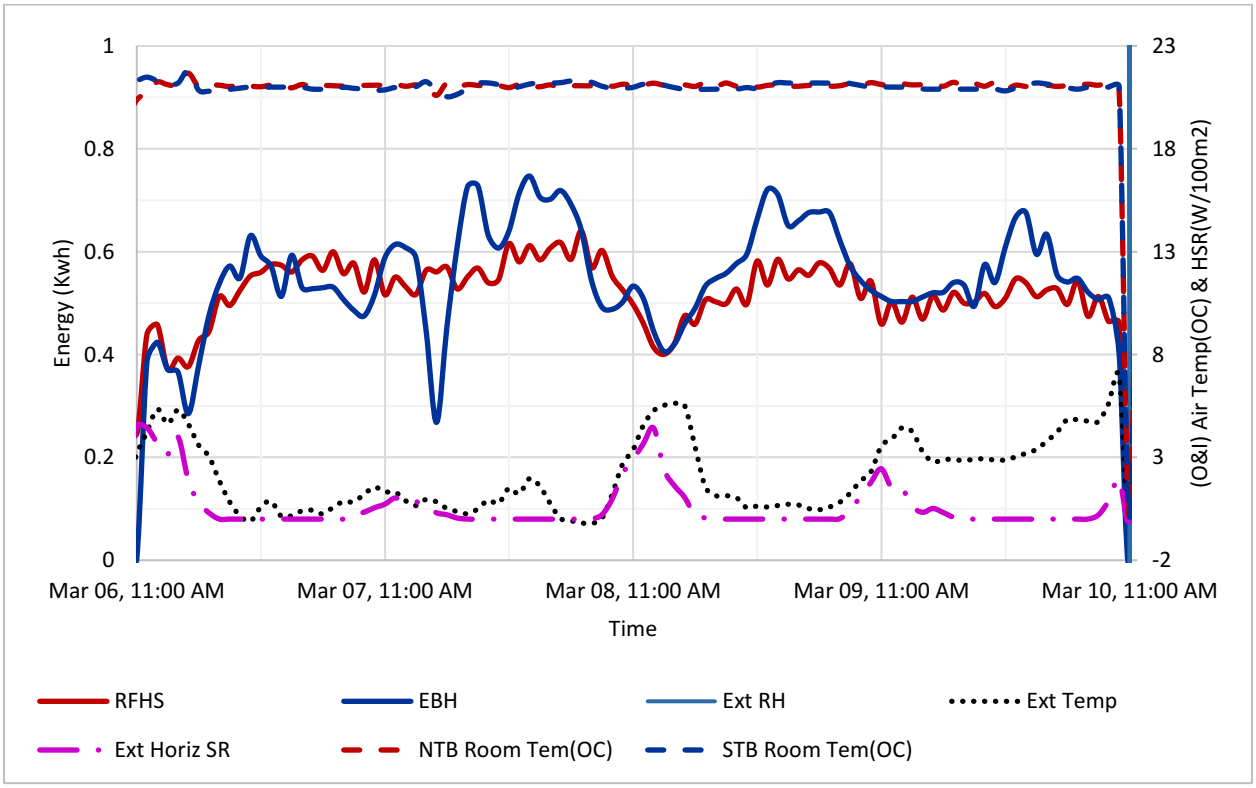

Figure 90: Thermal Energy profile of RFHS and EBH with indoor and outdoor conditions.

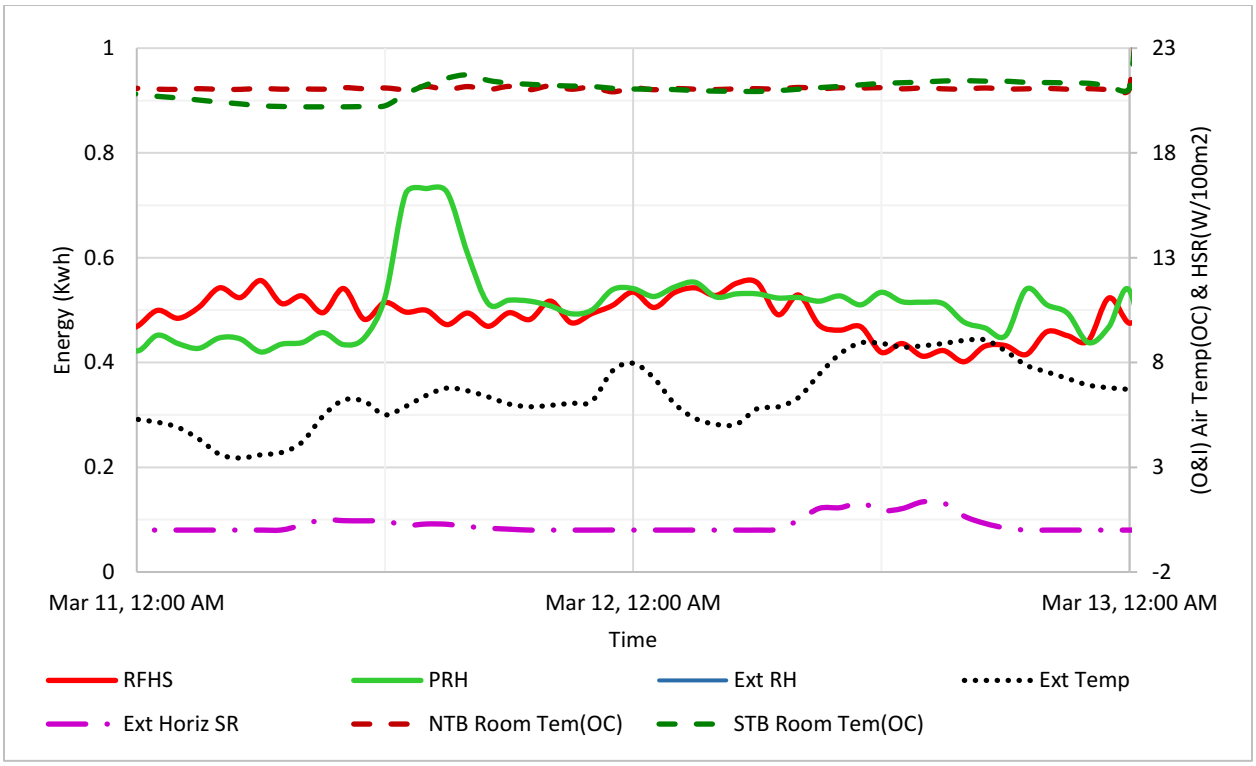

Figure 91: Thermal Energy profile of EBH and HP with indoor and outdoor conditions.

Section 2

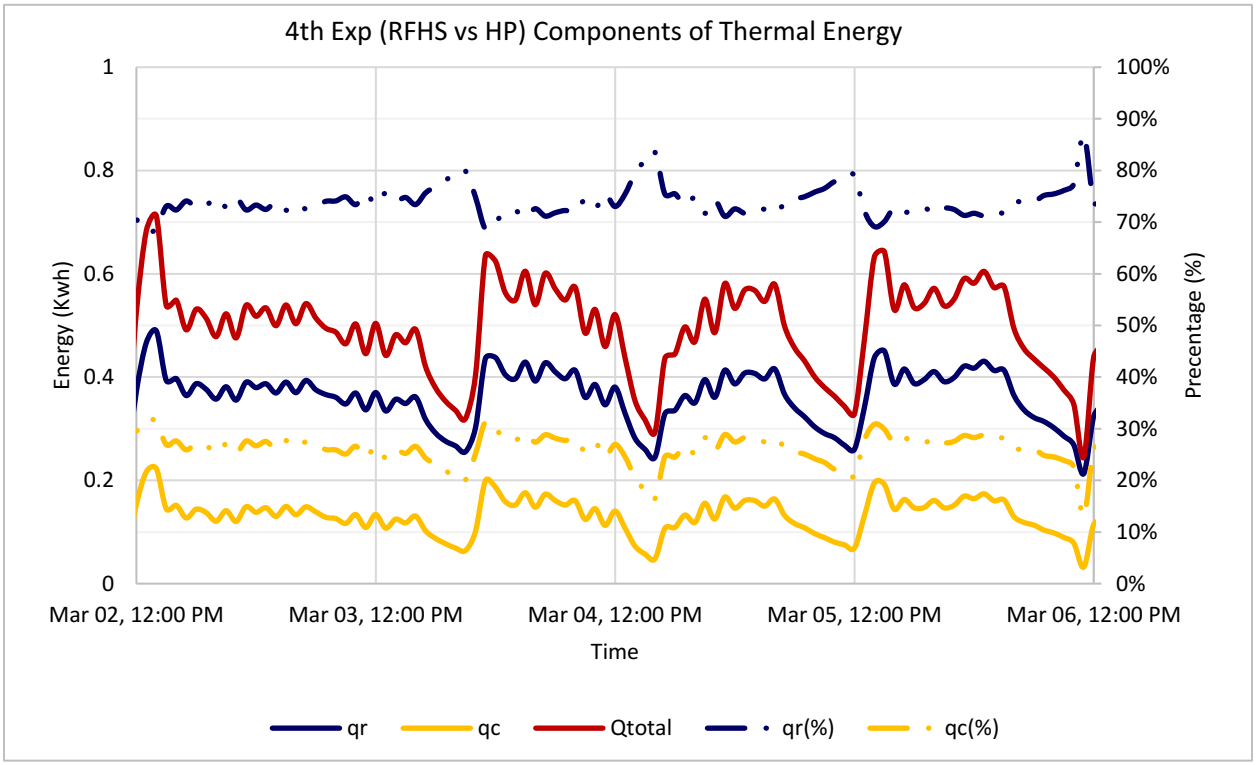

Figure 92 Components of thermal energy delivered by RFHS.

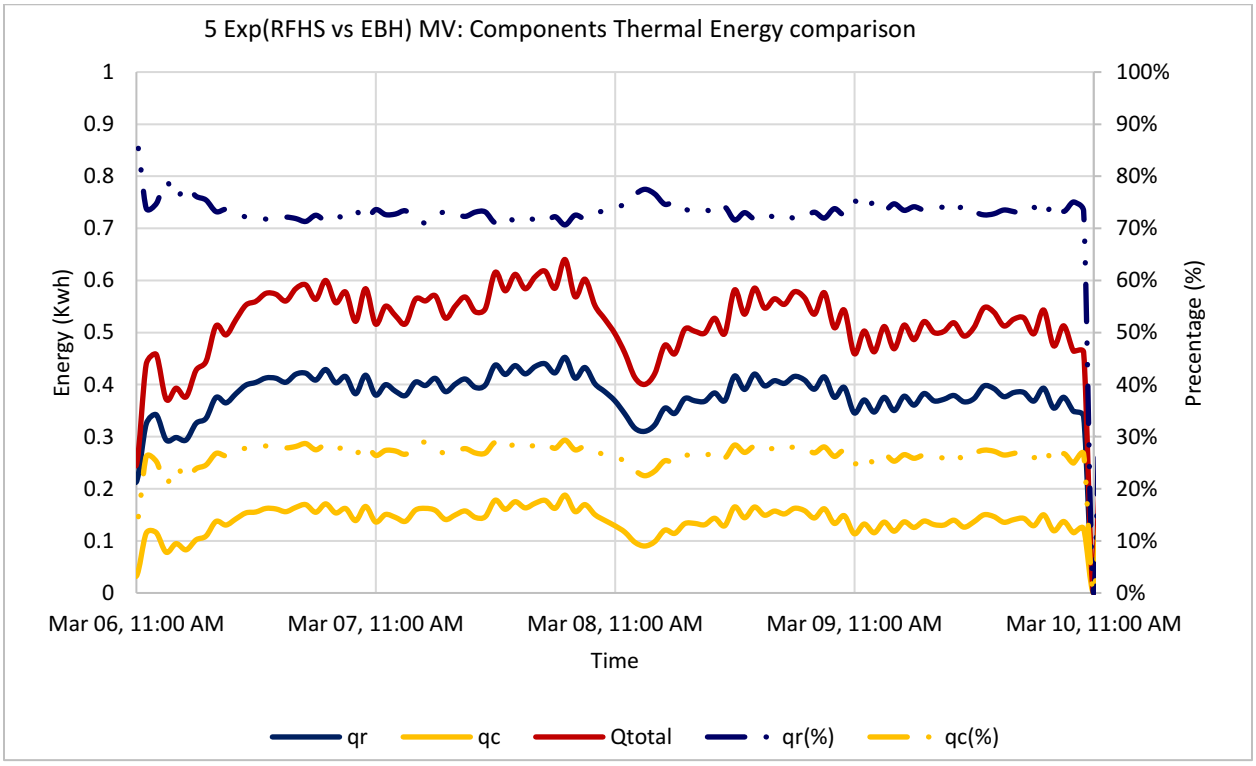

Figure 93: Components of thermal energy delivered by RFHS.

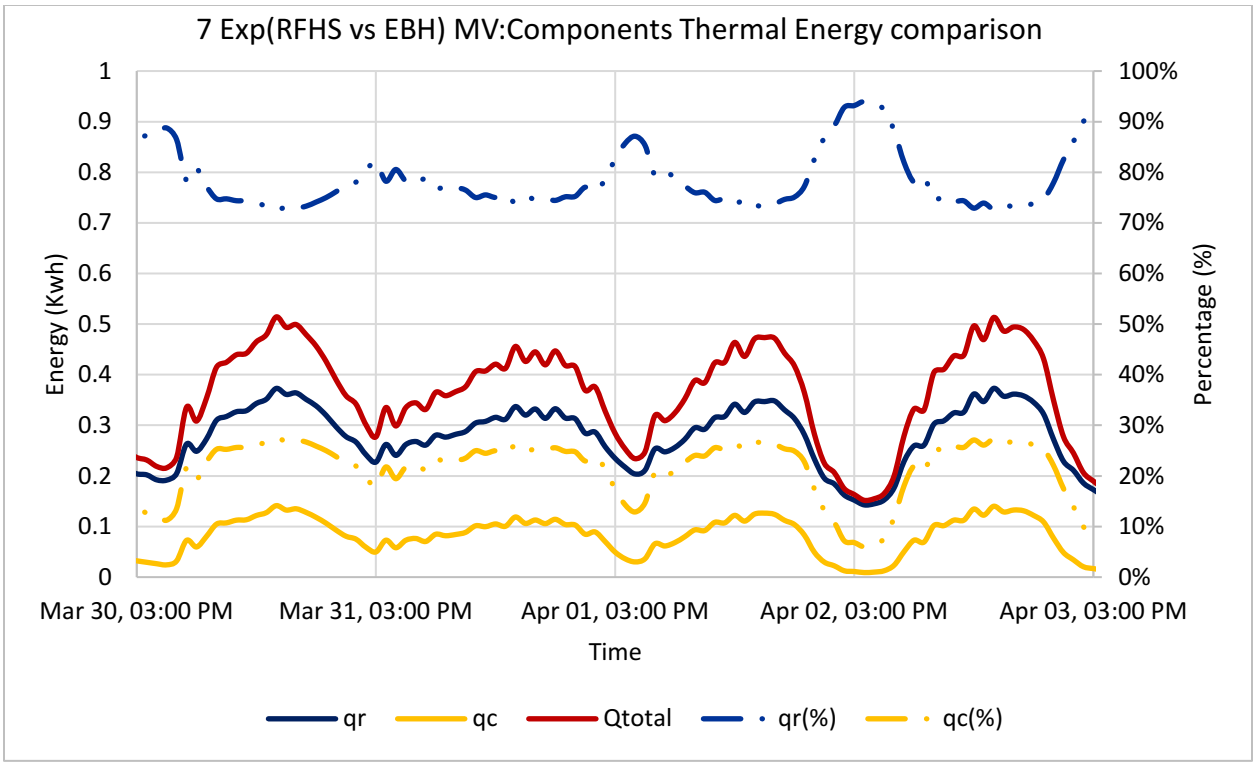

Figure 94: Components of thermal energy delivered by RFHS.

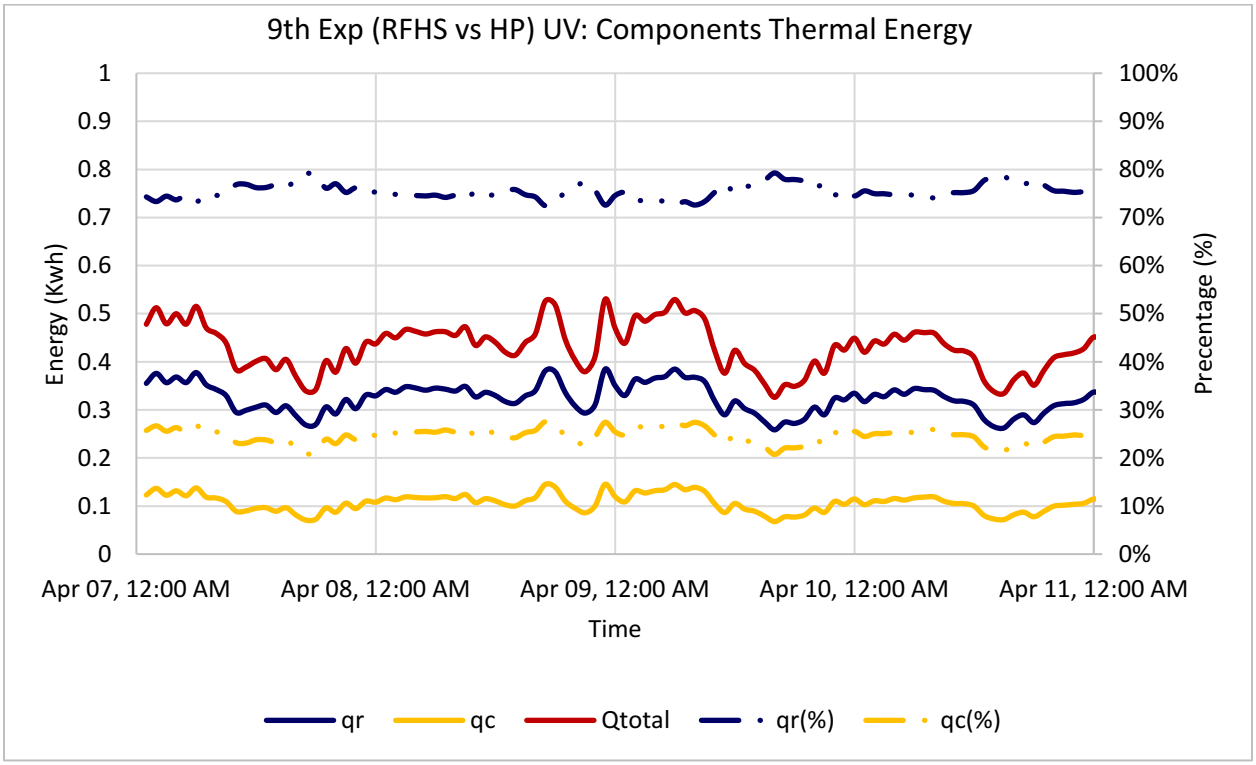

Figure 95: Components of thermal energy delivered by RFHS.

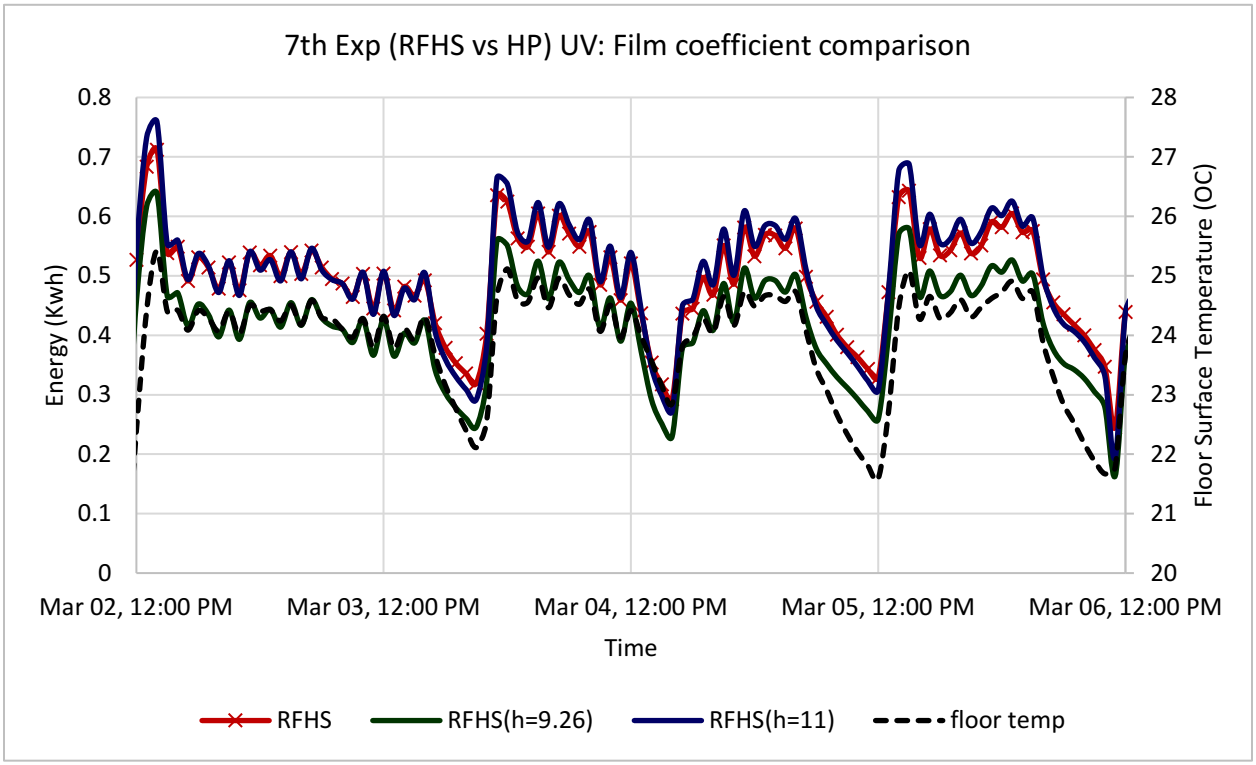

Figure 96: Film coefficient comparisons during 7th Experiment.

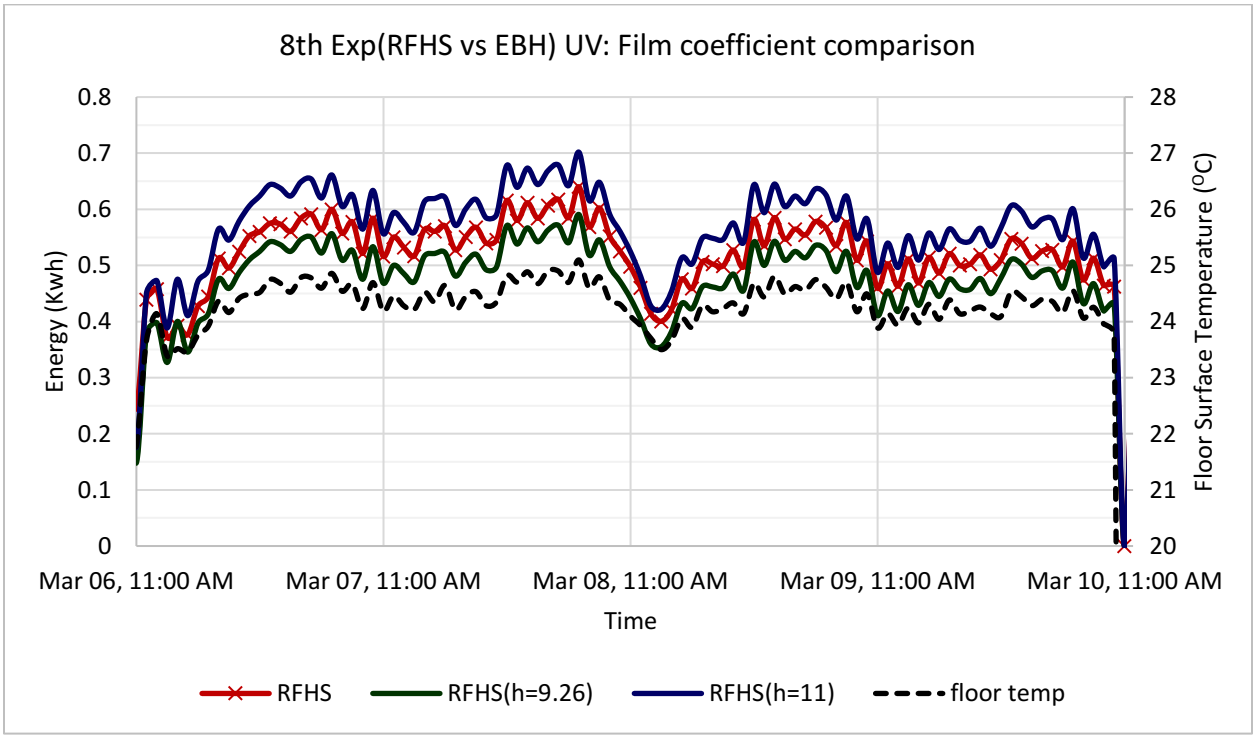

Figure 97: Film coefficient comparisons during 8th Experiment.

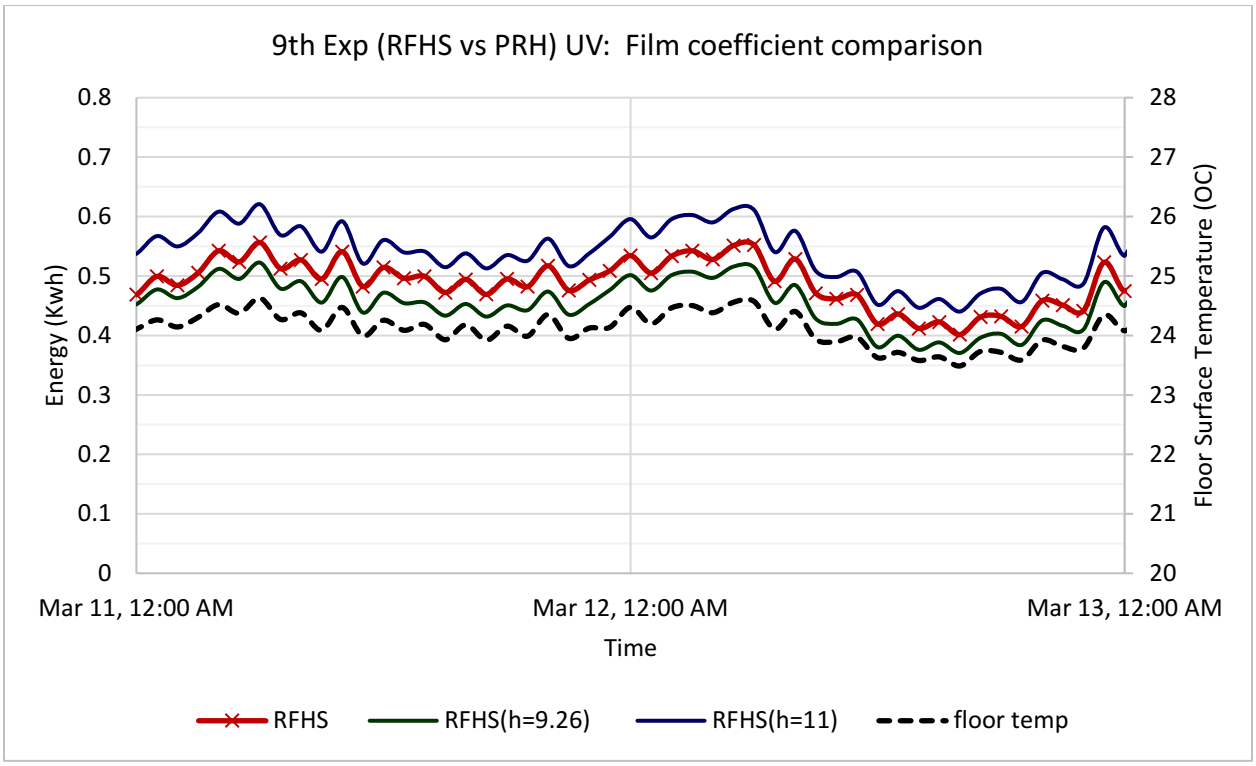

Figure 98: Film coefficient comparisons during 9th Experiment.

Section 4: Temperature Distribution

Indoor temperature distribution											
Heating systems											
Radiant floor heating system (RFHS)						Heat pump (HP)					
P4	20.9	20.8	21.2	20.7	20.3	P4	21.7	21.6	22.2	22.1	21.4
P3	21.1	20.7	21.3	20.7	20.6	P3	21.4	20.7	21.8	20.9	20.4
P2	21.0	20.7	21.3	20.7	20.7	P2	20.7	19.8	20.9	20.4	19.0
4th	L5	L4	L3	L2	L1	4th	L5	L4	L3	L2	L1
P4	20.8	20.8	21.2	20.6	20.2	P4	20.8	20.8	21.3	21.0	20.1
P3	21.1	20.6	21.3	20.6	20.4	P3	20.4	19.7	20.8	19.9	19.3
P2	21.0	20.7	21.3	20.6	20.5	P2	19.3	18.8	19.8	19.4	18.0
5th	L5	L4	L3	L2	L1	3rd	L5	L4	L3	L2	L1
P4	20.9	20.9	21.2	20.7	20.2	P4	21.5	21.2	21.5	21.5	21.0
P3	21.1	20.6	21.3	20.6	20.4	P3	20.8	20.1	21.1	20.3	19.7
P2	21.0	20.7	21.3	20.6	20.5	P2	18.9	18.4	19.5	18.6	17.8
6th	L5	L4	L3	L2	L1	1st	L5	L4	L3	L2	L1
Electrical baseboard heater (EBH)						Portable radiator heater (PRH)					
P4	20.4	20.1	20.9	20.7	19.9	P4	21.1	21.1	21.3	21.4	21.2
P3	20.0	19.4	20.4	19.7	19.1	P3	20.6	20.0	20.8	20.1	19.7
P2	18.9	18.8	19.5	19.3	17.9	P2	19.1	18.8	19.7	19.7	18.4
1th	L5	L4	L3	L2	L1	3rd	L5	L4	L3	L2	L1
P4	21.4	20.9	21.4	21.3	21.0	P4	21.0	20.9	21.2	21.4	20.9
P3	20.7	19.9	21.0	20.2	19.6	P3	20.5	20.0	20.8	20.0	19.6
P2	18.9	18.5	19.5	18.6	18.0	P2	19.2	18.8	19.9	19.3	18.5
2nd	L5	L4	L3	L2	L1	2nd	L5	L4	L3	L2	L1
P4	22.7	22.7	23.3	23.0	22.8	P4	22.2	22.2	22.8	22.8	21.9
P3	21.9	21.3	22.6	21.7	21.0	P3	21.4	21.0	22.0	20.9	20.6
P2	20.9	19.6	20.8	19.9	18.9	P2	20.7	19.9	20.9	20.8	19.2
5th	L5	L4	L3	L2	L1	6th	L5	L4	L3	L2	L1

Color Legend		
Ave of Min	Ave	Ave of Max
15	20	25

Figure 99: Temperature distribution with four heating systems and UV.

Section 5: Surface temperature distribution.

Surface temperature distribution							
Heating systems							
Radiant floor heating system (RFHS)							
PC	20.9		21.3		21.2		21.2
P4	20.0		20.8		20.9		
P3	19.4	17.8	21.2	19.3	20.9	18.4	
P2	20.4		21.6		21.4		
P0	25.7		21.9		25.8		26.0
Win			18.2				17.4
5th	E/L5	ES-C3	S/L2	SW-C2	W/L1	NE-C1	N/L4
PC	21.0		21.4		21.3		21.3
P4	19.5		21.1		21.2		
P3	19.6	18.4	21.4	20.0	21.2	19.0	
P2	20.4		21.8		21.5		
P0	24.6		24.0		24.6		24.7
Win			19.1				18.3
6th	E/L5	ES-C3	S/L2	SW-C2	W/L1	NE-C1	N/L4
Heat pump (HP)							
PC	20.9		23.3		20.1		21.6
P4	20.1		21.1		21.7		
P3	19.9	19.7	19.9	19.6	20.5	19.4	
P2	17.7		18.9		19.0		
P0	15.8		17.6		18.0		16.6
Win			22.1				16.7
UV4	E/L5	ES-C3	S/L2	SW-C2	W/L1	NE-C1	N/L4
PC	21.6		22.2		20.3		21.4
P4	20.8		22.1		21.8		
P3	20.5	20.3	21.9	21.3	21.0	19.9	
P2	18.7		20.8		19.9		
P0	17.8		19.0		18.5		17.9
Win			23.3				18.0
UV7	E/L5	ES-C3	S/L2	SW-C2	W/L1	NE-C1	N/L4
Electrical baseboard heater (EBH)							
PC	19.9		20.7		20.1		19.7
P4	18.1		20.7		20.4		
P3	17.5	19.4	21.0	18.8	19.6	17.1	
P2	17.2		19.5		18.6		
P0	16.0		17.3		17.1		16.7
Win			18.5				15.9
1st	E/L5	ES-C3	S/L2	SW-C2	W/L1	NE-C1	N/L4
PC	22.3		24.6		21.6		22.3
P4	21.6		22.5		23.0		
P3	21.3	21.0	21.0	20.8	21.7	20.6	
P2	18.8		20.1		20.2		
P0	17.1		19.0		19.0		17.8
Win			23.9				16.9
5th	E/L5	ES-C3	S/L2	SW-C2	W/L1	NE-C1	N/L4
Portable radiator heater (PRH)							
PC	20.8		22.2		21.8		21.1
P4	19.4		21.4		21.7		
P3	19.0	20.4	21.0	20.2	21.0	18.9	
P2	18.3		20.4		20.3		
P0	16.6		17.0		18.1		16.8
Win			19.4				18.1
UV5	E/L5	ES-C3	S/L2	SW-C2	W/L1	NE-C1	N/L4
PC	22.1		23.8		21.2		22.0
P4	21.4		22.3		22.5		
P3	21.0	20.7	21.2	21.4	21.7	20.5	
P2	19.1		20.6		20.9		
P0	17.5		20.5		19.4		18.0
Win			19.5				17.9
UV9	E/L5	ES-C3	S/L2	SW-C2	W/L1	NE-C1	N/L4

Color Legend		
Ave of Min	Ave	Ave of Max
14	20	24

Figure 100: Surface temperature distribution using four heating systems with UV.

Section 6: RH distribution.

Relative humidity distribution											
Heating systems											
Radiant floor heating system (RFHS)						Heat pump (HP)					
P4	46.0	46.2	45.7	47.6	46.4	P4	34.9	35.3	34.8	36.5	36.6
P3	45.7	46.3	45.9	47.1	45.5	P3	39.6	39.2	37.3	40.1	40.7
P2	45.3	46.2	46.2	46.9	45.3	P2	40.1	40.2	41.1	42.5	39.2
5th	L5	L4	L3	L2	L1	1st	L5	L4	L3	L2	L1
P4	48.7	48.8	48.6	50.5	49.0	P4	41.9	41.2	41.9	43.5	43.5
P3	48.5	49.0	48.6	50.0	48.0	P3	44.6	44.8	42.7	45.8	46.9
P2	47.9	49.0	48.9	49.8	48.0	P2	46.8	45.5	47.0	47.3	45.9
6th	L5	L4	L3	L2	L1	3rd	L5	L4	L3	L2	L1
Electrical baseboard heater (EBH)						Portable radiator heater (PRH)					
P4	35.7	34.9	35.0	37.0	36.7	P4	38.7	39.4	37.5	40.9	42.2
P3	37.5	36.9	37.0	38.5	37.5	P3	42.8	42.5	42.2	44.2	43.2
P2	39.6	37.8	39.2	40.3	37.9	P2	44.9	41.1	45.2	47.0	43.0
1st	L5	L4	L3	L2	L1	3rd	L5	L4	L3	L2	L1
P4	44.4	45.3	44.6	48.3	46.9	P4	42.6	41.7	43.6	45.3	44.9
P3	49.6	48.9	47.6	51.5	52.2	P3	47.0	47.7	46.1	49.3	50.3
P2	50.8	51.2	52.7	54.3	51.2	P2	48.5	44.2	49.6	50.8	49.0
2nd	L5	L4	L3	L2	L1	6th	L5	L4	L3	L2	L1

Color Legend		
Ave of Min	Ave	Ave of Max
15	20	25

Figure 101: RH distribution with four heating systems and UV.

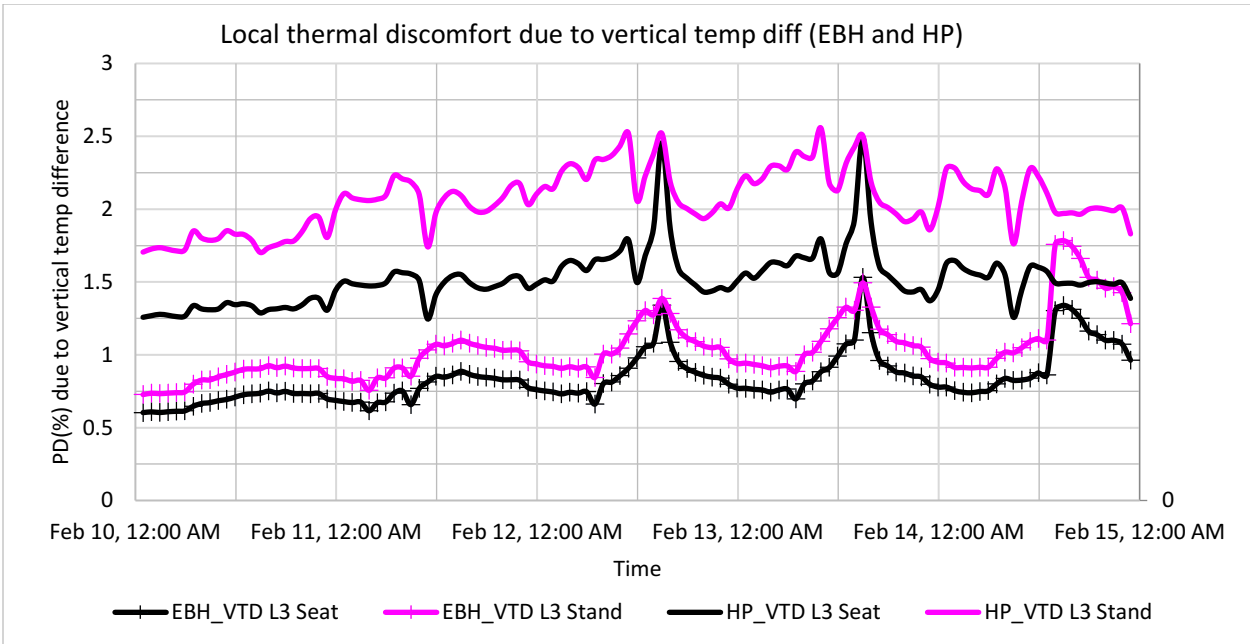

Figure 102: Local thermal discomfort due to a vertical temperature difference using EBH and HP.

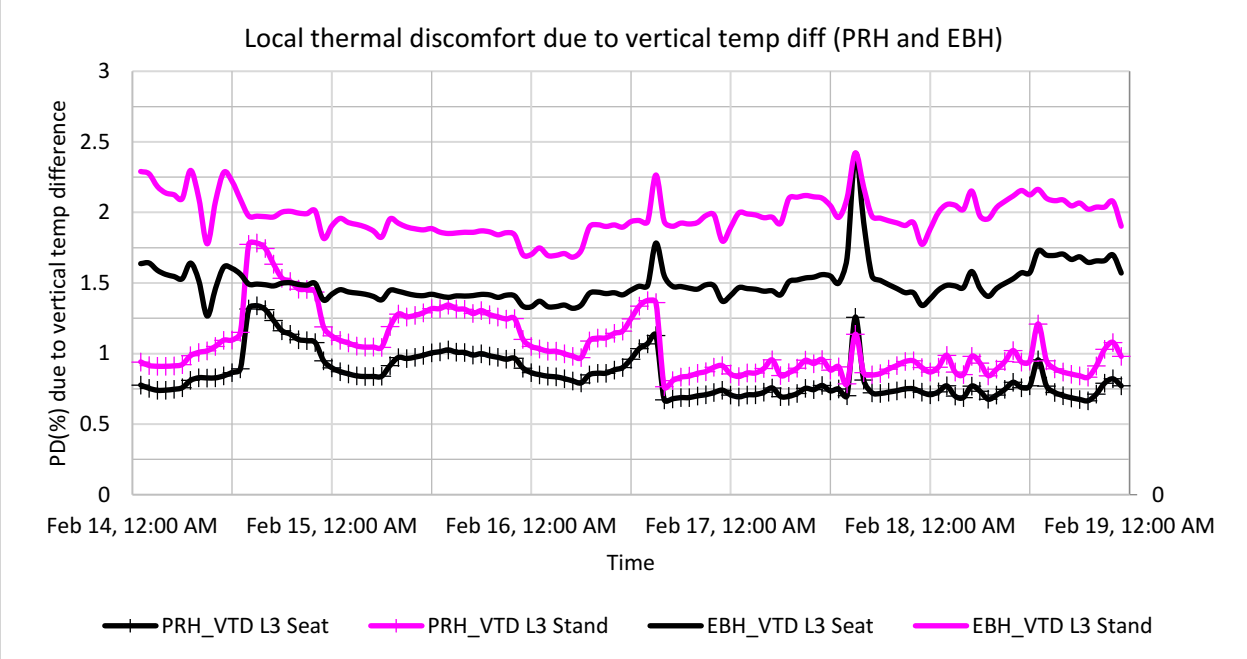

Figure 103: Local thermal discomfort due to a vertical temperature difference using PRH and EBH.

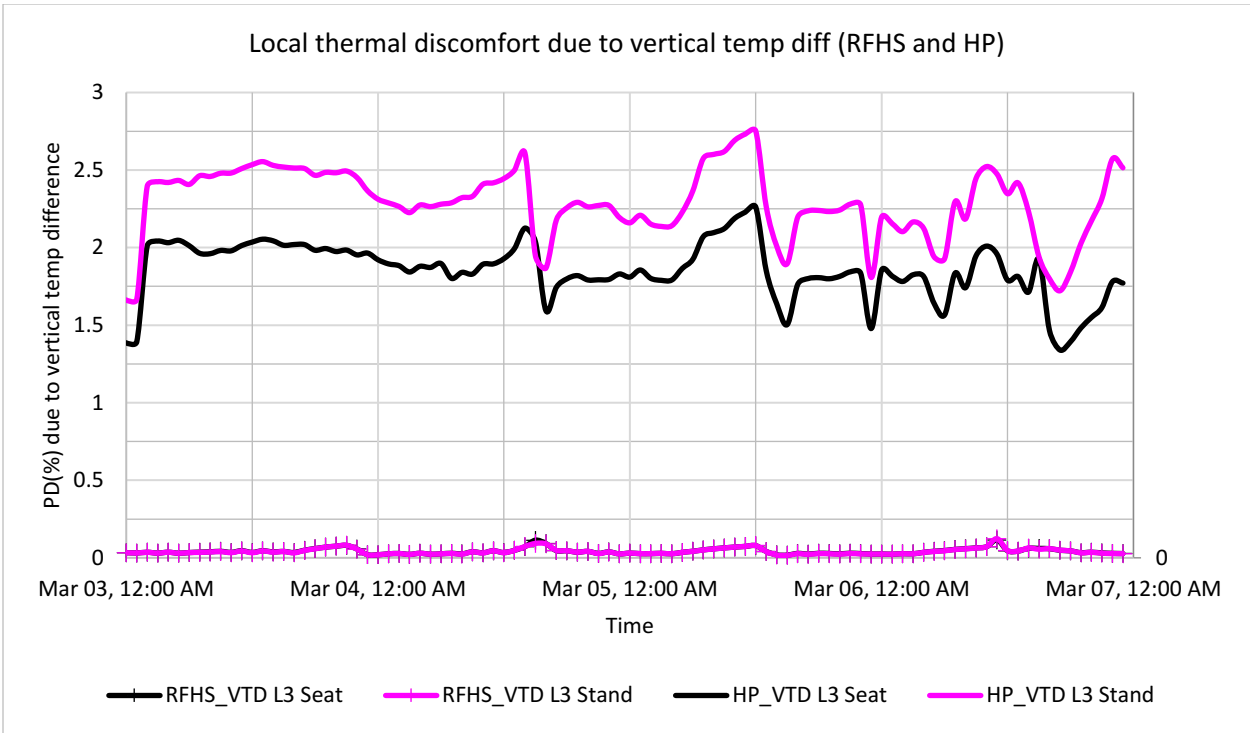

Figure 104: Local thermal discomfort due to a vertical temperature difference using RFHS and HP.

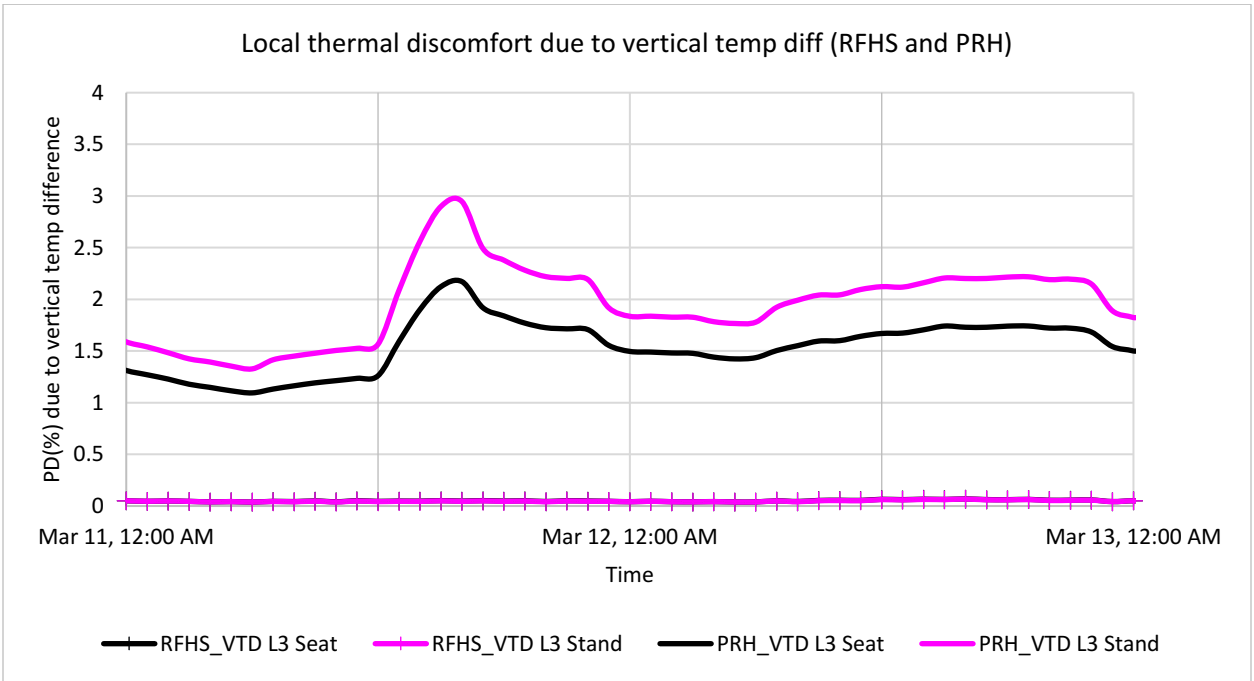

Figure 105: Local thermal discomfort due to a vertical temperature difference using RFHS and PRH.

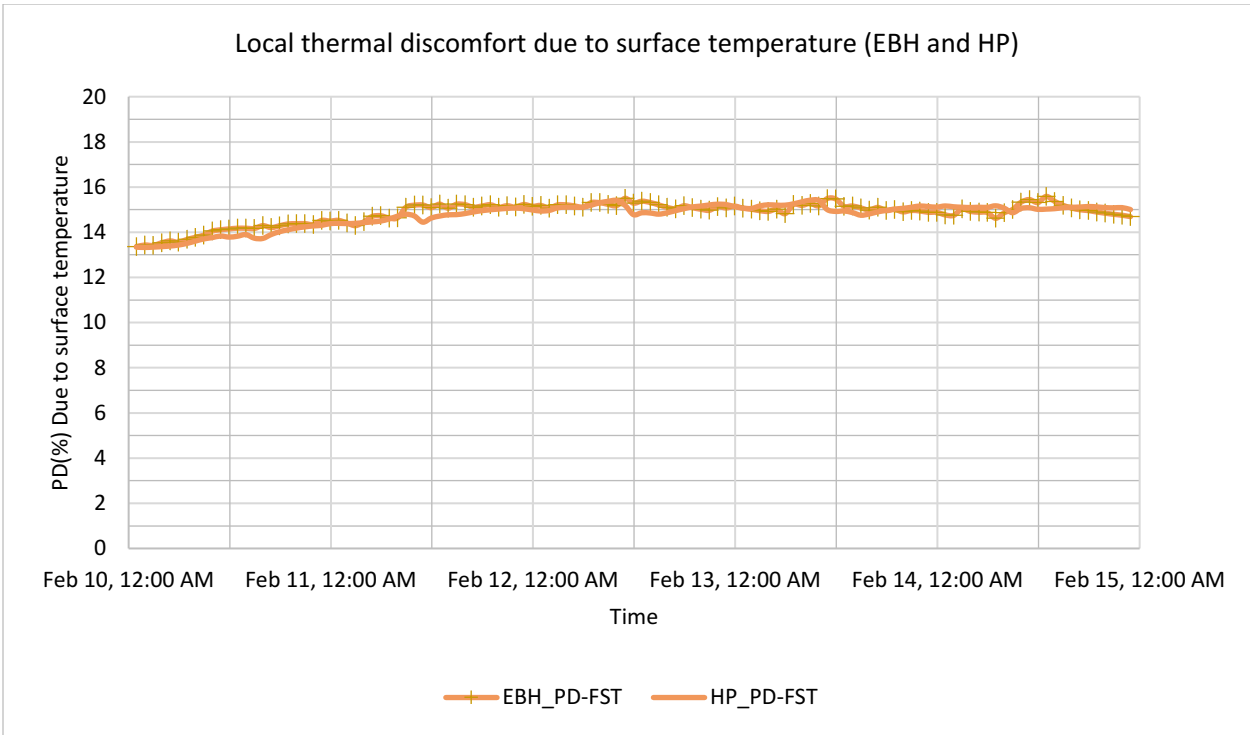

Figure 106: Local thermal discomfort due to surface temperature using EBH and HP.

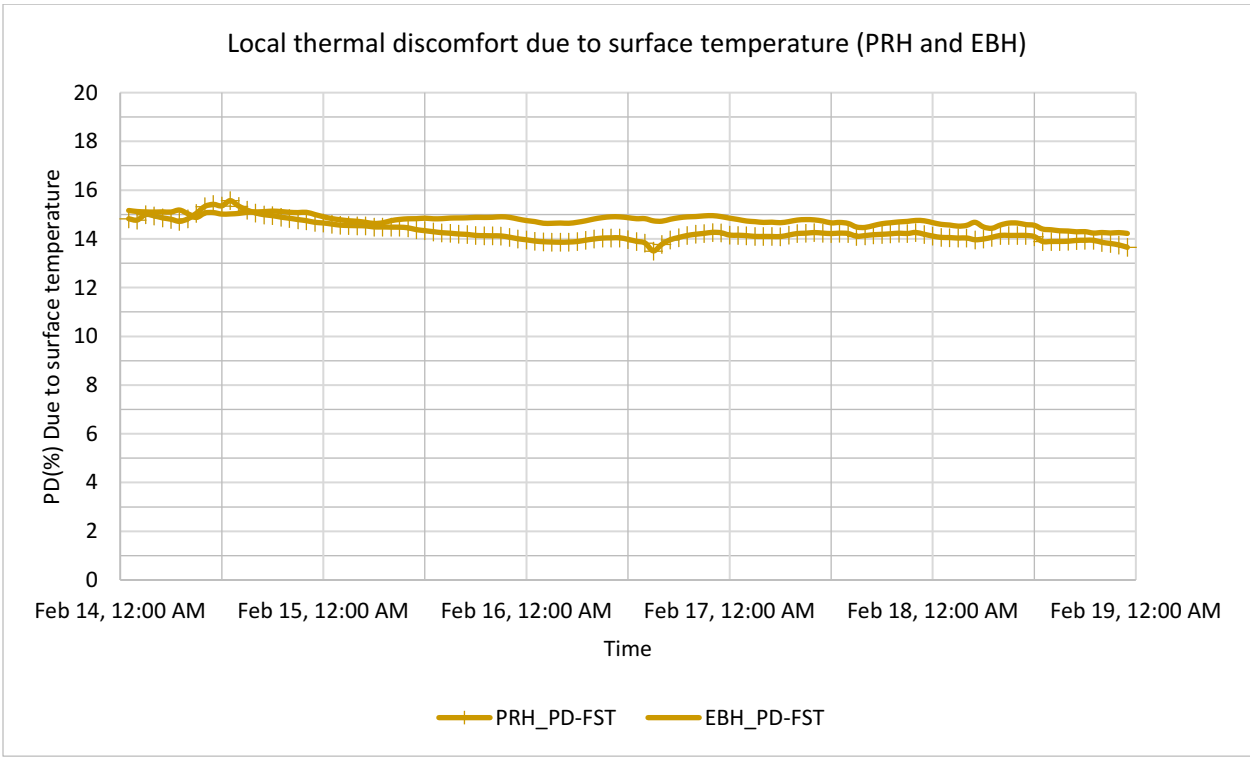

Figure 107: Local thermal discomfort due to surface temperature using PRH and EBH.

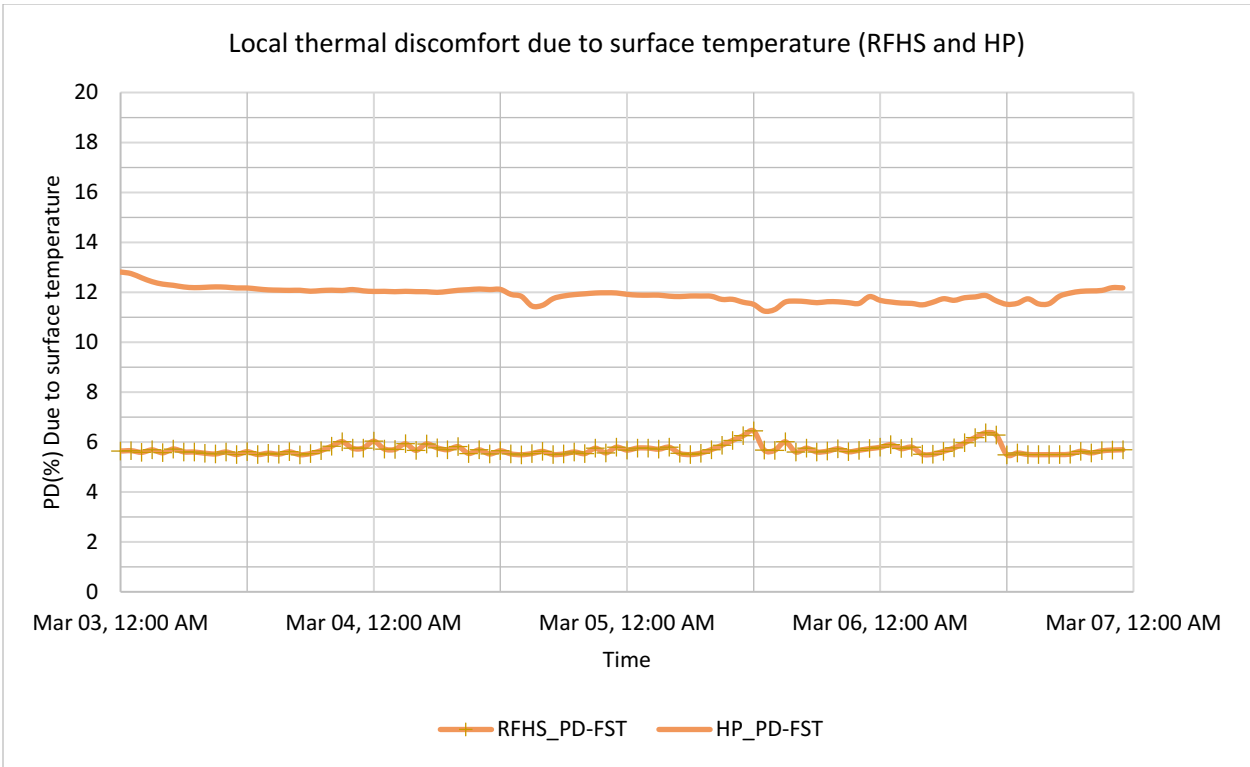

Figure 108: Local thermal discomfort due to surface temperature using RFHS and HP.

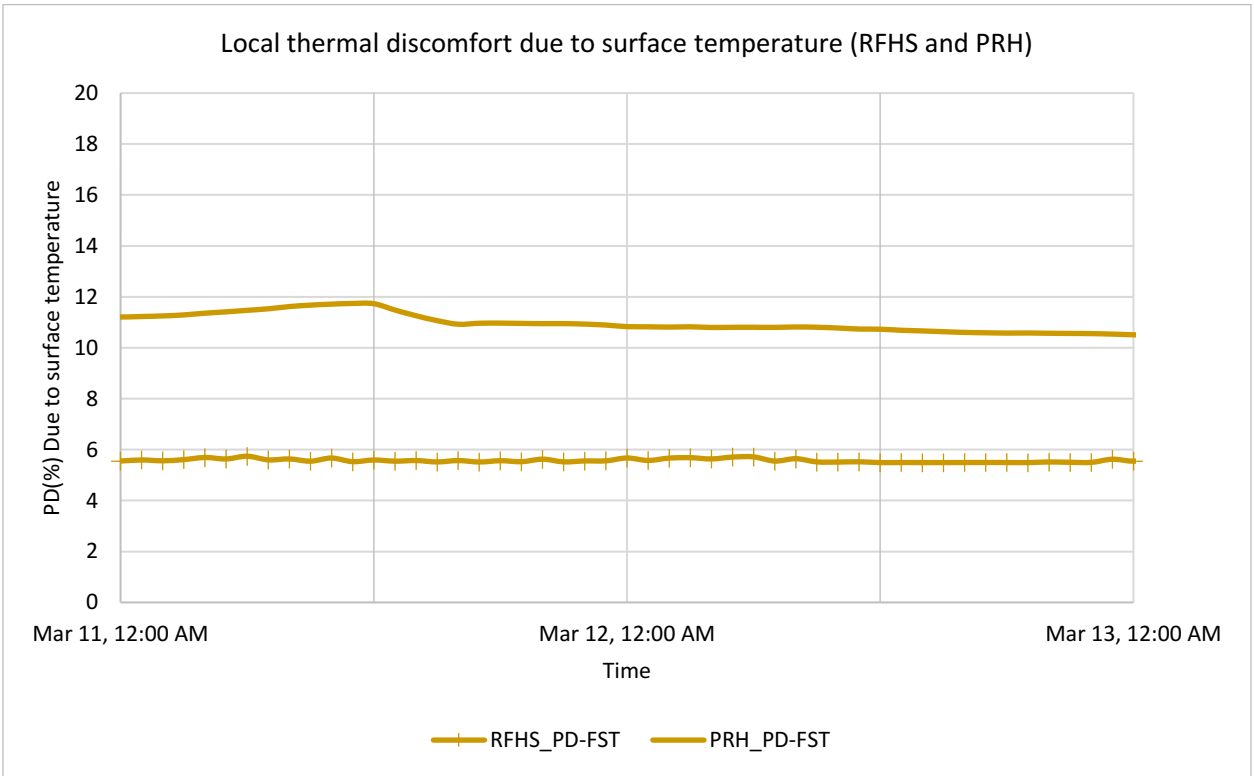

Figure 109: Local thermal discomfort due to surface temperature using RFHS and PRH.

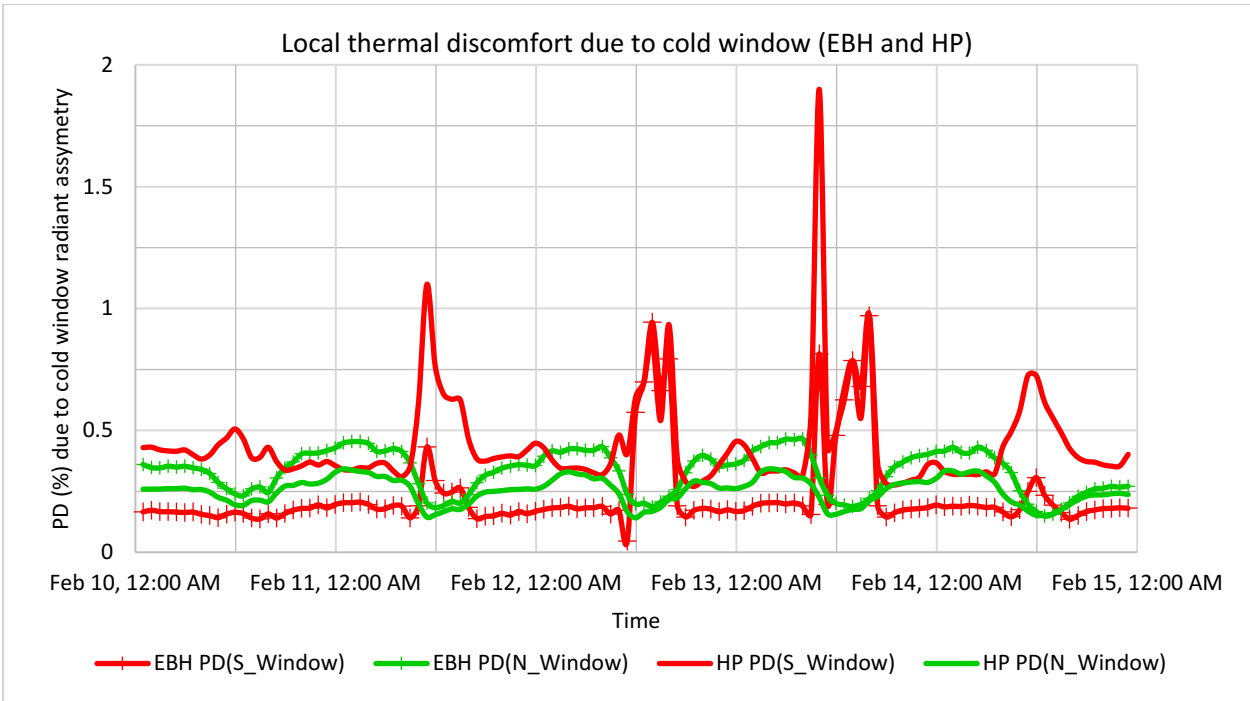

Figure 110: Local thermal discomfort due to cold window radiant asymmetry using EBH and HP.

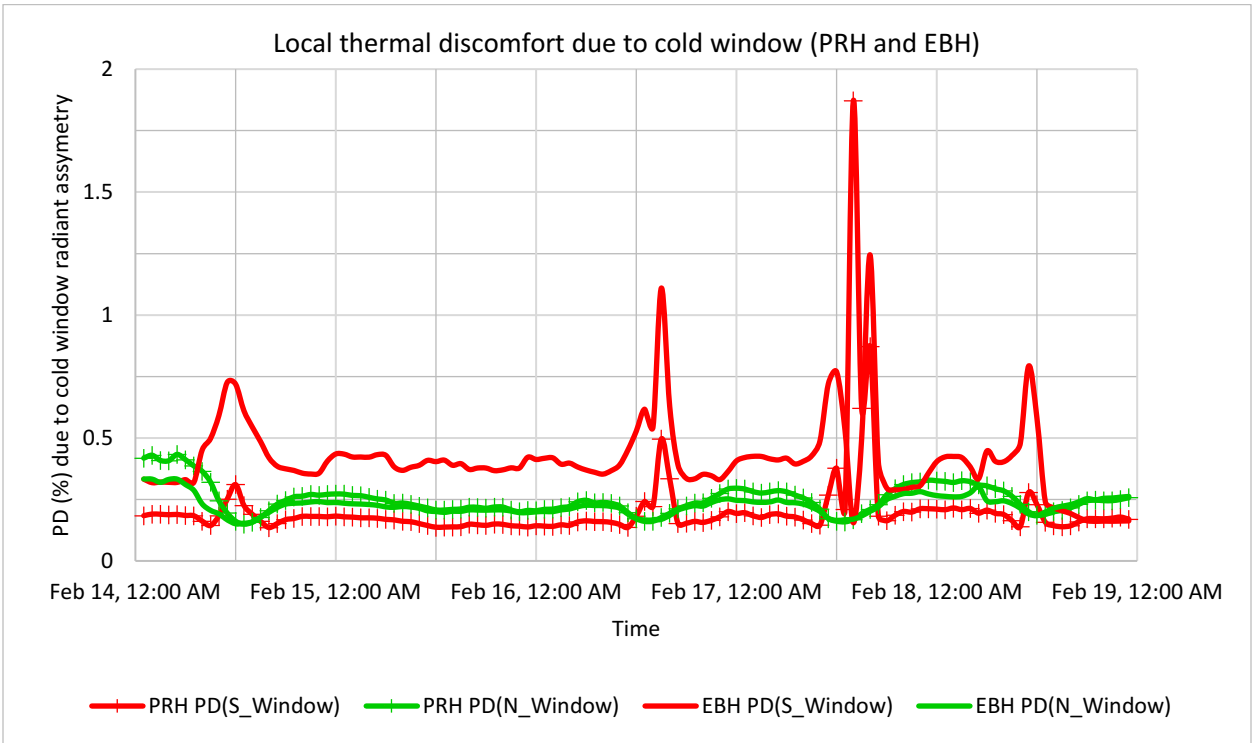

Figure 111: Local thermal discomfort due to cold window radiant asymmetry using PRH and HP.

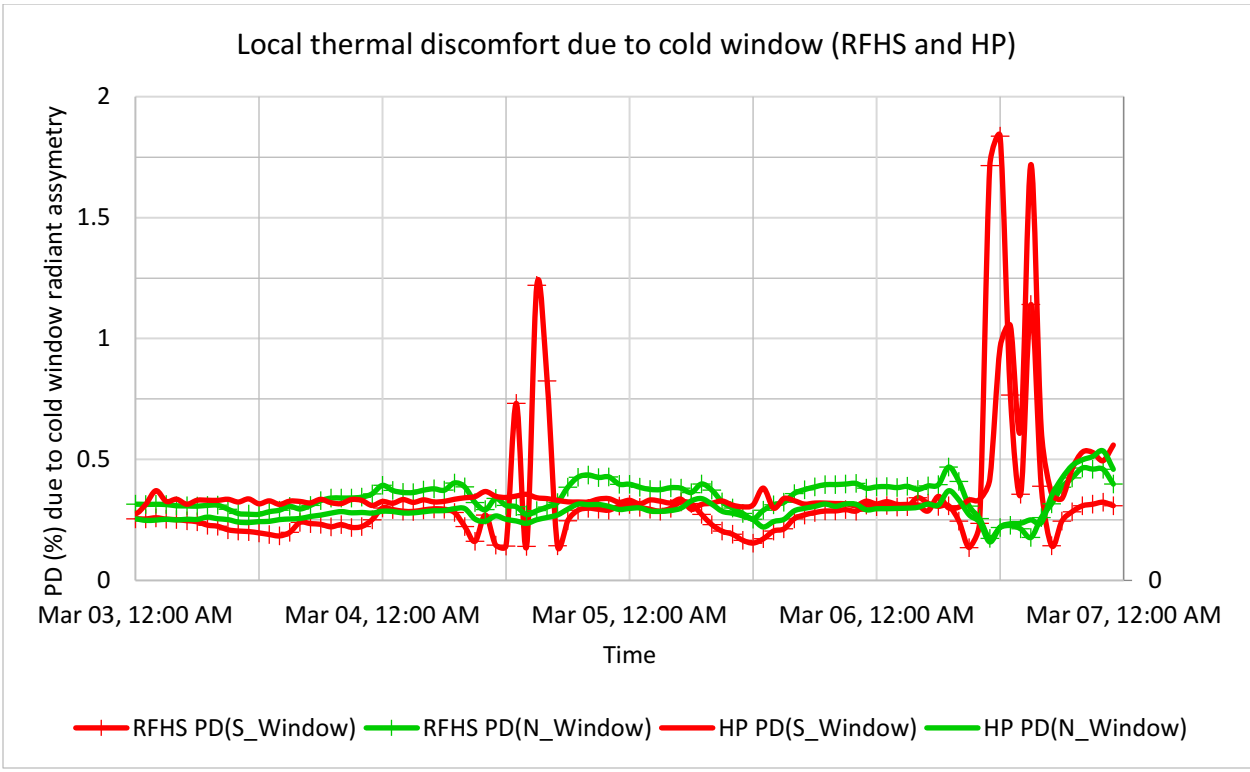

Figure 112: Local thermal discomfort due to cold window radiant asymmetry using RFHS and HP.

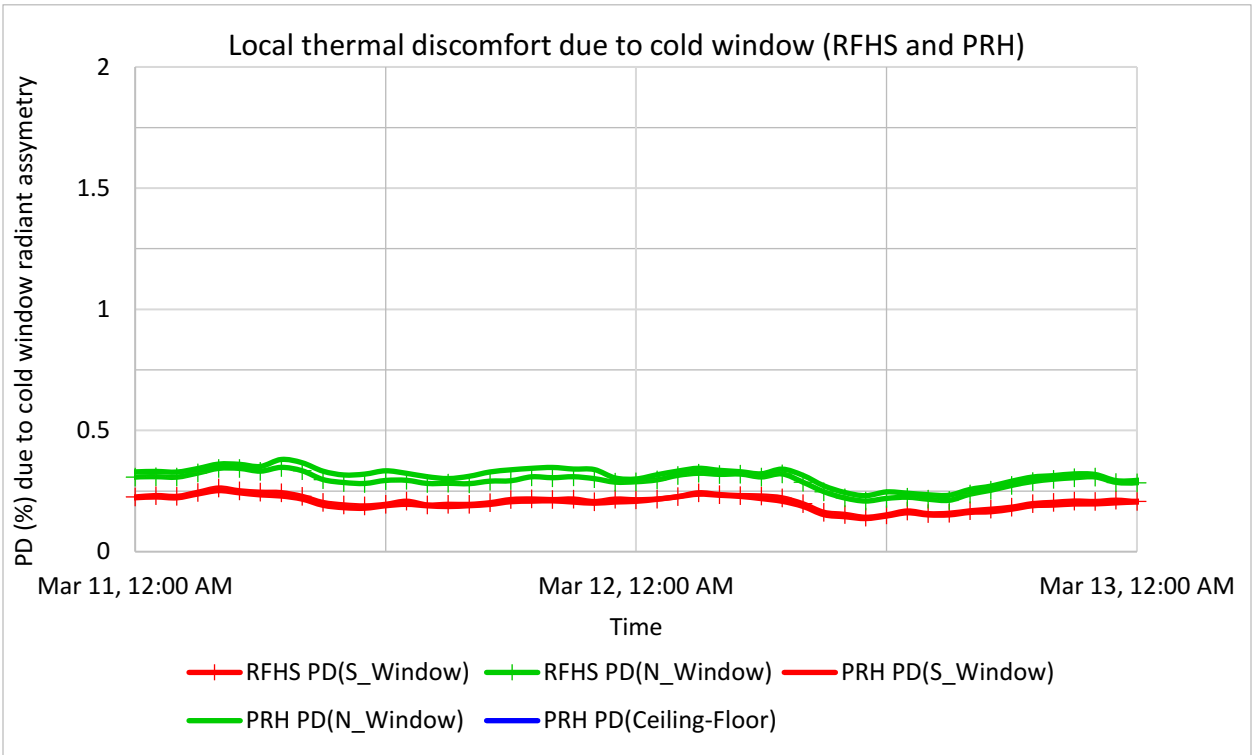

Figure 113: Local thermal discomfort due to cold window radiant asymmetry using RFHS and PRH.

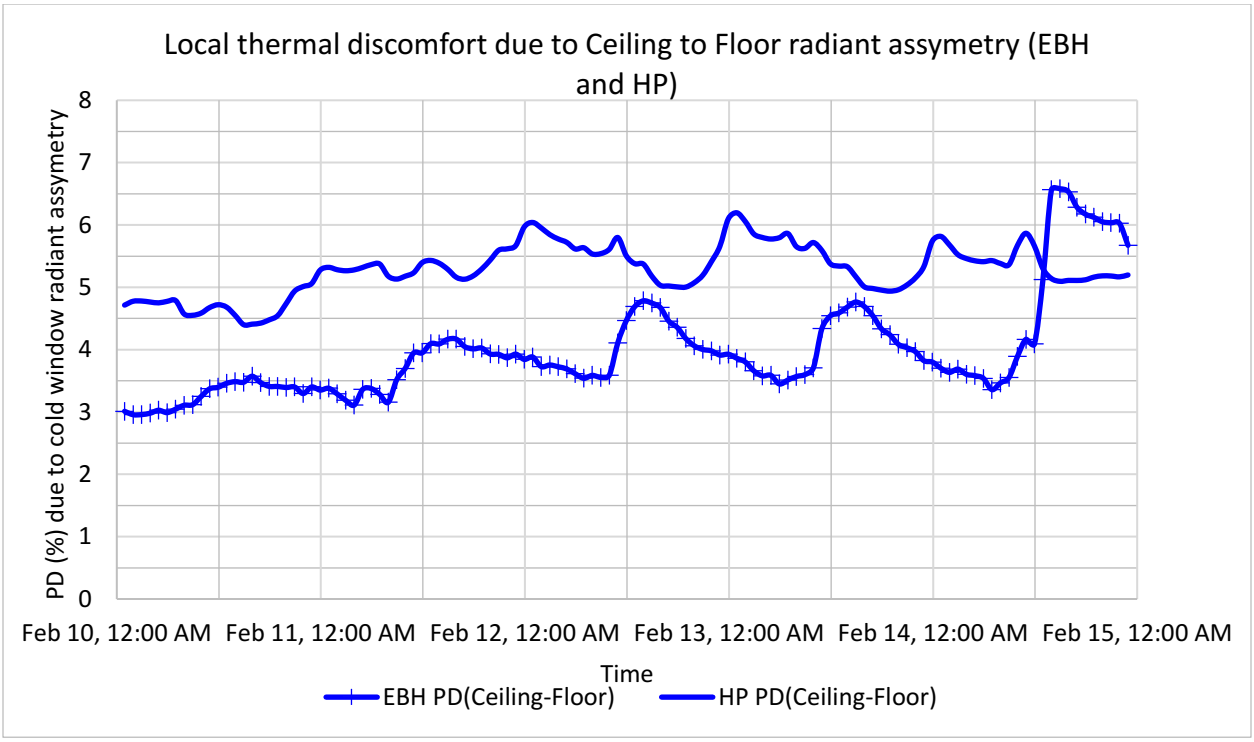

Figure 114: Local thermal discomfort due to the ceiling to floor radiant asymmetry using EBH and HP.

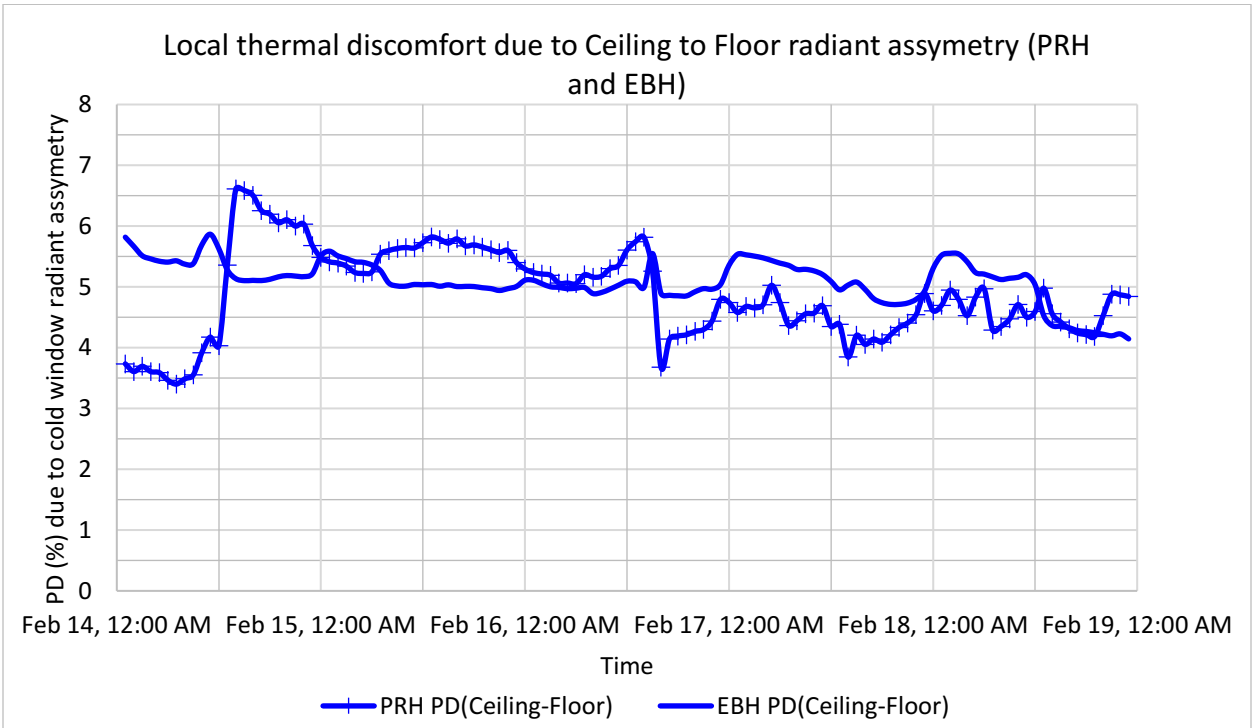

Figure 115: Local thermal discomfort due to the ceiling to floor radiant asymmetry using PRH and EBH.

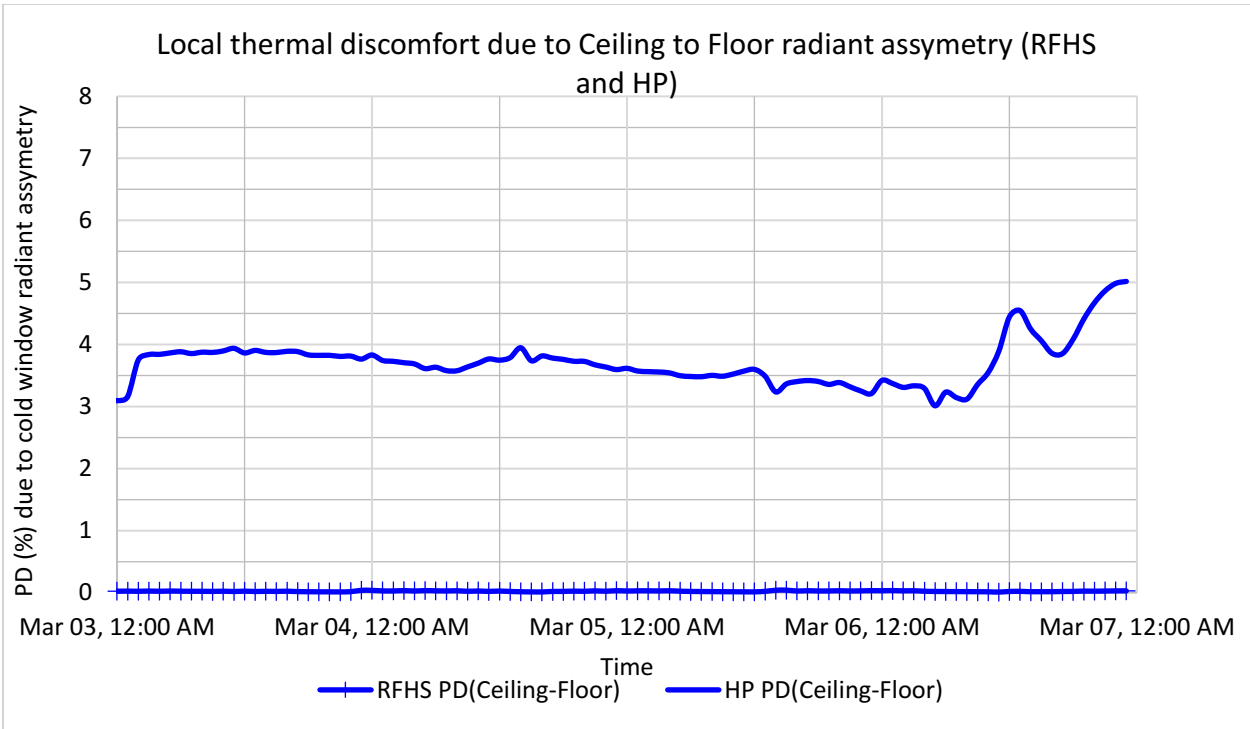

Figure 116: Local thermal discomfort due to the ceiling to floor radiant asymmetry using RFHS and HP.

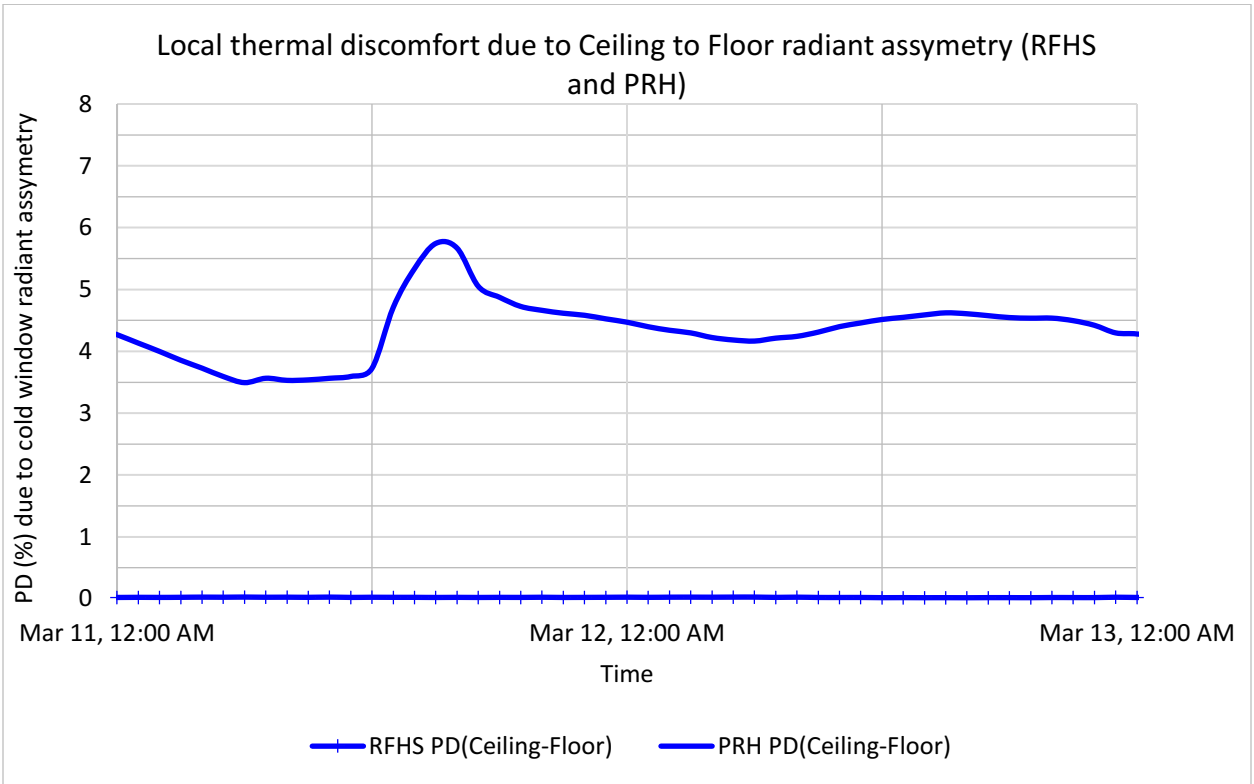

Figure 117: Local thermal discomfort due to the ceiling to floor radiant asymmetry using RFHS and PRH.

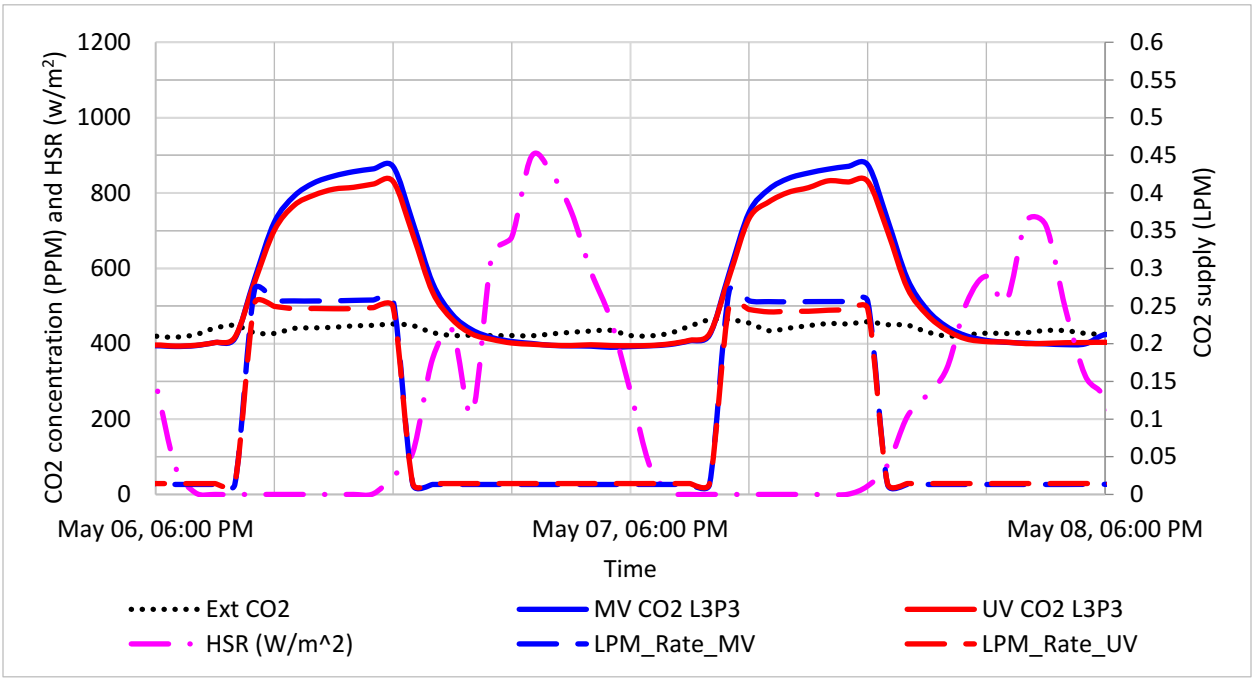

Figure 118: Transient CO2 profile at L3P3 in a room with the similar heating system (HP) and different ventilation strategy (MV and UV).

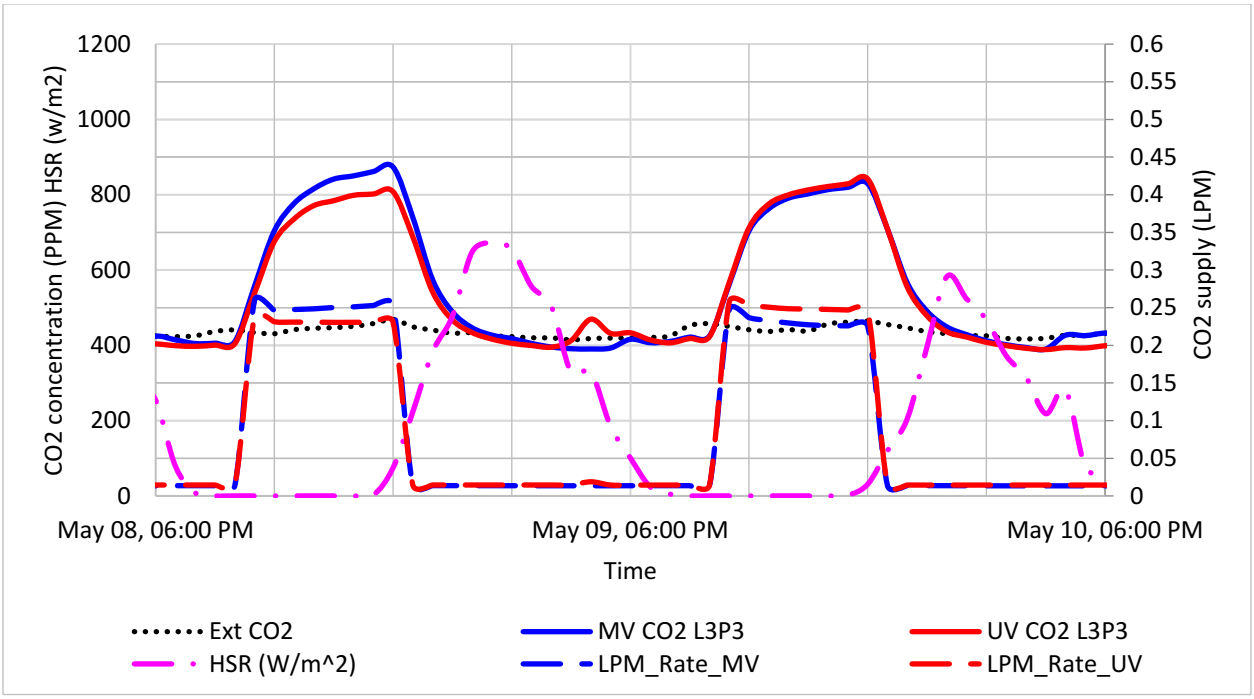

Figure 119: Transient CO2 profile at L3P3 in a room with the similar heating system (RFHS) and different ventilation strategy (MV and UV).

Section 11

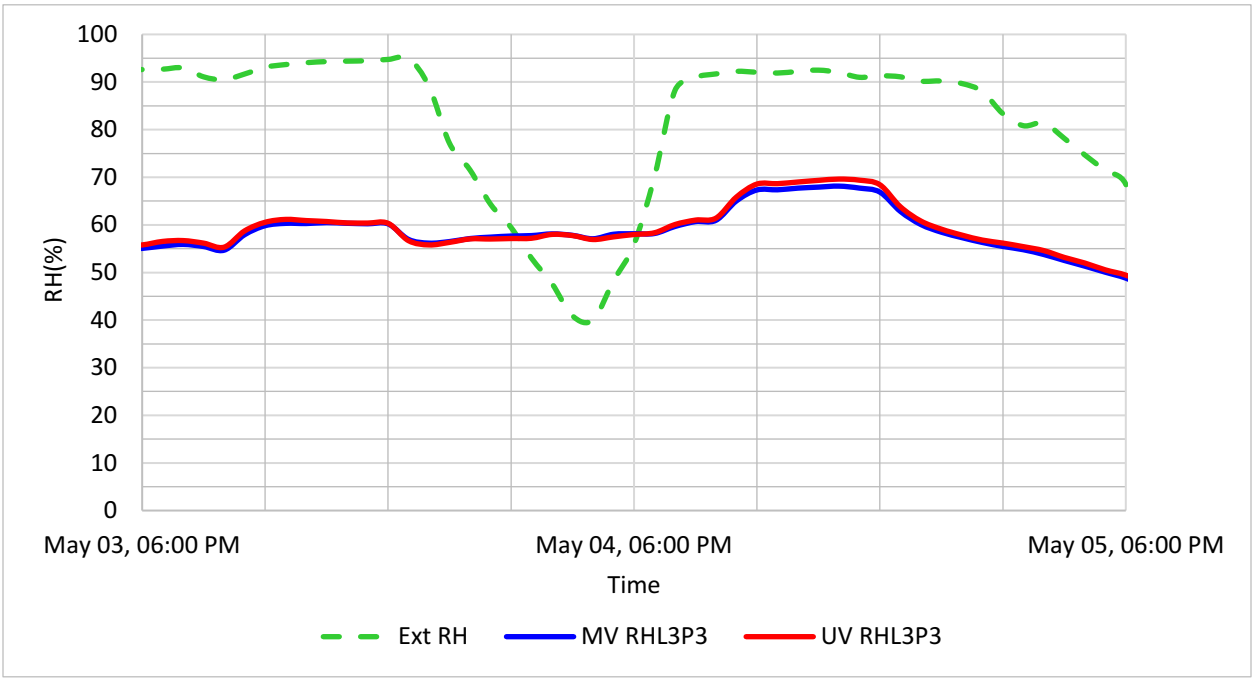

Figure 120: The relative humidity profile at L3P3 in a room with the similar heating system (EBH) but different ventilation strategy (MV and UV).

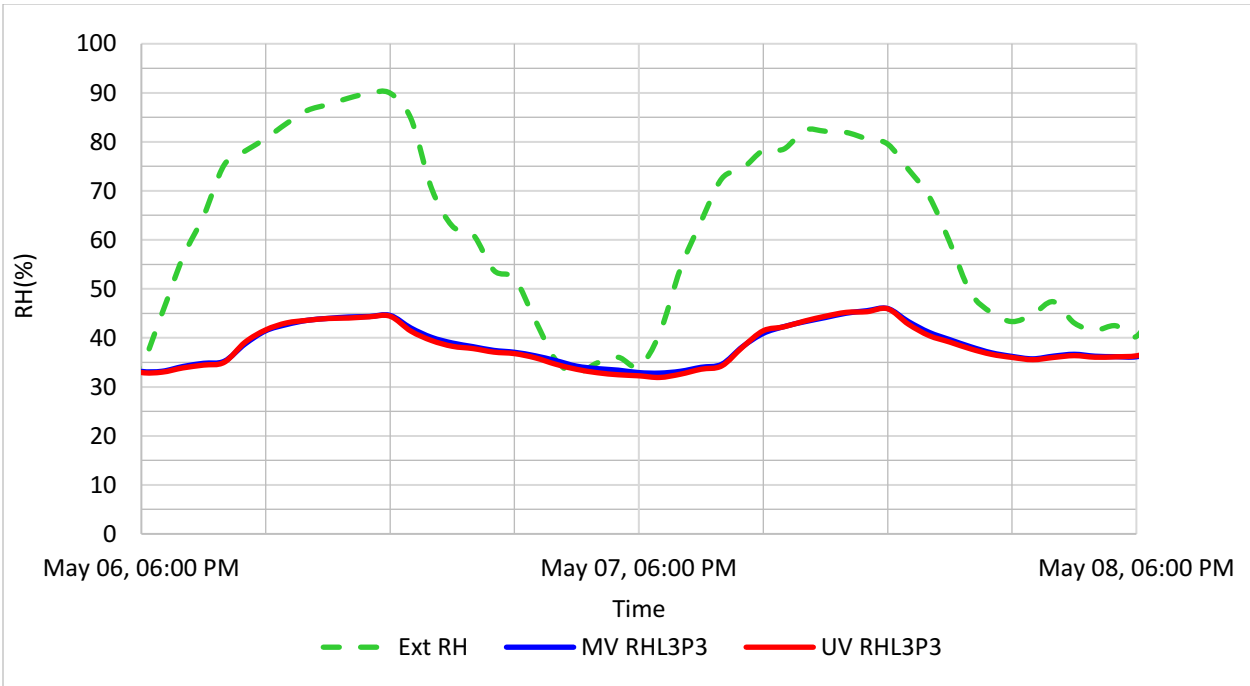

Figure 121: The relative humidity profile at L3P3 in a room with the similar heating system (HP) but different ventilation strategy (MV and UV).

Section 12,

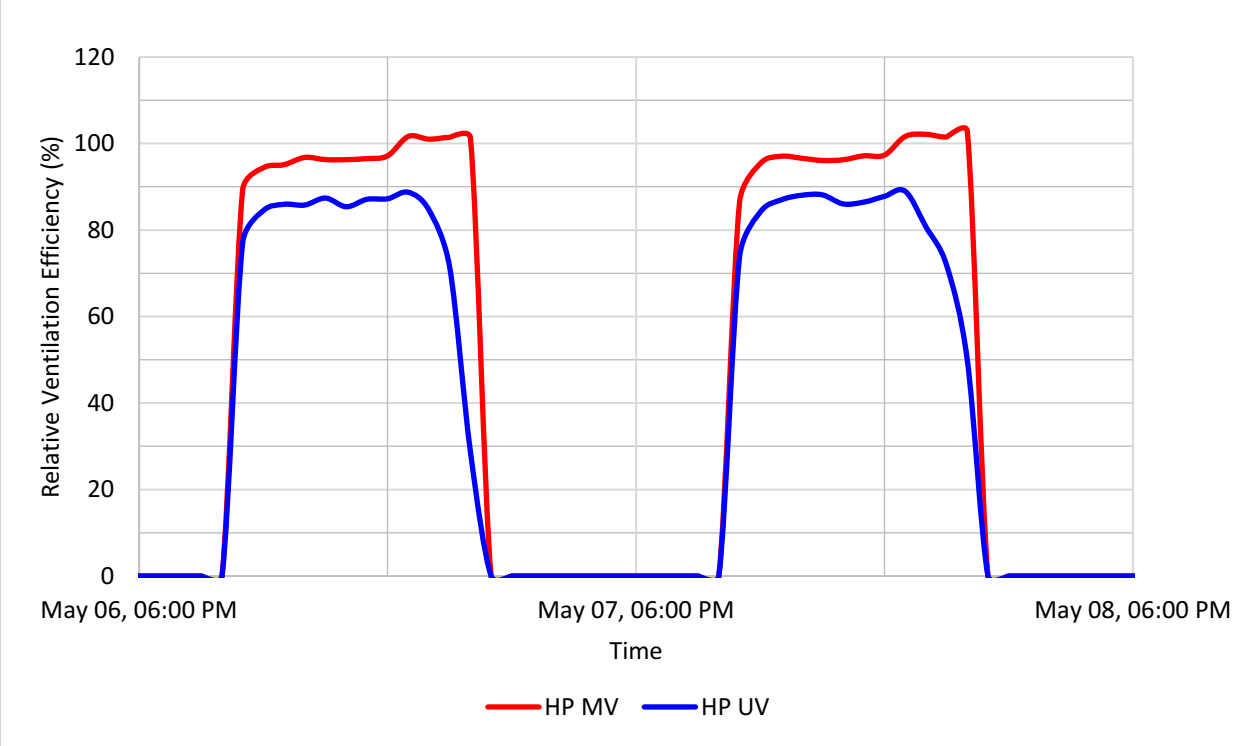

Figure 122: GVE in a test room with MV and UV both heated by HP.

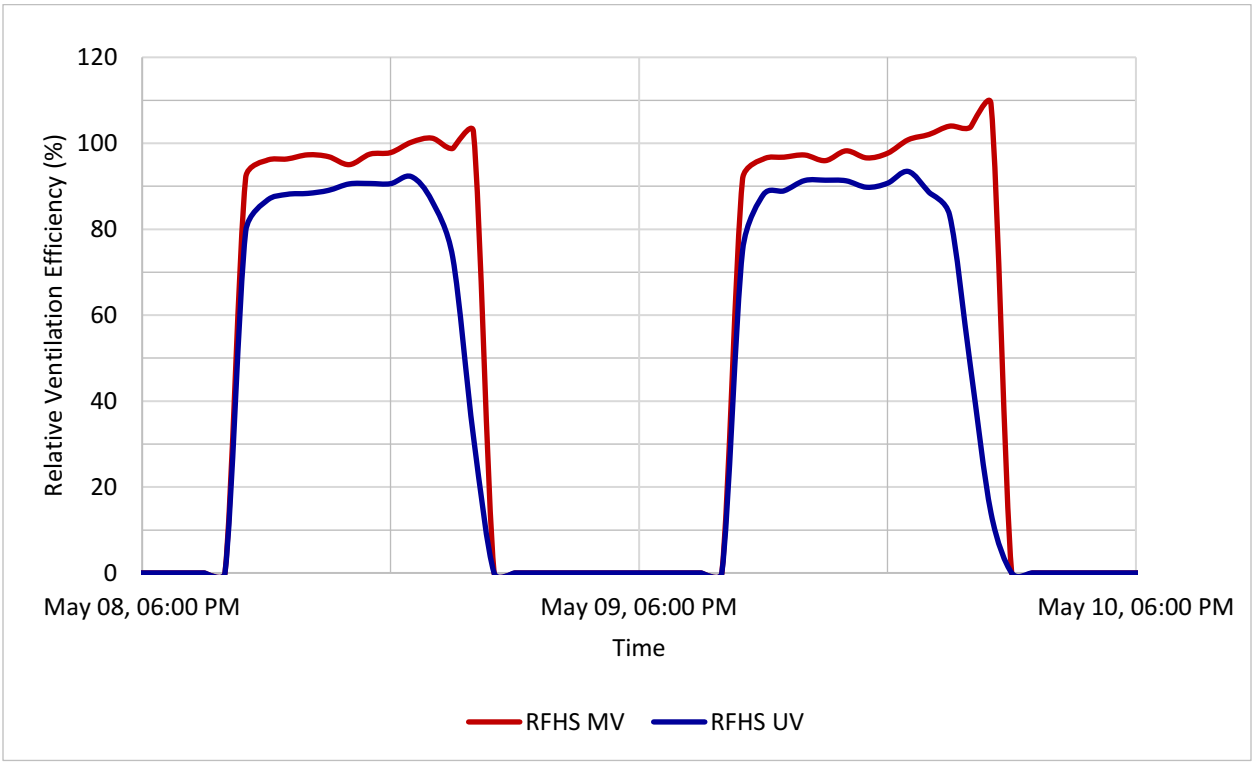

Figure 123: GVE in a test room with MV and UV both heated by RFHS.

Section 11: Temperature distribution UV

Heating systems	Ventilation flow rate										Difference				
	15cfm					7.5cfm					Abs(15cfm – 7.5cfm)				
Radiant Floor Heating system (RFHS)	P4	24.2	23.1	24.3	24.2	P4	24.0	23.0	24.2	24.2	P4	0.2	0.1	0.1	0.1
	P3	24.3	23.9	24.3	24.2	P3	24.0	23.8	24.4	24.0	P3	0.2	0.0	0.1	0.1
	P2	24.3	24.0	24.2	24.3	P2	23.8	23.6	24.1	24.2	P2	0.5	0.3	0.1	0.1
	P1	24.1	24.1	24.1	24.3	P1	24.1	23.9	24.2	24.3	P1	0.1	0.2	0.0	0.1
		L5	L4	L3	L2		L5	L4	L3	L2		L5	L4	L3	L2
Eclectic baseboard Heather (EBH)	P4	24.6	23.1	24.6	24.8	P4	24.4	22.8	24.3	24.6	P4	0.2	0.3	0.2	0.2
	P3	24.0	23.8	24.0	24.1	P3	23.9	23.7	23.7	24.0	P3	0.1	0.1	0.2	0.2
	P2	23.8	23.7	23.8	24.0	P2	23.7	23.5	23.6	23.8	P2	0.1	0.2	0.2	0.2
	P1	23.2	23.2	23.3	23.4	P1	23.4	23.3	23.5	23.4	P1	0.2	0.1	0.1	0.0
		L5	L4	L3	L2		L5	L4	L3	L2		L5	L4	L3	L2
Heat pump (HP)	P4	24.6	23.6	24.7	24.6	P4	24.7	23.4	24.8	24.8	P4	0.0	0.2	0.1	0.2
	P3	24.3	24.4	24.4	24.3	P3	24.5	24.3	24.5	24.4	P3	0.1	0.0	0.1	0.1
	P2	24.2	24.2	24.2	24.3	P2	24.3	24.1	24.2	24.4	P2	0.1	0.1	0.1	0.1
	P1	23.8	23.9	23.9	24.1	P1	24.1	24.0	24.0	24.2	P1	0.2	0.1	0.1	0.1
		L5	L4	L3	L2		L5	L4	L3	L2		L5	L4	L3	L2
	7.5cfm					5cfm					Abs(7.5cfm – 5cfm)				
Heat pump (HP)	P4	24.6	23.6	24.6	24.6	P4	24.5	23.3	24.6	24.7	P4	0.1	0.3	0.0	0.1
	P3	24.3	24.3	24.3	24.3	P3	24.3	24.2	24.4	24.3	P3	0.0	0.1	0.1	0.0
	P2	24.1	24.1	24.1	24.3	P2	24.1	23.9	24.0	24.2	P2	0.0	0.2	0.1	0.1
	P1	23.9	23.9	23.9	24.0	P1	23.9	23.9	23.9	24.1	P1	0.0	0.0	0.0	0.0
		L5	L4	L3	L2		L5	L4	L3	L2		L5	L4	L3	L2
Eclectic baseboard Heather (EBH)	P4	24.6	23.4	24.5	24.7	P4	24.4	23.0	24.3	24.5	P4	0.2	0.4	0.3	0.2
	P3	24.1	24.0	24.1	24.2	P3	24.0	23.7	23.9	24.0	P3	0.1	0.3	0.3	0.2
	P2	24.0	23.9	23.9	24.1	P2	23.8	23.5	23.6	23.8	P2	0.2	0.4	0.3	0.3
	P1	23.7	23.6	23.6	23.8	P1	23.6	23.5	23.6	23.6	P1	0.1	0.1	0.0	0.2
		L5	L4	L3	L2		L5	L4	L3	L2		L5	L4	L3	L2

Color Legend				
Ave of Min	Ave	Ave of Max	Min	Ave of Max
22	23.5	25	0	1

Figure 124: Interior temperature distribution comparison of 15 cfm, 7.5 cfm, and 5 cfm with UV.

Heating systems	Ventilation flow rate										Difference				
	15cfm					7.5cfm					Abs (15cfm – 7.5cfm)				
Radiant Floor Heating system (RFHS)	P4	0.03	0.20	0.07	0.07	P4	0.09	0.17	0.06	0.09	P4	0.06	0.03	0.01	0.02
	P3	0.02	0.07	0.05	0.08	P3	0.08	0.06	0.04	0.09	P3	0.06	0.01	0.00	0.01
	P2	0.01	0.06	0.08	0.09	P2	0.10	0.06	0.04	0.08	P2	0.08	0.01	0.04	0.01
	P1	0.03	0.07	0.10	0.08	P1	0.07	0.05	0.07	0.06	P1	0.04	0.02	0.04	0.02
		L5	L4	L3	L2		L5	L4	L3	L2		L5	L4	L3	L2
Eclectic baseboard Heather (EBH)	P4	0.00	0.14	0.04	0.04	P4	0.01	0.15	0.01	0.05	P4	0.00	0.01	0.03	0.01
	P3	0.00	0.04	0.01	0.00	P3	0.00	0.03	0.02	0.00	P3	0.00	0.01	0.01	0.00
	P2	0.00	0.03	0.01	0.00	P2	0.00	0.02	0.01	0.00	P2	0.00	0.02	0.00	0.00
	P1	0.01	0.04	0.01	0.01	P1	0.00	0.01	0.01	0.00	P1	0.01	0.03	0.00	0.01
		L5	L4	L3	L2		L5	L4	L3	L2		L5	L4	L3	L2
Heat pump (HP)	P4	0.05	0.19	0.05	0.11	P4	0.05	0.17	0.03	0.10	P4	0.01	0.02	0.02	0.01
	P3	0.06	0.06	0.05	0.09	P3	0.06	0.05	0.04	0.08	P3	0.00	0.01	0.01	0.01
	P2	0.05	0.04	0.06	0.07	P2	0.05	0.03	0.06	0.08	P2	0.01	0.01	0.00	0.01
	P1	0.06	0.04	0.08	0.06	P1	0.03	0.03	0.06	0.06	P1	0.03	0.02	0.02	0.00
		L5	L4	L3	L2		L5	L4	L3	L2		L5	L4	L3	L2
	7.5cfm					5cfm					Abs (7.5cfm – 5cfm)				
Heat pump (HP)	P4	0.06	0.21	0.06	0.12	P4	0.07	0.18	0.04	0.11	P4	0.02	0.03	0.02	0.01
	P3	0.07	0.06	0.05	0.10	P3	0.07	0.05	0.04	0.10	P3	0.00	0.01	0.01	0.00
	P2	0.06	0.04	0.07	0.09	P2	0.06	0.04	0.06	0.10	P2	0.00	0.01	0.01	0.01
	P1	0.05	0.04	0.10	0.08	P1	0.04	0.04	0.07	0.08	P1	0.01	0.00	0.03	0.00
		L5	L4	L3	L2		L5	L4	L3	L2		L5	L4	L3	L2
Eclectic baseboard Heather (EBH)	P4	0.00	0.15	0.04	0.03	P4	0.00	0.15	0.02	0.04	P4	0.00	0.00	0.02	0.01
	P3	0.00	0.04	0.00	0.00	P3	0.00	0.04	0.00	0.00	P3	0.00	0.01	0.00	0.00
	P2	0.00	0.03	0.02	0.00	P2	0.00	0.02	0.01	0.00	P2	0.00	0.01	0.00	0.00
	P1	0.02	0.03	0.00	0.00	P1	0.00	0.01	0.00	0.00	P1	0.02	0.02	0.00	0.00
		L5	L4	L3	L2		L5	L4	L3	L2		L5	L4	L3	L2

Color Legend				
Ave of Min	Ave	Ave of Max	Min	Ave of Max
0	0.05	0.15	0	0.05

Figure 125: Interior air velocity distribution comparison of 15 cfm, 7.5 cfm, and 5 cfm with UV.

Section 6.3: RH distribution UV

Heating systems	Ventilation flow rate										Difference				
	15cfm					7.5cfm					Abs (15cfm – 7.5cfm)				
Radiant Floor Heating system (RFHS)	P4	48.6	54.5	48.7	48.8	P4	51.8	60.7	51.7	51.6	P4	3.2	6.2	3.0	2.8
	P3	49.0	50.5	48.6	48.8	P3	53.8	55.4	50.7	52.2	P3	4.8	4.9	2.1	3.3
	P2	49.1	51.3	48.2	49.4	P2	48.6	51.3	49.5	51.5	P2	0.5	0.0	1.3	2.1
	P1	47.9	48.8	47.7	47.9	P1	50.9	52.1	51.3	50.2	P1	2.9	3.3	3.5	2.3
		L5	L4	L3	L2		L5	L4	L3	L2		L5	L4	L3	L2
Eclectic baseboard Heather (EBH)	P4	49.8	55.5	49.2	47.9	P4	51.2	60.3	51.3	50.4	P4	1.4	4.9	2.1	2.5
	P3	52.3	52.9	51.2	50.7	P3	57.1	56.5	52.2	53.6	P3	4.8	3.6	1.0	2.9
	P2	52.8	51.7	51.2	50.1	P2	51.2	51.7	51.9	52.8	P2	1.7	0.0	0.6	2.7
	P1	52.6	53.3	50.7	49.3	P1	54.7	55.5	54.1	52.4	P1	2.1	2.2	3.4	3.1
		L5	L4	L3	L2		L5	L4	L3	L2		L5	L4	L3	L2
Heat pump (HP)	P4	49.6	54.9	49.3	48.7	P4	51.1	59.3	51.3	51.1	P4	1.5	4.4	2.0	2.4
	P3	50.8	51.4	50.0	49.7	P3	54.9	54.9	50.5	52.5	P3	4.1	3.6	0.5	2.8
	P2	50.8	51.7	50.7	50.3	P2	49.6	51.7	51.7	51.8	P2	1.2	0.0	1.0	1.5
	P1	51.2	52.2	50.9	50.4	P1	53.1	53.9	53.2	51.9	P1	1.9	1.8	2.4	1.5
		L5	L4	L3	L2		L5	L4	L3	L2		L5	L4	L3	L2
	7.5cfm					5cfm					Abs (7.5cfm – 5cfm)				
Heat pump (HP)	P4	56.8	62.7	56.4	56.0	P4	55.4	64.1	56.6	56.5	P4	1.4	1.4	0.1	0.5
	P3	58.1	58.9	57.3	57.1	P3	60.7	59.2	54.6	57.9	P3	2.6	0.2	2.6	0.8
	P2	57.2	56.3	58.1	56.7	P2	54.4	56.3	57.1	56.5	P2	2.8	0.0	1.0	0.2
	P1	58.5	59.9	58.5	58.0	P1	57.7	58.6	58.1	56.3	P1	0.8	1.3	0.4	1.8
		L5	L4	L3	L2		L5	L4	L3	L2		L5	L4	L3	L2
Eclectic baseboard Heather (EBH)	P4	64.1	70.6	63.7	62.6	P4	64.6	74.6	64.7	63.9	P4	0.5	4.0	0.9	1.2
	P3	66.9	67.4	65.3	64.7	P3	71.1	69.9	65.6	66.8	P3	4.2	2.5	0.3	2.1
	P2	65.6	64.0	66.0	63.8	P2	62.1	64.0	64.8	64.1	P2	3.6	0.0	1.2	0.3
	P1	66.7	68.0	65.1	64.2	P1	67.9	69.3	68.3	65.3	P1	1.2	1.2	3.2	1.1
		L5	L4	L3	L2		L5	L4	L3	L2		L5	L4	L3	L2

Color Legend				
Ave of Min	Ave	Ave of Max	Min	Ave of Max
30	55	80	0	5

Figure 126: Interior RH distribution comparison of 15 cfm, 7.5 cfm, and 5 cfm with UV.

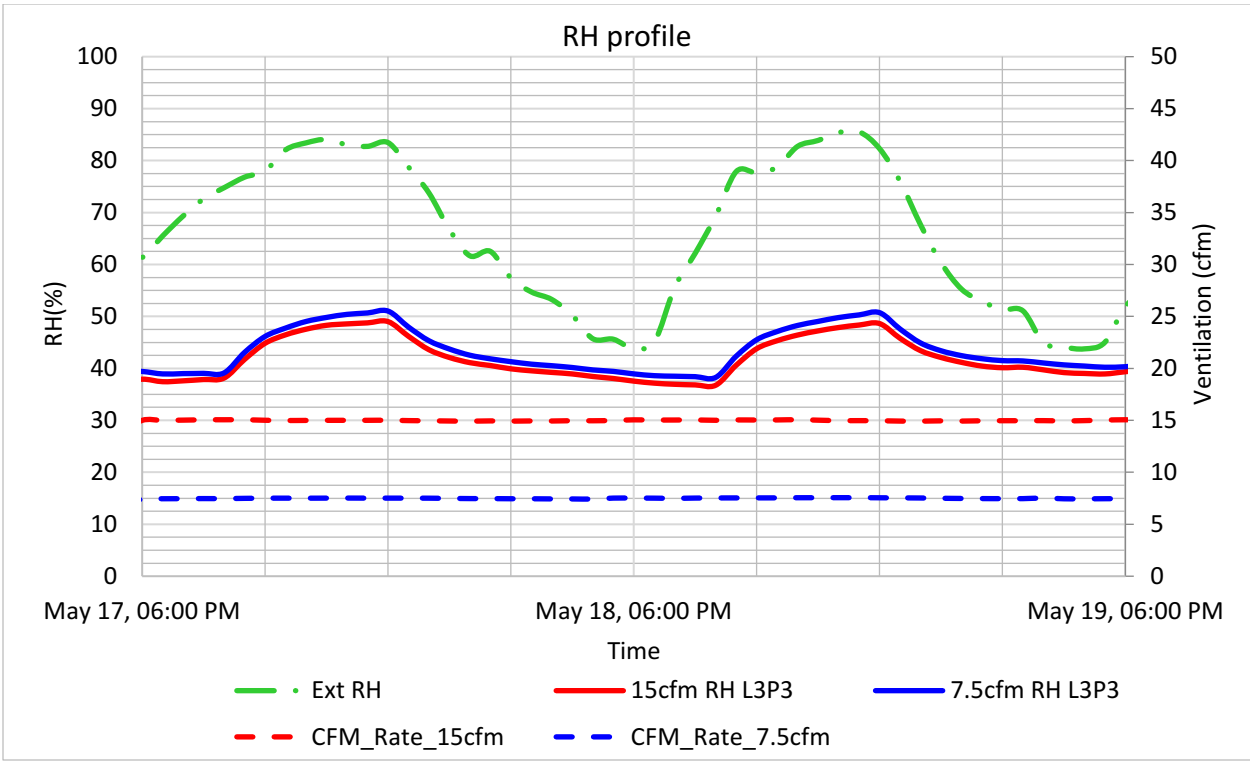

Figure 127: The relative humidity profile at L3P3 comparing 15 cfm 7.5 cfm using EBH and UV.

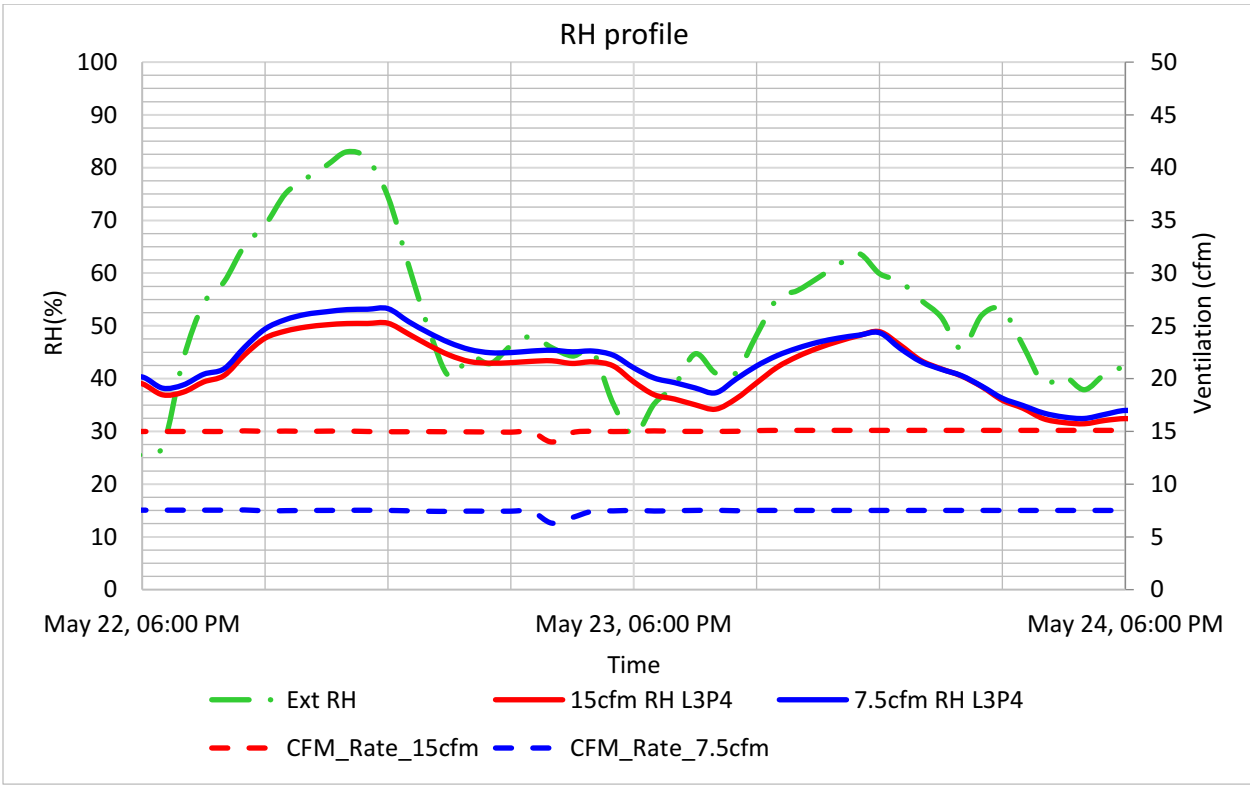

Figure 128: The relative humidity profile at L3P3 comparing 15 cfm 7.5 cfm using EBH and UV.

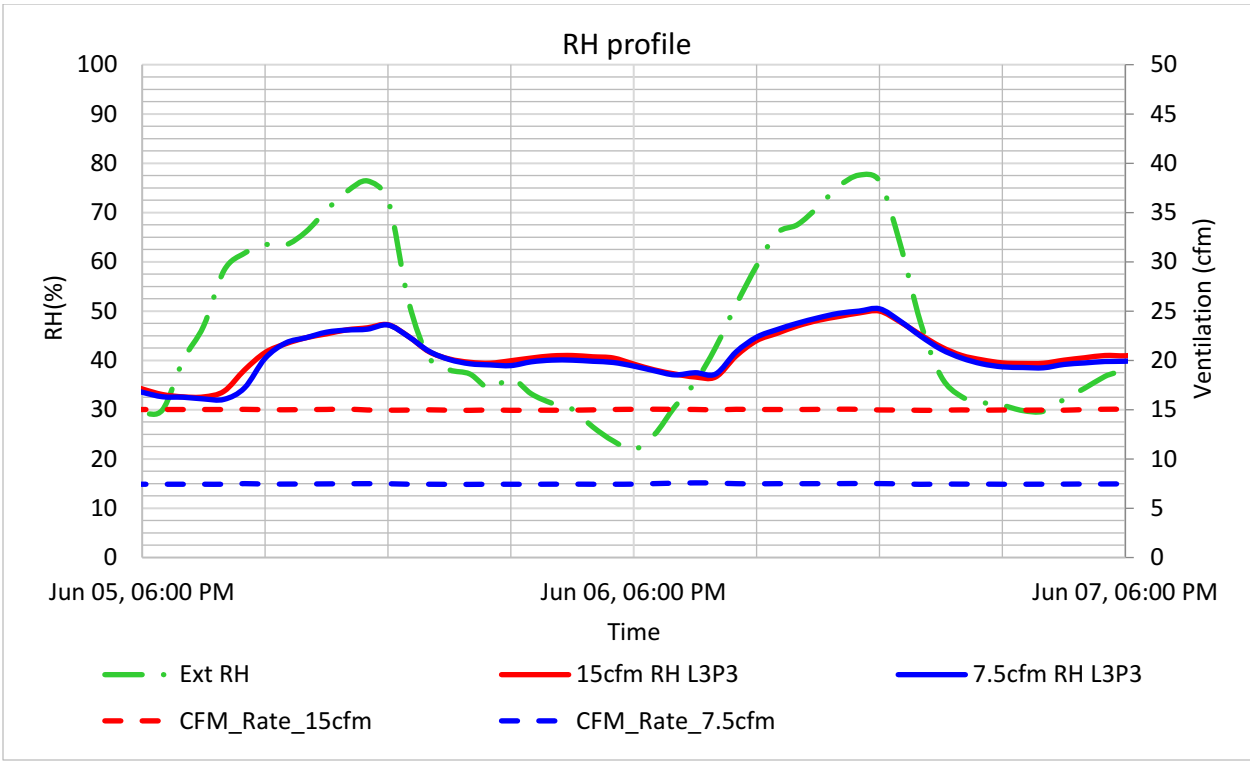

Figure 129: The relative humidity profile at L3P3 comparing 15 cfm 7.5 cfm using HP and UV.

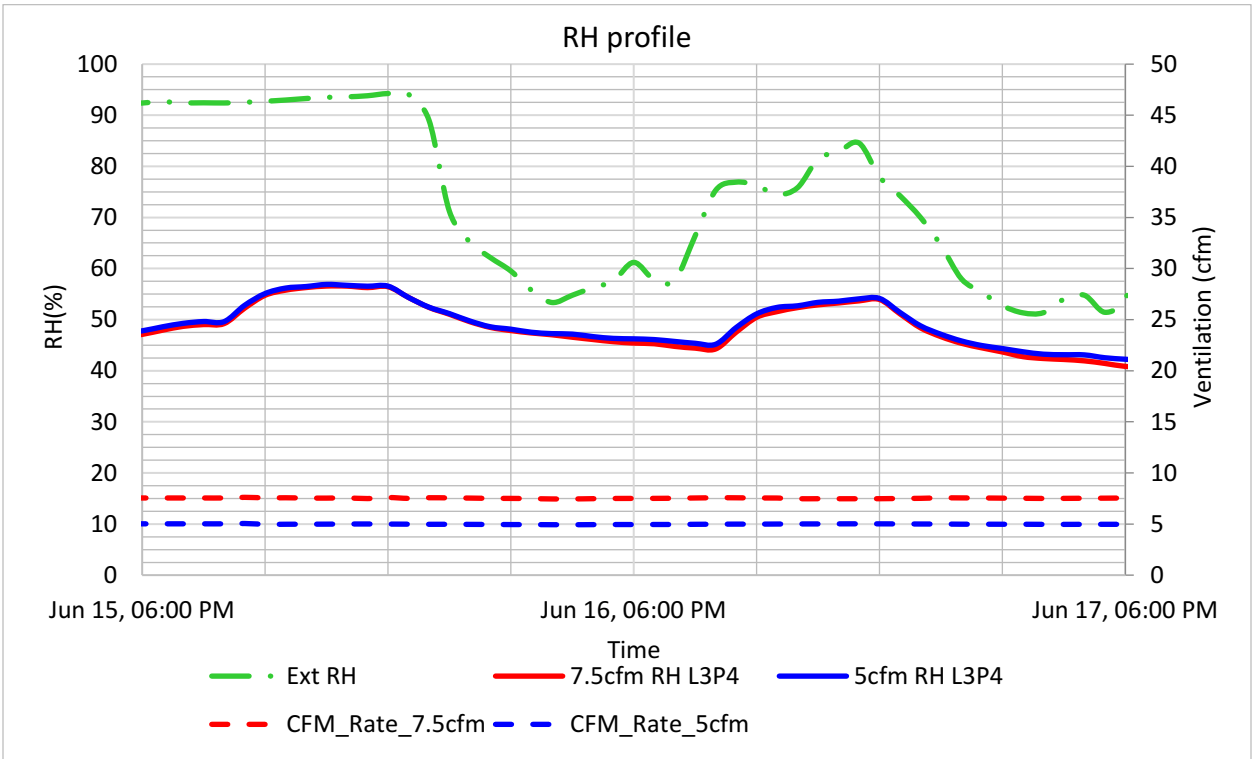

Figure 130: The relative humidity profile at L3P3 comparing 15 cfm 7.5 cfm using EBH and UV.

Section 6.4: CO2 distribution UV

Heating systems	Ventilation flow rate												Difference											
	15cfm						7.5cfm						Abs (15cfm – 7.5cfm)											
Radiant Floor Heating system (RFHS)		P4	434	506	432	442		P4	562	657	560	581		P4	128	151	128	139						
		P3	435	578	426	442		P3	515	666	540	559		P3	80	88	114	118						
		P2	392	458	462	441		P2	537	590	558	536		P2	145	133	96	95						
			L5	L4	L3	L2			L5	L4	L3	L2			L5	L4	L3	L2						
Eclectic baseboard Heather (EBH)		P4	416	495	411	418		P4	516	591	522	535		P4	100	96	111	118						
		P3	429	466	425	391		P3	504	566	511	517		P3	75	101	86	126						
		P2	402	422	419	363		P2	540	535	499	459		P2	138	113	80	95						
			L5	L4	L3	L2			L5	L4	L3	L2			L5	L4	L3	L2						
Heat pump (HP)		P4	421	496	418	424		P4	521	626	533	554		P4	119	128	118	130						
		P3	389	489	428	421		P3	443	619	520	538		P3	78	143	101	119						
		P2	359	443	421	418		P2	507	547	537	514		P2	140	108	101	102						
			L5	L4	L3	L2			L5	L4	L3	L2			L5	L4	L3	L2						
	7.5cfm						5cfm						Abs (7.5cfm – 5cfm)											
Heat pump (HP)		P4	601	692	587	605		P4	622	732	606	633		P4	21	40	18	28						
		P3	607	650	591	596		P3	579	693	587	612		P3	29	43	4	16						
		P2	559	604	609	587		P2	622	627	605	578		P2	62	22	4	9						
			L5	L4	L3	L2			L5	L4	L3	L2			L5	L4	L3	L2						
Eclectic baseboard Heather (EBH)		P4	617	739	609	624		P4	647	732	629	651		P4	30	7	20	27						
		P3	642	680	607	597		P3	614	687	607	627		P3	28	7	0	30						
		P2	555	635	596	571		P2	637	652	606	550		P2	82	18	9	21						
			L5	L4	L3	L2			L5	L4	L3	L2			L5	L4	L3	L2						
	Color Legend																							
	Ave of Min						Ave				Ave of Max		Min				Ave of Max							
	350						500				650		0				200							

Figure 131: Interior CO2 distribution comparison of 15 cfm, 7.5 cfm, and 5 cfm with MV.

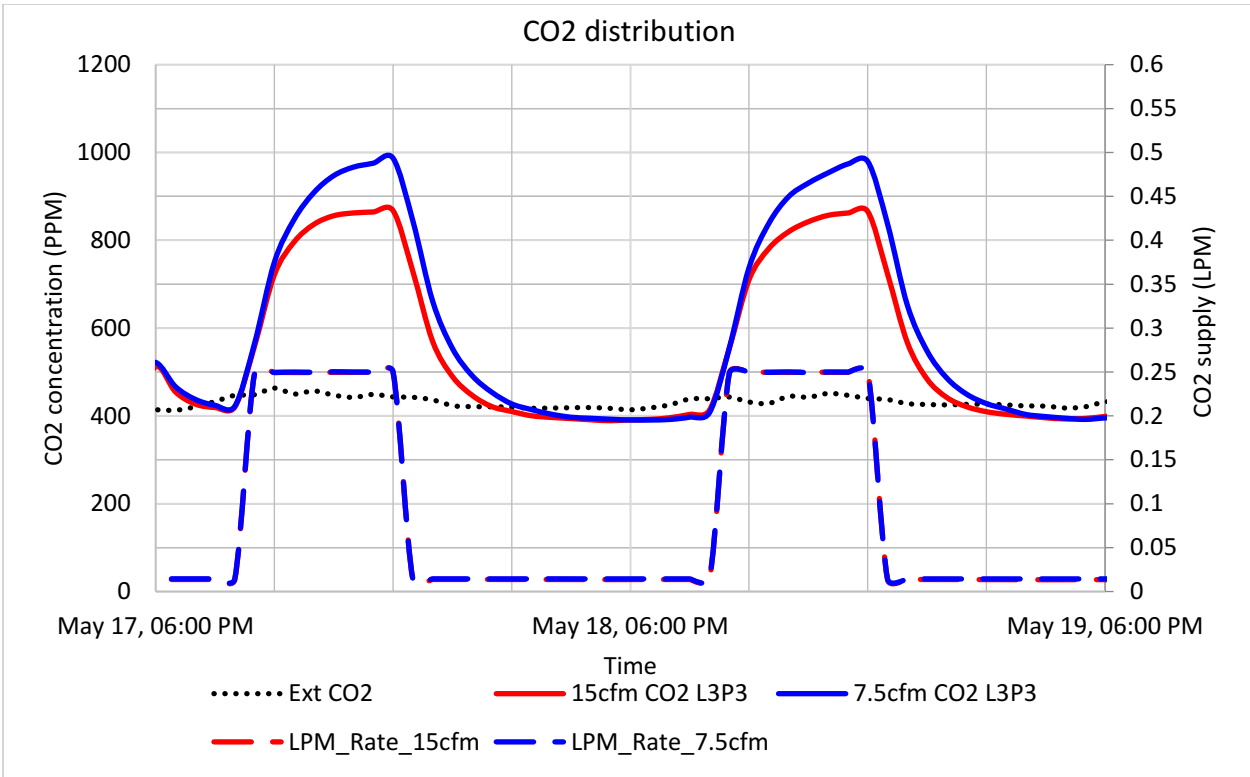

Figure 132: CO2 profile comparing 15 cfm and 7.5 cfm with RFHS and UV.

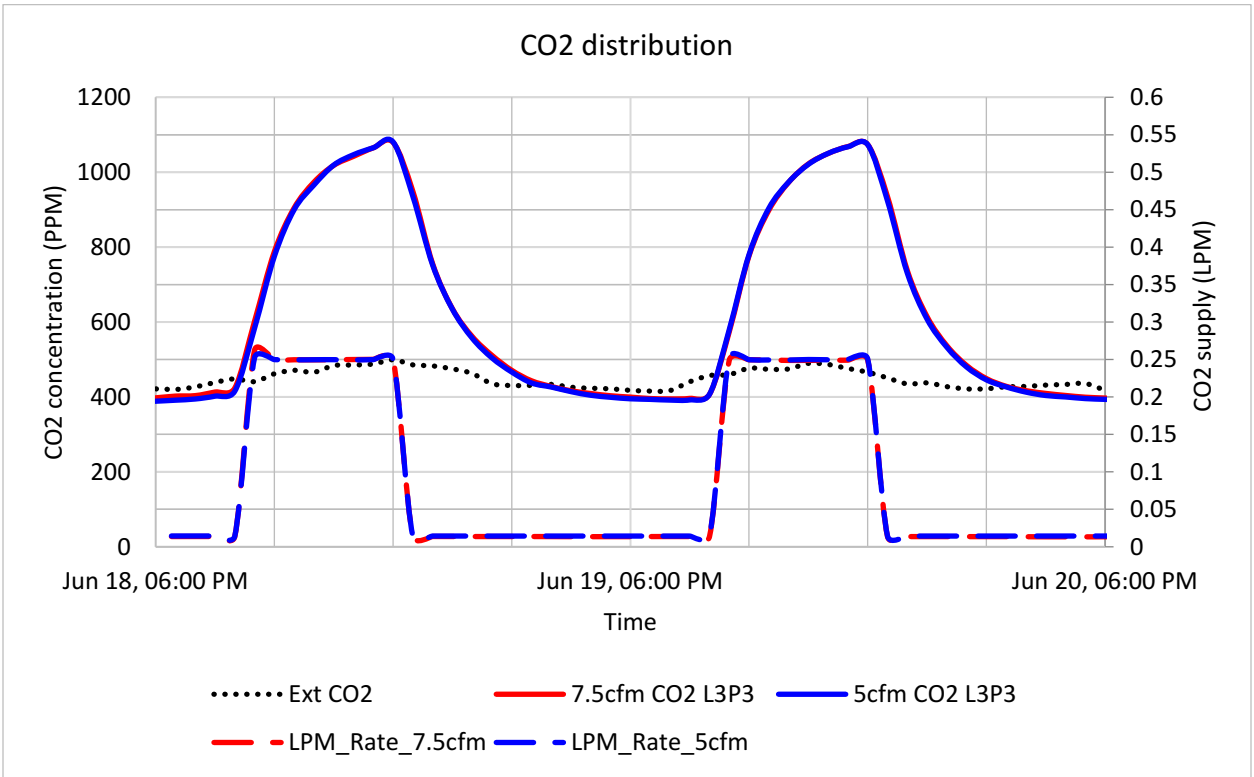

Figure 133: CO2 profile comparing 7.5 cfm and 5 cfm with EBH and UV.

Section 6.5: Absolute ventilation efficiency distribution UV

Heating systems	Ventilation flow rate											Difference				
	15cfm					7.5cfm						Abs (15cfm – 7.5cfm)				
Radiant Floor Heating system (RFHS)	P4	101.7	87.1	102.0	99.7	P4	95.5	81.6	95.7	92.2		P4	6.2	5.5	6.3	7.5
	P3	101.4	76.3	103.6	99.9	P3	104.2	80.5	99.3	95.9		P3	2.8	4.2	4.2	4.0
	P2	112.5	96.4	95.5	100.0	P2	99.8	90.8	96.1	100.0		P2	12.7	5.5	0.6	0.0
		L5	L4	L3	L2		L5	L4	L3	L2			L5	L4	L3	L2
Eclectic baseboard Heather (EBH)	P4	87.4	73.4	88.3	87.0	P4	88.9	77.7	87.8	85.7		P4	1.5	4.2	0.5	1.3
	P3	84.7	78.0	85.5	93.0	P3	91.1	81.0	89.7	88.8		P3	6.3	3.0	4.2	4.2
	P2	90.3	86.1	86.8	100.0	P2	84.9	85.8	92.0	100.0		P2	5.4	0.3	5.2	0.0
		L5	L4	L3	L2		L5	L4	L3	L2			L5	L4	L3	L2
Heat pump (HP)	P4	94.9	77.5	95.6	93.5	P4	93.0	77.9	93.6	90.0		P4	1.9	0.4	2.0	3.5
	P3	92.8	81.0	96.5	96.6	P3	98.6	78.8	97.4	94.3		P3	5.8	2.2	0.9	2.4
	P2	101.0	91.1	92.9	100.0	P2	93.8	91.7	94.4	100.0		P2	7.2	0.6	1.6	0.0
		L5	L4	L3	L2		L5	L4	L3	L2			L5	L4	L3	L2
	7.5cfm					5cfm						Abs (7.5cfm – 5cfm)				
Heat pump (HP)	P4	97.8	85.0	99.9	97.1	P4	93.1	79.3	95.5	91.5		P4	5	6	4	6
	P3	96.7	90.5	99.3	98.5	P3	99.9	83.6	98.5	94.6		P3	3	7	1	4
	P2	104.9	97.2	96.5	100.0	P2	93.1	92.4	95.7	100.0		P2	12	5	1	0
		L5	L4	L3	L2		L5	L4	L3	L2			L5	L4	L3	L2
Eclectic baseboard Heather (EBH)	P4	92.6	77.2	93.7	91.5	P4	85.1	75.2	87.5	84.5		P4	7.5	2.0	6.2	7.0
	P3	88.9	84.0	94.0	95.6	P3	89.6	80.1	90.6	87.7		P3	0.7	3.9	3.4	7.8
	P2	103.0	90.0	95.8	100.0	P2	86.4	84.4	90.9	100.0		P2	16.6	5.6	4.9	0.0
		L5	L4	L3	L2		L5	L4	L3	L2			L5	L4	L3	L2

Color Legend				
Ave of Min	Ave	Ave of Max	Min	Ave of Max
700	950	1200	0	200

Figure 134: Interior CRE distribution comparison of 15 cfm, 7.5 cfm, and 5 cfm with UV.

Section 6.7: Indoor air quality number UV

Heating systems	Ventilation flow rate										Difference				
	15cfm					7.5cfm					Abs (15cfm – 7.5cfm)				
Radiant Floor Heating system (RFHS)	P4	5.1	4.4	5.1	5.0	P4	3.0	2.5	3.0	2.9	P4	2.1	1.8	2.1	2.1
	P3	5.1	3.8	5.2	5.0	P3	3.2	2.5	3.1	3.0	P3	1.8	1.3	2.1	2.0
	P2	5.6	4.8	4.8	5.0	P2	3.1	2.8	3.0	3.1	P2	2.5	2.0	1.8	1.9
		L5	L4	L3	L2		L5	L4	L3	L2		L5	L4	L3	L2
Eclectic baseboard Heather (EBH)	P4	4.4	3.7	4.4	4.4	P4	2.8	2.4	2.7	2.7	P4	1.6	1.3	1.7	1.7
	P3	4.2	3.9	4.3	4.7	P3	2.8	2.5	2.8	2.8	P3	1.4	1.4	1.5	1.9
	P2	4.5	4.3	4.3	5.0	P2	2.6	2.7	2.9	3.1	P2	1.9	1.6	1.5	1.9
		L5	L4	L3	L2		L5	L4	L3	L2		L5	L4	L3	L2
Heat pump (HP)	P4	4.8	3.9	4.8	4.7	P4	2.9	2.4	2.9	2.8	P4	1.9	1.5	1.9	1.9
	P3	4.6	4.1	4.8	4.8	P3	3.1	2.5	3.0	2.9	P3	1.6	1.6	1.8	1.9
	P2	5.1	4.6	4.7	5.0	P2	2.9	2.9	2.9	3.1	P2	2.1	1.7	1.7	1.9
		L5	L4	L3	L2		L5	L4	L3	L2		L5	L4	L3	L2
	7.5cfm					5cfm					Abs (7.5cfm – 5cfm)				
Heat pump (HP)	P4	3.0	2.6	3.1	3.0	P4	2.3	1.9	2.3	2.2	P4	0.8	0.7	0.8	0.8
	P3	3.0	2.8	3.1	3.1	P3	2.4	2.0	2.4	2.3	P3	0.6	0.8	0.7	0.8
	P2	3.3	3.0	3.0	3.1	P2	2.3	2.3	2.3	2.4	P2	1.0	0.8	0.7	0.7
		L5	L4	L3	L2		L5	L4	L3	L2		L5	L4	L3	L2
Eclectic baseboard Heather (EBH)	P4	2.9	2.4	2.9	2.9	P4	2.1	1.8	2.1	2.1	P4	0.8	0.6	0.8	0.8
	P3	2.8	2.6	2.9	3.0	P3	2.2	2.0	2.2	2.1	P3	0.6	0.7	0.7	0.8
	P2	3.2	2.8	3.0	3.1	P2	2.1	2.1	2.2	2.4	P2	1.1	0.7	0.8	0.7
		L5	L4	L3	L2		L5	L4	L3	L2		L5	L4	L3	L2

Color Legend				
Ave of Min	Ave	Ave of Max	Min	Ave of Max
0	3	6	0	4

Figure 135: Interior IAQN distribution comparison of 15 cfm, 7.5 cfm, and 5 cfm with UV.

Section 6.8: Relative ventilation efficiency and indoor air quality number: Low ventilation flow rate comparison

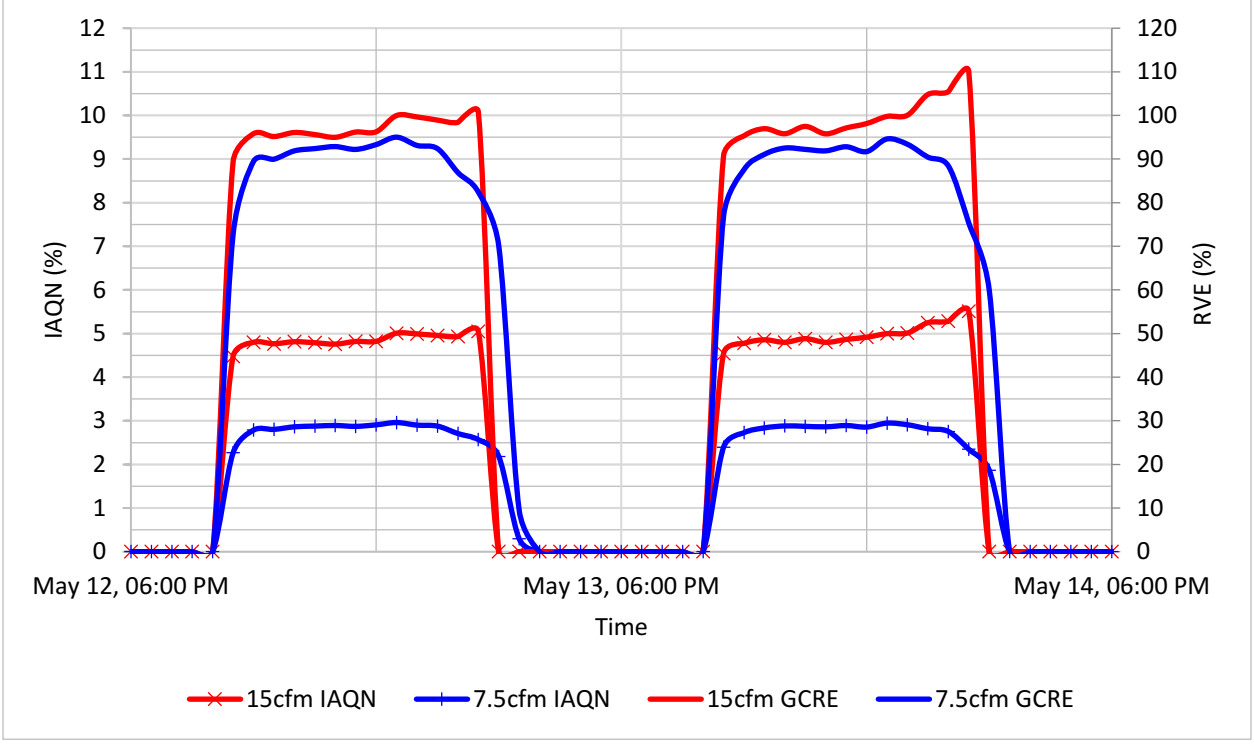

Figure 136: IAQN and GCRE room with RFHS (15 cfm vs 7.5 cfm) UV.

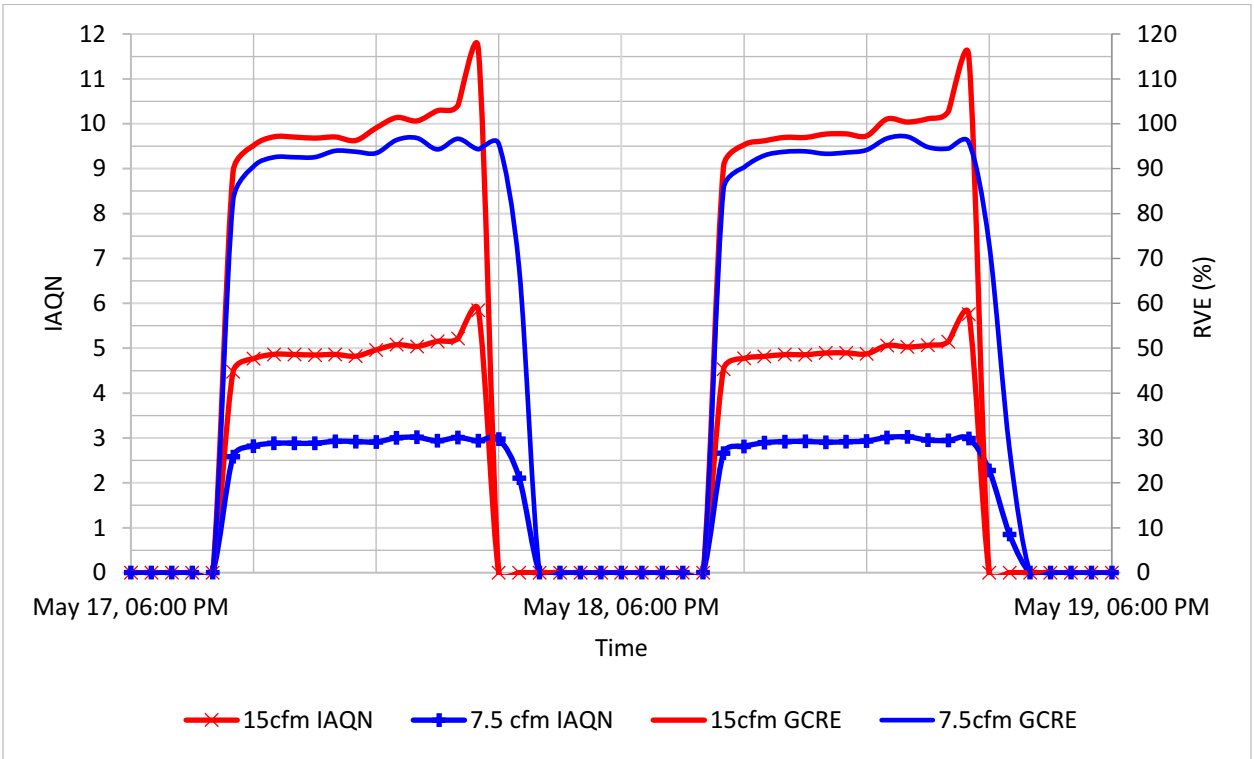

Figure 137: IAQN and GCRE room with RFHS and UV.

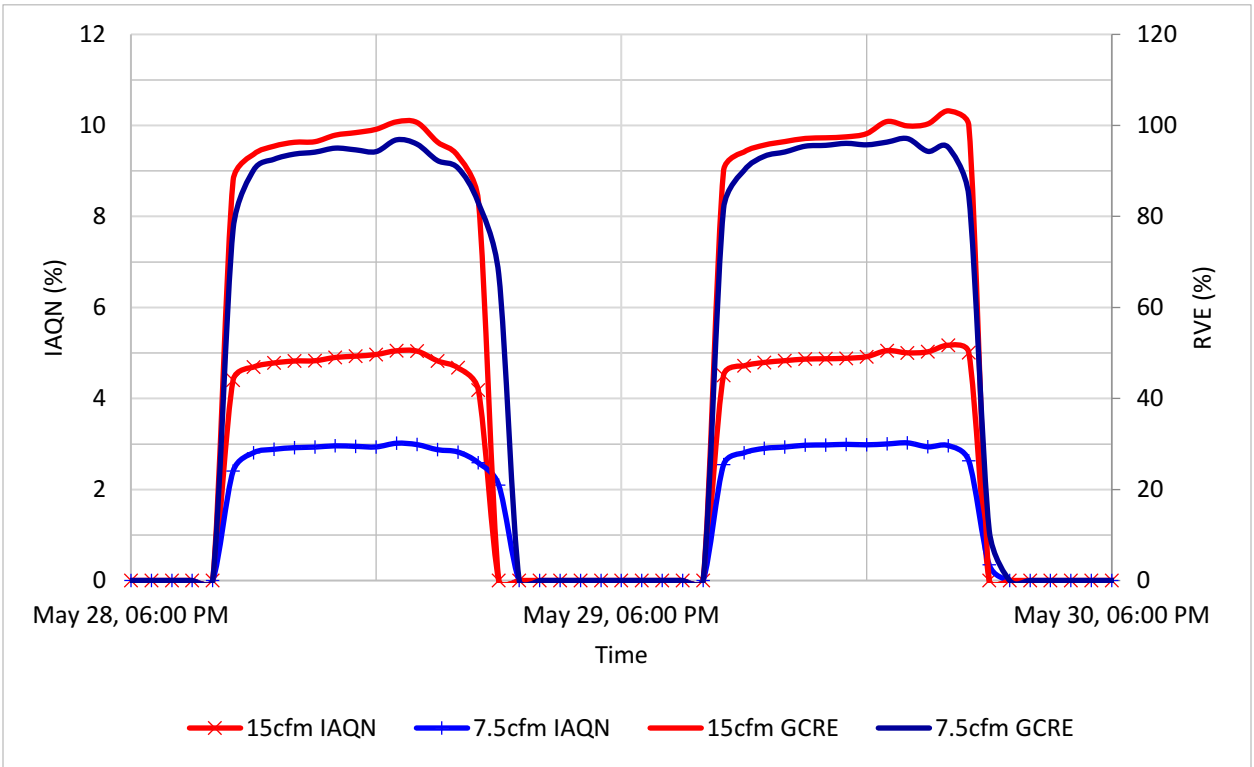

Figure 138: IAQN and GCRE room with EBH (15 cfm vs 7.5 cfm) UV.

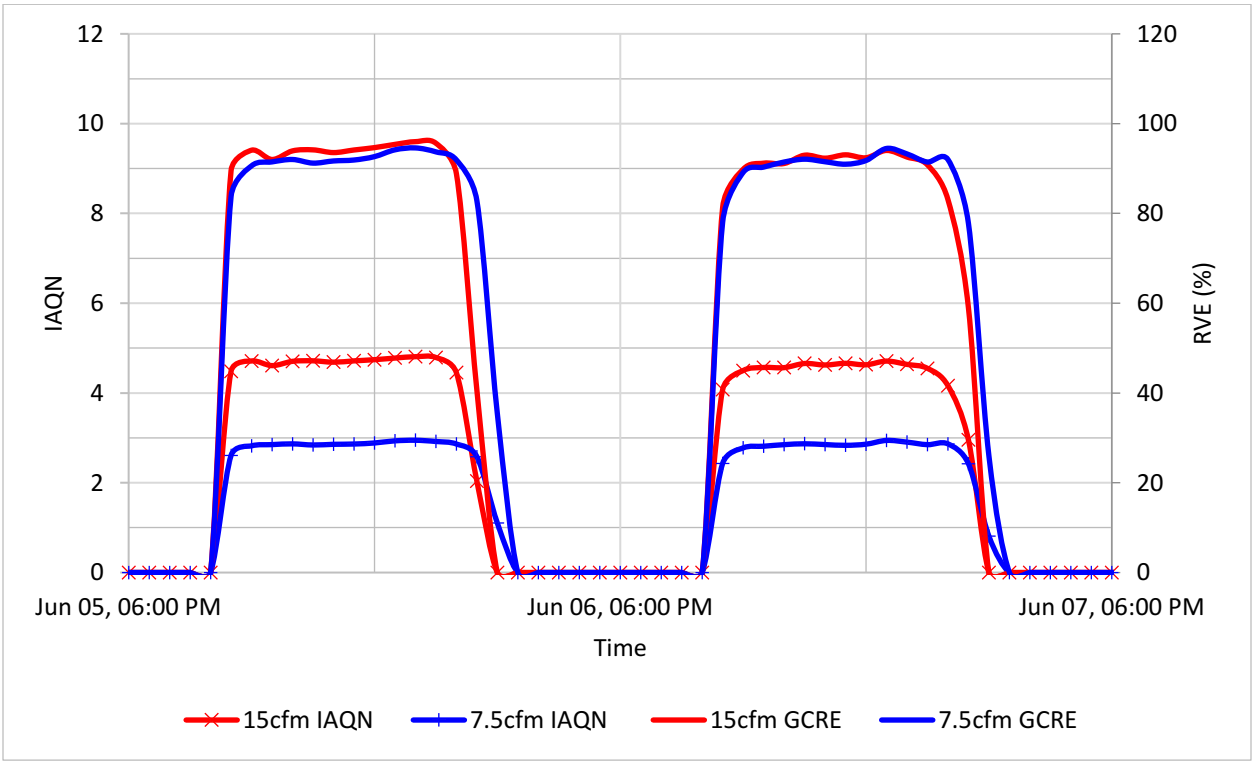

Figure 139: IAQN and RVE room with EBH (15 cfm vs 7.5 cfm) MV.

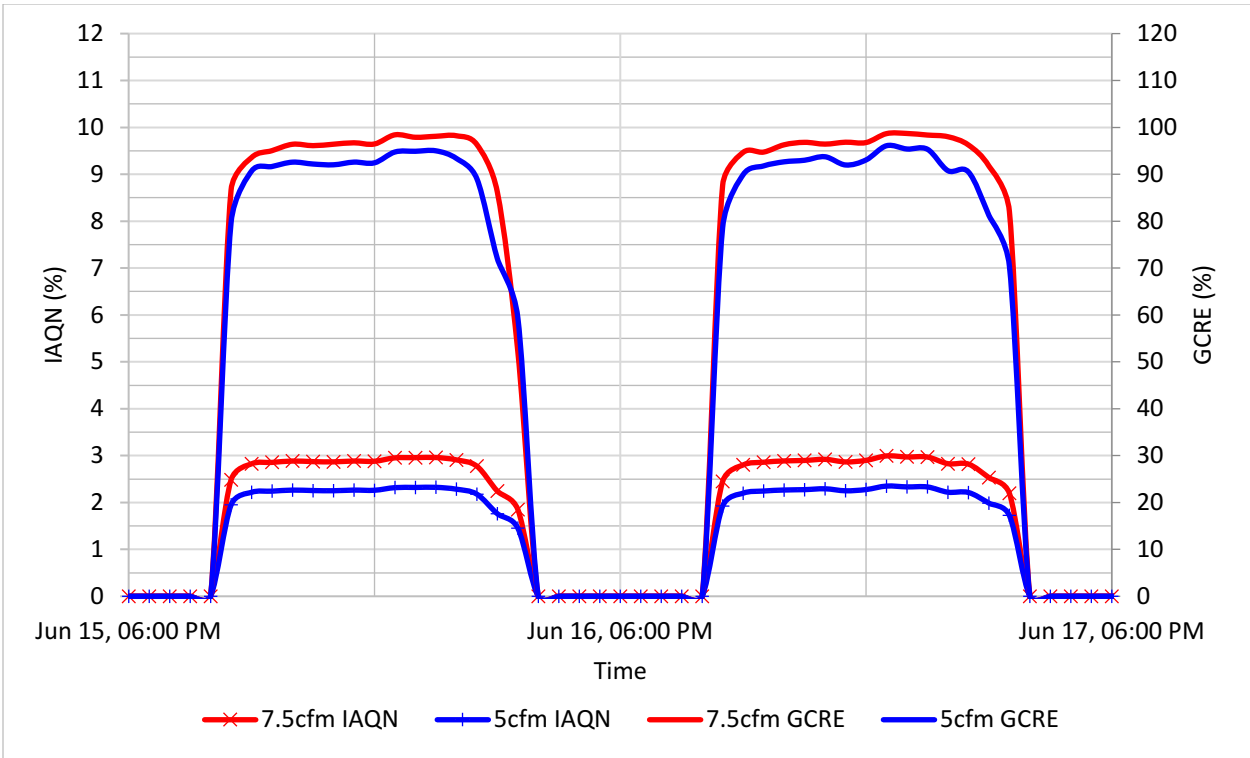

Figure 140: IAQN and RVE room with HP (15 cfm vs 7.5 cfm) UV.

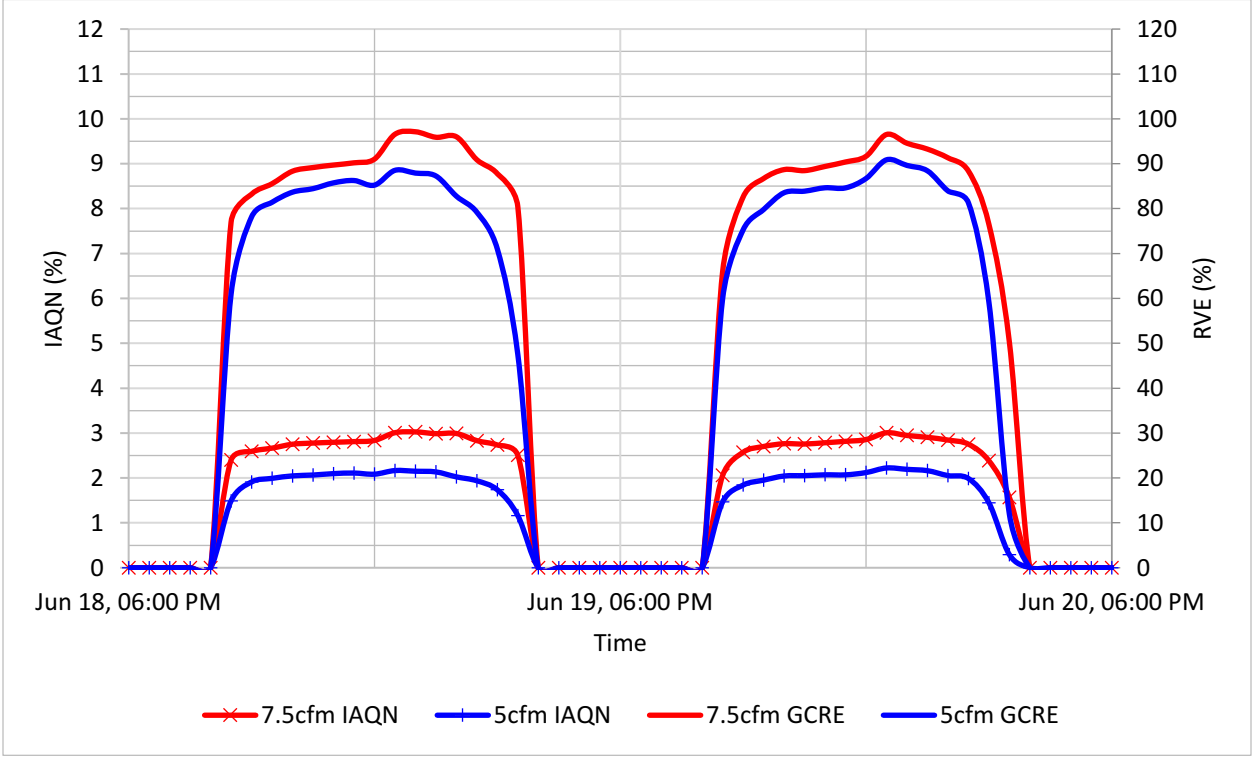

Figure 141: IAQN and RVE room with EBH (7.5 cfm vs 5 cfm) UV.

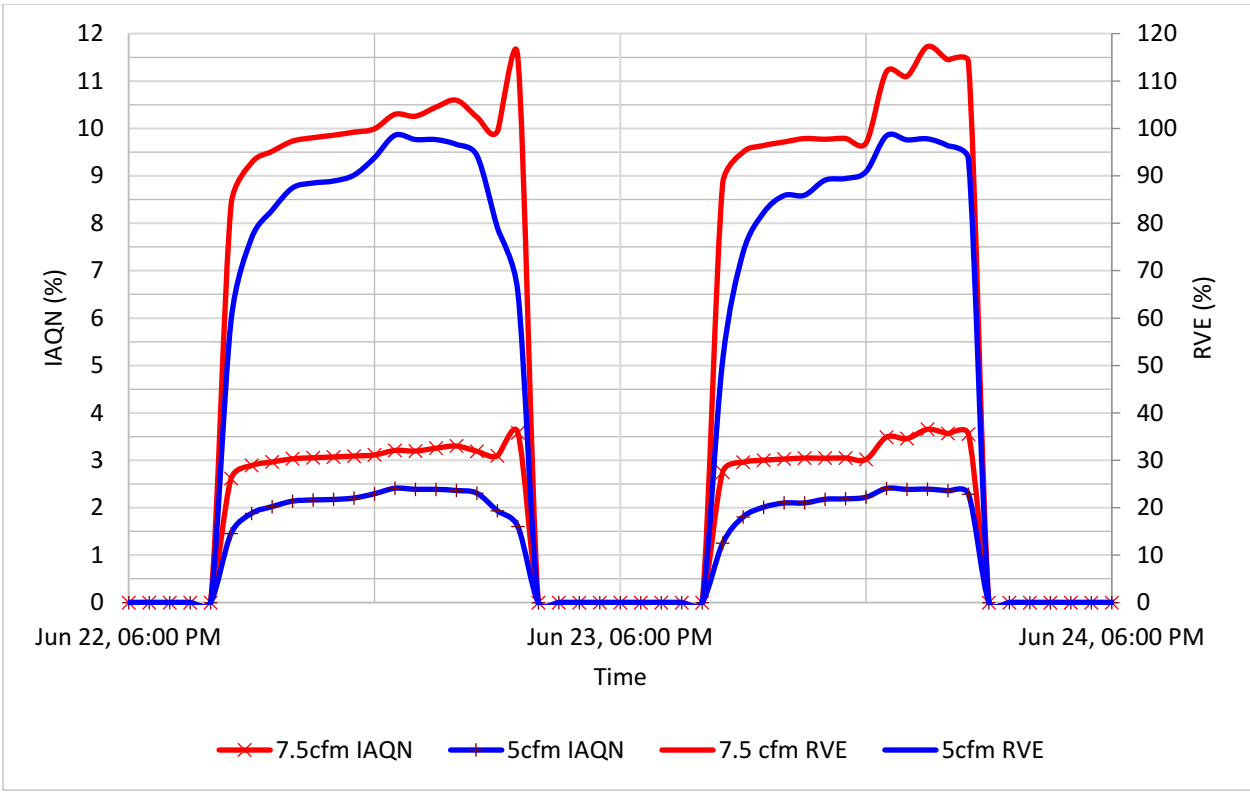

Figure 142: IAQN and RVE room with EBH (7.5 cfm vs 5 cfm) MV.

Section 6.9: Energy penalty

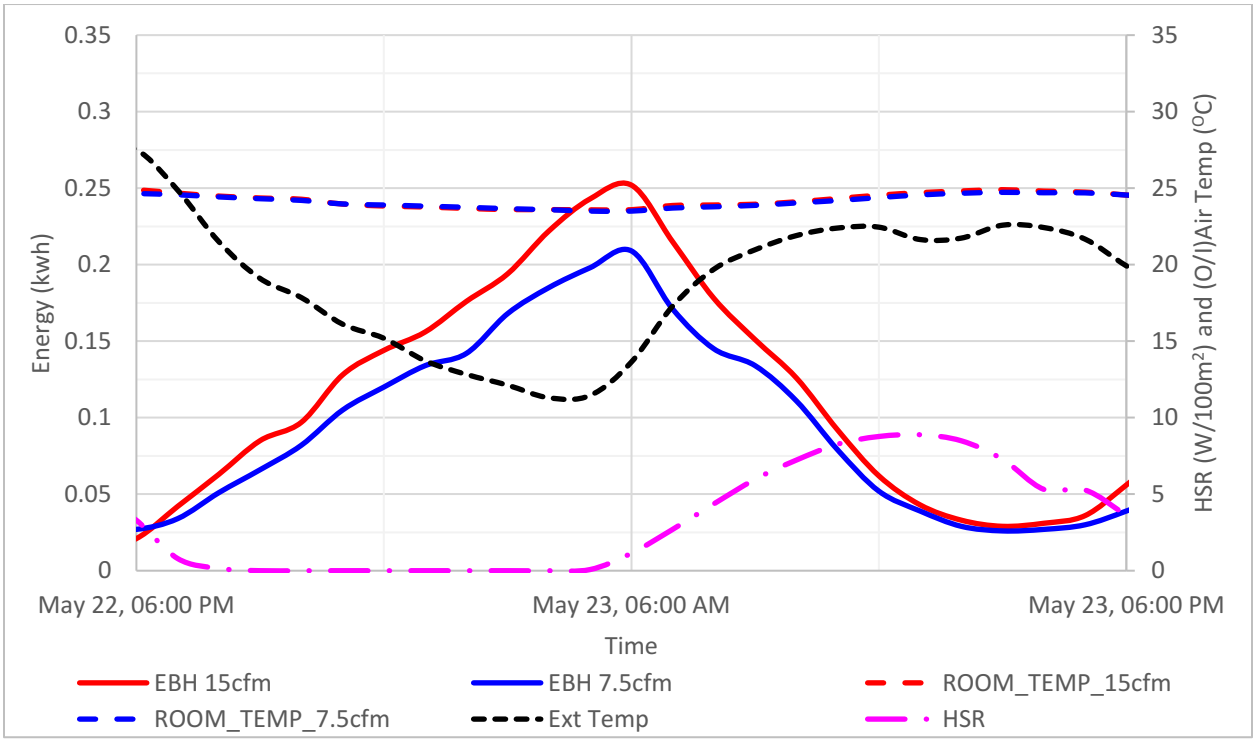

Figure 143: Energy profile of EBH and UV with 15 cfm and 7.5 cfm.

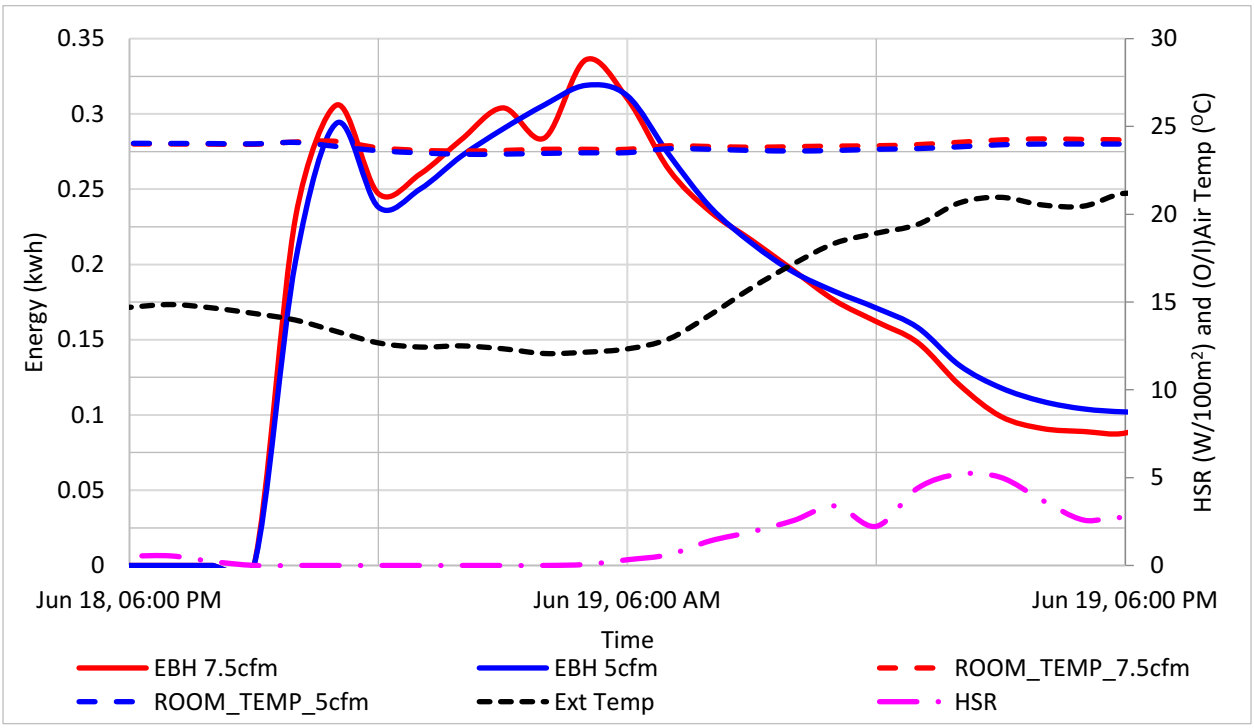

Figure 144: Energy profile of EBH and UV with 7.5 cfm and 5 cfm.

11 REFERENCE

Nghana, B., & Tariku, F. (2016). Phase change material's (PCM) impacts on the energy performance and thermal comfort of buildings in a mild climate. *Building and Environment*, *99*, 221-238.

Pedram, S., & Tariku, F. (2014). Moisture Buffering Effect of Gypsum Board in a Marine Climate: A Field Experimental Study. In *Advanced Materials Research* (Vol. 1051, pp. 763-773). Trans Tech Publications.

Tariku, F.; Simpson, Y. (2013). Development of a Whole-Building Performance Research Laboratory (WBPRL) for an Integrated Study of Energy Efficiency, Indoor Environmental Quality and Building Envelope Durability**.** Zero Energy Mass Customization Housing, International Conference (ZEMCH2013), Miami, USA, November 2013.

Fernández-González, A. (2007). Analysis of the thermal performance and comfort conditions produced by five different passive solar heating strategies in the United States Midwest. *Solar Energy*, *81*(5), 581-593.

Krajčík, M., Simone, A., & Olesen, B. W. (2012). Air distribution and ventilation effectiveness in an occupied room heated by warm air. *Energy and Buildings*, *55*, 94-101.

John R. Howell, Robert Siegel. 2010 "Thermal Radiation Heat transfer" 5th Edition CRC Press, ISBN-10:1439805334.

A. Hesaraki, S. Holmberg **"**Energy performance of a low-temperature heating system in five newly built Swedish dwellings: A case study using simulations and on-site measurements." Building and Environment 64(2013) 85-93.

Olesen, B. W. (2002). Radiant floor heating in theory and practice. *ASHRAE journal*, *44*(7), 19.

Causone, F., Olesen, B. W., & Corgnati, S. P. (2010). Floor heating with displacement ventilation: an experimental and numerical analysis. *HVAC&R Research*, *16*(2), 139-160. B. Olesen, B. W., Simone, A., Krajcĺik, M., Causone, F., & Carli, M. D. (2011). Experimental study of air distribution and ventilation effectiveness in a room with a combination of different mechanical ventilation and heating/cooling systems. *International Journal of Ventilation*, *9*(4), 371-383.

Pean, T. Q., Gennari, L., Kazanci, O. B., & Olesen, B. W. (2016). Evaluation of the Energy and Comfort Performance of a Plus-Energy House under Scandinavian Summer Conditions. In *Proceedings of the 12 th World REHVA Congress–CLIMA 2016*.

Zhang, D., Cai, N., & Wang, Z. (2013). Experimental and numerical analysis of lightweight radiant floor heating system. *Energy and buildings*, *61*, 260-266.

Olesen, B. W., Mortensen, E., Thorshauge, J., & Berg-Munch, B. (1980). Thermal comfort in a room heated by different methods. *ASHRAE transactions*, *86*(1), 34-48.

Nilsson, H. O. (2007). Thermal comfort evaluation with virtual manikin methods. *Building and Environment*, *42*(12), 4000-4005.

Catalina, T., Virgone, J., & Kuznik, F. (2009). Evaluation of thermal comfort using combined CFD and experimentation study in a test room equipped with a cooling ceiling. *Building and Environment*, *44*(8), 1740-1750.

Schøtt, J., Andersen, M. E., Kazanci, O. B., & Olesen, B. W. (2016). Simulation Study of the Energy Performance of Different Space Heating Methods in Plus-energy Housing. In *12th REHVA World CongressREHVA World Congress*.

Peeters, L., De Dear, R., Hensen, J., & D'haeseleer, W. (2009). Thermal comfort in residential buildings: Comfort values and scales for building energy simulation. *Applied energy*, *86*(5), 772-780.

Yang, L., Zmeureanu, R., & Rivard, H. (2008). Comparison of environmental impacts of two residential heating systems. *Building and Environment*, *43*(6), 1072-1081.

Kulkarni, M. R., & Hong, F. (2004). Energy optimal control of a residential space-conditioning system based on sensible heat transfer modeling. *Building and Environment*, *39*(1), 31-38.

Tye-Gingras, M., & Gosselin, L. (2012). Comfort and energy consumption of hydronic heating radiant ceilings and walls based on CFD analysis. *Building and Environment*, *54*, 1-13.

Krajčík, M., Simone, A., & Olesen, B. W. (2012). Air distribution and ventilation effectiveness in an occupied room heated by warm air. *Energy and Buildings*, *55*, 94-101.

Holz, R., Hourigan, A., Sloop, R., Monkman, P., & Krarti, M. (1997). Effects of standard energy conserving measures on thermal comfort. *Building and environment*, *32*(1), 31-43.

Bertsch, S. S., & Groll, E. A. (2008). Two-stage air-source heat pump for residential heating and cooling applications in northern US climates. *International journal of refrigeration*, *31*(7), 1282-1292.

Wu, X., Olesen, B. W., Fang, L., & Zhao, J. (2013). A nodal model to predict vertical temperature distribution in a room with floor heating and displacement ventilation. *Building and Environment*, *59*, 626-634.

Zhai, Z. J., & Chen, Q. Y. (2005). Performance of coupled building energy and CFD simulations. *Energy and buildings*, *37*(4), 333-344.

Krajčík, M., Simone, A., & Olesen, B. W. (2012). Air distribution and ventilation effectiveness in an occupied room heated by warm air. *Energy and Buildings*, *55*, 94-101.

Olesen, B. W., Simone, A., KrajcÍik, M., Causone, F., & Carli, M. D. (2011). Experimental study of air distribution and ventilation effectiveness in a room with a combination of different

mechanical ventilation and heating/cooling systems. *International Journal of Ventilation*, *9*(4), 371-383.

Awbi, H. B., & Gan, G. (1993, July). Evaluation of the overall performance of room air distribution. In *Proceedings of the 6th International Conference on Indoor Air Quality and Climate, Helsinki* (Vol. 5, pp. 283-288).

Sandberg, M. (1981). What is ventilation efficiency? *Building and environment*, *16*(2), 123-135.

Cho, Y., Awbi, H. B., & Karimipanah, T. (2002). A comparison between four different ventilation systems. In *Proceedings of the 8th International Conference on Air Distribution in Rooms (Roomvent 2002)* (pp. 181-184).

Krajčík, M., Simone, A., & Olesen, B. W. (2012). Air distribution and ventilation effectiveness in an occupied room heated by warm air. *Energy and Buildings*, *55*, 94-101.

Causone, F., Olesen, B. W., & Corgnati, S. P. (2010). Floor heating with displacement ventilation: an experimental and numerical analysis. *HVAC&R Research*, *16*(2), 139-160.

Olesen, B. W., Simone, A., Krajcĺik, M., Causone, F., & Carli, M. D. (2011). Experimental study of air distribution and ventilation effectiveness in a room with a combination of different mechanical ventilation and heating/cooling systems. *International Journal of Ventilation*, *9*(4), 371-383.

Dougan, D. S., & Damiano, L. (2004). CO2-based demand control ventilation: Do risks outweigh potential rewards?. *ASHRAE Journal*, *46*(10), 47.

Holmberg, S., & Chen, Q. (2003). Air flow and particle control with different ventilation systems in a classroom. *Indoor air*, *13*(2), 200-204.

Yoshino, H., Murakami, S., Akabayashi, S. I., Kurabuchi, T., Kato, S., Tanabe, S. I., & Adachi, M. (2004, September). Survey on minimum ventilation rate of residential buildings in fifteen

countries. In *Proceedings of the 25th AIVC Conference-Ventilation and retrofitting, Prague* (pp. 227-238).

Yang, L., Zmeureanu, R., & Rivard, H. (2008). Comparison of environmental impacts of two residential heating systems. *Building and Environment*, *43*(6), 1072-1081.

Wan, M. P., & Chao, C. Y. (2005). Numerical and experimental study of velocity and temperature characteristics in a ventilated enclosure with underfloor ventilation systems. *Indoor air*, *15*(5), 342-355.

Fountain, M. (1991). Laboratory studies of the effect of air movement on thermal comfort: a comparison and discussion of methods.

Fong, M. L., Lin, Z., Fong, K. F., Chow, T. T., & Yao, T. (2011). Evaluation of thermal comfort conditions in a classroom with three ventilation methods. *Indoor Air*, *21*(3), 231-239.

Krajčík, M., Simone, A., & Olesen, B. W. (2012). Air distribution and ventilation effectiveness in an occupied room heated by warm air. *Energy and Buildings*, *55*, 94-101.

Krajčík, M., Tomasi, R., Simone, A., & Olesen, B. W. (2013). Experimental study including subjective evaluations of mixing and displacement ventilation combined with radiant floor heating/cooling system. *Hvac&r Research*, *19*(8), 1063-1072.

Tomasi, R., Krajčík, M., Simone, A., & Olesen, B. W. (2013). Experimental evaluation of air distribution in mechanically ventilated residential rooms: Thermal comfort and ventilation effectiveness. *Energy and Buildings*, *60*, 28-37.

Janbakhsh, S., & Moshfegh, B. (2014). Experimental investigation of a ventilation system based on wall confluent jets. *Building and Environment*, *80*, 18-31.

Murakami, S., Kato, S., & Zeng, J. (2000). Combined simulation of airflow, radiation and moisture transport for heat release from a human body. *Building and environment*, *35*(6), 489-500.

Ho, S. H., Rosario, L., & Rahman, M. M. (2011). Comparison of underfloor and overhead air distribution systems in an office environment. *Building and Environment*, *46*(7), 1415-1427.

Karimipanah, T., Awbi, H. B., Sandberg, M., & Blomqvist, C. (2007). Investigation of air quality, comfort parameters and effectiveness for two floor-level air supply systems in classrooms. *Building and Environment*, *42*(2), 647-655.

Dorer, V., & Breer, D. (1998). Residential mechanical ventilation systems: performance criteria and evaluations. *Energy and Buildings*, *27*(3), 247-255.

Chiang, W. H., Wang, C. Y., & Huang, J. S. (2012). Evaluation of cooling ceiling and mechanical ventilation systems on thermal comfort using CFD study in an office for subtropical region. *Building and Environment*, *48*, 113-127.

Wu, X., Olesen, B. W., Fang, L., & Zhao, J. (2013). A nodal model to predict vertical temperature distribution in a room with floor heating and displacement ventilation. *Building and Environment*, *59*, 626-634.

Cho, Y., Awbi, H. B., & Karimipanah, T. (2002). A comparison between four different ventilation systems. In *Proceedings of the 8th International Conference on Air Distribution in Rooms (Roomvent 2002)* (pp. 181-184).

Cheng, Y., & Lin, Z. (2016). Experimental investigation into the interaction between the human body and room airflow and its effect on thermal comfort under stratum ventilation. *Indoor air*, *26*(2), 274-285.

Cheng, Y., & Lin, Z. (2015). Experimental study of airflow characteristics of stratum ventilation in a multi-occupant room with comparison to mixing ventilation and displacement ventilation. *Indoor air*, *25*(6), 662-671.

Cho, Y., Awbi, H. B., & Karimipanah, T. (2008). Theoretical and experimental investigation of wall confluent jets ventilation and comparison with wall displacement ventilation. *Building and Environment*, *43*(6), 1091-1100.

Lin, Z., Tian, L., Yao, T., Wang, Q., & Chow, T. T. (2011). Experimental and numerical study of room airflow under stratum ventilation. *Building and Environment*, *46*(1), 235-244.

Lin, Z., Chow, T. T., Tsang, C. F., Fong, K. F., & Chan, L. S. (2005). CFD study on effect of the air supply location on the performance of the displacement ventilation system. *Building and environment*, *40*(8), 1051-1067.

Skistad, H., Mundt, E., Nielsen, P. V., Hagström, K., & Railio, J. (2002). Displacement ventilation in non-industrial premises.